The Transfer, Mixing and Wear Behaviour of an Al-Si-SiC Metal Matrix Composite Under Plasticity Dominated, Low Speed Reciprocal Sliding Conditions

By

Richard Allen Lawrence

A Thesis

Submitted to the University Of Manitoba

in fulfillment of the

thesis requirement for the degree of

MASTER OF SCIENCE

in

Mechanical and Industrial Engineering

Winnipeg, Manitoba, Canada

THE UNIVERSITY OF MANITOBA

FACULTY OF GRADUATE STUDIES

*****

COPYRIGHT PERMISSION PAGE

THE TRANSFER, MIXING AND WEAR BEHAVIOUR OF AN Al-Si-SiC METAL MATRIX COMPOSITE UNDER PLASTICITY DOMINATED, LOW SPEED RECIPROCAL SLIDING CONDITIONS

BY

RICHARD ALLEN LAWRENCE

A Thesis/Practicum submitted to the Faculty of Graduate Studies of The University of Manitoba in partial fulfillment of the requirements of the degree of

Master of Science

ACKNOWLEDGEMENTS

I would like to thank my advisor, Dr. K.N. Tandon for his support on this project. I am grateful for opportunity that was given to me. I would also like to thank Dr. J.R. Cahoon for help along the way. I would like to express my gratitude to my mother, Gloria, for being there during my schooling, and to my father, Bill, for the interest he gave me in engineering and technology. This project was made possible by financial support from NSERC, the Natural Science and Engineering Research Council of Canada, as well as funding from the University of Manitoba.

ABSTRACT

Current research has established that surface mechanical mixing can occur during sliding wear, causing a wear resistant surface layer to form and increasing tribological performance. Many studies have identified the benefits of surface mechanical mixing, however the sliding conditions required for a mechanically mixed layer (MML) to increase wear performance remain uncertain. The greatest factors in a mechanical mixed layer forming are the two materials in contact and the correct sliding velocity and pressure to allow beneficial exchange between surfaces to occur.

This study examines the mechanical mixing behaviour of an Aluminum-Silicon Metal Matrix Composite (Al-MMC) reinforced with 20vol% SiC particulate. This material has been established in most unidirectional studies to have superior wear resistance over the unreinforced binary Al-Si alloy. Wear of the A356-20vol%SiC composite has been demonstrated to result in surface MML formation during dry unidirectional sliding against a hard steel counterface. The central question to be answered in this study is if surface mechanical mixing can form with reciprocal sliding conditions, with different counterfaces and with different applied loads and sliding velocity than so far established in literature. In other words, more factors need to be examined (dominant wear mechanisms required, role of debris reprocessing, integration of counterface elements and oxides) as they relate specifically to mechanically mixed layer (MML) formation, allowing its wear resistance to be more fundamentally understood.

Effort is taken to understand the transfer of elements and counterface material that occurs in forming mechanically mixed layers between sliding surfaces by using different

counterface materials in dry sliding contact against the composite aluminum. Three steel counterface materials, 316 stainless, 440C, and 52100 bearing were tested against the A356 Al-20% SiC to compare elemental transfer and MML formation behaviour. Al-6061 a counterface softer than the composite with high compatibility was examined for mechanical mixing behaviour. A K-Monel nickel alloy counterface was compared in terms of mixing and transfer behaviour to the 316 stainless steel counterface, as both materials had similar hardness but entirely different compositions. Two ceramics, Al_2O_3 and Si_3N_4, were tested in comparison to the metallic counterfaces for mixing behaviour. Unlubricated reciprocal, ball on block, testing was chosen to examine its effect on the reprocessing of debris between surfaces in contact and to help further understand how contact geometry affects mechanical mixing.

It was observed that under reciprocating motion a MML caused by transfer of steel across the interface is less likely to form on the Al-MMC. Mixing of elements of both surfaces is seen to be limited by mass transfer of the Al-MMC to the steel counterface (high adhesion). The formation of a mechanically mixed layer is proposed to depend more directly on the dominant surface wear mechanisms and debris particle dynamics than on the hardness or composition of the counterface during sliding wear. For high Al-composite mixing, continued counterface abrasion and low overall weight loss from the sliding system to all simultaneously occur, the debris once produced had to be 1) small, 2) retained in the interface and 3) remixed into the composite surface. Abrasion of the steel counterface was required to dominate over adhesive transfer of the Al-composite for Fe mixing to form a MML surface. In addition the sliding contact pressure had to be high enough to plastically mix the composite surface while abrasion of the counterface occurred.

Since adhesion of mixed Al-MMC to the steel counterface dominated transfer that was occurring for most reciprocal sliding conditions tested the result was the formation of a Surface Mixed Layer, SML, which comprised of debris produced by continual transfer and back transfer mixed of the Al-composite during sliding. The formation of a SML was proposed to be the result of different surface wear mechanisms than the formation of a MML; The former considered to form by smearing and high adhesive transfer to the counterface, with the latter considered to form by greater reprocessing of debris and high abrasion of the counterface. K-monel was observed to result in lower adhesion of the Al-MMC surface and experienced greater abrasion and as a result, caused the formation of a semi-stable MML. However, the MML formed by K-monel did not significantly increase wear performance due to low remixing of debris into the surface layer under the reciprocal sliding conditions. The differences between SML and MML phenomenon observed here and in literature are discussed.

A stable SML was not observed to form for any counterface tested under the reciprocal sliding conditions. High adhesion of the composite became unstable at low pressures causing random delaminations of the transferred material, and resulting in random "patches" of surface mechanical mixing. The counterface was observed to significantly affect the stability of transferred mixed Al-MMC material, with the ceramics acting as the most stable substrate for mixed material to adhere. Tribological performance of the different counterfaces in terms of weight loss and surface damage is discussed.

TABLE OF CONTENTS

LIST OF FIGURES

Chapter 2

LIST OF TABLES

Chapter 2

Chapter 3

Chapter 4

CHAPTER 1 INTRODUCTION

1.11 INTRODUCTION TO TRIBOLOGY OF AL-SIC COMPOSITES

The use of discontinuously reinforced composites in a tribological application is met with understandable pessimism when considering the surfaces that are brought into contact. Notably, hard ceramic reinforcement protrude from a polished surface of the composite, and provide a sense that increased abrasion potential exists and that probable surface damage caused by particle detachment or pullout would outweigh the increase in wear resistance in comparison to the use of monolithic aluminum alloys. Under dry sliding conditions the resistance to wear has been related to mechanical mixing with the counterface on the composite surface, providing a wear resistant *tribolayer*. The plastic deformation required for the formation this mechanical mixed layer (MML) is substantial and although it may provide increased wear performance under laboratory dry sliding conditions, the process of transfer and mixing is yet to be fundamentally understood, so that use of Al-MMCs and incorporation of the phenomenon of MML formation comes with great uncertainty. This is especially true under lubricated conditions and noting that the plastic deformation required in forming a MML on the surface of Al-composites may not be tolerable in most applications. However research into the wear properties of aluminum-discontinuously reinforced metal matrix composites (Al-MMCs) has almost universally demonstrated improved wear resistance can be achieved in comparison to the use of unreinforced aluminum alloys. In addition, studies that have observed a stable MML to form have found very low wear rates for dry sliding conditions, and which can allow these

Al-MMCs to become contenders with equivalent or better wear performance compared to steels in many tribological applications.

Nonetheless, the existence of the reinforcement requires consideration of how the hard particles would become third-body debris and the effect on the sliding system. Here the size, shape, and orientation, bonding etc. of the ceramic particles become extremely important. The reinforcement phase is a major variable that controls surface mechanical mixing behaviour. For surface integrity of the composite Al-MMC surface, particle pull-out cannot be tolerated.

The dry sliding conditions that would best simulate reciprocating engine components would have high sliding velocities and relatively low normal contact forces. High speed sliding conditions have been extensively studied, in part due to the amiable combination of high thermal conductivity and high strength exhibited by Al-MMCs, making this class of material excellent for applications such as brake rotors or cylinder liners. Tremendous potential also exists for aluminum metal matrix composites in tribological applications such as gears, bearings, or pressure plates, at much greater compressive stresses and lower sliding velocities. However, the "plasticity dominated" or cold wear sliding conditions of these applications have not been systematically studied, and consequently little development has been made in use of Al-MMCs in these areas. A considerable range of sliding conditions has been investigated, allowing for wear performance predictions to be made for some of stated potential applications. Some of the prolific authors involved in the study of wear properties of aluminum composites are Venkataraman and Sundararajan, Li and Tandon, Alpas and Zhang, Wang and Rack, Harris and McColl, to name a few.

In any case, the plastic deformation that can be tolerated must be kept at a minimum for adequate component life. This being known, great improvements in wear resistance can be made in conjunction with the formation of a "tribolayer" or a distinct surface microstructure formed by mechanical, physical, and chemical interactions, that has been established to occur during the process of wear of *some* Al-MMCs. This study is focused of the conditions that allow a tribolayer or MML to form for any discontinuously reinforced aluminum metal matrix composite. Some variables are examined as they related to transfer, mixing and wear for an Al-Si-20%SiC composite. With this composite it has been already established that excellent wear resistance can be obtained. For this and other aluminum metal matrix composites, the study of mechanically mixed layers that allot much of the wear resistance is necessary to establish if further improvements in wear behaviour are made based on incorporating this phenomenon. Better wear resistance for aluminum metal matrix composites requires that the surface tribolayer is stable, therefore this investigation focuses on some of the variables such as elemental transfer and mixing that allow this layer to be regenerated.

1.12 GOALS OF STUDY

GOAL 1: REVIEW WEAR OF AL-MMCS

To accumulate published research specifically on the wear behaviour of Al-MMC under plasticity dominated, "cold" wear sliding conditions. Clear trends in literature need to be established to allow for decisions to be made of composite morphology including the right size, shape, volume fraction, morphology and type of reinforcement, choice of alloy

and heat treatment, as well as the choice of counterface for the sliding conditions. Focus is made on the use of Al-Si composites with SiC reinforcement.

GOAL 2: ESTABLISH WEAR RESISTANCE OF AL-MMC

Examine if an improvement in wear resistance occurs through use of a SiC reinforced Al-Si-MMC as compared to using an unreinforced binary Al-Si alloy. To allow for comparison, dry sliding wear rates are determined for a HP Al, an Al-Si hypoeutectic alloy and an Al-Si-20vol%SiC_p metal matrix composite. Improvements in the reinforced aluminum over the monolithic alloy need to be observed before tribological application of the composite material is justified. Improvement in the wear resistance cannot come at the cost of increased counterface abrasive wear, which negates the wear resistance of the composite when considering the tribological pair. All three aluminum materials are tested against 52100 bearing steel, known to make a good choice for a counterface material from previous work [90]. Change in mass transfer to the counterface, adhesion and abrasion wear occur through the introduction of the brittle Si phase and secondly through the addition of the SiC reinforcement. Focus is on the wear mechanisms which are limiting the wear performance of the tribological use of the tested aluminum materials.

GOAL 3: EXAMINE THE EFFECT OF COUNTERFACE

Establish a better understanding of how the counterface affects SiC interactions, Al-SiC adhesion and resistance to reinforcement abrasion. Steels, the most popular counterface materials, are examined in terms of the influence of hardness and composition. Three counterface steel compositions, 316 stainless, 440C, and 52100 bearing steel are

tested against A356 Al-20% SiC to compare wear, elemental transfer, and mechanical mixing behaviour. Mechanical mixing of iron oxides has been identified as a common occurrence, however if the same mixing behaviour exists with a chromium oxide for stainless steels has not been established. The effect of change in hardness for the same steel composition is also examined. 52100 bearing steels were annealed to allow testing over a hardness range, allowing examination of hardness as a variable on transfer, mixing and wear behaviour, independent of steel composition. Other counterface materials were tested to examine wear and mixing behaviour: Al-6061, which has a lower hardness than the composite, K-Monel which allows for elemental mixing of Ni and Cu, and Al_2O_3 and Si_3N_4 ceramics with very high hardness. The ceramic counterfaces do not possess metallic compatibility but can vary based upon friction and mixing behaviour, as well as capability of elastic interaction with the SiC reinforcement.

GOAL 4: EXAMINE THE EFFECT A DIFFERENT CONTACT GEOMETRY

Unlubricated reciprocal, ball on block, testing is chosen to examine its effect on the reprocessing of debris between surfaces in contact and to help further understand how contact geometry affects mechanical mixing. Debris that remains in the interface is expected to contribute to mechanical mixing caused by dry sliding contact. For mixing to occur of the debris once it is produced, it must not be ejected from between the contact surfaces. How debris was generated is the origin to the debris particle dynamics that follow, which alone is very particular to the contact geometry of the sliding system.

The plastic deformation experienced during reciprocal testing can prevent cumulative strain hardening in the sliding direction that occurs for unidirectional sliding.

Cumulative strain behaviour has been identified as determining the subsurface depth at which shear instability is most likely to occur. The effect of reciprocal sliding induced strain on shear instability, the resulting adhesive/delamination wear, and the ability of the SiC to reinforce the subsurface has yet to be compared to behaviour under unidirectional strain for the composite material.

GOAL 5: EXAMINE VARIABLES FOR MECHANICAL MIXING

During dry sliding wear, extrinsic factors need to be examined (sliding speed, applied pressure, debris reprocessing, counterface) as they relate specifically to mechanically mixed layer (MML) formation, allowing its wear resistance to be more fundamentally understood. Effort is taken to understand the transfer of elements and counterface material that occurs in forming mechanically mixed layers between sliding surfaces by using different counterface materials in dry sliding contact against composite aluminum.

1.13 LONG TERM GOALS FOR WEAR STUDIES

Three broad goals can be stated for improving acceptance and increasing confidence in the application of these aluminum composites in tribological applications.

A) Understand the potential for increased abrasion due to the reinforcement, especially under lubricated conditions. The important variables are the percent

volume of reinforcement, size of reinforcement and the choice of the counterface. The role of hard ceramic particles in the interface is also very important.

B) Understand the conditions that cause delamination wear. The most important variables are load and velocity, microstructure of the composite and the choice of counterface. Excessive delamination and adhesion behaviour results in impractical wear rates to justify use of an Al-MMC.

C) Determine if the formation of a mechanically mixed layer as a wear surface can provide a stable condition for increased wear resistance. This requires knowing the conditions under which a MML is expected to form, the reliability of a MML for a long sliding distance, and if the extent of deformation that is required can be accommodated without loss of service tolerances.

CHAPTER 2 LITERATURE REVIEW

2.11 PROPERTIES OF ALUMINUM AS THEY RELATE TO WEAR

Non-transition metals such as Al, Zn, Cu, Ag tend to have very low natural hardness for the pure metal. High ductility of the FCC structures causes these metals to be susceptible to high amounts of plastic deformation during sliding contact, often preventing the formation of a coherent, protective surface oxide layer. Bowden [1] made the analogy that sliding of soft aluminum covered by Al_2O_3 likened to sliding on mud covered with a thin layer of ice. On the other hand, transition metals such as Cr, Mn, Fe, Ni, Co, Mo have higher densities, higher natural hardness, and in comparison, generally better wear resistances. A comparison of natural hardness values obtained for these materials is listed in Table 2.1.

Pure element	HV [kgF/mm^2]	Density [g/cm^3]
Al	**17**	**2.7**
Zn	26	7.14
Cu	37	8.92
Ag	26	10.49
Cr	108	7.14
Fe	62	7.87
Ni	65	8.91
Mo	155	10.28

Table 2.1 List of pure element hardness values [4]

A lot of importance is placed on hardness as experience has shown this to be the most influential mechanical property in predicting wear [2]. Rabinowicz [3] predicted that two thirds of all wear damage is by either adhesion (which includes delamination and low-cycle fatigue) or abrasion mechanisms. Both of these dominant wear mechanisms have been found to correlate well with the original Holm-Archard equation [1], which states that the wear rate is inversely proportional to the hardness of the softest material paired. The second independent mechanical strength parameter that may contribute to wear resistance is toughness, although this is not always significant:

> ...if a comparison is made of the wear resistance of two materials of the same hardness, but widely different toughness, it seems instinctive that the tougher one should wear much less, while (the Holm-Archard equation based on hardness alone) would give the same wear rates. In practice adhesive wear seems quite independent of strain; in fact the use of anti-wear coatings of very hard materials with limited elongations, of which hard plated chromium is the prime example, is feasible only because hardness rather than toughness determines adhesive wear resistance [3]

Pure aluminum has the lowest natural hardness of the metals listed in Table 2.1. Therefore aluminum alloys and composites will have an inherent limitation from the intrinsic hardness of the aluminum [5] for wear applications.

Of the metals listed in Table 2.1, the most substantial amount of wear research has been performed on steels, with aluminum alloys generally considered to have comparably worse wear resistant properties. For aluminum alloys to supercede steels in tribological applications, plastic deformation must be limited, which has been achieved through the use of high silicon Al-Si alloys and hard reinforcement phases for aluminum composites. The addition of these hard ceramic phases limits metallic wear to the aluminum fraction [6]. Since the Al matrix phase is always present, it is desirable to achieve high deformation

resistance of these inherently natured plastic "zones" in the binary or composite microstructures to further improve overall wear. This must be done without large delamination or adhesive wear occurring, as this form of wear damage is generally more severe than abrasive wear. With increased reinforcement phase toughness becomes increasingly more important due to the high damage experienced with particle pullout and particle fracture. Toughness is most often reduced when trying to reduce ductility through increased reinforcement. There is also increased risk of cracks linking in the subsurface at higher volume fractions and therefore higher danger of shear instabilities and adhesive fracture through low-cycle fatigue. Shear instability and delamination is often further promoted by strain localization at the interface of hard and soft phases when forced to simultaneously deform [7]. In other words, toughness of the microstructure has become more relevant to wear resistance for aluminum composites compared to the dominant role in which hardness had be given in predicting wear for monolithic alloys. A recent study by Straffelini [8] has demonstrated that the hardness of a composite aluminum could be increased by using a large reinforcement size and a high volume fraction, however this resulted in a much higher wear rate than a softer composite, due to more extensive particle fracture and pull-out for the less damage tolerant microstructure.

Researchers have frequently observed that aluminum when mated against various counterface materials experiences wear by significant transfer across the wearing interface, i.e. adhesion [9]. Adhesion of the aluminum matrix to the counterface material results in large delaminations of the aluminum surface and can be considered a root cause of poor wear performance [10,13,14]. For this reason, wear performance of aluminum is not only

affected by intrinsic hardness and toughness properties but also on the contribution of the counterface material in promoting adhesive or abrasive wear.

2.12 METHODOLOGY FOR IMPROVING WEAR RESISTANCE

(I) WEAR REGIMES

Wear regimes essentially separate the wear performance of a metal into two groups of sliding conditions: sliding where a mild rate of wear occurs and sliding where a severe wear rate is expected. A transition between what is mild wear and what is severe wear must be defined. The transition is most often defined by a rapid rise in wear rate as a sliding variable is increased beyond a particular point, for example a critical applied pressure and/or a critical sliding velocity. The transition between wear regimes can also be correlated with a critical sliding distance or a critical surface temperature; however these two transitions are most often dependant on and are derivable from the primary sliding variables of applied pressure and sliding speed.

When defining a transition between wear regimes, it is essential to investigate the transition in wear mechanisms that has occurred. Change in the wear mechanism is an intrinsic transition, governed by any extrinsic variable, including applied pressure, sliding speed, distance, or temperature. Studies that refer to mild and severe wear transitions that are not correlated to a change in wear mechanism or specific wear rate are not particularly instructive. Transitions between wear regimes are therefore best defined chronologically, starting with the definition of what can be considered a mild wear rate for that particular alloy, and ending with defining the intrinsic cause of mild/severe wear transitions based on

the material properties, Figure 2.1. Understanding the reason for the change in the wear mechanisms that occur for a transition between mild and severe wear, is fundamental in improving and insuring wear performance.

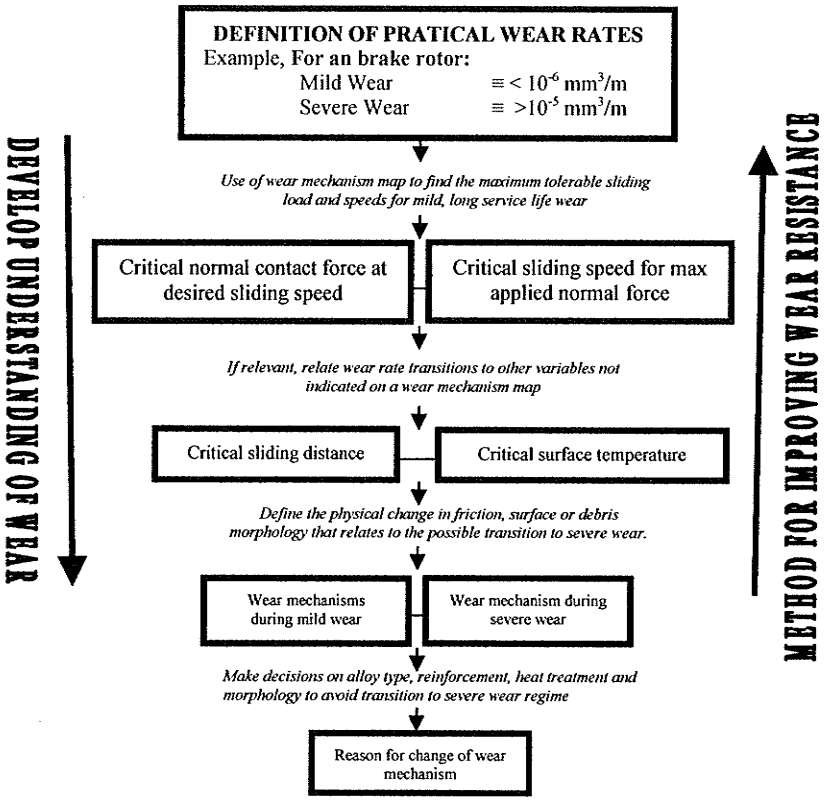

Figure 2.1 Proposed organization for wear study. Top to bottom: increased understanding for transitions in wear behaviour. Bottom to top: using collected data to make changes to the alloy to improve its wear resistance.

Finding a critical normal contact force that can cause a severe rise in the wear rate, the starting point of Figure 2.1, does not answer the question as to why this has occurred. Knowing that the severe rise in wear rate was a result of surface delaminations does provide a better overall description although still limited in usefulness. Relating the change to delamination wear to a microstructural feature such as particle/matrix interface provides

the most significant insight into the cause of severe wear from which changes to the alloy can be made in an attempt to improve the wear performance. The systematic approach, shown in Figure 2.1, is required to progress from simply collecting data for different aluminum composite materials, to specifically optimizing an aluminum metal matrix composites (Al-MMCs) for improved wear resistance. This can be difficult and requires the cumulative effort of many researchers. If no attempts are to be made in improving the inherent wear resistance of the aluminum alloy or composite for the particular sliding system, the first step, defining the transition points for the chosen aluminum composite and avoiding the operating conditions that exceed these limits, may prove to be the more practical design approach. A summary of critical loads and sliding velocities, has recently been made possible by the development and use of wear mechanism maps for aluminum alloys [15,16,17], and Al-MMCs [12,18].

Due to wear transitions, wear rates often do not increase monotonically. In Figure 2.6, representing the results obtained by Alpas and Zhang for the wear of Al composites reinforced with SiC or Al_2O_3, a large wear rate transition was observed over a narrow range of applied loads. An increase in volume fraction of reinforcement resulted in a higher normal load at which this I/II (mild/severe) transition occurred. Below the transition load, the composite with coarse SiC particles demonstrated superior wear resistance (by a lower wear rate) compared to the composite reinforced with fine SiC [11].

The separation between mild and severe wear classifications can be observed here. Regime I, mild wear, was associated with the transfer of an iron oxide layer and a low wear rate for the composite aluminums tested ($<.10^{-5}mm^3/m$). Although SiC particle protrusions

can be produced by careful polishing, however a polished surface was not required to reduce wear rates by iron oxide transfer at the low contact forces in regime I (≈2-20N).

Regime II, severe wear, was defined after the transition load, and related to a much higher wear rate of the composite (> $10^{-3}mm^3/m$). The transition load was consistent with a rapid rise in particle fracture. Comminution of SiC particles was indicative that sliding conditions in regime II (≈20-200N).

Some mechanical mixing of the Al-matrix and reinforcement was observed for the range of applied loads in regime II. However, low amounts of iron and iron oxides were mixed into the composite surface. Since only a small amount of iron transfer was detected, protection of the MMC surface by an iron transfer layer was no longer occurring at normal contact forces past regime I. No I/II transition was observed for the unreinforced aluminum alloy. In regime II wear rates between the unreinforced and composite aluminum materials were similar.

A third wear regime (III), characterized by very severe wear, was defined by another rapid rise in the wear rate, and was correlated to a critical surface temperature inducing severe delaminations (≈340°C). Iron and iron oxides were mechanically mixed on the surface and in the deformed subsurface, which was characterized by extensive reinforcement fracture and counterface transfer. The depth of deformation was up to 10x greater than in regime II. Galling or large delamination wear occurred in response to the extensive deformation, causing the surface to rapidly deteriorate.

As can be seen by this breakdown, the reason for changes in wear regimes were related to changes in wear mechanisms. First the loss of the iron oxide protection layer (I/II), then extensive particle fracture (II), then finally sliding temperature induced

delaminations. By defining the wear regimes, the wear mechanisms, and reasons for the change in wear behaviour, the work by Alpas and Zhang [11] has been fundamental to the understanding the wear of aluminum metal matrix composites and has been quoted extensively in literature. The transition to severe wear was found to be primarily due to particle fracture. With this understanding, altering the reinforcement variables to prevent fracture can be focused upon as the principal method of further improving wear resistance if sufficiently low load is the sliding condition..

(II) WEAR MECHANISMS

Wear mechanisms describe the material damage that is occurring in the respective wear regime. Defining the cause of wear in a mild wear regime appears trivial if only one source of material damage or only one wear mechanism is occurring. However, wear that is shown to simultaneously involve several sources of material damage, cannot be simply classified in terms of one wear mechanism. This is most often the case for wear of Al-MMCs, where during sliding simultaneous and competitive wear mechanisms can include adhesive transfer, abrasion, crack propagation and fracture, surface delamination, plastic deformation causing smearing or extrusion, brittle fracture of the reinforcement, high rates of oxidation, oxide spalling, ploughing of debris, development of anisotropic properties and refinement of the microstructure. A summary of wear mechanisms is given in Figure 2.2.

In this section the most important categories of wear mechanisms are related to the wear of particle reinforced aluminum composites, namely plastic deformation, adhesion (delamination wear), and abrasion.

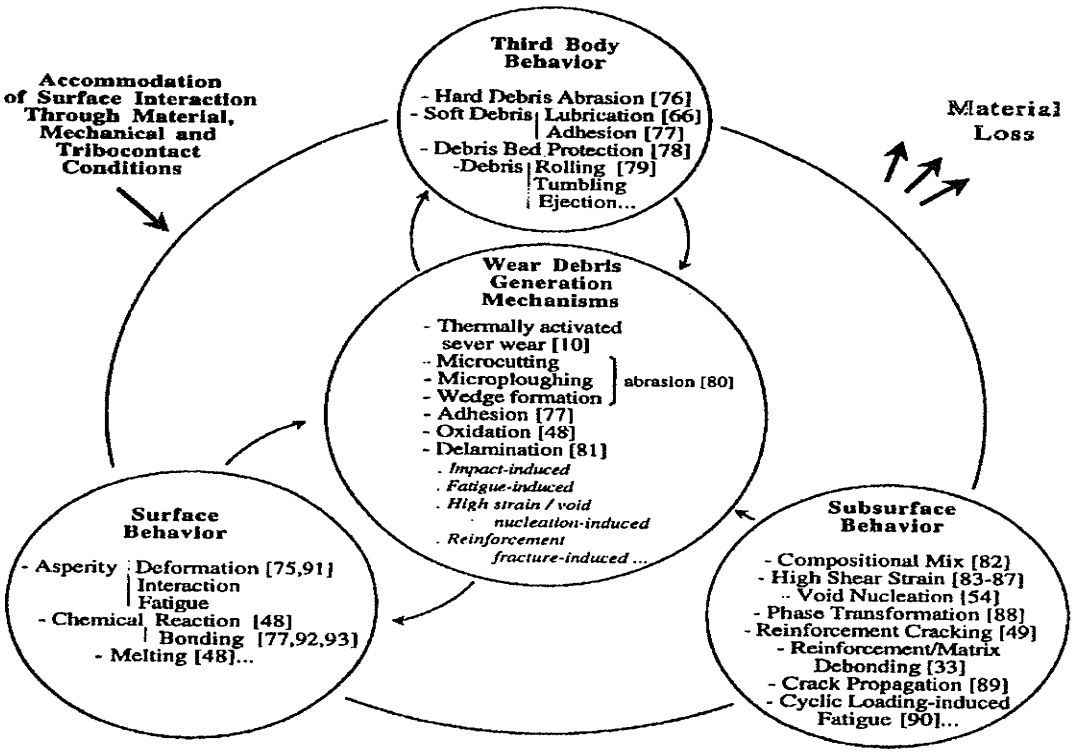

Figure 2.2 Organizational chart for defining wear mechanisms. The generation of debris, through surface, subsurface, and third-body behaviour is placed as the central focus of wear and wear transitions. Sannino and Rack [20], 1995.

To make sense of this, the relative importance of the rival wear mechanisms must be identified. For most practical purposes where the goal is to maintain design tolerances for a maximum service life, the most critical wear mechanism is easily identified as causing the greatest material loss. More eloquently stated:

> ...for steady-state wear, the relative amount by which a mechanism contributes to the total wear is approximately proportional to the area fraction occupied by the scars of that mechanism. Thus, in combating the wear of devices with rival mechanisms operating, efforts should be focused on the mechanism that damages the largest surface area fraction and not on the mechanism that produces the largest individual scars [30]

With this understanding, counterface adhesion and shear instabilities that result in large surface delaminations are the most hazardous wear mechanisms for aluminum alloys and aluminum composites as demonstrated by wear rates in Regime III [11]. A risk of using an Al-MMC that introduces hard particles into the wear system is increased abrasion of both surfaces, yet the risk of an increase in this wear mechanism may be acceptable if the additional reinforcement phase is preventing surface spalling and large adhesive-delamination wear.

When dry sliding contact is unavoidable (as is the case for most lubricated conditions!), researchers have noted that it is desirable to have the aluminum or aluminum composite to come into contact with the counterface under conditions that produce fine particle debris [9,15]. In other words, wear by fine particle detachment as the dominating wear mechanism causes the most gracious surface damage as compared to other wear mechanisms such as adhesion transfer and delamination fracture.

(A) *PLASTIC DEFORMATION*

Aluminum, with a close packed FCC structure and high stacking fault energy, retains high ductility over its useable temperature range, with the resistance to continued plastic deformation through work hardening much lower than steel materials. Large plastic strains have been observed to be generated in the subsurface under dry sliding conditions for short sliding distances and to significant depths from the surface. For example, after a sliding distance of just 30 m plastic deformation was observed to extend 40μm below the surface for an applied pressure of approximately 0.7 MPa [27]. Exhaustion of the strain hardening capacity was observed at up to 5x equivalent strain being experienced in the

matrix for a cast, T6-aged, A356Al-Si alloy [27]. When strain hardening capacity was surpassed, either work softening occurred due to void formation, or fracture occurs. In general, work softening involves the overload of the dislocation mechanisms responsible for strengthening the aluminum and preventing it from plastically deforming [10]. Excessive plastic deformation is an obstacle for long term wear performance of ductile metals such as most aluminum alloys and MMC. Local instabilities are difficult to avoid in heterogeneous microstructures that experience accumulation of large plastic strains. Local instabilities result in favourable conditions in the subsurface for large delaminations to occur, producing debris which is frequently in the order of 1-3 mm in size for aluminum alloys [13]. Steels, in comparison, maintain a shallower subsurface depth of deformation due to higher rates of work hardening [40]. While delamination wear can result in severe damage due to large surface fractures for steels and irons, the scale of the delaminations for aluminum materials are often much greater, therefore causing the wear surface to rapidly loose integrity. Needless to say, reduction in subsurface plastic deformation must be avoided to avoid unacceptable wear rates controlled by delaminations, especially in the presence of second phase particles.

The formation of a mechanically mixed layer (MML) with high hardness has been found to reduce wear by reduced matrix plastic deformation [8,33]. Li and Tandon [25,35] observed a transition from a linear wear rate vs. applied normal force to a much lower than expected rate of wear at high loads capable of significant plastic deformation due to the phenomenon of MML formation. When a MML was able to form, initially requiring high plastic deformation, the wear mechanism appeared to be dominated by smaller delaminations of the MML, not from subsurface cracks in the highly deformed matrix [33].

(B) ADHESIVE WEAR

Adhesive wear is loosely defined by transfer of material, metallic or non-metallic, from one surface to another during contact. The mechanisms of adhesion can be modeled as nearest neighbor, atomic bonding at the free surface [50] as well as by localized welding where the bulk of the contact material remains in the solid phase [51]. Mechanical interlocking is another mechanism which has gained in importance when considering composite materials where hard particles are found between contacting surfaces. Mechanical interlocking is caused by a relatively hard protrusion becoming "pressed in" to a softer surface to an extent that the surface provides enough resistance to shear off the hard protrusion from its original surface, i.e. mass transfer between surfaces occurs [76]. This mechanism has been observed to also cause mixing and transfer between two metals of different hardness [19]. This is also a mechanism of reinforcement particle pull-out by a metallic counterface.

The pressure and frictional heat due to plastic deformation between asperities must be high enough to bond surfaces in the classical adhesion theory by Rabinowicz [1]. Mechanical interlocking assumes no atomic bonding mechanism, instead it depends entirely upon the relative hardness between surfaces and resistance of asperity contacts to fracture. The potential for increased adhesion resistance can be seen for either case with increased hardness, or increased resistance to plastic deformation, however, improving wear resistance by increasing the hardness of one material is insufficient as it is the relative hardness between surfaces that will determine if adhesive transfer will occur. Considering the hardness ratio of the material pair, conditions where an increase in hardness would not increase adhesive wear resistance are:

a) When the softer Al matrix hardness is increased, this causes an unacceptable decrease in fracture toughness. When mated against a much harder steel counterface, more adhesion-delamination wear could be promoted – increasing wear by this mechanism [9].

b) Increasing the hardness of the harder material of the pair (for example using a ceramic instead of steel as the counterface material) may facilitate greater plastic deformation of the softer material (Al-MMC) causing extrusion of the surface that can result in gross material transfer and severe wear [46].

c) A small increase in hardness (for example from 70-110 HV for T6 aging of an A356-20% composite) would have little consequence when hard particles such as oxides and reinforcement phase at the interface dominate the plastic deformation and adhesion transfer between surfaces [33].

Despite these exceptions, wear by adhesion can most often be related to the hardness of the softer material in contact. The Archard equation states that the wear resistance is inversely proportional to hardness of the softest material, and provides an excellent starting point to predict wear by simply relating lower wear rates to reduced plastic deformation.

Drastic contradictions have been established that show that wear cannot simply be related to hardness. For example, major changes in wear rates due to the "compatibility" of metals in contact, subsurface controlled delamination and fatigue mechanisms, and mechanical mixing obscuring a simple understanding of hardness and work hardening at

the interface. Therefore, predictions based on hardness may or may not compare to experimental results and should only be used with the principal understanding that hardness, as a variable, offers only a partial insight into the subsequent wear of sliding surfaces. Even so, the original Holm-Archard equation has been shown to satisfactorily estimate the wear rate to ductile metal pairs [3]:

$$W = \frac{K \cdot d \cdot P}{3H}$$

K = wear coefficient d = sliding distance P = applied normal force
H = indentation hardness

K is a dimensionless experimentally determined constant for the soft material of the wear couple. The statement that wear is inversely proportional to hardness has been shown to have good correlation compared to other mechanical property indicators such as ductility and ultimate tensile strength [47]. In addition, many of the mechanical properties including yield stress, proportional limit, resilience, and yield strain can be related to hardness [3]. Toughness, on the other hand, cannot be related to hardness and as noted earlier, cannot be disregarded because of the significant control over adhesive wear it can have for Al-MMCs.

(C) DELAMINATION WEAR

A delamination occurs due to instability in the presence of a flaw, or more appropriately, any inhomogeneity that may cause the matrix to fracture under strain. The sources of instability can include second phase particles, composite reinforcement, porosity, or inclusions. Cyclic surface contact can accumulate plastic deformation in small

increments which can result in void formation; from which crack propagation ensues to generate delaminated wear particles from the surface.

The applied contact pressure and fracture toughness factor into the extent of crack propagation before an instability results in surface delamination. Oxygen assisted flaking [86] can be described as a delamination wear mechanism in the mild wear regime of Al-MMCs that experience iron oxide transfer layers. Adhesion-induced tribofracture [20] is an excellent wear mechanism description of the delaminations that occur when significant transfer of the Al-MMC was observed to the harder counterface at higher loads [14].

The significance of delamination theory is that metallurgical structure and sub-surface deformation have rate controlling effects on wear. In other words, material lost from the surface is at a rate determined by instabilities nucleated in the metal matrix. This can have greater relevance on the wear rate than the hardness of a material due to the bulk of the delaminated particle not experiencing direct plastic deformation before it is fractured off the surface, resulting in wear independent of surface plastic deformation resistance.

Delamination theory proposes that the production of surface delaminations is the fundamental outcome of wear by adhesion, fretting, fatigue and oxide layer fracture mechanisms. Consequently, the magnitude of what is delamination debris can change drastically. For aluminum alloys, the dominant range of large delamination debris can be revealed in wear mechanism maps, as originally proposed by Antoniou and Subramanian [15]. Sliding conditions that cause "melt wear" of aluminum alloys can be considered to establish upper boundaries on the velocity and normal contact pressures that delamination mechanisms of wear can be used to describe the wear process. On the other end of the spectrum, delamination theory does not appear to apply to sliding conditions that cause the

formation of fine equiaxed particles, which have been observed in literature to arise more from mechanisms of ploughing, abrasion and/or microcutting [21,22,23,24]. The wear mechanism map proposed by Antoniou and Subramanian in shown in Figure 4.15.

An intermediation outcome, wear debris of compacted plates of equiaxed particles, has been related to delamination of a mechanically mixed surface layer for aluminum alloys [25,52] and Al-composites [33]. Compacted plates of equiaxed particle debris from the mechanically mixed layer are produced and have been related to subsurface shear instabilities originating within the MML.

For all sliding conditions that cause aluminum alloys to experience some form of delamination wear, the depth and extent of plastic deformation is expected to be reduced as the coefficient of friction is reduced [26]. This result can correlate well with a lower wear rate, Figure 2.3. Acting as an exception to this trend, the formation of a mechanically mixed layer offers the potential for a relatively low wear rate despite the existence of a high coefficient of friction.

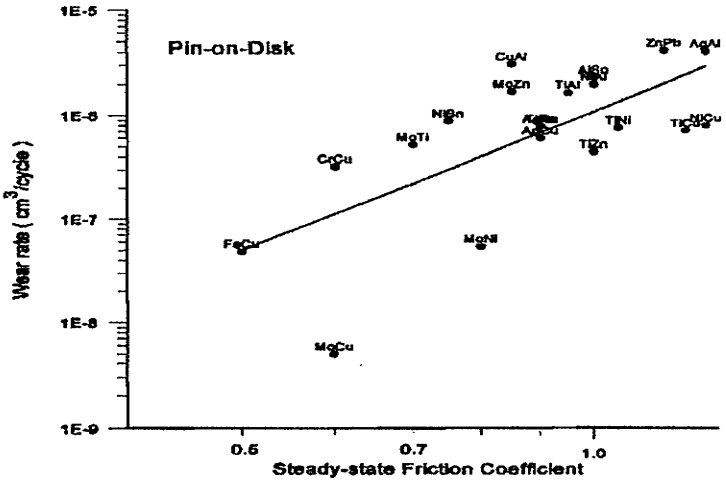

Figure 2.3 General trend of increased wear rate for metal pairs which exhibited high steady state friction, Hwang *et al.* [47], 1999

(D) DELAMINATION MODELS

Delamination models help to define the depth at which cracks initiate and propagate in relation to microstructure [27]. For ductile metals such as aluminum, models based on elastic fracture mechanics have limited suitability or relevency in relation to the high levels of plastic deformation observed [29]. Accordingly, delamination models for ductile materials during wear have been based upon:

1) A critical shear strain that initiates subsurface cracking and softening [74]

2) Damage accumulation and void growth at second phase particles causing ductile fracture [28,43]

3) A local region with lower flow strength than the surrounding matrix and critical subsurface stress intensity [26]

From the shear instability model proposed by Rosenfield [26], delamination can be predicted when the deformation resistance of a small subsurface region is less than the shear strength of the surrounding material. This causes fracture to initiate in that region. In terms of stress intensities, the stress intensity due to the sliding contact exceeds the sustainable stress intensity of the local subsurface region, due to a particular flaw, crack, or void that exists at that depth. In the subsurface region where instability is initiated, the local maximum shear strength is exceeded and a crack rapidly propagates, producing a surface delamination.

Rosenfield derived the shear stress intensity in the subsurface at a flaw due to a surface distributed load to be:

$$K_{II} = \frac{2S_o a^{1/2}}{\pi^{1/2}} H(k, p, \mu, n)$$

(Eqn. 1)

Where H(k',*p*, μ, n) is a geometric integral. This integral, given in Table 2.3, defines the dimensions of the flaw in relation to the distance from the surface contact, H=*f*(k,*p*). It also defines the dimensions of the crack in relation to the magnitude of applied contact force, H=*f*(μ,*n*).

a	One half of the crack length (m)
A_r	Real area of contact – sum of asperities (m^2)
A_n	Nominal (apparent) area of contact (m^2)
B, C	Constants determined by linear regression from strain profile
α_t	Constant used for Tabor's junction model, α_t = 12 experimentally determined for steels
F	Distributed force (N)
x_o	Distance in front of applied load where center of crack located (m)
k	Normalized offset of the crack from the applied load with respect to the crack size = x_o/a
k'	Center of crack tip related to leading edge of a distributed force
y	Depth of crack from surface (surface corresponds to y = 0)
y	Depth below the surface (m)
ε(y)	Subsurface strain@ y
ε_{sat}	Critical saturation strain for work hardening
p	Normalized depth of the crack from the surface with respect to the crack size = y/a
N	Number of individual asperities
n	Parameter related the to the contact width to distributed force, normalized to crack length $F = 2 \cdot n \cdot a \cdot S_o$ or $n = F/2 \cdot S_o \cdot a$ (m)
H	Geometric dependant integral – defines stress intensity based upon the location, size, and orientation of the crack with respect to the applied surface force ($N \cdot m^{3/2}$)
H_o	Room temperature surface hardness – equivalent to surface flow strength, S_o
$H_o(y)$	Room temperature hardness at depth of y (N/m^2)
I	Geometric dependant integral – defines stress intensity due to point surface contact load ($N \cdot m^{3/2}$)
θ	Shear angle (determined from microstructural markers)
r_a	Contact radius of an asperity for an applied normal contact force and frictional shear stress (m)
r_o	Radius of pin
S_o	The flow strength of the material at the surface (N/m^2)
$S_f(y)$	The subsurface flow stress of the plastically deformed material (N/m^2)
S_{sat}	Saturation stress for maximum strain hardening (N/m^2)
μ	Coefficient of friction

Table 2.2 Symbols, definitions and units of material and geometrical wear parameters

Note that a distributed load is assumed for the surface, however, approximations of the asperity size for range of hardness achieved by Al and Al-MMC materials indicate that a point force analysis of the stress distribution, I(k,p,μ) could be used without loss of accuracy [26].

The a maximum stress intensity that can be inherently resisted by the plastically deformed subsurface can be stated as:

$$K_c = S_f \cdot \sqrt{\pi a} \qquad \text{(Eqn. 2)}$$

Where S_f is the material shear strength at a particular depth.

Shear instabilities leading to delamination wear are predicted to occur when the applied stress intensity at a particular subsurface depth (defined by the H(k',p, μ, n) integral) exceeds the sustainable stress intensity that can be resisted by the plastically deformed metal at that depth. This can be expressed as,

$$K_{II} = K_c$$

Or for any stress intensity K_{II} greater than K_c the delamination model will predict shear instability to occur. Equating the applied stress intensity, K_{II}, with the maximum supportable material stress intensity, K_c, (Eqns 1 & 2) results in the relation,

$$H(k, p, \mu, n) \geq \frac{S_f \pi^2}{2S_o}$$

Observation of this analysis indicates the importance of defining the subsurface strain hardening behaviour of a metal in sliding contact. This can be found by:

$$\frac{\partial S_f}{\partial \varepsilon} \cdot \frac{\partial \varepsilon}{\partial z} = \frac{\partial S_f}{\partial z}$$

where the strain as a function of depth can be determined by markers as in Figure 2.4a, while the strain hardening can be found by microhardness testing at different depths, Figure 2.4b. Subsurface strain hardening behaviour is shown for an aluminum alloy and an Al-MMC where a surface MML has formed. It can be noted that a drop in shear strength, causing a low K_c occurs once the strain hardening capacity of the subsurface has been surpassed, Figure 2.4.

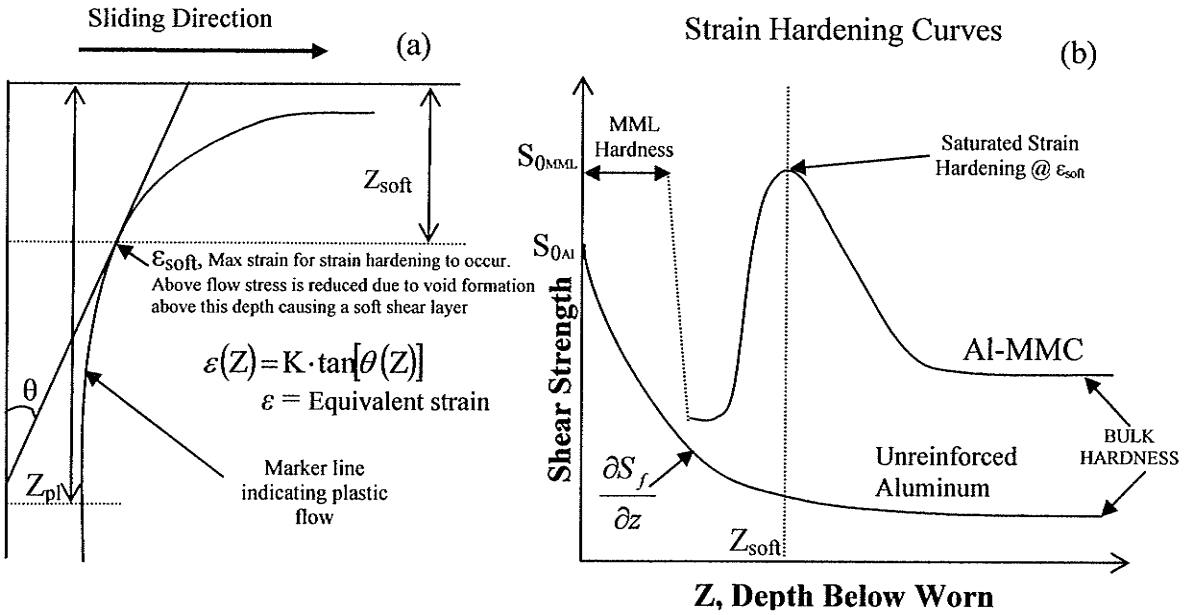

Figure 2.4 (a) Equivalent strain hardening analysis for subsurface strains observed under unidirectional sliding. (b) Variation in th strain hardening subsurface behaviour for a pure aluminum and an Al-MMC that forms a surface MML. The resulting shear strength at any depth will determine the prospect of delamination wear. Adapted from Venkataraman and Sundararajan [33], 2000

As expected, shear strength can vary significantly based on the extent of plastic deformation in the subsurface. It is desireable to define S_f at the observed delamination depth. Zhang and Alpas [27] noted that the strain hardening behaviour of the composite can be defined by the maximum strain hardening capacity and the rate of strain hardening, Table 2.3. Delaminations can occur in the subsurface at continually greater depths as the depth of subsurface deformation increases, Figure 2.13.

Some important guidelines for prediciting and avoiding delamination wear emphasized by Rosenfield [26] are:

1) Stress intensity and thus the driving force for delamination wear increases with increased friction

2) A threshold applied load exists for instability to occur. For greater applied loads (in relation to this threshold) shear instability is possible at various depths beneath the surface.

Modelling of the magnitude of point loads introduces significant uncertainty into predicting delamination wear, the extent and depth that the stress intensity extends and therefore the depth at which delamination will result. Using a distributed load based upon the nominal contact area is not correct except when the applied load is very high, Figure 2.5. The summation of asperity contacts, consisting of the real area of contact, Ar, in most cases is a small fraction of the apparent contact area, An, resulting in point contact pressures that are significantly higher than the perception given by much larger visibile contact surfaces.

Description	Equation	Ref
Equivalent plastic strain	$\varepsilon = \frac{\sqrt{3}}{3}\tan\theta$	32
Strain as a function of depth below the surface	$\varepsilon = C \cdot e^{(-B \cdot y)}$	32
Flow stress as a function of the strain @ y rel. to maximum saturation strain	$S_f = S_{sat} - (S_{sat} - S_o) \cdot e^{\left(\frac{-\varepsilon}{\varepsilon_{sat}}\right)}$	27
Work hardening rate	$\frac{\partial S_f}{\partial \varepsilon} = \frac{S_{sat}}{\varepsilon_{sat}}\left(1 - \frac{S_f}{S_{sat}}\right)$	27
Estimation of flow stress	$S_f = \frac{1}{3}H(y)$	27
Approximation of surface flow strength, S_o	$S_o = \frac{1}{3}H(y=0)$	26
Mean pressure on an asperity (Local hardness)	$\frac{F}{A_r} = S_o$	44
Number of asperities	$N = \left(\frac{r_a}{r_o}\right)^2 \frac{F}{A_n \cdot S_o}\left(1 - \frac{F}{A_n \cdot S_o}\right) + 1$	44
Stress intensity, point force, I	$I(k,p,\mu) = \int_0^{\pi}(1+\cos\psi)\left[\frac{p(k+\cos\psi)\{p+\mu(k+\cos\psi)\}}{\{(k=\cos\psi)^2+p^2\}^2}\right]d\psi$	26
Stress intensity, distributed force, H	$H(k',p,\mu,n) = \int_0^{2n}\int_0^{\pi}(1+\cos\psi)\left[\frac{p(k+\cos\psi)\{p+\mu(k+\cos\psi)\}}{\{(k=\cos\psi)^2+p^2\}^2}\right]d\psi \cdot dz$	26
Approximation of real contact area	$A_r = \frac{F}{H_o}\cdot\sqrt{(1+\alpha_t \cdot \mu^2)}$	44
Asperity contact radius for circular pin contact	$r_a = \sqrt{\frac{A_r}{A_n}} \cdot r_o \cdot N$	44

Table 2.3 Useful equations in estimating surface contact, subsurface strain, and delamination wear.

Surface roughness and surface waviness contribute to a large variation in asperity sizes and stress concentrations [1,36]. To quantify "small" for a steel ball sliding over a machined bronze surface, nominal contact pressures less than 10 MPa were observed to cause Ar/An ratios less than 2%. At a very high applied pressure of 65 MPa, Ar/An reached a maximum of 12% when considering elastic-plastic deformation of the asperities [36].

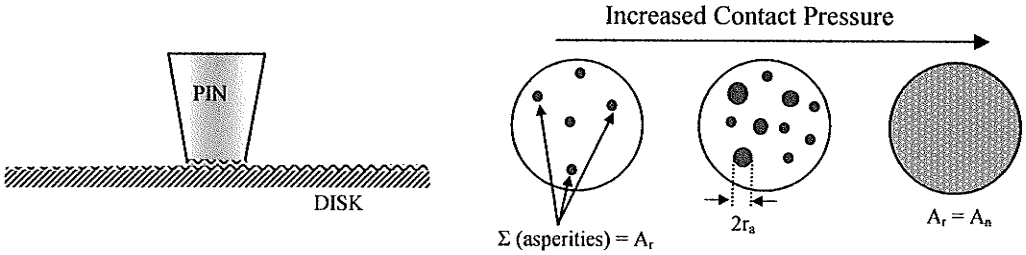

Figure 2.5 Distribution of asperity contacts. For intermediate pressures the number of contacts points reaches a maximum, with size distribution dependant on surface roughness. At low loads the real contact area is a very small fraction of the nominal contact area due to the asperities remaining elastic. At very high loads junction growth removes individual asperity contacts. Adapted from Lim and Ashby [44], 1987

In relation to these approximations it is important to note that the real area of contact is proportional to the applied normal load and can be considered independent of the size of the contacting bodies [91].

A mechanically mixed layer on the surface changes the distributed load characteristics. Modelling based on flattening asperity junctions is folly in lieu of hard particles penetrating and mechanically deforming the surface while supporting the contact pressures in the processs. A doubtful assumption used for analysis of most friction or delamination models is that the harder of the two materials, in particular its asperities, do not plastically deform [54]. Plastic deformation of the contact points must be substantial as

can be estimated from the extensive deformations in the substructure observed by cross-sections of the worn composites[25,34]. Plastic deformation makes stress intensities based on point or distributed loads hard to predict. Therefore, predictions of delamination behaviour of ductile materials (including Al-MMCs) cannot be accurate even by the elastic-plastic fracture mechanics approach taken by Rosenfield [27]. Nonetheless, this model is important as it provides guidelines for how changes in friction, normal applied load, and surface flow stress can initiate delamination wear.

More recently Kapoor and Franklin [29] developed the rachetting failure approach to predicting delamination wear, considered to be more suited for ductile materials such as Al-MMCs. The premise is that each pass of the counterface causes an incremental increase in strain, $\Delta\varepsilon$ to develop in the surface and subsurface, causing a corresponding increase in the subsurface flow stress ΔS_f, at any depth that experiences strain. When the accumulated strain at the surface exceeded the critical equivalent strain, ε_{sat}, considered to be in the range of 5-20, loss of surface material would occur causing low wear rates. However, if the imposed shear stress in the subsurface exceeded the work hardened shear strength of the material, many "layers" would be removed causing high wear rates. Due to the high strain observed for Al-MMCs this model based on accumlated plastic deformation can be considered a significant improvement over earlier predictions.

Adhesion and low-cycle fatigue are stated as the causes of delaminations which subsequently can constitute the majority of surface damage under plasticity dominated wear conditions [3]. As stated earlier, the importance of the pursuit of delamination modelling can be related to the fact that large delaminations limit the use of Al-MMCs in tribological applications.

2.21 BASE ALLOY CHOICE AND THE IMPACT ON WEAR

2000, 5000, 6000, and 7000 series aluminum alloys have been utilized for the choice of matrix for aluminum composites. The primary choice of matrix could ultimately be related to the choice of processing route, with the most common methods being stir-casting, powder metallurgy, and melt-infiltration. Al-Si alloys such as A356 and A359 are popular choices for casting discontinuously reinforced aluminum metal matrix composites [57]. Additionally the choice of matrix alloy could be based the strength obtainable through age hardening, toughness and corrosion resistance in the presence of alloying elements. Most of these alloys can be heat treated (aged) to obtain higher matrix hardness. However peak hardness through age hardening of the composite has been found to have little effect on improving wear resistance for 356 cast Al-Si matrix alloy [35] and was actually found to decrease wear resistance for a 2124 matrix alloy [37] and 6061 matrix alloy [38] used to make SiC reinforced composites. Causes were stated as increased particle pullout [37] and subsurface softening through plastic deformation [38] in the peak aged condition. Mechanical mixing of the steel counterface was also found to decrease in the peak aged condition for 2024 [41] and 7075 [33] matrix alloys used for composites compared to the use of these matrix alloys in the softer solution annealed state. Therefore the decision to use a matrix alloy based on its ability to increase hardness through precipitation hardening, so far, cannot be justified.

(I) ALUMINUM-SILICON ALLOYS

In these alloys, the Si phase is hard relative to the aluminum matrix, in part increasing resistance to plastic deformation. The hard particles have been identified as promoting mechanical mixing and mutual transfer at the wear surface when mated against a steel counterface [78,83]. Increasing silicon content in the range of 4-24% Si was found to generally improve the wear resistance of the aluminum alloy [73]. This was concluded over a 0.105 - 1.733 MPa pressure range and 0.19 - 0.94 m/s range of speed [73]. A smaller debris morphology was found for the hypereutectic compositions (Si > 11.7 wt%) as compared to the hypoeutectic compositions. Increasing the Si content from 2-13% was observed to also promote more mechanical mixing by transfer from the steel counterface [6].

Seizure pressure increased when %Si was increased from 7 to 23%, with seizure pressures in the range of 5-7 MPa [75]. Increased wear resistance through the addition of silicon will undoubtedly reach a maximum, however, due to the loss of fracture toughness with decreased ductility and therefore greater likelihood of surface delamination. Increased instability due to low toughness for high % Si alloys has been shown to prevent mechanical mixing [75]. For example, absence of a mixed surface layer and significant counterface abrasion through direct Si particle contact resulted for dry sliding wear of the 23%Si alloy [75]. In comparison, a 13%Si alloy formed a surface mixed layer and caused low counterface wear. *In situ* mixed surface layers were observed to form up to 17%Si, above which instability under compression prevented stable surface mixing [75]. Mild wear occurred at low loads where delaminations are not produced. Instead during mild wear a layer of fine granular particles, formed by fracture and compaction of an ultra fine grained

surface microstructure, was found essential for improved wear resistance [92]. In an earlier study of the wear of Al-Si alloys, Sarkar [83] similarly recommended the use of a near-eutectic composition to prevent counterface abrasion and ensure toughness, without knowing that the surface mechanical mixing was causing the improved wear resistance for this range of compositions he was observing.

While increasing the Si content above 13% *may* not improve wear resistance, SiC additions clearly can: Martinez *et al.* [72] observed that at room temperature, primary Si in a hypereutectic Al-20%Si alloy was prone to particle cracking, while no particle cracking and lower wear rates occurred with the choice of a near-eutectic composition Al-7Si alloy reinforced with 20% SiC (13μm).

Si phase can protect the Al-Si from matrix contact if the particle size is large enough to protrude and contact the counterface asperities, similar to the role of protruding SiC particles [77,84]. The effect of Si or reinforcement phases in protecting matrix contact was postulated to reduce the wear in proportion to the area fraction in contact with the counterface [85,86] by an equation of the form,

$$\dot{w} = \dot{w}_p f_p + \dot{w}_m f_m$$

where f_p and f_m are the surface contact volume fractions of particles and matrix respectively. This wear rate prediction applies best at higher sliding speeds, or more specifically, between the sliding conditions where debris does not accumulate readily on the surface (debris accumulation may be considered more dominant at low sliding speeds below 1 m/s) [25,45,59,60] and very high sliding speeds where frictional melting and

softening of the surface occurs [15,21,79,90]. Predictions of this nature have been shown to be invalid [20,32,42] under plasticity-dominated wear [44], where particle fracture, plastic deformation and mechanical mixing are most important to the wear behaviour.

It is important to re-instill the importance of the sliding conditions in relation to observed increase in wear resistance. In studies that examine severe wear conditions (high applied force or substantial frictional heating) resulting in seizure (the rapid disintegration of the material due to gross material transfer) it has been almost uniformly concluded that an increase in hard particles, whether higher additions of Si or SiC reinforcement, can improve on wear resistance [12,72,75]. Seizure is typically associated with a critical surface temperature being reached, with the transition to seizure occurring due to any particular combination of applied load, sliding velocity, (and also heat dissipation) that causes frictional heating past a stable temperature limit. When relating seizure wear findings to subsequent applications for Al-Si alloys, improved seizure resistance does not conclusively state improved wear resistance, as operating at more moderate sliding conditions would most often be practically required in a design. Attempting to obtain the maximum sustainable operating temperature for the Al-MMCs can be paramount in establishing these materials as contenders against steels in many tribological applications [126].

(II) EFFECT OF MICROSTRUCTURE

The morphology of the brittle Si phase can be a much more influential factor in Al-Si alloy wear resistance when compared to the effect of small variations in Si content. Cast hypereutectic Al-Si microstructure has large primary Si particles in comparison to the

eutectic formed Si needle-like phase formed without modifier elements such as Na and Sr. The interfacial region between the Si particles and the matrix is prone to microcracking [87,88]. Microcracking becomes more prominent at low operating temperatures, therefore at low sliding speeds where frictional heating is not as significant [89]. At a sliding speed of 1 m/s, just outside the cold wear regime due to some observed surface heating, a cast 11.3% eutectic Al-Si alloy had better wear resistance than 23.3% hypereutectic Al-Si alloys containing the relatively large primary Si phase. Here it was concluded that cracking of large primary Si particles, 26-55μm in size, did not allow an increase in wear resistance at low speeds.

Looking at the effect of further refining the Si particle size, Eyre and Davis [6] compared the wear properties of a eutectic, sand cast Si structure to an alloy with a purposely refined small particulate Si structure produced by a melt-spray technique. Both Al-Si alloys had 11wt%Si and were tested at a very low sliding speed of 0.01m/s. Under this low speed sliding condition friction was found to be independent of these silicon morphologies. The sand cast aluminum-silicon alloy had initially a relatively coarse, needle-like dispersed Si phase which experienced pulverization during dry sliding wear, resulting in a fine Si dispersion of particles as the worn surface/subsurface microstructure. Accumulation of the hard, wear resistant Si phase was apparent by higher percentage of Si on the surface. The Al-Si alloy with an initially small Si particulate phase experienced the opposite effect: Si particles were removed during sliding, leaving more of the matrix phase unprotected. Therefore, mechanical mixing of the Si phase during sliding resulted in the coarse sand-cast microstructure having a better wear resistance under the tested boundary lubrication conditions. Dry sliding wear of all the Al-Si alloys resulted in a mixed iron and

aluminum oxide layer, with a high hardness and black appearance [6,92]. Accumulation of a mechanically mixed "oxide" layer has been found to increase the wear resistance of Al-Si alloys independent of Si particle accumulation [59] with more severe wear occurring at high surface loads that cause the oxide/MML to delaminate.

In conclusion, for wear of the Al-Si base alloy without reinforcement, a mechanically mixed layer of oxides, possibly containing fractured Si phase, was observed to often comprise the active surface layer during tribological contact. The mixing of the Si phase in the active layer was found highly dependent on the initial microstructure, specifically the Si morphology and size. It all the cited studies, mixing of the Si phase in addition to a mechanical mixed surface containing counterface elements was found unanimously to increase wear resistance whenever it was observed to occur.

(III) AGE HARDENING

Alpas and Embury stated that the size and distribution of second phase particles were influential when surface delamination is the dominant wear mechanism for an aluminum metal matrix composite [28]. The corollary of this was that distribution of second phase particles could determine the size and likelihood of delamination wear occurring. Subsurface cracks nucleated at the particle matrix interface were found to be influential in causing delamination wear [28]. This can also apply to the distribution of Si particles due to the alloy heat treatment in a precipitation hardened matrix.

Age hardening has the possibility of reducing plastic deformation. However peak-age hardened alloys may not provide the expected increase in yield strength and hardness expected due to over-aging caused by local frictional heating [85]. Li and Tandon observed

that a T6 heat treatment to an as-cast A356-20vol%SiC composite did not significantly improve the wear resistance [35]. *In situ* coarsening of Mg_2Si precipitates occurred during sliding due to plastic deformation effects; frictional heating was low and was considered to not contribute significantly to the coarsening of precipitates. Under lubricated conditions Pan *et al.* observed that wear rates were lower for a 2124-20vol%SiC composite in the over-aged condition. This was attributed to decreased particle pullout through the corresponding increase in fracture toughness [108]. Overall, the increase in hardness through precipitation hardening has not been proven to significantly reduce wear, and in fact may have a detrimental effect on wear resistance through increased SiC particle debonding or particle fracture.

2.22 REINFORCEMENT CHOICES AND THE IMPACT ON WEAR

For all wear rate regimes, SiC particulate can improve wear performance of the unreinforced aluminum alloy by:

1) Allowing higher surface temperatures at which a transition from particle mixing/oxidation to bulk delamination occurs. Therefore reinforcement improves thermal stability, and allows operation at higher temperatures [12,72,85,126]

2) Acting as load bearing surfaces. SiC protrusions from worn surface can protect the matrix phase [109,130]. Reducing metal adhesion through

ceramic particles creating surface separation [11]. Distribution of particles reduces delamination size [27,61,77] and decreases plastic deformation and matrix flow at the surface [25,71,75,109].

3) Promoting transfer and mixing. SiC hard particles can transfer counterface metal and oxides to the composite surface, as well as fracture and redeposit on the surface increasing surface hardness [68,76,77,109].

(I) EFFECT OF REINFORCEMENT SIZE

(A) PARTICLE SIZE AND APPLIED LOAD

This section is concerned with the effect of particle size on wear rates observed over a range of applied loads, under plasticity dominated wear conditions found at low sliding speeds. Here, contact pressure is more important than applied normal contact force [18]. Alpas and Zhang have investigated the influence of different size ceramic reinforcement on the wear of aluminum composites against steel [11]. The wear rate and transition loads were altered as a result of coarse or fine particle size. A summary of some of the results are repeated in Figure 2.6.

In regime I, an iron oxide transfer layer, formed by abrasion of the reinforcement particles, resulted in a mild wear rate. The block-on-ring setup makes contact pressures more difficult to approximate due to increasing wear scar breadth with sliding distance, however, noting the wear volume and approximating the contact surface by simple geometry an estimated maximum nominal contact pressures of 0.4 MPa can be associated

with the observed maximum normal applied force of 20 N for ultra-low wear behaviour in regime I. The composite with coarse particles (15.8μm vs. 2.4μm) achieved lower wear rates below this maximum applied pressure and resisted the I/II transition to severe wear up to a greater normal applied contact stress than did the fine particle reinforced composite [11]. Sato and Mehrabian provided data for even larger particle sizes of 20μm and 46μm under sliding conditions in Regime I (Load 3 N, pin on disk tester, cast 2xxx Al 15%vol SiC_p MMC, 0.3 m/s, 52100 steel, 63HRC) [68]. The study observed that the increase in particle size in this size range resulted in *higher* wear rates. It has been relatively postulated that particulate cracking has more probability of occurring for particulate above 15-20μm [69]. Sannino and Rack found consistent results that increased particle size from 13 to 29 μm increased wear rates for loads in Regime II (>1 MPa) and sliding speeds less than 0.4 m/s [20,111,112].

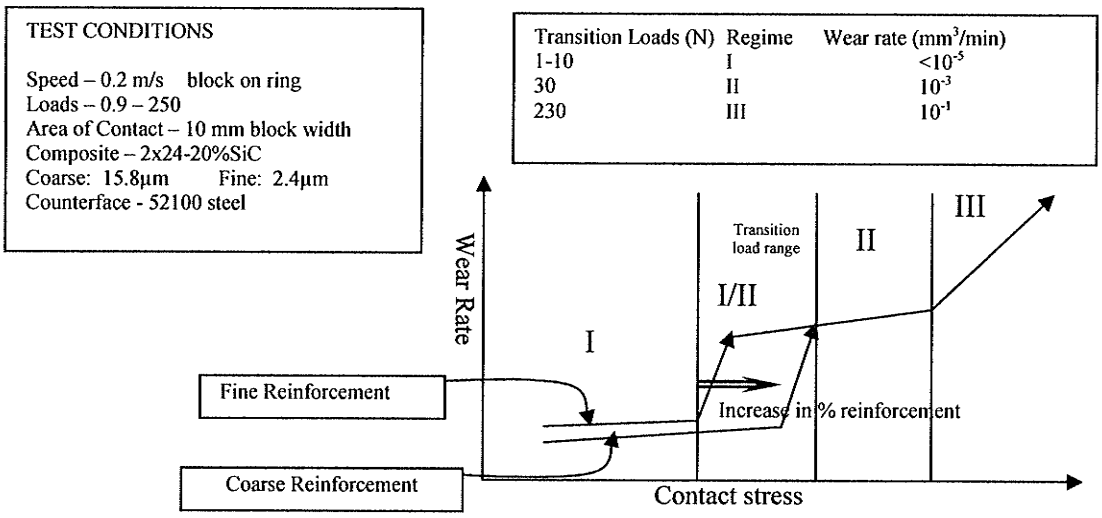

Figure 2.6 The effect of the choice of a larger particle size at low loads. The coarse particle size had a lower wear rate at the same applied load in Regime I. A transition was caused by significant particle fracture in the I/II stress range. Past this transition point increased particle size did not lower wear rates. Adapted from Alpas and Zhang [11], 1994

Chung and Hwang [109] examined the effect of particle size during short reciprocal sliding. Tests were performed with a reciprocating track of 1 mm, average sliding speed of 0.05 m/s, applied pressure of approximately 0.3 MPa and a pin-on-disk setup, both of the same composite material. Wear rates were found to decrease with successively larger particle sizes from fine (2-5μm) to medium (15-25μm) to coarse (70-85μm) ranges [109]. Higher wear resistance for the coarse 70-85μm particle size contradicts the earlier observed behaviour [68,69,111,112] that would predict the opposite effect. This shows the importance of the counterface and contact geometry in composite wear behaviour. Against a like-composite counterface at a very low sliding speed, fine and medium sized particles were more likely to a) be pressed into or "buried" in the matrix, b) to have greater likelihood of particle pull-out and c) be agglomerated into larger abrasive debris particles, increasing plowing interactions with the soft matrix material [109]. These effects were considered to be more dominant than the effect of increased particle fracture for the large particle reinforcement. Despite this being the case for a like composite counterface, no comparison was made with the wear rates of the composite against a steel counterface, which may cause more significant particle fracture due to increased hardness. Also, at higher applied normal contact pressures, a MML has the possibility of forming instead of the increased plowing observed of agglomerated smaller particle debris.

(B) Particle Size and Sliding Speed

Several studies have shown agreeable results that the choice of large reinforcement particles for Al-SiC composites results in improved wear resistance at high (approximately

above 1 m/s) sliding velocities [39,41,21,22,79,80]. To quantify "large", similar wear resistance was found for an as-cast A356-20vol% SiC composite with an average particle size of 10μm compared to an Al-4.5%Cu-13vol%SiC composites with 27.4 and 38.7μm average particle sizes [21,79]. However, a 6061-15vol%SiC composite with an average particle size of 1.6μm had a much worse response to increased sliding velocity, experiencing gross material transfer and seizure wear damage at lower sliding speeds than the composites with larger particles. The composite with 1.6μm particles failed due to gross material transfer (seizure) at any sliding speed greater than 1 m/s with contact pressures between 0.15-0.3 MPa. In comparison, the 27.4μm particles did not seize up to a contact pressure of 0.5 MPa and sliding speed of 5 m/s. This was the same resistance achieved by the composite with "medium" sized particles of 10μm. Nevertheless, the composites with a larger particle size (approx 30μm) achieved an equivalent or better wear resistance at high sliding speeds than the composite with a smaller particle size (10μm) but larger volume fraction (13% vs. 20%). Interestingly, the composites with the 1.6μm and 10μm particle sizes had the lower wear rates over the range of applied loads (0.12-1.2MPa) at the lowest sliding speed tested of 1 m/s, again indicating that composites with smaller particle size may have better wear resistance in the plasticity-dominated wear regime (II).

(C) PARTICLE SIZE AND ADHESION

The observable fact that aluminum and aluminum composites experience wear by transfer and adhesion to the counterface [14,78] remains a setback in achieving consistent wear performance at low sliding velocities. Increased size of reinforcement has the potential to reduce shear strains caused by matrix adhesion [77]. Sasada *et al.* further

proposed that reduced adhesion results from fine ceramic particles in the interface, which even though most likely much smaller than asperity contacts at an average diameter of 3μm, were found to accumulate of the metal surface promoting less direct matrix contact [61]. The overall trend from a study by Hoskings *et al.* was that increased SiC particle size from 1-142μm decreased the adhesive wear that was occurring [76]. However the corresponding improvement in wear, caused by the wear mechanism changing from purely adhesive to mixed mode oxidation-abrasion [109] may only be valid at the very low pressures tested as demonstrated by Alpas and Zhang [11,42].

Besides surface shear, equal importance must be given to the influence of particle size on adhesion-delaminations which originate in the subsurface. Zhang *et al.* [22] demonstrated that a larger particle size (Al-20% 8.8 μm Al_2O_3 vs. Al-20% 1.8 μm SiC) can withstand higher contact pressures (2.65 MPa vs. 0.79 MPa) before the development of cracks that lead to an adhesion-delamination severe wear transition. At lower contact pressures abrasion was the dominant mechanism. In terms of subsurface damage it has been well established that maximum strengthening and minimized particle fracture will occur with the choice of the smallest possible particle size with the same overall volume fraction of reinforcement [123]. If particle cracking was resulting in delamination instabilities the opposite trend of increased adhesion-delamination with increased (1.8 to 8.8μm) particle size would have been observed over this range of sizes [22]. This may indicate that void formation at the particle/matrix interface was a principal source of flaws that initiate subsurface instability [27,44]. With void formation as the dominant cause of delamination wear, for the same volume fraction, small particles could have the additional

effect of increasing adhesion-delamination wear through crack linking of more evenly distributed small particles in the subsurface [80].

To summarize, it can be stated that increasing particulate size may decrease wear rates at low normal pressure (Regime I) however the wear performance improvement that can be achieved is limited by particle fracture and pull-out as the reinforcement size is increased past a particular size for sliding pressures in Regime II. In general, fracture and pull-out occurs to a lesser degree at higher sliding speeds, therefore a larger particle size can be used with less risk of severe wear by either of these wear mechanisms. Overall, it could be seen that particles in the order of 20 μm had superior wear resistance at speeds greater than 1 m/s [79], while this size of wear particle had much worse wear resistance at speeds less than 0.4 m/s. Tests at these lower speeds showed superior wear resistance for particles around half this size due to decreased cracking. The effect of increased load at any applied speed can be considered to increase the risk of particle pull-out and fracture for the chosen reinforcement size.

(II) REINFORCEMENT ORIENTATION AND SHAPE

Reinforcement orientation and shape can affect wear performance through [20]:

1) Rotation, deflection and load bearing capacity.
2) Reinforcement fracture and possibility of intermixture of the fragments and matrix.
3) Preferential matrix crack nucleation points and void formation sites.

Reinforcement orientation determines the pattern of reinforcement fracture under matrix strain. How the reinforcement fractures significantly affects the expected debris morphology and delamination size. Wang *et al.* observed a lower wear rate with SiC whiskers perpendicular to the sliding surface as compared to parallel, [118]. More recently, Goto and Omori [125] similarly observed that alumina fibers normal to the wear surface resulted in lower wear rates. This was explained by better load carrying capacity of normal fibers under frictional shear as compared to the parallel fiber orientation.

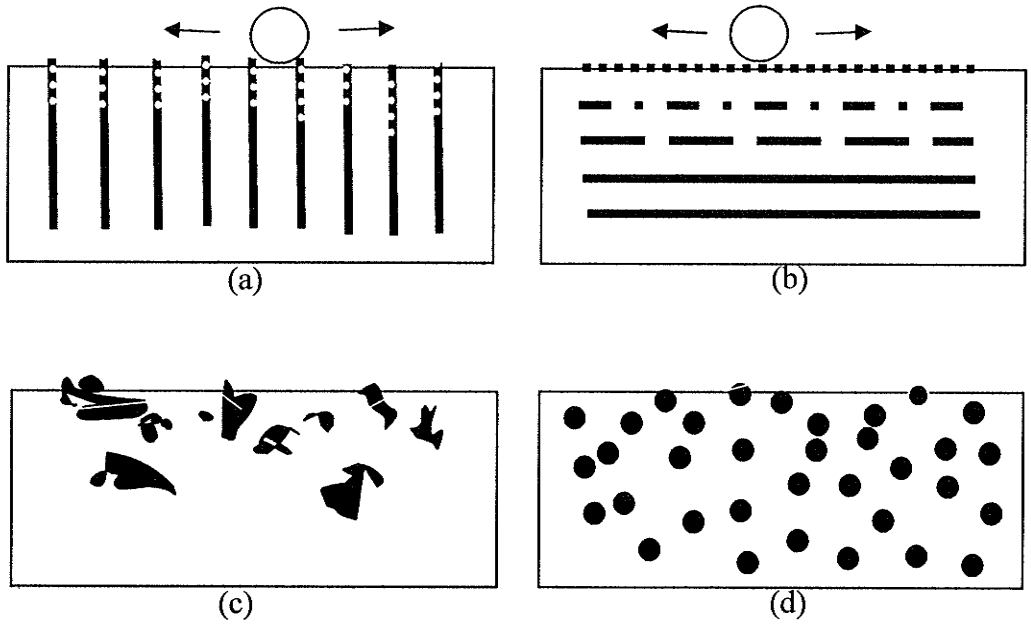

Figure 2.7 Reinforcement orientations (a) Normal, high aspect ratio, (b) Parallel, high aspect ratio. Orientation of fractured reinforcement can affect particle mixing or surface particle pullout. (c) Irregular shaped particles can have a larger strain field reinforcement effect than the spherical particles and ability for strain damage absorption. (d) Spherical particles have a lower likelihood of fracture, void formation, and potential for more homogeneous subsurface strain distribution

Orientation and shape are essential to reinforcement against plastic deformation. The magnitude of elastic loading, and therefore its contribution to work hardening, is highly influenced by particle size and aspect ratio under strain [7]. Brechet *et al.* stated that

under strain as induced by surface sliding, the strength imparted by reinforcement through sharing of elastic strain is lost by 1) particle cracking or 2) plastic relaxation of the matrix at the particle interface [7]. Larger sized SiC reinforcement, in this study between 5-25 μm, had greater probability of cracking due to a greater elastic stress retained by the particle under strain [7]. As a result of particle cracking matrix stress relaxation occurs, causing impairment of the plastic deformation resistance. A larger particle by way of a higher aspect ratio in the direction of stress allows for higher average stresses to be transferred to the particle. However again this results in greater probability of cracking.

Comparatively, very fine reinforcement sizes are less likely to fracture due to proportionately lower elastic loading through the interface. However, plastic relaxation occurs by deformation of the matrix surrounding the particle at a lower stress magnitude. Matrix flow around the particle at lower stress levels also impairs the plastic deformation resistance.

Shape variables can be divided into two categories, 1) by how uniform it is geometrically, i.e. sphere, cylindrical, or random faceted, and 2) its length/diameter or aspect ratio. A benefit of irregular shaped particles is a large far-field resistance to deformation under strain, as compared to a geometrically smooth sphere [122].

(III) REINFORCEMENT DISTRIBUTION

A uniform distribution of SiC_p has been found to be a considerable factor for improved Al-composite wear resistance [98]. Particle clusters result in high localized strain hardening due to disproportionate sharing of matrix stresses [122]. Due to the difference in CTE during casting of a MMC, the matrix tensile stress is proportionally higher in the

immediate vicinity of clusters. Incomplete matrix flow in clusters results in high porosity, causing these regions to be loosely bonded to the matrix and therefore easily pulled out during wear [128]. Under plastic deformation clusters can also cause heterogeneous subsurface strain promoting delamination wear. Finally at low pressures that prevent surface fracture of these regions, particle clusters can act as asperities increasing abrasion of the counterface [20].

In conclusion, shape, orientation and distribution of the reinforcement phase has a major effect on the contribution to plastic deformation resistance and wear resistance through the sharing of elastic loads and distributing damage to prevent large scale fracture.

(IV) % VOLUME OF REINFORCEMENT

An increase in volume fraction of reinforcement can become detrimental to the sliding pair by further introducing hard third body debris particles into the interface that can potentially increase both composite and counterface wear [20,108]. However, higher particle volume fractions can accommodate greater normal contact stresses where abrasion will remain the dominant wear mechanism due to a decreased load on each particle acting as an asperity [22]. This is beneficial since a severe wear transition, which occurs with the dominant wear mechanism becoming adhesion, plastic deformation and particle fracture, will occur at higher contact stresses [22,23,38]. The transition to severe wear is also extended to higher contact pressures by the complementary benefit of increased shear strength in the subsurface through increased volume fraction of reinforcement [11,22]. Increasing the volume fraction will have a similar effect to increasing particle size in that

both allow reduced potential for adhesive wear by reduction of the contact-interaction with the matrix phase [76], providing the size of the particles which are being added are of large enough size to act in part as asperity contacts.

Chung and Hwang observed wear resistance increase with increased SiC particle content from 0-30 wt% [109]. Similarly, Venkataraman and Sundararajan observed the wear rate to decrease with increased reinforcement from 10 to 40 vol% SiC particles, of average size 2.5 μm [31]. However, increased wear resistance of the Al-MMC comes at a cost: in most cases higher volume fraction of hard reinforcement has been shown to cause a significantly increase in counterface wear [22,23,80]. To balance the wear rates several reviews of Al-MMC wear behaviour have concluded that an optimal reinforcement volume fraction for particle reinforced aluminum composites is in the range of 25-35% [20,57,76, 144]. Higher volume fractions of reinforcement than this range can be expected to experience higher damage accumulation through increased particle cracking or pull-out at higher elastic matrix stresses [123]. Secondly, linking cracks between reinforcement particles at higher volume fractions can add to tensile instability [27,123].

Therefore, a major consideration for increased volume fraction of reinforcement is the decrease in fracture toughness. Similar to the effect of high Si content in an Al-Si binary alloys, increased SiC results in a greater likelihood of surface instability and delamination/ adhesive fracture under high compressive stress. To support this, wear scars have been observed to have increased "white" fracture surfaces (caused by edge charging effects for SEI imaging) when the reinforcement fraction was increased in the range of 10-40% SiC at equivalent applied loads [32,71].

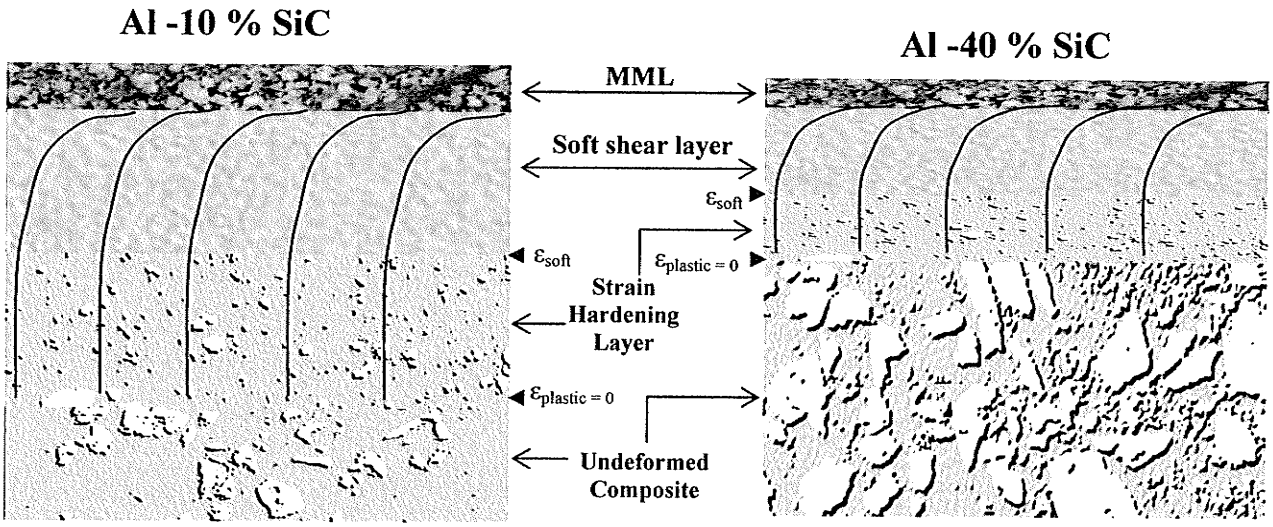

Figure 2.8 The effect of increased % SiC on the depth of penetration of subsurface strains. Three layers exist: 1) surface MML, 2) Subjacent soft shear layer, and 3) Strain hardened Al-MMC observed under unidirectional sliding. Adapted from Venkataraman and Sundararajan [33], 2000.

Several studies have noted that above 10%SiC adhesion to the steel counterface (delamination fracture) dominates wear more significantly than abrasion by the steel counterface [45,70,80]. This seems contradictory to the expected effect of more reinforcement phase, that is abrasion as a mechanism would be expected to increase, however, at the low 10% volume fraction smearing may dominate, causing low adhesion, while at the higher volume fraction smearing cannot occur as easily leading to more stick-slip induced adhesion delamination fracture [71].

(V) TYPE OF REINFORCEMENT

The degree of improvement allotted over the base alloy depends significantly on the nature of the reinforcement [71]. In Al-MMCs, Al_2O_3 and SiC reinforcement have been

used most extensively. Of these two the wear properties of SiC reinforced have been shown to be generally superior due to less localized cracking, fracture, and pullout [11,41]. There are some studies that show otherwise [22,38,80], although some of these findings are more related to the composites, not the reinforcement particles. For example, improper oxidizing of the SiC to prevent interfacial reaction would produce an inferior SiC reinforced composite when compared to the non-reactive Al_2O_3, due to the resulting poor matrix bonding [118].

In their review of discontinuously reinforced aluminum metal matrix composite wear, Sannino and Rack [20] concluded that SiC offers one of the best choices for reinforcement, however TiB_2 and B_4C are also on par in terms of their respective composite wear resistance [68]. Wear resistance of SiC has been shown to be significantly reduced if Al_4C_3 is observed to form at the interface due to high processing temperatures [113]. This is avoided through keeping temperatures well below 1023°K [114], use of powder metallurgy (P/M), and increased silicon content in the casting alloys [8,115].

As stated earlier, it is generally well known that the use of the smallest reinforcement size possible allows for the maximum strengthening effect [123], higher fatigue strength [102], less particle fracture damage under compression and higher fracture toughness [127]; all around better mechanical properties. It is also known that higher volume fractions of reinforcement (>30%) can achieve the higher strengths, although this becomes deleterious to the toughness and fatigue bulk mechanical properties of the composite [123] and therefore is usually not recommended.

However, the above discussion indicates that what provides the best choice for the bulk mechanical properties is not the best choice for wear resistance, when considering the

addition of a reinforcement phase. Attempting to maximize the volume fraction of hard particles on the surface appears to appreciably increase wear resistance [130], if this can be achieved without significant occurrence of severe wear mechanisms of pull-out and particle fracture. This is a very big "if", since particle pullout and cracking was generally observed for all particles greater than 10 μm in size for the short duration laboratory tests, indicating that use of large particles for an expected long service life may often not be practical. In contrast, smaller particles were frequently smeared in the matrix and removed through bulk delamination [109]. Particle inundation is a problem especially as the load is increased, such as for Hertzian contact pressures found in roller bearings. At high loads, high volume fractions are required to resist smearing and extensive plastic deformation with small particle reinforcement. Therefore, the goal of maximizing the SiC particles on the surface of a size not prone to smearing, fracture or pullout can be stated as the encompassing goal for optimization of the reinforcement phase for maximum wear resistance of discontinuously reinforced Al-MMCs.

2.31 EXTRINSIC VARIABLES

(I) SLIDING SPEED AND APPLIED LOAD

This study is designed to focus on "low speed" sliding behaviour of aluminum metal matrix composites; that is, frictional heating is expected to not significantly increase the bulk temperature of the composite. As a result plasticity-dominated wear mechanisms are expected to govern wear under these sliding conditions. Lim and Ashby [44] defined a relationship of the wear rate being independent of sliding velocity from experimental data

collected for steels at sliding velocities below 0.1m/s. The wear rate at these low speed sliding conditions was considered to increase linearly based on applied pressure only, and was modeled based on Archard's law of plasticity dominated wear {See Adhesion Wear},

$$\widetilde{W} = k_A \cdot \widetilde{F}$$

where k_A is the wear coefficient based upon the material hardness. Antoniou and Subramanian [15] proposed that aluminum alloys (and here we can also classify aluminum composites) have definite velocity dependence at relatively low sliding velocities and predicted the wear rate using a new wear coefficient which includes the normalized sliding velocity into the equation,

$$\widetilde{W} = k_B \cdot \frac{\widetilde{F}}{\widetilde{V}}$$

The predictions of wear rates when placed on a wear mechanism map are shown in Figure 2.9. Normalized parameters are given in section 2.32.

When including velocity dependence, for the same normalized pressure a lower wear rate is predicted as the velocity is increased. This can be seen in by comparing the intersection of the equivalent wear rate contours in Figure 2.9b). This behaviour has been observed [12,39,45] and appears to have greater validity for aluminum alloys than the original model proposed by Archard. However, the model developed by Antoniou and Subramanian may be inaccurate at low sliding loads due to the mechanisms of oxide transfer and transition to particle fracture not observed in the monolithic alloys[20].

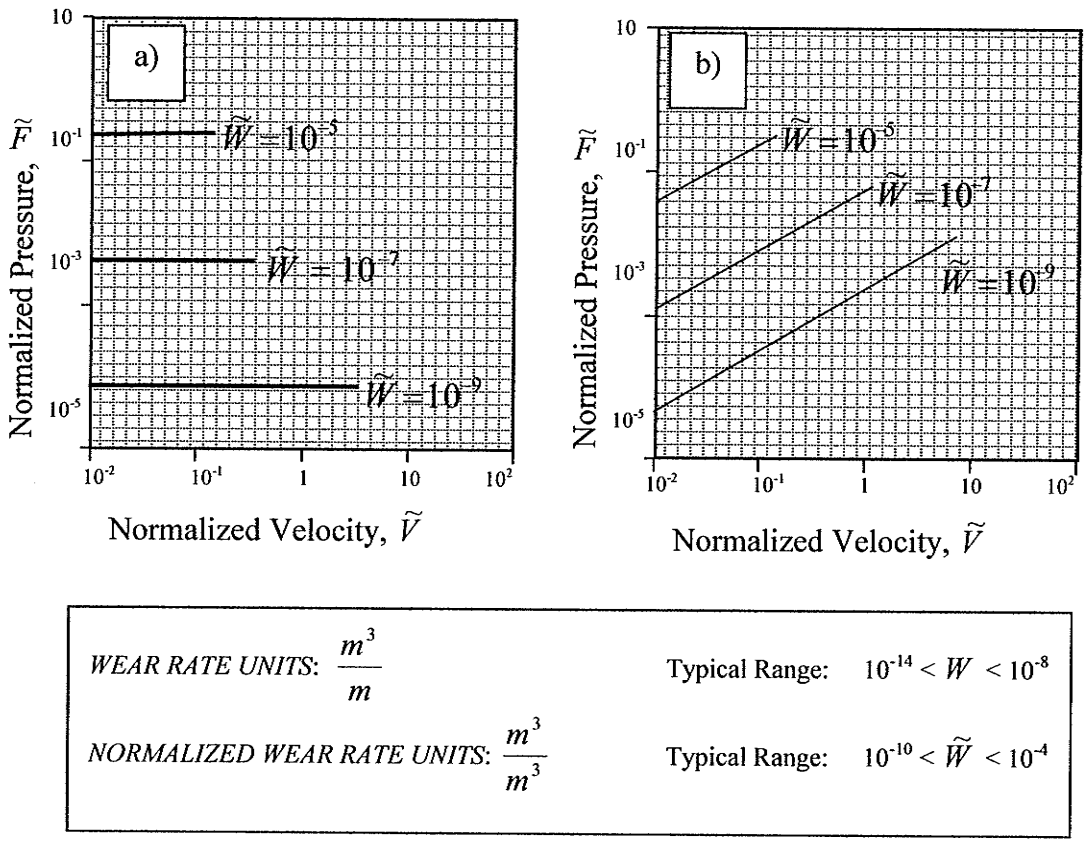

Figure 2.9 Illustration of wear rate predictions. a) Velocity independent (Archard's equation) prediction of plasticity-dominated wear, typical for steels. b) Velocity dependence for wear rate as proposed by Antoniou and Subramanian for aluminum alloys and composites. Compare contours to Figure 2.14. Numbers are for illustration only.

Wear rates may be independent of velocity in the ultra-mild wear regime in which little to no particle fracture is observed, but suddenly increase disproportionately with an increase in velocity at slightly higher loads that can initiate particle fracture [11,12]. Experimental results of the effect of increased sliding speed are shown for an aluminum alloy and aluminum composite in Figure 2.10.

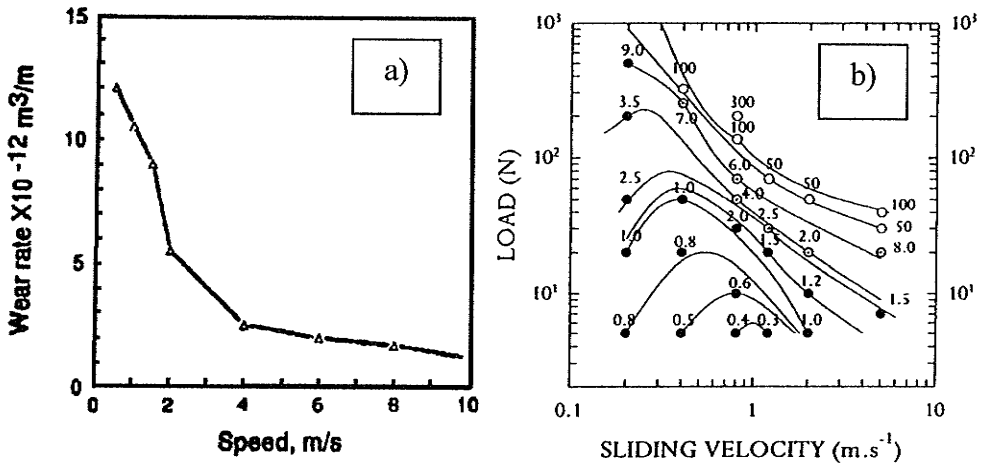

Figure 2.10 a) Decrease in wear rate at an applied normal pressure of 2 MPa using for a 356-20%SiC composite against steel, Ravikiran and Surappa [30]. b) Ware rate map for 6061 Al against a 52100 steel counterface. Note that at loads below 100 N and sliding velocities between 0.2-1 m/s consecutive contours indicate a decreased wear rate as sliding velocity increases. At higher velocities, consecutive contours show an increased wear rate for the same applied load, Zhang and Alpas [13].

Clearly a maximum sliding velocity exists at which the "cold" wear mechanisms no longer apply although there are too many variables to define this specifically. Considering frictional heating, higher applied loads would induce lower sliding velocities at which a transition based on wear mechanism would occur.

As the sliding speed is increased debris agglomeration and reprocessing becomes less prevalent for the same contact geometry. This causes a reduction in high fluctuations of the coefficient of friction, resulting in a relatively smooth friction trace in response to debris being simply removed from the interface [10,46,50,61]. The reduction in high fluctuations of the coefficient of friction can act as a good indication that the plasticity-dominated wear regime, which is significantly influenced by the interaction and character of the debris, has been surpassed in response to increasing sliding speed. At a relatively low load of 42N, Cho *et al.* observed the wear of several Al-SiC composites to linearly

decrease from 0.15 to 0.65 m/s, with a corresponding decrease in debris agglomeration size over this range [98]. At higher speeds than 0.65 m/s wear increased and was attributed to surface temperature rise, clearly indicating that the cold wear sliding conditions had been surpassed. Wang and Rack [45] reported that below a sliding speed of 1.2 m/s microcracking, debris generation, and third body abrasion caused low Al-20vol%SiC_w composite wear resistance. Above this sliding speed, abrasion and adhesion became more dominant wear mechanisms and the wear rates were observed to decrease up to the maximum tested sliding velocity of 3.6 m/s. Similarly, Ravikiran and Surappa [39] observed a high wear rate at 2 MPa contact pressure and a low sliding speed of 0.5 m/s. At this speed large coefficient of friction fluctuations occurred and SiC particles were fractured and removed from the surface. At a sliding speed of 4 m/s coefficient of friction fluctuations disappeared, the overall coefficient of friction was lower, and it was observed that both the number of SiC particles undergoing fracture and the wear rate decreased. The same change in friction behaviour with velocity was observed during reciprocating motion [24,90]. At a low average reciprocating speed of 0.075 m/s high fluctuations in the coefficient of friction were observed for an Al(Cu)-20vol%SiC composite. The friction fluctuations disappeared and a much lower average friction coefficient was observed as the reciprocating speed was brought to 0.6 m/s. In this study [24] periodic friction behaviour was observed against a martensitic stainless steel, hard tool steel, and Si_3N_4 counterface, providing some indication that the friction behaviour was not as much controlled by the material pair as compared to the effect of the extrinsic sliding variables such as contact geometry, load, and speed [87]. Again in all cases the high fluctuating coefficient of friction at low speeds resulted in the highest composite wear as compared to higher sliding

speeds. Rigney [10] also recently stressed the role of third-body interactions in causing the fluctuating coefficient of friction. To supplement this, Hwang et al. [46] confirmed that the frictional fluctuations are related to the accumulation and ejection of debris from the interface based on the contact geometry, through use of intermittent tests. Fluctuations in the coefficient appear a common characteristic aluminum metal matrix composites at low sliding velocities and define the region of sliding conditions that focus is placed on for this study. The best deduction to make is that mechanical mixing, transfer and back transfer, and the interaction of debris in the interface are more prominent at low sliding velocities, and are the interactions which relate to observed friction fluctuations, the presence of a mechanically mixed layer, and relatively high or low transitions in the rate of wear.

(II) RECIPROCAL VS. UNIDIRECTIONAL SLIDING

(A) CUMULATIVE STRAIN AND THE SOFT SHEAR LAYER

Soft shear layers are an important phenomenological occurrence during the wear of metal matrix composites. No soft shear layers have been found for HP aluminum and most Aluminum alloys, however a soft shear layer has been identified as forming during the dry sliding wear of Al-MMCs [31,32]. A soft shear layer can be seen to be formed between layers of comminuted SiC reinforcement [14]. The soft shear layer has also been identified as forming subjacent to a protective mechanically mixed layer [25,32]. This behaviour has been related to damage accumulation and void nucleation at the reinforcement phase, in addition to the maximum strain hardening capability of the matrix phase. The soft shear layer is illustrated for two different volume fractions of reinforcement based on a previous study [33], Figure 2.8.

Voids have been identified as forming at the particle matrix interface which results in inefficient reinforcement of the subsurface [27,28,32]. That is, the reinforcement phase is expected to promote some void nucleation. Void formation and coalescence has been identified as causing softening of plastically deforming metal as the strain is increased past a maximum sustainable level. To clarify, a critical strain exists for void nucleation; beyond this deformation level no further increase in strain hardening will be achieved due to voids forming.

Venketaraman and Sundararajan [32] observed that the strain at fracture for Al composites in uniaxial tensile loading is in proportion to the strain observed in the shear layer formed under compression and shear stresses during wear, Figure 2.12. Under tensile load, strain softening results causing void coalescence, crack propagation and fracture. Under the hydrostatic pressure of the counterface on the wear surface void formation is suppressed, allowing greater strain to occur without fracture [26,27,32,69]. This can be seen by comparing ε_{frac} and ε_{soft} for the same composite reinforcement in Figure 2.12.

Understanding conditions for void formation is essential as voids cause a reduction in the composite resistance to stress deformation. Greater strains before fracture can achieve greater strain hardening effects. Venkataraman and Sundararajan noted greater peak strain hardening to occur in the plastically deformed region as the sliding load was increased from 52 to 122N for the same sliding velocity [32]. Under sliding conditions where no MML was formed large delaminations and thus a severe wear rate can result from delaminations originating in the soft shear layer, Figure 2.11 [27]. With a MML present a soft shear layer may prevent the MML from becoming a stable surface phenomenon. Therefore if soft shear layers are identified as forming, changing the contact force, velocity,

or subsurface strain capacity of the composite could improve upon wear surface stability by preventing the surface from reaching this softening limit.

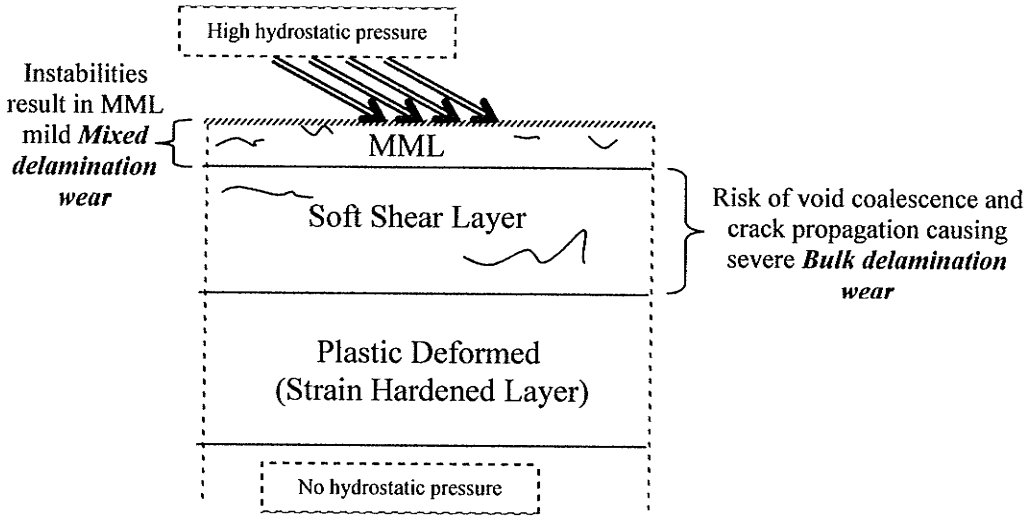

Figure 2.11 Potential delamination size based upon subsurface plastic deformation. If no mixing occurs bulk delamination wear can be mild at near surface depths.

(B) THE BAUSCHINGER EFFECT

During cyclic loading, the composite first strained in tension commonly does not achieve the same stress resistance when the loading is reversed, due to relaxation and plastic flow where microscopic strain hardening had initially occurred. The described Bauschinger effect results in plastic yielding at lower reversed stresses, or permanent softening of the material. This effect is perpetuated by inhomogeneous plastic flow at the reinforcement phase under strain [121].

The effect of permanent softening under the reciprocal stresses is dependant on both the aging treatment forming dispersed precipitates and the reinforcement phase.

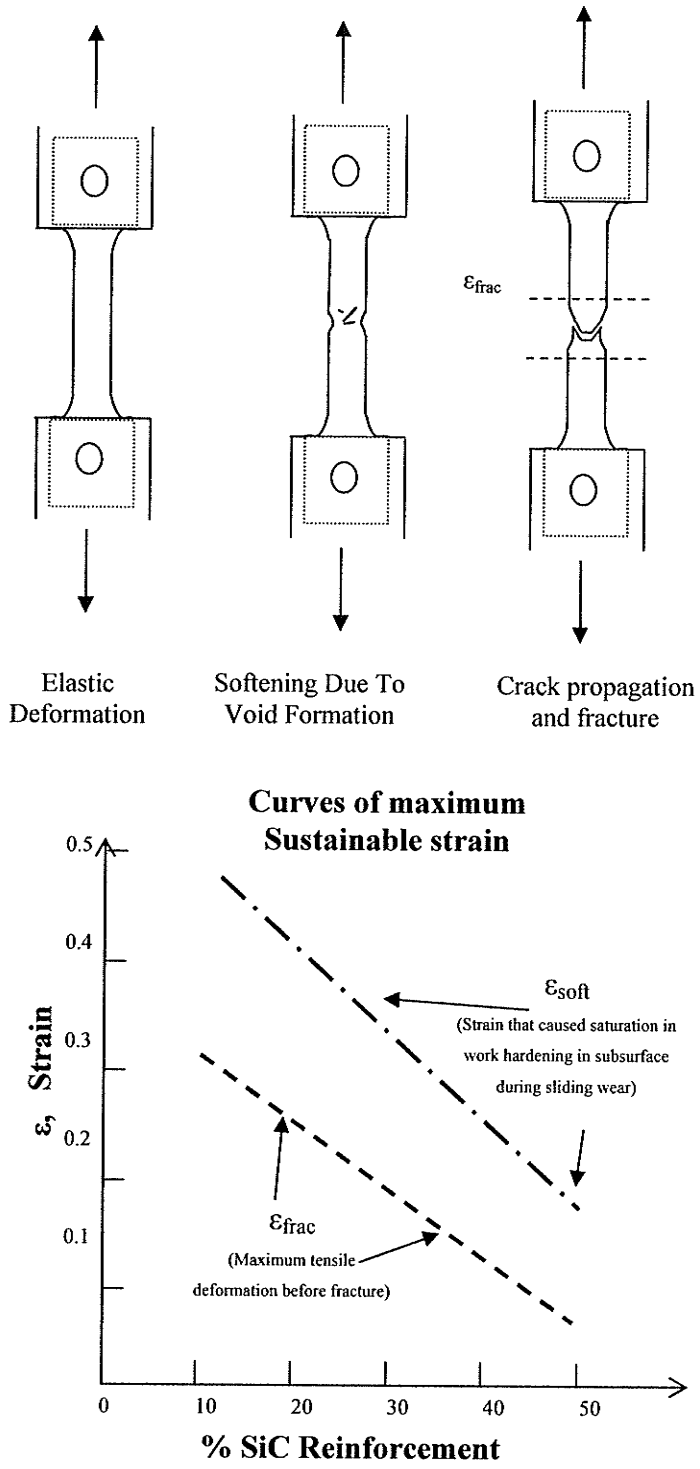

Figure 2.12 The relationship between tensile composite properties and subsurface strain hardening under dry sliding wear. Strain at fracture, ε_{frac}, decreases with increased reinforcement under tensile load. The equivalent subsurface strain required for work softening to occur, ε_{soft}, was observed to also decrease in proportion to higher % SiC reinforcement. Adapted from Venkataraman, and. Sundararajan [32], 1996

Using a A356 20vol%SiC composite, the Bauschinger strain was found to increase (indicating increased softening) with aging as the precipitate size increased (T61→ T4→ OA200→ OA300); this was attributed to more substantial long-range stress distribution for larger precipitates [121].

Considering the reinforcement phase, permanent softening under reverse loading conditions was related to damage accumulation by 1) plastic flow around the particles and 2) particle cracking [121]. Therefore relaxation of the internal stress by either form of particle damage (also the effect of overaging) has the potential to increase permanent softening behaviour under reversed loading reciprocal siding conditions. This can prevent the accumulation of strain hardening in the subsurface observed under unidirectional sliding [27].

(C) REPROCESSING OF DEBRIS AND RECIPROCATING LENGTH

Great insight into debris reprocessing and mixing can be found by comparing wear behaviour under fretting, reciprocal and unidirectional sliding conditions. During fretting wear the relative velocity between the contacting surfaces is low causing the debris to stay where it is generated [124], resulting in a more pronounced effect of debris interaction in the interface. McColl *et al.* [52] observed equiaxed debris particles, 1 to 2 μm in size, agglomerated into flakes and ejected from the wear scar. This occurred under fretting at a pressure of 5.6-9.7 MPa, reciprocating amplitude of 0.04 mm and 3μm SiC particle size. Li and Tandon [25] similarly observed plate-like debris aggregates to be formed of fine equiaxed particles, 0.2-3 μm in size, under unidirectional block-on-ring sliding with 10μm SiC average particle size. Sliding speed for under fretting conditions was approximately

0.003 m/s [52], while under unidirectional sliding the speed was set at 0.2 m/s [25]. Comparing these two results, the manner of particle debris agglomeration must be similar despite drastically different sliding conditions.

Under the fretting conditions [52], the debris agglomerations were stated as forming by a process of first mass transfer of the composite to the counterface, then buildup of transfer "mounds" by continued adhesion of submicron thick matrix material particles, and finally ejection of the compacted mound [52]. The process resulted in patchy adhesive induced transfer to the steel counterface and ejection of the compacted material as plates.

In another wear study using a significantly longer reciprocal amplitude of about 6mm, similar patchy transfer to the steel counterface was observed to occur during the reciprocal sliding [14]. In both the reciprocal sliding and fretting studies [14,52], the transferred mounds of Al-MMC were observed to become unstable and delaminate from the counterface, introducing plate debris into the interface which was easily ejected from the wear scar. Additionally both studies observed only small fractions of steel to become mixed in the debris formed by this adhesion-delamination process, indicating that adhesion wear was a more dominant mechanism than abrasion [52]. Finally, the piles of adhered and mechanically mixed Al-MMC were observed to cause significant damage to the composite surface, acting as large plows once they had formed to significant size. Therefore despite a much greater track length when comparing fretting and sliding conditions, the process of transfer, agglomeration and ejection of debris remained similar during reciprocal motion.

Similar to both fretting and reciprocal studies, the unidirectional study observed ejection of compacted plates composed of equiaxed transfer particles. However, under the unidirectional sliding condition a mixed *layer* of transferred material and debris formed

(MML), not mounds, and significantly more transfer of the steel counterface occurred [25]. This indicated a distinct difference in how debris agglomerated between reciprocal sliding (of any amplitude) and unidirectional sliding: while adhered particles transferred to the counterface to form "mounds" under reciprocal sliding, layered structures were able to form by redeposit of the adhered material parallel to the contacting surfaces in the unidirectional condition. An illustration of the different debris agglomeration behaviour is shown in Figure 2.13.

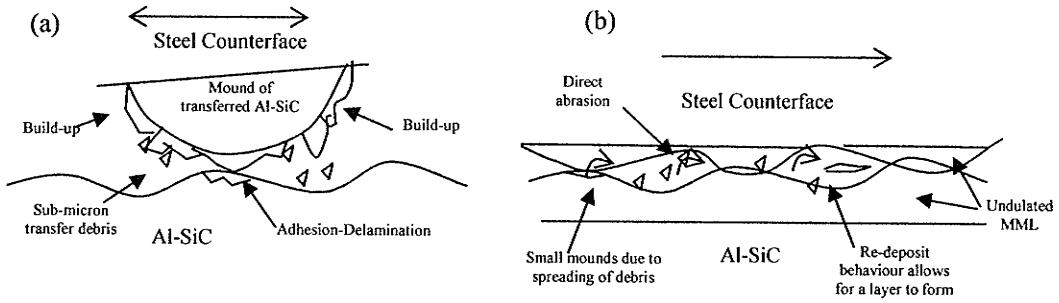

Figure 2.13 Illustration of the effect of debris reprocessing on mechanical mixing. And transfer (a) Reciprocal sliding causing build-up and separation of surfaces due to adhered heap volumes. Patchy deposits are observed on the counterface (b) Unidirectional sliding that allows for better distribution of debris formed by adhesion-delamination. A layered mechanically mixed layer is observed to form on the counterface.

The patchy transfer of the Al-SiC by local adhesion was found to be affected by fretting amplitude. The number of patches of compacted debris increased with increased stroke from 40 μm to 120 μm, whereas the area and thickness of these patches generally diminished [60]. The Fe content of the surfaces was also found to increase due to increased abrasion at the greater reciprocating/fretting amplitude. Overall it can be seen that both

adhesion and abrasion mechanisms are contributing to wear at all sliding amplitudes. Furthermore it may be proposed that the balance of adhesion/abrasion mechanisms contributing to wear can be seen to shift from predominantly adhesive to significantly abrasive as the sliding amplitude is increased from fretting, to reciprocal sliding, to unidirectional conditions [60].

As a final remark, debris must be expelled or removed from the interface to allow for wear, defining wear by a weight loss. Reprocessing of debris indicates that it will not contribute to wear through ejected lost from the sliding system, however its accumulation in the interface may be as equally damaging to the wear surface. Patches of mixed material caused severe ploughing of the unmixed surface as compared to when a continuous MML was present. Therefore the function of contact geometry in contributing to adhesive transfer, mixing, and mass loss from the system is a major consideration when formation of a mechanically mixed layer is desired [100].

(III) SLIDING DISTANCE

The most significant advantage of *in situ* formed mechanically mixed layers is that time dependant failure of the tribosurface can be avoided by regeneration. This is contrary to fatigue-lifetime limited wear coatings and finite surface treatments. Therefore a time-dependant wear transition should not occur for wear protection through MML formation. That is, it must be a perpetual phenomenon during sliding. Wear transitions for Al alloys and Al-MMCs have been identified due to the surface temperature exceeding a critical value [12,21,45,79], accumulation of debris [74,92], and reduction of contact stresses for non-conformal contacts [96]. A transition to a lower wear rate is expected with the

formation of an oxide tribolayer from the counterface [8,11,77] or the formation of an MML on the composite surface [25,33]. Both transitions are dependant on cumulative transfer and mixing as sliding distance is increased.

2.32 WEAR MECHANISM MAPS

Subramanian proposed five observable wear mechanisms for aluminum alloys [15]:

(i) Formation of fine equiaxed particles
(ii) Delamination of compacted equiaxed particles
(iii) Delamination of deformed aluminum alloy
(iv) Gross material transfer
(v) Melt wear

These wear mechanisms were further developed by Liu *et al.* [16] to include oxidation dominated wear at low sliding speeds and contact pressures that would be known to produce (i) and (ii) debris morphologies. The development of wear-mechanism maps is crucial for cross-study comparisons of the wear, wear mechanisms and wear rates for different sliding conditions [18]. The normalized equations used by Lim and Ashby [44] are given due to the importance that they be used for this study of Al-MMC wear.

The importance of including a wear-mechanism map is that it predicts the field of dominance of one wear mechanism and when its contribution becomes less important [18]. Considerable development is still required in defining the dominant mechanisms in the cold wear regime for aluminum alloys and aluminum composites.

Mechanical mixing is not aforementioned as a wear determining mechanism for aluminum alloys. Wilson and Alpas provided a wear mechanism map of A356-20%SiC composite and concluded that debris produced by mechanical mixing/oxidation describes the wear of this material for most normal loads and sliding speeds that due not produce large surface delaminations, mechanism (iii). Speculatively under sliding conditions where a MML forms, for aluminum or aluminum composites, mechanical mixing could provide the most correct description of the wear mechanism, as compared to attempts to separate gross material transfer (iv) and delamination of fine equiaxed particles (ii). Examples of wear-mechanism maps currently developed for aluminum alloys and aluminum metal matrix composites is shown in Figure 2.14

$$\widetilde{W} = \frac{W}{A_n}$$ Normalized Wear Rate

$$\widetilde{F} = \frac{F}{A_n \cdot H_o}$$ Normalized Pressure

$$\widetilde{V} = \frac{V \cdot r_o}{a}$$ Normalized Sliding Velocity

SYMBOL	*UNITS*
W = wear rate	m^3/m
A_n = nominal contact area	m^2
F = applied normal force	N
H_o = room temp. hardness	N/m^2
V = sliding velocity	m/s
r_o = contact radius	m
a = thermal conductivity	m^2/s

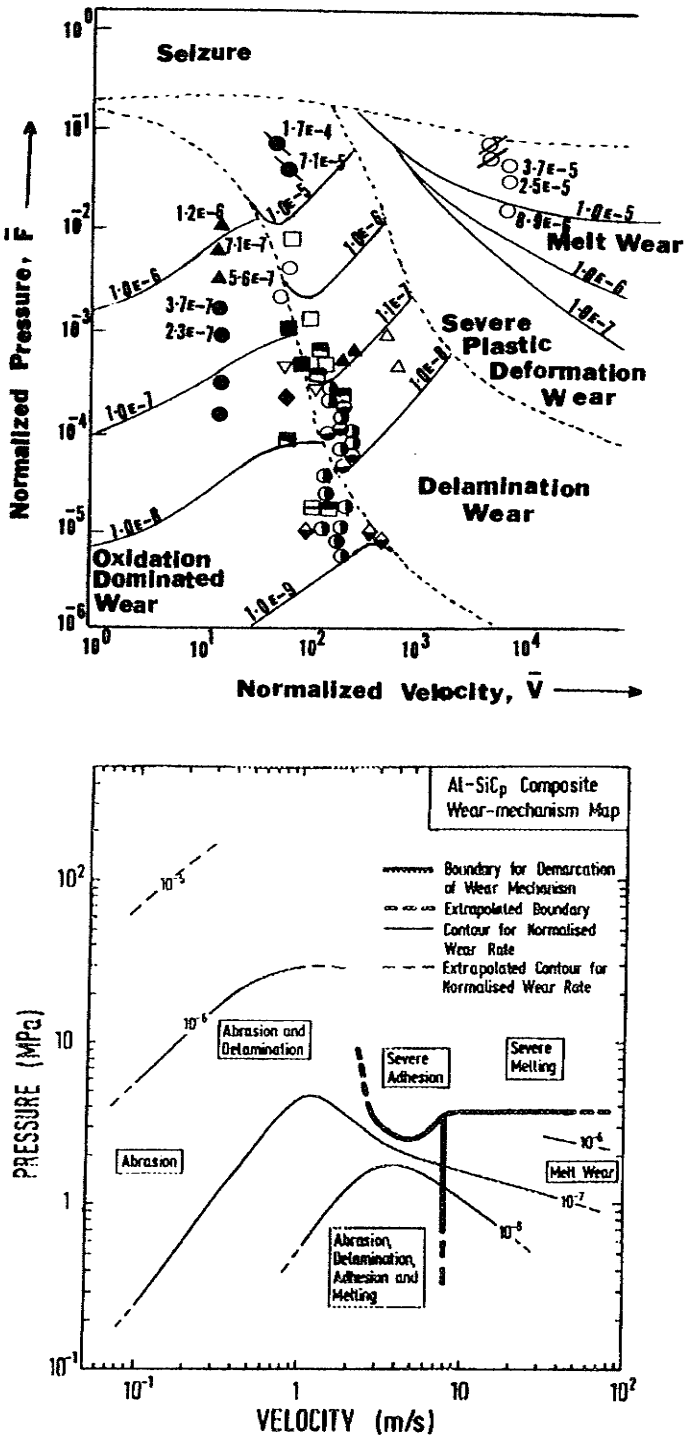

Figure 2.14 TOP: wear mechanism map proposed for aluminum alloys [92]. BOTTOM: wear mechanism map proposed for an aluminum-metal matrix composite [91]. Constructing maps for Al-composites suffers from the fact that many of the physical processes that cause sliding wear are not fully understood.

2.33 CHOICE OF COUNTERFACE MATERIAL

In general, the contribution of the counterface on the wear behaviour of a material has not been as well documented in comparison to the effects of load or speed [58]. Hwang *et al.* [47] examined the effects of metal combinations on the frictional and adhesive behavior of different tribological pairs. The significant conclusions were:

1) Initial coefficient of friction showed a decreasing trend as the hardness ratio of the materials paired increased. This was attributed to the relative ease in which plastic deformation is induced in the softer metal of the metal pair.

2) Adhesive transfer increased for metals paired with similar hardness. The softer metal of the pair tends to transfer to the harder metal surface.

3) Wear rates and coefficient of friction were, in general, higher for identical metals paired. This leads to the well established conclusion that different materials should be used for dry sliding wear as plastic deformation and adhesion effects tend to be reduced.

4) An increaseed wear rate was found to correlate well with increased coefficient of friction, Figure 2.3.

5) No definitive trend was observed for wear rates or the steady state coefficient of friction with respect to hardness ratio or theoretical adhesion compatibility of the metals paired.

6) While the material pair has a significant effect on friction and wear, the greatest influence was related to extrinsic factors such as wear particle dynamics, contact forces, velocity, and geometry.

The choice of counterface will determine properties of asperity contacts such as hardness and sustainable elastic pressures, as well as the nature of its own wear particles. The counterface affects the adhesion properties and oxide formation that can control the nature of the other materials wear debris. M. Bai *et al.* [90] examined the effect on wear behaviour of using three different counterface materials under reciprocal sliding conditions against an Al(Cu)-20vol%SiC composite, average particle size of 10 μm. The three counterface materials are ranked in Table 2.4 based upon which caused the minimum wear of the aluminum composite. The silicon nitride caused the highest wear rates for the low sliding speed, low sliding load conditions. The study proposed that this was possibly due to the lack of oxide formation [90] on the ceramic counterface. Also, increased wear caused by the ceramic counterface could relate to dominating interactions with the SiC particles encountered which would be fractured. The softer martensite stainless steel also caused a high wear rate of the Al-Cu-SiC composite pins at the low sliding speed of 0.075 m/s and below 1MPa nominal applied pressure. When the pressure was increased, composite wear rates drastically increased against the stainless steel counterface over 1MPa, making 4Cr13

the worst choice of the three counterfaces materials for low speeds over a range of applied loads.

Counterface Material	Hardness (HV)	Rating low speed, low load (0.075m/s, <1MPa)	Rating low speed, high load (0.075m/s, 1-4 MPa)	Rating high speed, high load (0.6m/s, 1-4MPa)	*Overall rating for least amount of composite wear*
4Cr13	501±8	2	3	3	3
$W_{18}Cr_4V$(T1)	**857±30**	**1**	**1**	**1**	**1**
Si_3N_4	1450±50	3	2	2	2

Table 2.4 Comparison of three different counterface materials based on weight loss under reciprocal dry sliding wear, M. Bai *et al.* [90], 1996

The softer stainless steel consistently caused much more severe wear of the composite than the hard T1 tool steel. Under high speed, high load conditions (Table 2.4) the tool steel again caused the least amount of composite wear. This work thus demonstrated that the counterface does significantly determine the wear resistance of a metal matrix composite and that the hard T1 tool steel provided the best overall wear resistance for materials paired.

The observation that a ceramic counterface can cause more severe rates of wear at low sliding speeds was earlier observed by Alpas and Zhang [11]. At a low sliding speed of 0.2 m/s a ceramic counterface (mullite, $3Al_2O_3{\cdot}2SiO_2$) caused the transition from ultra-mild wear rates to occur at lower applied loads when compared to a plot made with the composite paired against a 52100 bearing steel, Figure 2.15. The I/II wear transition observed was related to the initiation of particle fracture during the dry sliding contact. As illustrated in Figure 2.15, the ceramic counterface shifts the transition so that more severe wear occurs at lower contact stresses.

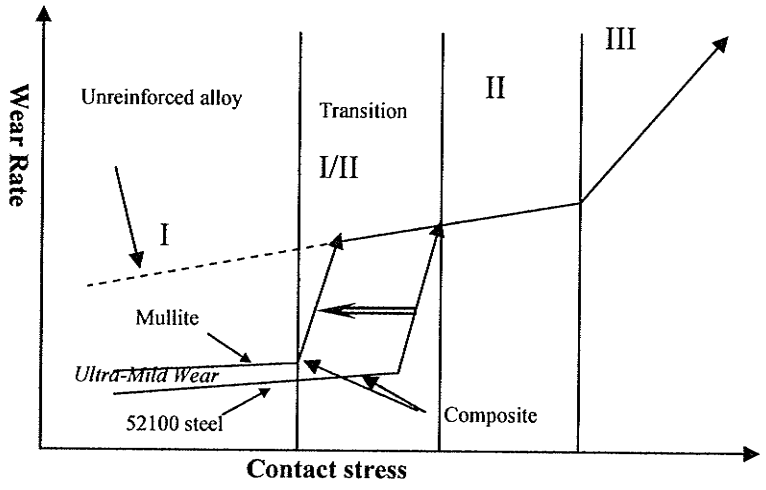

Figure 2.15 The effect of the counterface on the transition load and wear rates at low contact stresses. The ceramic counterface caused fracture of SiC particles at a lower contact stress resulting in an earlier transition to severe wear. Alpas and Zhang [11], 1994

Subramanian [58] examined various metal counterfaces for an unreinforced Al-Si alloy, solution annealed to spherodize the Si phase. Sliding velocities from 0.1-10 m/s and applied loads from 4.5-225N (block-on-ring setup, ring diameter of 30mm) were used to construct linear plots of the normalized wear rate for each counterface material. Ratings were given based upon the lowest wear rate of the binary Al-Si alloy and are listed in Table 2.5. In terms of wear performance at low sliding speeds (the primary focus of this report) the Partially-Stabilized Zirconia (PSZ) ceramic counterface caused an order of magnitude higher Al-Si wear rate than when the aluminum alloy was mated against the hard die steel counterface. Again, the hard die steel was determined to be the best choice for a counterface material, this time based on its causing the lowest wear rate for the matrix alloy alone. These experimental results [11,58,90] indicate that hard ceramics at low sliding speeds appear to act as a worse choice for a counterface material for both Al-Si alloys and aluminum metal matrix composites compared to hardened steel. Noting the rating of the

steels listed in Table 2.5, in can be concluded that the wear rates for aluminum-silicon alloys can be reduced as the hardness of the steel counterface is increased. This observation has also been demonstrated for Al-SiC composites [14,90]. This behaviour should be noted when comparing wear results with different steel counterfaces.

MATERIAL	HARDNESS HV (kg/mm^2)	RATING	AL-SI WEAR RATE
Al -12.3wt%Si (block)	**39**	-	**↓COUNTERFACES↓**
Copper	52	7	$\widetilde{W} = 162\left(\widetilde{F}/\widetilde{V}\right)^{0.69}$
Cu-4.6Al	76	6	$\widetilde{W} = 95.5\left(\widetilde{F}/\widetilde{V}\right)^{0.73}$
Cu-7.5Al	114	2	$\widetilde{W} = 5.5\left(\widetilde{F}/\widetilde{V}\right)^{0.55}$
Mild Steel	114	4	$\widetilde{W} = 19.5\left(\widetilde{F}/\widetilde{V}\right)^{0.52}$
4340 Steel	440	3	$\widetilde{W} = 18.6\left(\widetilde{F}/\widetilde{V}\right)^{0.55}$
Die Steel	770	1	$\widetilde{W} = 2.1\left(\widetilde{F}/\widetilde{V}\right)^{0.43}$
PSZ	1027	5	$\widetilde{W} = 34.7\left(\widetilde{F}/\widetilde{V}\right)^{0.57}$

Table 2.5 Comparison and ranking of different counterface materials against a 12.3wt% Al-Si alloy. Subramanian [58], 1991

Finally, the wear rates of the Al-Si significantly decreased as the hardness of the counterface increased for pure copper to harder Cu-4.6%Al and Cu-7.5%Al alloys. This may be related to a reduction in adhesion, which is the crux of poor aluminum wear resistance at any applied load. If surfaces are of comparable hardness and metallic composition adhesion theories predict very strong asperity junctions will form, resulting in much more severe adhesive-transfer wear [50,91,116]. The hardness of the softer alloy copper was close to the Al-Si alloy promoting adhesion, while the Cu-Al alloys had compatibility due to the Al solubility promoting adhesion. Comparing the two variables for

the counterface it can be seen that increased hardness had the more significant effect, as increased compatibility did not impair wear resistance.

2.41 REQUIREMENTS FOR MECHANICAL MIXING TO OCCUR

(I) DEFINITION OF A MML OR TRIBOLAYER

A distinction must be made between mechanically mixing and tribolayer. A tribolayer can consist of a heavily deformed surface, evolved from the motion of surfaces in contact that has been microstructurally and compositionally altered. A suggestive interpretation is that a tribolayer *is produced by a process* of mechanical mixing. Of course this does not apply to all observed tribolayer phenomenon, however it does apply to the fine particle surface mixtures found at the surface of binary Al-Si alloys and Al-composites. The process of mechanically mixing can include cyclic debris compaction and generation, matrix deformation, reinforcement fracture, chemisorption, or transfer across the interface that occurs by events of adhesion and delamination fracture. It is important to articulate that these mechanisms of mechanical mixing can occur abundantly without a tribolayer forming.

A tribolayer, by some definitions [57], must include mutual material transfer between the two surfaces in contact. A distinct surface formed by cumulative strain often better describes the case where only one surface is altered when in sliding contact and where no elemental transfer occurs. Being mindful of what is defined as a layer, a minimum thickness of a tribolayer should cover the bulk metal surface. In this sense, a tribolayer should be a relatively stable in covering the unmixed subsurface. Patchy surface

adhesive transfer of the Al-MMC found under reciprocal sliding should not be defined as a tribolayer [14,24]. A surface mixed layer, SML [99], was identified to form during reciprocal wear of an Al-20%SiC MMC. This layer was tentatively produced by a mechanism of smearing and attrition of the SiC reinforcement, since very little transfer of the steel counterface occurred [64]. This SML was observed to be removed at long sliding distances [64]. Since the layer was not stable and did not contain counterface mixing it was not considered a MML. Under unidirectional sliding for this composite, a stable and continuous mixed surface was observed to form for long sliding distances containing significant transfer from the counterface steel, therefore fitting under the definition of a MML [25,34].

As a final point, for a MML to be particularly beneficial, this tribolayer must impart some degree of wear resistance. Ideally the bulk of surface wear should be contained in the tribolayer, providing an inherent wear resistant coating. The terms MML and tribolayer are often used interchangeably; however a MML is a specific tribolayer phenomenon and is the preferred term to describe the mechanical mixing found on the surface of Al-materials during dry sliding wear.

For Al-MMC materials two forms of continuous tribolayer phenomenon have been observed against a steel counterface: 1) A oxide tribolayer that has formed predominantly by abrasive transfer of iron and oxidized aluminum [11,12,39] and 2) A mechanical mixed tribolayer containing comminuted SiC, Al matrix under high strain, iron oxides and transferred elemental iron from the steel counterface [25,32,33,34]. The second observed mechanically mixed layer has been formed through and found to require significant deformation of the composite surface.

(II) SLIDING CONDITIONS THAT FAVOUR MML

For two metals in intimate contact, a MML has been described as occurring through very high shear strains (in the order of 10-100 times) causing 'tongues' to form of what were once asperities, which overlap, become interlocked, then are mixed and compacted into a single solid [19]. For conditions were the debris is observed to play a major role, the formation of the tribolayer has been described as formed by a process debris transfer from one surface to another, followed by compaction and consolidation of the debris particles into a coherent layer [92]. For this process, Deuis and Subramanian [57] suggest that conditions of high sliding speeds and high contact pressures allow fewer transfer and back transfer events that favor the formation of a tribolayer. Clarke and Sarkar [78] further noted that for a transfer layer to be stable and reduce the rates of wear on each surface, continued transfer between surfaces must occur.

A MML is favored by a mechanism of transfer, directly or through debris, of matrix units of a small size [29]. Small adhesive particles or abraded debris of sizes significantly less than the surface roughness are more likely to be integrated into a mechanically mixed layer and less likely to be ejected from the interface. As a result, larger debris sizes produced through adhesion-delamination can simultaneously reduce wear performance by 1) greater surface damage of the composite as compared to having abrasion as the more dominant mechanism and 2) *reduction of mechanical mixing due to the larger debris size being more easily removed from the interface* [2]. Reduction in mechanical mixing may also occur due to increased reinforcement particle size and/or increased volume fraction as a result of the more difficult situation for hard debris to redeposit and penetrate into a surface with a greater area fraction of hard reinforcement phase.

As mentioned earlier, for a MML to subsist it requires continued debris production and deformation to generate and regenerate this mechanically mixed surface. Therefore the sliding conditions that allow a MML or tribolayer to form are rarely near the operating parameters desired for a design, due to tolerances that must be maintained. For example, for a 5/1000" tolerance specification, deformation above 150μm cannot occur. Mixed depths greater than this have been often associated with reported MML formation [33,34]. An additional negative result of the high surface deformation required is a relatively high coefficients of friction, Table 2.6.

PIN **Material Pair** *DISK*	**1045** (220HV) ***On*** **1045** (220HV)	**HP Al** (42HV) ***On*** **HP Al** (42HV)	**HP Al** (38HV) ***On*** **Steel** (532HV)	**7075 ST** (85HV) ***On*** **Steel** (532HV)	**7075 Aged** (185HV) ***On*** **Steel** (532HV)	**Al-40% SiC** (78HV) ***On*** **Steel** (532HV)	**A356-20% SiC** (55HV) ***On*** **Steel** (60HRC)
Initial C.O.F.	0.1	0.3	0.1	0.1	0.1	0.5	-
Steady State C.O.F.	0.6-0.8	0.4-1.4	0.4	0.35-45	0.15-0.2	0.65-0.75	0.45-0.65
Degree of mechanically mixed surface	No MML	No MML	20 μm MML	5 μm MML	10 μm MML	15 μm MML 2.5 μm SiC	Iron Oxide Transfer Layer 40 μm SiC
Sliding speed (m/s)	0.1	0.1	1	1	1	1	1
Contact Pressure (MPa)	0.45	0.45	1.8 [50N]	1.8	1.8	1.8	2
Study	Hwang *et al.* [47]	Hwang *et al.* [47]	Venk & Sund [33]	Venk & Sund [33]	Venk & Sund [33]	Venk & Sund [33]	Ravikiran & Surappa [39]

Table 2.6 C.O.F. obtained for dry sliding and observed mechanical mixing for various materials in pin on disk unidirectional tests.

Noting the relative coefficient of friction (C.O.F.) between no MML and a thin MML present, the existence on an MML alone does not appear to have as significant of effect on C.O.F. as does hardness and volume fraction of reinforcement.

(III) REQUIREMENT OF A SECOND PHASE

Venkataraman and Sundararajan [32] stated that for a MML to form, a reinforcement phase harder than the mating disk material is required. This statement is not falsified by an MML found on high purity Al and Al-Si alloys, as hard particles promoting mechanical mixing of the steel disk into the aluminum surface can be identified as aluminum oxide and Si eutectic particles respectively [66]. To advance this statement, Li [34] stated that a *reinforcement* particle with a higher hardness than the original material is not a necessity for an MML to form.

A thicker MML was found to form on an Al/SiC composite surface as compared to a finer surface mixed layer formed on the unreinforced alloy [33] . The difference in behaviour was attributed to the presence of SiC acting as sites for the nucleation of shear instability, resulting in promotion of turbulent plastic flow. Instability caused by hard second phase particles may be the cause of the critical maximum thickness of observed transfer layers [116]. Subsurface cracks initiate delaminations of the transfer layer; as a result in situ MML growth is constrained by fracture events. Consequently the hardness of the MML layer and the applied load has direct consequence on MML fracture and stability.

2.42 ROLE OF OXIDATION

In the ultra-mild-wear regime, wear can be controlled by the following oxidation process [55]:

1) Frictional heating results in the formation of an oxide layer on the asperities in contact with the counterface

2) Localized fracture and spalling of the oxide layer occurs during wear

3) Subsequent reformation of the oxide film occurs through frictional heating, filling in holes in the oxide layer topography.

The, protection by an oxide film by this process will be dependant on sliding distance as well as the peak frictional temperatures thus achieved, controlling the rate of oxide formation [1]. The contribution of this oxidation wear process is generally considered low under plasticity dominated wear conditions, where frictional heating is minimal. Al-Si alloys have been observed to experience high wear rates during the initial "wear in" during dry sliding, which decreased in severity due to the supposed buildup of an oxide "film" [107]. The degree of Si particle comminution was stated to provide indication of the alloys ability to maintain oxide film protection during sliding deformation [84]. Additions of Si increased the yield strength of the alloy and therefore were expected to improve the retention of a brittle oxide layer. This early observation by Eyre and Davis was later contradicted by Antoniou *et al.* [59,92], who observed that the dark surface film on worn Al-Si alloys was actually a composition of very fine particles of Al, Si and Fe counterface material, with relatively little aluminum oxide. This indicates that surface mechanical mixing forming a protective film was decreasing wear of Al-Si alloys rather than a retained surface aluminum oxide layer as previously postulated. For wear at low sliding speed this confirmed that surface oxidation may not play a critical role in increasing wear resistance of the matrix alloy.

It is also unclear how significant is the formation of an aluminum surface oxide layer in increasing wear resistance of aluminum metal matrix composites [57]. Aluminum oxide layer thickness at room temperature is very thin in the range of 0.01-0.1 μm [55,67] which compared to the average worn surface roughness of 1-4 μm [22] for a composite with small 1.8 μm SiC particles this layer is still very thin. Larger particles than 1.8 μm are more commonly used, with composites made with particles up to 100 μm in size, resulting in higher surface roughness and consequently higher ratios of the oxide thickness to the asperity size. This is based on a reasonable assumption that reinforcement of larger sizes constitute a considerable number of the asperity contacts. Therefore a nascent formed oxide layer on an aluminum asperity [84] at low sliding temperatures is unlikely to be the dominant cause of ultra-mild wear rates due to the aluminum oxide-counterface oxide interaction not prevailing as the dominant interaction with SiC asperities present.

Considering wear at low pressures, a transition to high wear resistance of the composite when in air has been interconnected with oxide transfer from the steel counterface. A compacted and sufficiently thick iron oxide layer, in the order of several micrometers has been observed to be the cause ultra-mild rates of wear [8,11]. For Al-MMCs the reinforcement phase allows this formation of a stable oxide tribolayer usually not achievable by the unreinforced alloy. The SiC causes increased oxide abrasion, producing layered oxide deposits on the composite surface [62]. Furthermore, the presence of SiC disrupts a continuous aluminum oxide film, which therefore can rupture easily, resulting in greater mixing of the small oxide particles at the sliding interface [117]. For aluminum, it has been observed that almost complete oxide-rupture occurs under lubricated conditions during steady state sliding, primarily due to plastic deformation matrix beneath

the oxide-metal interface [55]. Finally as debris, the hard ceramic particles in the interface are stated as promoting chemisorption, resulting in higher surface oxidation and higher amounts of surface aluminum oxide capable of resisting wear [61]. Pramilla Bai [71] found higher percentages of oxides on the Al-Si-SiC surface as compared to the base metal alloy worn surface. Higher oxide was also found with an increase in SiC reinforcement from 15 to 25% [71]. Therefore for Al-MMCs, mixing of oxides and the formation of a compacted oxide tribolayer can improve wear resistance at low sliding pressures that allow this layer to be stable [8,11].

At very low pressures a mechanism that incorporates the role of the aluminum oxide layer has been proposed [118]. When an oxide-covered aluminum asperity comes into contact with the counterface at low pressures, high interfacial shear stresses at the interface may develop at the junction, causing the hard oxide to act as an anchor and promoting adhesion and small transfers of base matrix [55]. This process has been defined as oxidation assisted mild adhesion wear [118]. This interlocking/adhesion mechanism has been proposed to cause to mild wear in the lower left corner of the wear mechanism map, Figure 2.14.

At higher pressures, many observations have been made that contradict this proposed wear mechanism, primarily due to the viewpoint that oxidation can have a significant role in decreasing adhesion between the plastically deformed contact surfaces, and thus has the potential to decrease production of adhesive debris [51,61]. Larsen and Rigney [48] compared wear behaviour of an Al alloy and Al-MMC at high temperature in both air and vacuum environments. Under vacuum the aluminum alloy formed a smooth transfer layer on the steel counterface and experienced wear by smearing and extrusion,

resulting in very little debris, and a very low weight loss. In a gaseous (air) environment, oxidation disturbed the adhesion of the transfer particles between surfaces resulting in the ejection of large adhesion induced delaminations of the monolithic alloy. Very severe wear (over 1000x higher than in vacuum) resulted, with patchy transfer of the aluminum to the steel counterface [48]. In this case reduced adhesion by oxidation resulted, however it had a negative effect on wear resistance.

For a 2080-15%SiC MMC under vacuum, again transfer of the aluminum composite to the steel counterface resulted. However due to the presence of the SiC particles continued smearing could not occur and adhesion-induced delaminations were produced from the unstable surface and removed from the interface causing high composite wear. In comparison, for the composite aluminum tested in air no Al transfer to the steel counterface occurred, instead fine powder wear debris was mixed on the surface, and very low composite wear resulted [48]. In both cases the role of oxidation can be clearly seen to reduce adhesion, not promote it. Furthermore, oxidation was observed to tremendously increase the wear resistance of the composite material, and have the exact opposite effect on the monolithic alloy. The sliding speed was 0.02 m/s, with approximately 2.75 MPa applied pressure and a 410°C surface temperature [48].

Due to omnipresence of O_2 during environmentally exposed sliding wear conditions, confusion exists in the low speed / low pressure region of wear mechanism maps for Al metal matrix composites where the formation of an oxide layer can have the most significant effect. Wilson and Alpas [12] define the dominant wear mechanism as mixing/oxidation, Wang *et al.* [118] define the dominant wear mechanism as mild

oxidation, and Kwok [18] defines the dominant wear mechanism as abrasion, in what can be roughly considered the low speed, low pressure sliding conditions for these Al-MMCs, Figure 2.16. However a common observation of wear associated with these sliding conditions is the production of fine equiaxed debris particles, dark-grey to black in appearance, in agreement with the empirical wear-mechanism map by Subramanian for Al-Si alloys [15].

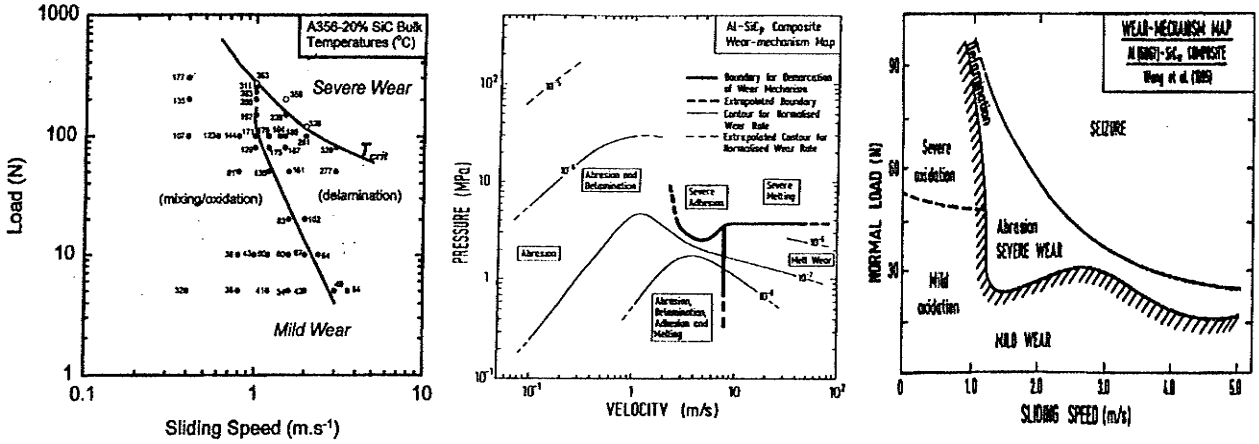

Figure 2.16 Three wear–mechanism maps for Al-MMCs. Left: Wilson and Alpas [12], Middle: J.K.M. Kwok [18] Right: Wang *et al.* [118]. Note confusion of the wear mechanism at low loads and low sliding speeds

These fine equiaxed debris particles have been analyzed to consist of α-Al_2O_3, FeAl, α-Al and α-Fe [34] and therefore cannot be stated as a product of pure abrasion or as purely formed through oxidation. Pure oxidation can only be stated as the dominant wear mechanism if a coherent oxide tribolayer forms, which has been observed to form at very low loads [11], however mechanical mixing of the matrix through abrasion is a major contributing mechanism for the lower left corner of the wear mechanism map and cannot be ignored.

In conclusion oxidation has an influential role in the wear behaviour, and appears to have more benefit in increased wear resistance for Al-MMCs compared to monolithic aluminum alloys.

2.43 ROLE OF DEBRIS

Sasada *et al.* [61] introduced the concept of a specific size required for the ceramic particles to act as abrasives, causing wear by plowing and cutting actions. It was concluded that fine ceramic particles would not promote abrasion if the size of the particles was below a critical (maximum) size. SiC, Cr_2O_3 and Al_2O_3 particles, average size of 3 μm, were introduced between different metal pairs at 0.05 m/s and an applied pressure of 0.08 MPa. Particles of this size were considered to be below the critical particle size for abrasion to occur [61]. Nonetheless, with the ceramic particles introduced into the interface wear still became more severe. This was correlated to the ceramic particles in the interface promoting an increase in adhesive transfer between surfaces.

Additionally, ceramic particles in the interface as a third-body were entrained by the surface which could provide the strongest mechanical/ chemical bonding, causing the ceramic particulates to be mixed and retained on the surface, which significantly reduced the wear rate. During initial sliding, few ceramic particulates were present on the surface and severe wear occurred through large adhesive delaminations. Therefore, similar to the role of oxidation, ceramic particles on the surface were observed to reduce adhesion by some degree, which ultimately improved the wear resistance of the some of the soft metals where adhesion would normally severely limit performance.

In the discussion so far hard particles have been stated as both increasing and decreasing adhesion. This can be clarified by noting different roles hard particles partake depending on their location: hard particles mixed into the surface decrease adhesion, while hard particles that remain as third bodies in the interface increase adhesion. Table 2.7 lists different metals pairs tested with hard particles in the interface, with a transition to a mild wear rate indicated for metal pairs where fine particles mix into the surfaces.

Hard ceramic particles in the interface is not sufficient on its own for a transition between mild and severe wear to occur as no transition was found for self mated Cu in the presence of small SiC particles, Table 2.7. Wear rates remained severe and no accumulation of a hard protective particle layer occurred. For all the metal pairs tested in Table 2.7, if no mixing occurred the wear rate would remain substantially higher than, or as a minimum, be unaffected by the presence of the hard ceramic particles. In other words, without mixing, the wear rate was never shown to decrease. Therefore, mixing of hard particles and hard debris can be seen as critical for achieving low wear rates, as without mixing the damage with these particles present can be expected to be much more severe. To support this, Ni on Ni was unaffected by ceramic particles in the interface, however when Ni was mated against a harder Mo counterface, a transition was observed to a lower wear rate, which also corresponded to transfer and mixing on the Ni surface in the presence of the fine ceramic particles. Besides also showing the critical importance of mixing, this also suggests that a material pair with considerably different hardness may be a factor in allowing for mechanical mixing behaviour in the presence of hard particles.

Tube / Disk	Al	Zn	Cu	Ni
Al	M	M	M	-
Zn	M	M	M	-
Cu	M	M	S	-
Ag	S	M	S	-
Ni	-	-	-	**N.E.**
Mo	-	-	-	**M**

M - Mild wear rate transition through surface mixing of ceramic particles

S - Severe wear with ceramic particles present in the interface

N.E. – Not affected by the addition of ceramic particles in the interface

V = 0.05 m/s P ≈ 0.08 MPa

Table 2.7 Summary of results with ceramic particles added in the interface. When the particles mechanically mixed into the surface a transition to a mild wear rate was observed. Oike, Emori and Sasada [40], 1987.

All discussion so far has been related to hard particles in the interface as this relates well to fine equiaxed debris particles produced during aluminum and aluminum composite wear. However a clear distinction must be made between the role of hard particles (debris) as a third-body in the interface and the role of hard particles deposited on the wear surfaces [2]. The most evident distinction is in how each contributes to mechanical transfer. Hard particles in the interface can mix with the metal surfaces before becoming ejected from the wear interface, essentially promoting small abrasion and adhesion transfer. An additional benefit of fine ceramic particles in the interface was observed by an active role it played in the reduction of debris agglomeration [61]. Large debris sizes are more easily removed from the interface promoting wear and can also cause severe surface damage before being ejected.

The role of ceramic particles on the surface, as noted earlier, can disrupt direct surface to surface transfer and therefore decrease adhesion wear. This is the opposite role of ceramic particles in the interface, which can promote surface to surface transfer,

although indirectly. The extent that fine ceramic particles accumulate on the surface as compared to particles remaining in the interface can affect adhesive transfer wear and therefore if a transition to mild wear will occur with a reduction of this wear mechanism.

Ceramic particle accumulation on the surface is analogous to the formation of a mechanically mixed layer. Accumulation of ceramic particles requires sufficient contact pressure to "press in" hard particles on the surface *and* the ability of the matrix to withstand the plastic deformation without cracking resulting in surface instability.

Overall, the possible role of hard ceramic phase is very different on the surface as compared to in the interface. A further conclusion may be drawn that if abrasion does not significantly increase (as noted for small ceramic particles) *and* surface mixing occurs, presence of a hard ceramic phase on the surface may act to reduce wear. For Al-composites, mixing debris containing a hard ceramic phase can be expected to depend upon the initial reinforcement size, morphology and extrinsic sliding conditions that make mixing possible.

2.44 FRICTION, MIXING, AND TRANSFER

(I) FRICTION MODELS

Any discussion on frictional behaviour must begin by recognizing the original work of Tabor [97], who stated that significant understanding of frictional behaviour can be found when the surface interactions are divided into 1) an adhesion term and 2) a plowing term. Suh and Kim further proposed that plowing of surfaces by asperities and wear particles was the most significant interaction to the frictional forces [56]. A vast number of

mathematical models have been proposed which all state sum assumptions of the nature of asperity contacts and the forces involved in these microscopic surface interactions. Models of friction for reinforced metal matrix composites cannot be simply made, since further assumptions are required to include the relative role of the hard reinforcement phase, in addition to the elastic/plastic behaviour of the matrix. Understandably, an no accurate friction model exists that considers transfer, mixing and surface/debris contact which are consistently present during dry sliding wear of ductile material under plasticity-dominated sliding conditions.

As a starting point, for composite materials, each material in contact can be considered to contribute a frictional component. Considering an Al matrix with SiC reinforcement,

$$\mu_{sliding} = f_1 \mu_1 + f_2 \mu_2$$

Al - Component 1
SiC - Component 2

f = the area fraction of the phase on the sliding surface
μ = the friction coefficient resulting from self-mated sliding

This model has been used to predict friction under lubricated conditions with adequate accuracy [129]. However, the above rule of mixtures approach to estimating friction has severe limitations in usefulness during dry sliding wear as:

1) With a mechanically mixed surface layer area fractions are unclear.

2) The interaction of debris has been observed to severely alter the C.O.F. as compared to simple monolithic Al or SiC phases in contact.

3) Conditions are common where delaminations vary the surface volume fractions of matrix/reinforcement in a cyclic manner.

In this study the greatest emphasis is placed on friction behaviour at low sliding speeds where asperity melting and bulk frictional heating do not regulate the frictional behaviour. Therefore friction remains best determined experimentally.

(II) TRANSFER OF ELEMENTAL FE AND COF

Variations in μ have been related to the extent of Fe transfer to the Al-composite surface. Greater Fe transfer caused more regularity in the recurrence of steel sliding against steel at the interface [130]. Gross material transfer to the Al-composite surface was related to a process of delamination/adhesion of debris or through abrasion of the steel counterface. Either process would result in iron deposits on the mixed surface. A high friction coefficient was correlated with the formation of the iron (not iron oxide) transfer layer causing like metals in contact at the interface [9]. Oscillations in the coefficient of friction could occur in accordance with the transfer and subsequent delamination of the iron from the Al-composite surface [130]. Transfer of relatively large steel debris and mechanical mixing were shown to generally increase friction when the transfer is patchy [39]. However, the continuous transfer layer of iron has been established as a primary mechanism in reducing the wear of Al-Si alloys [6,59,92] and Al-composites [11,106]. In most of these wear studies it is not fully clear if the transfer is predominantly of elemental iron or iron oxide. Nonetheless, an even distribution of the transferred counterface steel on

the composite surface has been consistently observed to reduce friction fluctuations and be the better case for wear resistance.

(III) TRANSFER OF IRON OXIDES AND COF

Mechanical mixing that results from iron oxides being transferred to the Al-composite surface from the steel counterface have been well documented [11,12,33, 45,62,130]. A mechanically mixed or abraded layer of iron oxides has been in part credited with improved wear resistance at low applied pressures. The reduction in wear occurred in a similar manner to the organic transfer layer formed by a brake friction material mated against Al-SiC, as observed by Howell and Ball [77]. Once the coherent transfer layer is formed through the abrasive action of the SiC, wear occurs through shearing of the soft layered material in the interface. Knowing this, a lower coefficient of friction has been related to sliding conditions that allow for the transfer of iron oxide layer. The built up iron oxide layer has a low shear strength, in comparison to sliding conditions that cause transfer of elemental iron [11]. The iron oxides, Fe_2O_3 (low temperature oxide) and Fe_3O_4 (high temperature oxide), when retained at the interface can provide a shear layer requiring minimal energy [97], due to high hardness (H) and low shear strength (τ_{sh}), or τ_{sh}/H [49].

(IV) MML AND COF

As stated earlier, for low loads that allowed the SiC to act as load bearing elements, and where abrasion of the steel counterface was a much more prominent occurrence than SiC particle fracture and mechanical mixing, a transfer layer of iron oxide was found to

form. A mixture of iron and iron oxides existing at the interface allowed for a low coefficient of friction and was described as providing some *in situ* lubrication at the junction [11]. As a result, a lower coefficient of friction resulted under conditions that cause fine iron oxides to form a transfer layer on the Al/SiC.

In contrast, when a MML was formed at higher loads abraded iron oxide was mixed into the surface and was incapable of providing an interfacial layer. This consequently resulted in a higher C.O.F. [32]. Venkataraman and Sundararajan noted that the presence of iron oxides was found to result in an increased MML hardness, with friction increasing in accordance with higher deformation energy of this layer [32]. It was further stated that the deformation of the contacting surfaces can be assumed to be concentrated in the MML, and for varying degrees of mechanical mixing, a parallel could be drawn between the coefficient of friction and the hardness of the of this layer [32].

(IV) % REINFORCEMENT AND COF

Variations in μ have been reported due to changes in the percentage of reinforcement exposed on the worn surface during sliding. As the sliding speed was increased from 0.5 to 10 m/s fracture of SiC particles continually decreased, allowing a greater percentage of SiC to remain as load bearing elements during sliding [39]. The coefficient of friction responded to changes in elemental transfer, due to changes in abrasion caused by protruding SiC particles that stand firm under the contact stresses, and changes in adhesion due to Fe/iron oxide transfer material fragmenting from and depositing to the surface differently at higher speeds. As a result of the high dependency of μ on the

counterface transfer, a simple increase or decrease in C.O.F. cannot be related to the percentage of reinforcement present on the contact surface.

The percentage of reinforcement intrinsic in the composite aluminum has the most obvious influence on the SiC exposed on the surface. Rana and Stefanescu [131] reported reductions in the sliding friction coefficient with increased volume fractions of SiC against steel, in agreement with earlier findings by Hoskings [76]. Intrinsic to the composite are also the size, shape, distribution and orientation of the reinforcement, shaping how the reinforcement presents itself on during sliding contact.

Sato and Mehrabian [68] provided wear and C.O.F. data for aluminum composites using TiC, Al_2O_3, Si_3N_4, and SiC as reinforcement. The volume percent of reinforcement ranged between 1-30% for the aluminum composites tested. A general conclusion was that the coefficient of friction decreased with increased sliding velocity in the range of 0.04-0.46 m/s. Covering as supplementary range of sliding speeds between 0.5 and 10 m/s, Ravikiran and Surappa [39,130] discovered that fluctuations in C.O.F. decreased as the sliding speed was increased. The steady state friction at 10 m/s was in the range of the fluctuating C.O.F at 0.5 m/s, however the fluctuations disappeared at the higher speeds and the composite experience a lower wear rate.

CONCLUSIONS FROM THIS REVIEW ARE GIVEN IN CHAPTER 5

2.51 POTENTIAL FOR ALUMINUM MMC IN TRIBOLOGICAL APPLICATIONS

Aluminum-silicon alloys have the potential to replace cast iron components in internal combustion engines [9]. By electrochemically removing the aluminum matrix, silicon particles protruded from the surface and it was observed that this surfaced offered the needed improvement in wear resistance to be used as a piston-cylinder bore [6]. Scuffing resistance of an Al-SiC MMC was further improved over the etched hypereutectic Al-Si alloys for this application [143]. Al-Si-SiC metal matrix composites can offer additional wear resistance through improved seizure temperatures [72], higher plastic limit, and improved fatigue strength [102]. Howell and Ball [77] recently demonstrated that a cast Al-Si-20vol%SiC composite used as brake rotor can achieve equivalent wear resistance and more stable friction behaviour than the most commonly used grey cast iron material. To achieve this, an organic friction lining was required that formed a stable transfer layer through SiC abrasion. Optimization of the particle reinforcement sizes of the brake rotor and semi-metallic brake pad has allowed for recent aluminum-composites to be on par or exceed the performance of the most common steels used in this application [126]. Despite improvements made, Al-MMCs most often exhibit a lower service life and relatively high wear rate in comparison to the use of steel for the same application.

(I) LUBRICATED WEAR

Mechanisms of dry sliding wear accurately extend to wear mechanisms under lubricated conditions. Microgrooves, ploughing and abrasive wear occur most commonly during lubricated wear; spalling, delamination and adhesion transfer increase during dry

sliding wear. With lubrication, chemical reactivity of the Al-matrix can be an inherent obstacle for Al-composites in tribological applications [103]. In low sliding speed applications such as gears and bearings, extreme pressure additives containing sulfur (sulphurized olefin) or chlorine (chlorinated paraffin) may increase oxidation of aluminum asperities under lubricated conditions [104]. The danger of chemical reactivity is reduced with higher solid solubility of iron in the aluminum alloy [105], which has given an impetus for mechanically alloyed Fe-Al composites to further increase tribological performance. Noting this, iron transfer, mechanical mixing and MML formation with high iron content against a steel counterface offers excellent potential for a reactive tribolayer on the Al-MMC surface under lubricated conditions as well as the documented [31,32] improved wear resistance shown under dry sliding conditions.

(II) INCORPORATION OF A MML OR TRIBOLAYER

Research by Bowden and Tabor has found that metal surface films possessing low shear strengths can allow for very low friction coefficients ($\mu<0.1$) and wear rates under dry sliding conditions [91]. Understanding this, Tabor further proposed two fundamental questions to incorporating a tribolayer as a means of reducing friction and wear:

1) How are the films attached to the substrate?
2) How do they break down?

Mechanically mixed layers found on Al-MMCs have exhibited high hardness, high shear strength and therefore high friction coefficient during dry sliding. Formation of a

subjacent soft shear layer in the bulk material that does not possess the deformation resistance of the mixed surface can cause the breakdown of the protection allotted by the MML, Figure 2.11, especially since the level of plastic deformation required to initially form this layer could not be continually maintained under engineering tolerances. Therefore, MML formation as so far observed has more setbacks than benefits for incorporation into a design to improve wear performance.

Further concern exists that mechanical mixing of hard particles will not occur under lubricated conditions. Fractured reinforcement increased friction and was observed to cause more damage though abrasion than the benefit it offered in wear resistance through surface mixing under lubricated conditions [125]. It has been proposed that Al-MMCs must be operated in the lubricated condition against a steel counterface for adequate performance [108,125]. Incorporation of a MML, with mixing of the reinforcement phase under lubrication has not yet been demonstrated practically. MML alternatives that could be more practically accomplished include incorporating a soft metallic phase to be mechanically mixed, or use of reinforcement of larger size to support a more stable tribolayer that is not as dependant on the mixing of the Al-MMC material.

To summarize, Kapoor and Franklin [29] simulated different possibilities for the mechanical properties of a MML and concluded that the desired properties for enhanced wear performance would be 1) a low coefficient of friction, 2) a high hardness, 3) high work-hardening ratio, and 4) high ductility. This can be considered a wish list for any wear surface.

The influence of forming a MML on reduced wear rates can be found by comparing wear rates for the wide range of Al-MMC composites examined in this literature review.

Wear rates are best described in terms of mg/m or mm^3/m with the composite density ranging from 2.8 to 3 mg/mm^3. Most dry sliding studies found the composite wear rate under "mild" plasticity-dominated conditions to be in the range of 10^{-2} to 10^{-3} mm^3/m. The minimum wear rate observed by Venketaraman and Sundararajan [31] with a MML present was about $3x10^{-3}$ mm^3/m. This lowest wear rate correlated to the minimum thickness of a MML, found for an Al-40%SiC composite with an average particle size of 2.5 μm. Most studies found higher wear rates than this for similar low speed plasticity-dominated sliding conditions [22,23,39,41,68,75,76,106,109].

This low wear rate was however comparable to that of most Al-Si-20%SiC composites with average particle sizes between 7-15 μm [16,52]. Larger 40 μm particles used by Surappa for the same matrix and volume fraction of reinforcement experienced significantly higher wear [39,130]. The Al-Si-SiC composites with smaller particle size were shown to exhibit MML behaviour [25,34], while the larger particles caused abrasive Fe transfer [39]. This demonstrated that for Al-Si-SiC composites in which this study is focused have excellent wear resistance compared to published wear rates for other Al-MMCs.

More recently, Straffelini [8] observed a wear rate of $1x10^{-3}$ mm^3/m, 3x lower than the lowest rate observed by Venketaraman and Sundararajan [32]. The composite used had 60vol% Al_2O_3 with particle sizes in the range of 1-5 μm. This composite also exhibited both plastic flow in the surface layer and the formation of an iron oxide transfer layer. This result shows promise in the use of a stable tribolayer in promoting superior wear resistance for Al-MMCs. Further it can be clearly seen that MML formation has allowed for some of the lowest wear rates published so far in literature.

CHAPTER 3 EXPERIMENTAL PROCEDURE

3.11 APPARATUS

All wear tests were performed using a ball-on-block reciprocating wear tester, used in previous studies [64,65,99]. A schematic of the machine is given in Figure 3.11 and pictured in Figure 3.12. The requirements of the ASTM standard G133-95 for testing methods were satisfied. No lubrication was used in any test. Friction was not measured. The steel ball was fastened to the reciprocating jig, causing it to experience continual contact; the block Al-SiC specimen was stationary causing the composite surface to experience the intermittent contact of the ball sliding. Contact geometry significant affects wear results, and in comparison to the ball on block geometry sliding geometry used here, most commonly published pin-on-disk experiments use the Al-SiC material as the pin, causing instead the composite to experience continual contact. Severe wear has been correlated to the use of the softer material as the intermittent contact surface, as is the case tested in this study [49]. Some predictions state that reduced transfer, reduced wear, and smoother friction traces are more likely to occur with the cohesively weaker material as the continuous contact surface [50,116]. This prediction so far holds true for Al-SiC composites against a steel counterface. Both block-on-ring and pin-on-disk apparatus testing have observed MML formation causing lower rates [25,33], and in both cases the Al-composites, the cohesively weaker material, experienced the continuous contact.

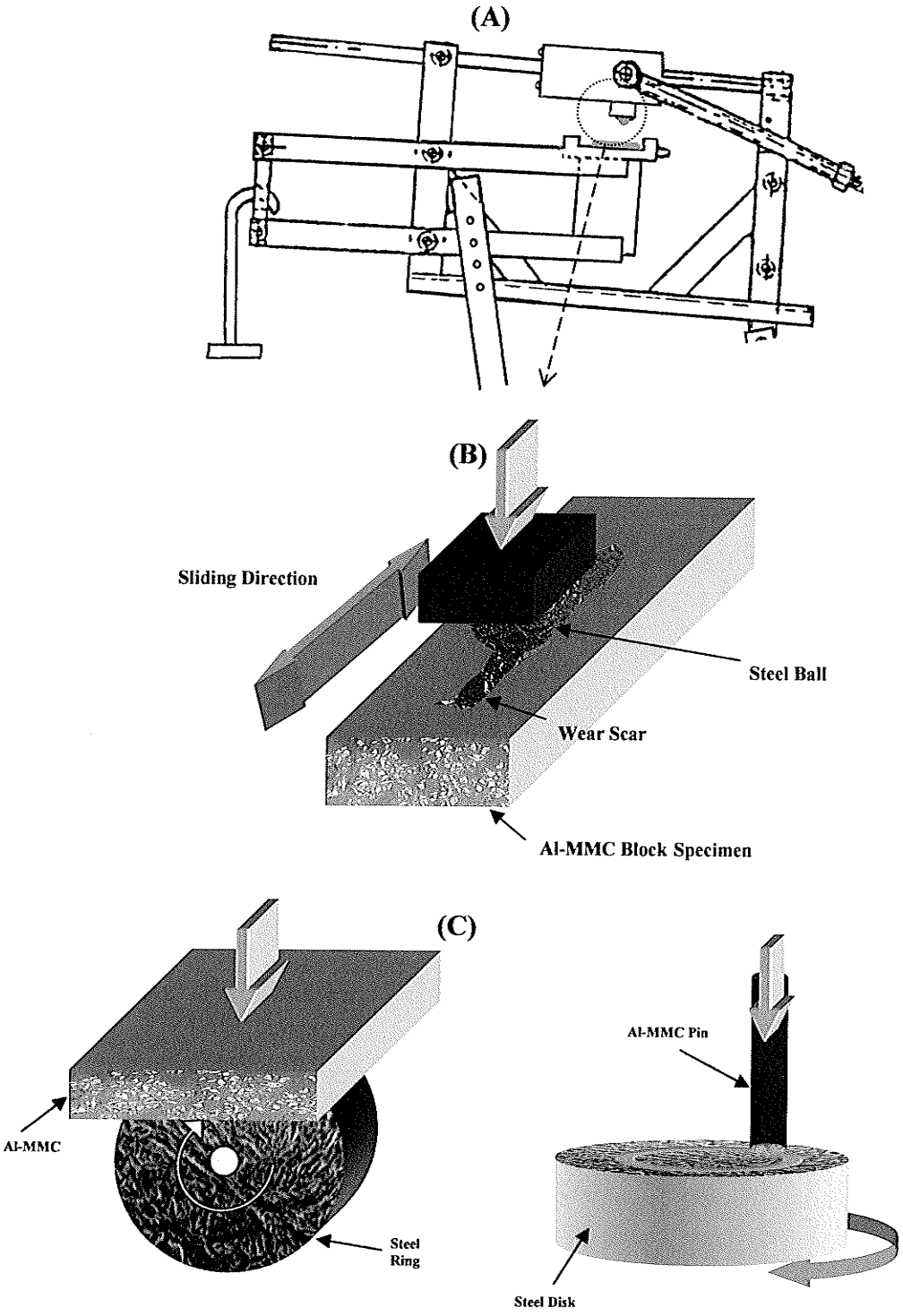

Figure 3.11 (A) Schematic of ball-on-block test apparatus used. (B) Image of composite specimen, steel counterface setup and wear scar produced from non-conformal reciprocal ball contact. (C) Comparison geometries. LEFT: Block-on-ring wear configuration, non-conformal, RIGHT: Pin-on-disk configuration, conforming contact with constant nominal contact area during wear if properly aligned.

With the Al-composite as the intermittent contact surface for ball-on-block testing the wear rates were considerably higher for equivalent applied load and sliding speed compared to the opposite geometry [90] and no continuous MML has been observed [14].

3.12 RECIPROCAL TESTING AND CHOICE OF VARIABLES

Two sets of reciprocal testing were used to examine wear, wear mechanisms, mechanical mixing and transfer of elements. First each counterface was tested over a range of applied loads. Each test had a total reciprocating sliding distance of 250m. To examine the progress of wear and elemental transfer, a low load of 2 N was applied over different sliding distances from 1 m to 2000 m for the steel counterfaces. Weight loss of the ball and sample was accurately measured to 0.1 mg for each counterface specimen for normal loads between 2 and 150 N. Sample to sample variance was a concern due to the non-uniform nature in which SiC was distributed; therefore, each test was done at least twice. Reciprocating track length was ¼". Sliding speed was on average 7.5 cm/s, slower than previous studies [34,99]. Velocity in reciprocal wear is stated as an average value, determined by:

$$\text{VELOCITY} = \frac{\text{contact distance of ball for reciprocated stroke (cm) x number of strokes}}{\text{Time of test (s)}}$$

Temperature rise of the sample did not noticeably occur for any test load. Temperature does not need to be considered as a significant variable for the experiments performed. Bulk surface temperature was examined by placing a thermocouple as near as possible to mating surfaces during wear which found the sliding surfaces not to be higher

than ambient. Mechanisms of "cold" wear as defined by Ashby [44] are expected to dominate. Tests were performed at room temperature, approximately 22°C, and between 40-60% relative humidity.

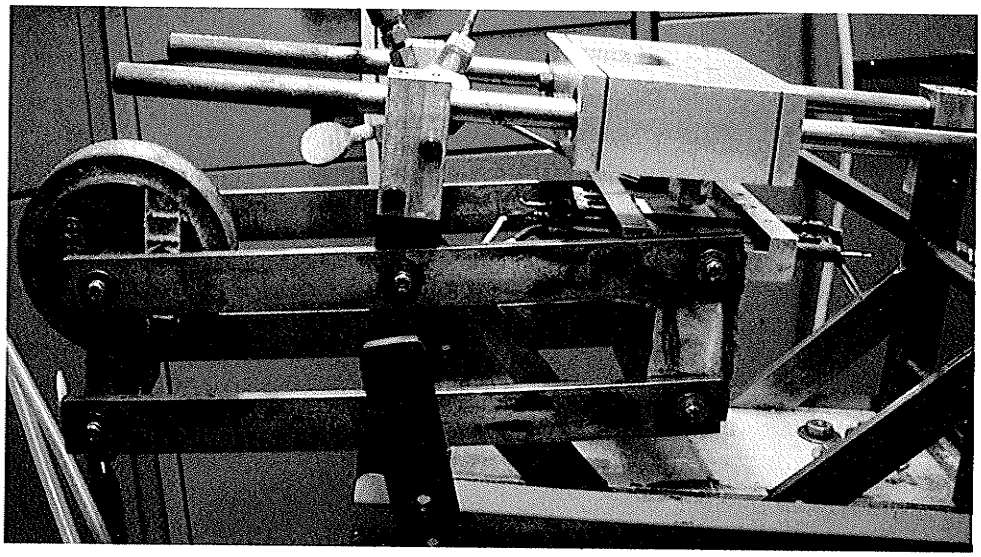

Figure 3.12 Ball-on-block testing apparatus

(I) NON-CONFORMAL CONTACT GEOMETRY

Wear-rate data has more significance when referenced to contact pressure instead of applied force [93]. Normalized pressures and velocities allow wear rates to be accurately compared for different testing configurations, geometries and variable ranges. Both block-on-ring and ball-on-block test methods result in reduced normalized pressure as surface wear causes the contact area to increase. These non-conformal contact geometries initially causing significantly higher contact pressures than data collected using a pin-on-disk apparatus, where, when properly aligned, the nominal contact pressure should remain constant.

(II) CONTACT PRESSURE

To be able to use the presented ball-on-block data usefully on a wear mechanism map, the contact pressure was estimated as a function of sliding distance. As the sliding distances increases the flat surface conforms to the spherical counterface due to wear, forming a concave groove. The nominal contact area can be approximated by an elastic Hertzian analysis, however since the surface deforms plastically this predicts a much smaller contact radius than in the actual case. Consequently, the apparent contact area was better approximated by the surface area of the spherical wear scar on the steel ball, Figure 3.13. Cross-sections of the worn Al-SiC allowed for measurement of the depth of the wear into the surface.

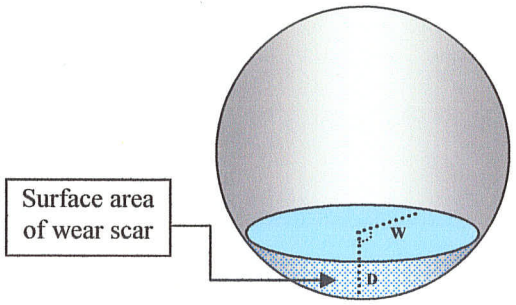

$$S = \pi \cdot \left[D^2 + W^2\right]$$

$$V = \frac{\pi}{6} \cdot \left[3W^2 + D^2\right] \cdot D$$

Figure 3.13 Approximation of nominal contact area of the steel counterface based on 2-D wear scar size and depth of scar found by transverse cross section of the composite. If wear of the ball is dominant (rare) then the wear volume can also be calculated. [99,125]

Using the wear scar depth and the worn spherical cap on the counterface the apparent area was estimated as a function of sliding distance. From this the range of apparent pressure was obtained as a function of sliding distance, Figure 3.14.

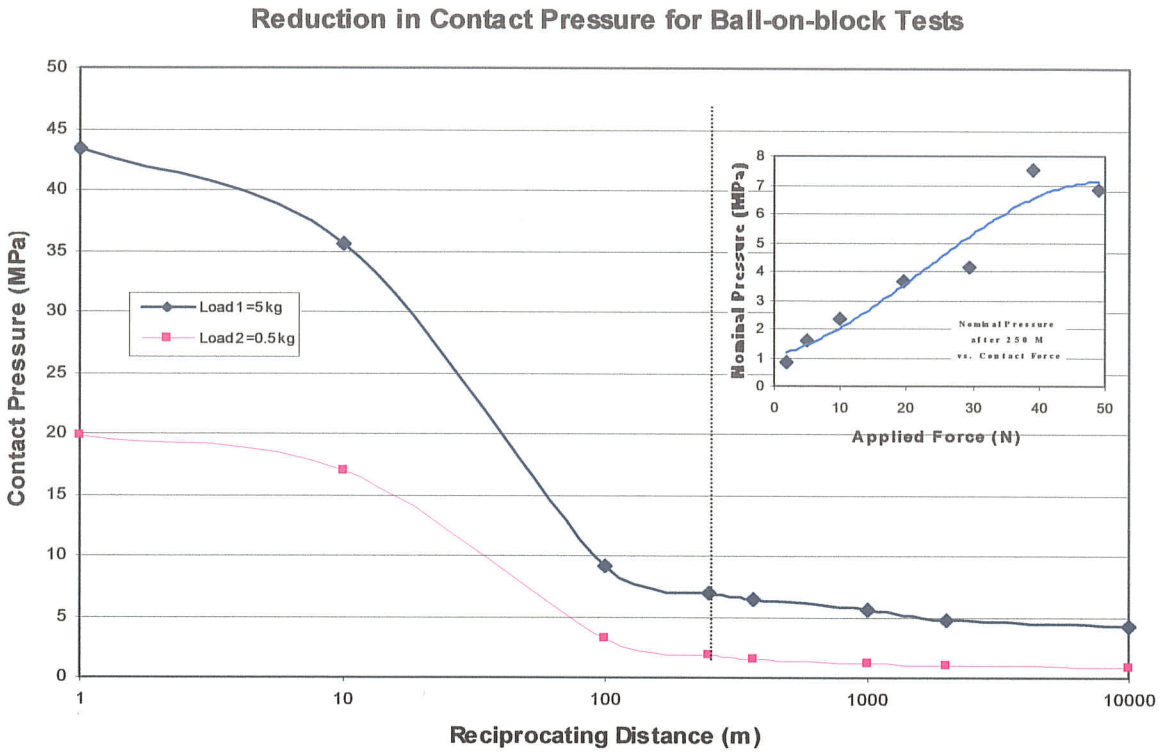

Figure 3.14 Estimate of the reduction in contact pressure due to the wear scar of the composite conforming to the steel counterface. A test sliding distance of 250 m was most commonly used. Initial pressures are very high (up to 1000MPa) as predicted by Hertzian analysis however plastic deformation lowers the pressure immediately. Wear scars of ¼" reciprocating track against a 52100 counterface.

A major benefit of ball-on-block testing is the ability to examine wear transitions over a range of applied pressures using a single sample. The wear rates are not expected to be constant as sliding continues due to the drop in contact pressure.

The contact area and therefore contact pressure depends upon the wear behaviour of the counterface as well as the composite. There are three forms of counterface wear behaviour, 1) pure adhesion from the composite, no weight loss, 2) mixed abrasion and adhesion causing a larger effective contact radius and 3) pure abrasion of the counterface, illustrated in Figure 3.15. Each case can slightly alter the nominal contact pressure.

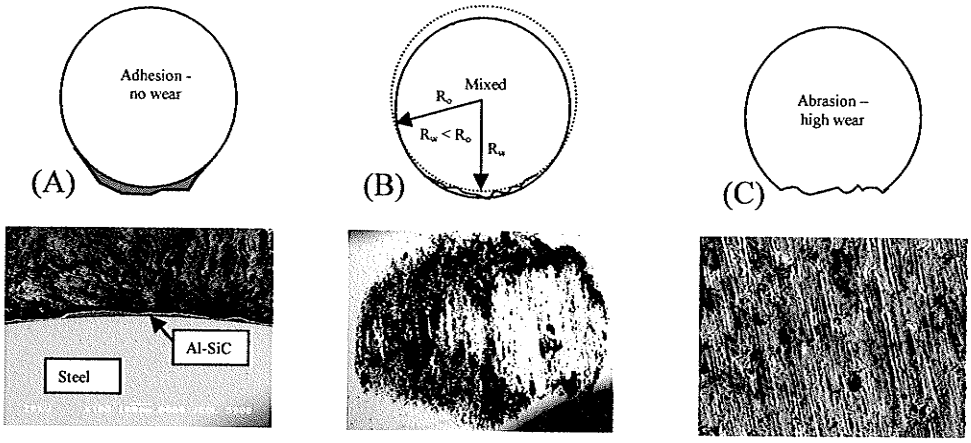

Figure 3.15 Different types of counterface wear. (A) Adhesion of the deformed composite prevents wear of the steel counterface. (B) Mixed wear of counterface causing as increase in contact radius. (C) Pure abrasion of the counterface. Each case presents a slightly different nominal contact area.

Using an approximate thermal diffusivity of 9.6×10^{-5} m^2/s [100] and using the wear scar radius as r_o, the range of normalized pressures and velocities were determined to be:

$$\mathbf{5 \times 10^{-3} < Normalized\ Pressure < 5 \times 10^{-2}}$$

$$\mathbf{0.3 < Normalized\ Velocity < 1.4}$$

H_o values are given in Table 3.3. Normalized equations are given in Section 2.32.

3.13 EXPERIMENTS PERFORMED

The experiments can be divided into four sections:

1. Comparison of the wear of Pure Al, Al-Si, and Al-Si-SiC

2. The influence of steel hardness and composition on the wear, transfer and mixing behaviour of Al-Si-SiC

3. Change in reciprocating distance from ⅛" to ¼" to ¾" corresponding to an average increase in sliding velocity from 3.75 to 7.5 to 22.5 cm/s

4. The influence of the type of counterface material on wear, transfer and mixing of Al-Si-SiC

All experiments were performed with variables similar to those outlined in Section 3.12. The general test conditions were high pressure, low speed reciprocal sliding.

In the first section, wear of three different aluminum materials are tested against a 52100 steel counterface. The reciprocating track length was ¼" for each material over a range of applied loads. Differences in the mass transfer to the steel counterface and surface wear mechanisms were observed. The magnitude increase in wear resistance gained by using composite aluminum material is established. The Al-composite can be described as "not ideal" for theoretically maximum wear resistance of these materials.

In the second section, effort is taken to evaluate the mixing and transfer of various elements between sliding surfaces based on the counterface materials in contact. A 316 stainless steel counterface, with a substantial percentage of Ni and Cr, introduces additional elements that may be mechanically mixed during sliding contact. 440C and 52100 bearing steels were also tested for comparison. Hardness and composition varied significantly amongst these three counterface materials. Ball bearings of the three steel alloys were obtained from Thompson Precision Ball with a diameter of 10 mm, and were counterfaced against rectangular coupons of the composite aluminum 8 mm thick, polished to 0.25 μm. Wear rates against three steel counterface materials, Table 3.2, were obtained against the composite aluminum over a range of applied loads.

In the third section, the influence of extrinsic parameters of reciprocating sliding

distance and sliding velocity were considered. All experiments used the composite aluminum against a 52100 steel ball. ¾" reciprocating was tested to examine the effect of reciprocating over a longer track length on the reprocessing of debris, transfer, and surface wear mechanisms. The sliding speed was set at three times faster the majority of the tests. Shorter track lengths were examined for similar reasons. The total sliding distance was kept the same for the longer ¾" track length by decreasing the number of cycles. For the shorter track lengths (⅛" and $^1/_{16}$") the number of sliding cycles was kept constant.

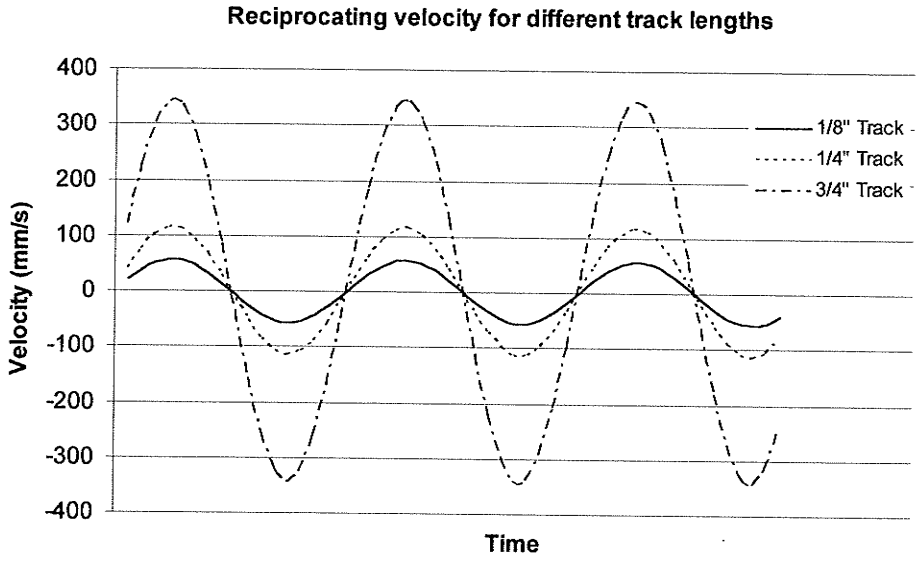

PARAMETERS	¾"	¼"	⅛"	$^1/_{16}$"
Machine Speed	345	345	345	345
Stroke Length	≈20 mm	≈6 mm	≈3 mm	≈1.5 mm
Average Sliding Velocity	22.5 cm/s	7.5 cm/s	3.3 cm/s	1.8 cm/s
Number Of Cycles	6,560	19,700	23,600	23,600
Total Sliding Distance	250	250	150	75

Figure 3.16 Different reciprocal ball on block sliding conditions tested.

Testing different counterface materials besides steels was examined in the final section. Tests were run for 1m, 10m, 100m and 250m at which point steady state sliding (or no change in operative mechanism) was assumed. The operative surface mechanisms were recorded at each sliding distance. The counterfaces chosen allowed for the study of a large hardness range, Table 3.4. The 316 stainless steel and K-Monel counterface materials were chosen as they had near the same hardness but very different compositions. Between 1 and 10 m sliding surface damage under high load is observed as affected by counterface hardness and composition. Also at short sliding distances the initial observation of the process of Al/SiC transfer to the counterface can be observed. Two test loads were used: 1) a low load of 2 N that promotes fatigue and micro-abrasion effects on surface wear and 2) a high load of 20 N that causes significant aluminum subsurface plasticity and SiC fracture during wear.

The key areas that were focussed upon for all sections were:

- Weight loss of the counterface and weight loss of Al-SiC composite
- Differences in mechanical mixing of Al-SiC surface.
- Transfer of elements from the counterface to the composite surface
- Change in wear mechanisms indicated by a change in debris

3.14 MATERIALS

A soft pure aluminum (HP Al, 99.99%) was chosen for comparison to the significantly harder and more wear resistant Al-Si and Al-SiC composite. The two Al-Si material nominal compositions are given in Table 3.1; the hardness values are given in

Table 3.3. The Al-Si alloy was solution annealed at 540°C for 8 hrs causing the as cast needle or acicular eutectic Si structure to become spherodized. Si particles are 3-5 μm in size. The alloy was then quenched and allowed to age at room temperature. Si particles are not uniformly dispersed due to cores of pro-eutectic solid solution aluminum formed prior to the eutectic reaction. Elongated plates of (Al-Fe-Mn-Si) intermetallics were found to exist and polished in relief, Figure 3.18. Most common intermetallic phases formed for 356 aluminum alloys are $FeSiAl_5$, $Fe_2Si_2Al_9$, Mg_2Si, and Si [115] with the first two intermetallic compounds fitting the results of semi-quantitative EDS scans.

The composite had 20vol%SiC with an average particle size of 10μm. The majority of particles were in the range of 5-15μm [99]. Particles were observed to be concentrated on the periphery of solidified grains, Figure 3.19. The distribution of SiC was consequently not uniform, potentially reducing wear resistance [39]. Particle clustering was accordingly observed causing a high likelihood of increased porosity in these regions [128]. SiC particles were faceted with parallel crystallographic planes easily observable and clearly irregular in shape. A fractured cluster showing a range of particle shapes and sizes is shown in Figure 3.19.

Hardness values for the steel counterfaces were measured with a Rockwell Hardness (RH) diamond indenter, using the HRA scale. The indenter was accurately aligned on the round counterface surface using a special fixture. For HP Al, Al-Si, Al-Composite, Al-6061counterface, the HRB or HRF hardness scales were chosen, then values were converted to Vickers Hardness using tabulated conversion data [95]. Microhardness measurements using a Diamond Pyramid Hardness (DPH) indenter and 25g load were required for the ceramic counterfaces, and were compared to the manufacturer specs.

A356.2 Alloy (wt%)

Si	Mg	Ti	Fe	Mn	Cu	Zn	Ni	Sn	Al
6.99	0.34	0.11	0.08	<0.01	<0.01	0.01	<0.01	-	Balance

A356 MMC (wt%)

Si	Mg	Ti	Fe	Mn	Cu	Cr	Ni	Sn	Al
6.5-7.5	0.17	0.20	0.20	0.10	0.20	0.25	0.5-1.5	0.5	Balance

Table 3.1 Composition of the aluminum-silicon alloy and Al-Si-SiC composite tested in the study. Compositions are given by supplier.

52100 (wt%)

C	Mn	Si	P	S	Cr	Ni	Cu	Mo	Fe
1.04	0.35	0.25	<0.02	0.05	1.45	-	-	-	Balance

440C (wt%)

C	Mn	Si	P	S	Cr	Ni	Cu	Mo	Fe
1.05	0.36	0.68	0.01	<0.001	16.91	0.12	0.03	-	Balance

316 (wt%)

C	Mn	Si	P	S	Cr	Ni	Cu	Mo	Fe
0.08	2.0	1.0	0.045	0.03	16-18	10-14	-	2-3	Balance

Table 3.2 Compositions of steel counterfaces tested.

STEEL BEARING MATERIAL	SURFACE HARDNESS [HRC]
316	31.4
440C	61.0
52100	64.8

AL WEAR MATERIAL	SURFACE HARDNESS (HV)
HP Al	45
Al-Si	82
Al-20%SiC	94

Table 3.3 Hardness values of material pairs

COUNTERFACE MATERIAL	HARDNESS (HV) – kgF/mm^2
Al-6061 (O temper)	75
K-Monel	302
316 Stainless	313
440C	722
52100	827
Al_2O_3	1365
Si_3N_4	1800

Table 3.4 Different counterface materials and converted hardness values

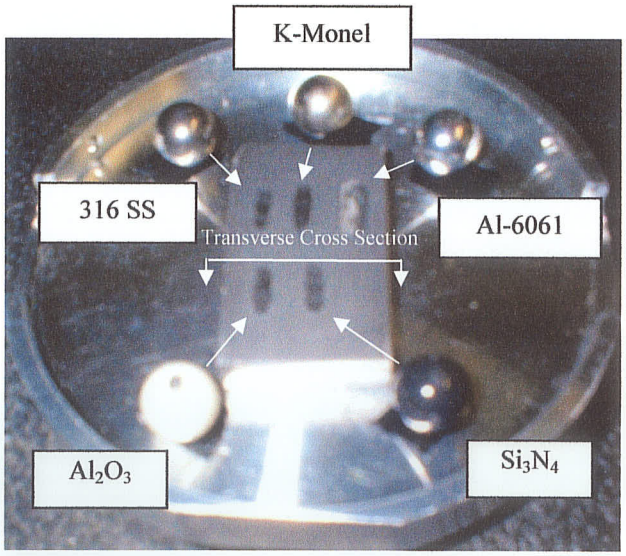

Figure 3.17 Different counterface materials and the wear scars that resulted from 250 m sliding contact with a 20 N applied load

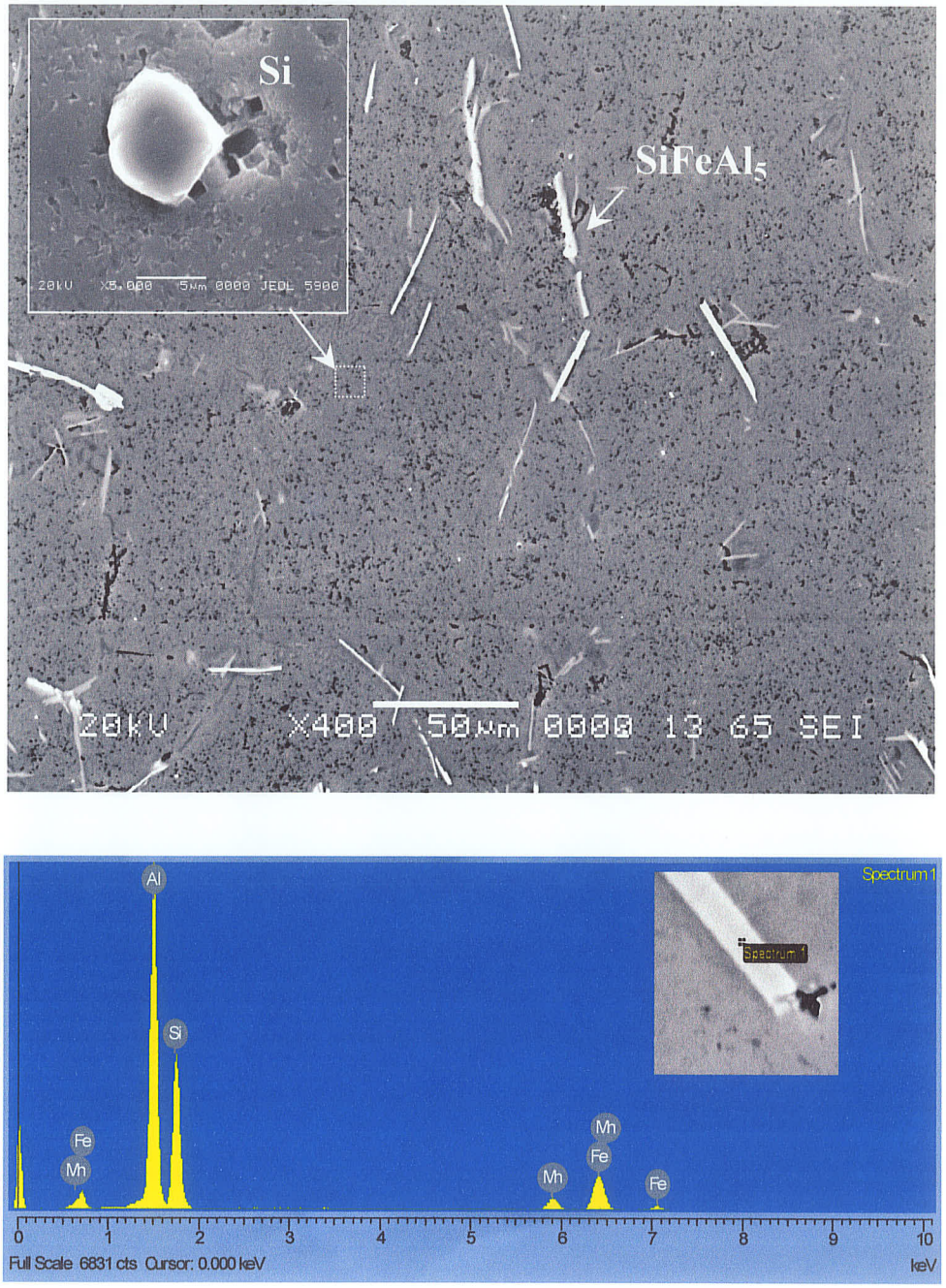

Figure 3.18 TOP: A356 alloy, solution annealed, T4. Insert shows size of spherodized Si phase. BOTTOM: EDS composition of white intermetallic stringers. Fe intermetallic compounds with a needle shape can act as crack initiation sites [132].

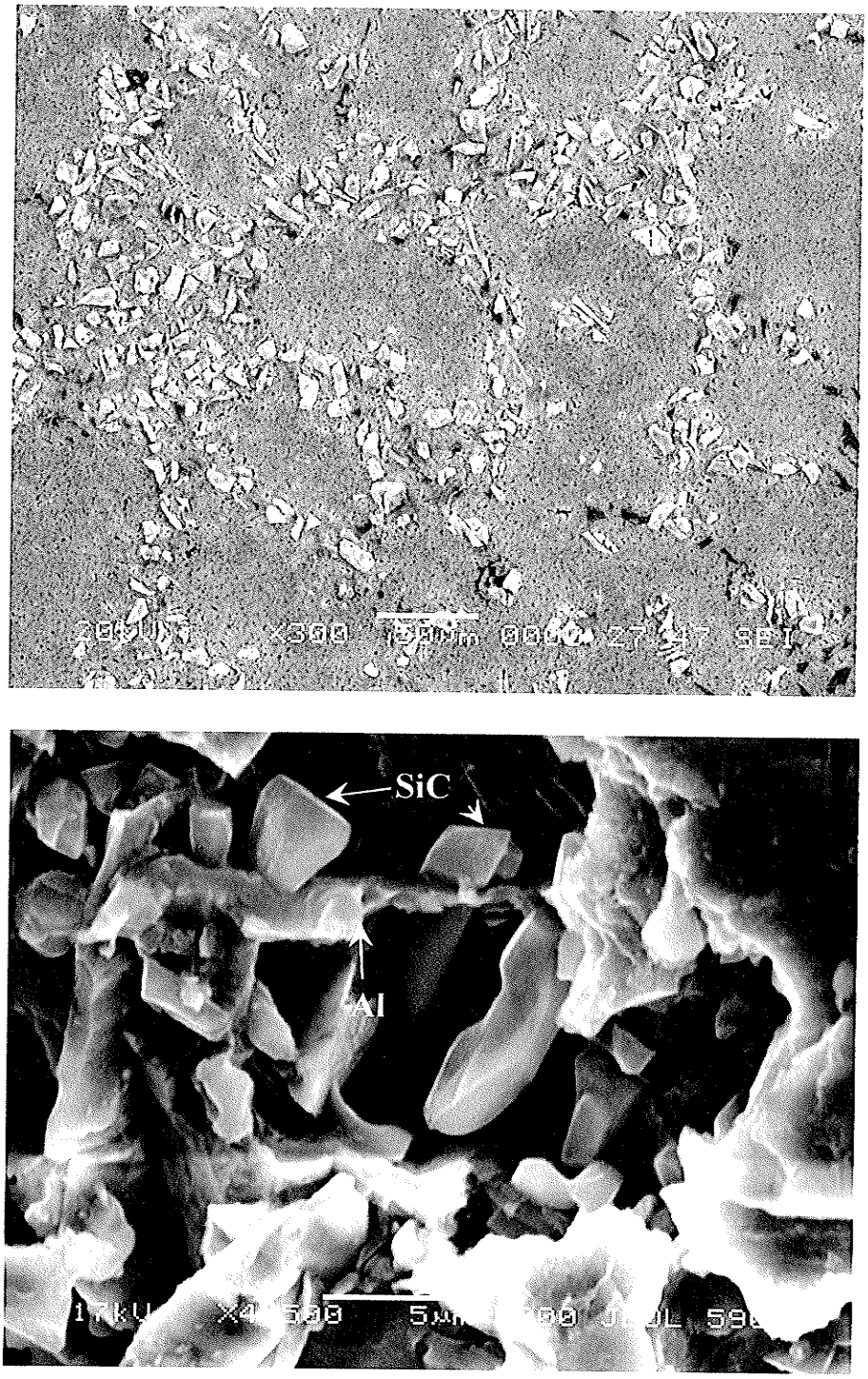

Figure 3.19 TOP: As cast A356-20vol%SiC MMC. A non-uniform distribution of SiC reinforcement exists with clustering on the periphery of solidified grains Sample is polished to 0.25 μm, unetched. Etching with Keller's Reagent and higher magnification reveals the Si eutectic network. BOTTOM: Delamination fracture of a particle cluster showing incomplete bonding and irregular sized SiC.

3.21 SAMPLE PREPARATION

Block samples 50mmx20mmx8mm were prepared from the cast aluminum and composite ingots. A carbide tipped band-saw blade was used to make rough cuts of the composite which were then milled into blocks using a tool steel cutter. A HSS blade rapidly deteriorated due to abrasion of the SiC. It was recommended to keep machining temperature to a minimum and use water based lubricant to reduce adhesion effects during machining [133,134]. Samples were rough sanded up to 1200 grit paper. Compressive surface residual stresses are expected to exist and are studied more extensively elsewhere [135,136]. Samples were fine polished to 0.25 μm using alumina powder using a minimal amount of water [101].

SiC and intermetallics polished in relief so that no etchant was required to view these microstructural characteristics. Immersing the polished composite in Keller's Reagent (2.5ml HNO_3, 1.5ml HCl, 1ml HF, and 95ml H_2O) for less than 30 s revealed the Si eutectic structure. 0.5vol% HF was also adequate. Using 1g NaOH in 100ml H_2O as an etchant, dabbing the alloy with a cotton ball for a few seconds worked to reveal the Si particle phase.

3.22 SCANNING ELECTRON MICROSCOPY

Transverse cross sections of the wear scar were made using a diamond cut-off wheel. The direction of the transverse cross section is illustrated in Figure 3.18. The samples were then cleaned of all surface contaminants and electroplated in a "strike" copper bath. The composite aluminum was made the cathode ("-") and placed in the

cyanide solution near a copper anode ("+") for one hour at an operating potential of 7 volts. The Cu plating produced was approximately 0.1 mm thick. Contaminated solutions used more than once provided poor Cu adherence. The plated composite was mounted in bakelite and polished. Bakelite registers as Si and O using EDS and can melt underneath improperly formed porous Cu plating, making it difficult to distinguish the true surface composition of these elements. The Cu surface plating was mainly required for edge protection during polishing and better imaging without charging of the non-conductive bakelite mount.

Semi-quantitative analysis of worn surfaces and debris was performed using a Jeol 5900LV SEM equipped with EDS. An operating voltage above 15 KeV was used for most analysis as the accuracy Fe, Cr, and Ni X-ray detection becomes questionable at lower beam energies. For examining aluminum and oxygen content a lower 8 KeV beam allowed for a better surface composition result due to the lower beam penetration. Debris was placed on adhesive carbon tape for imaging. The high depth of focus of SEM allowed tilting of the specimen to make delamination and smearing morphologies more apparent. Backscattered electron images (BSE) was used to indicate the distribution of SiC particles which appear slightly darker than the surrounding matrix. Nickel, Iron and iron intermetallics appear bright relative to the aluminum matrix due to higher atomic numbers.

3.23 EDS AND X-RAY MAPPING

X-Ray mapping was performed to identify elemental distributions of worn surface, debris, and subsurface found by transverse cross sections wear scar. Quantitative elemental

compositions by spot EDS detection can be expected to have inaccuracy up to 10%, especially for a surface composition and elements with low atomic numbers such as oxygen. As a result, EDS scan were predominantly used to qualify the relative magnitude of elements present.

CHAPTER FOUR RESULTS AND DISCUSSION

4.11 WEAR PERFORMANCE OF AL, AL-SI, AND AL-SI-SIC

Wear performance was measured by weight loss of the three aluminum materials listed in Table 3.1, which were exposed to a range of pressures during reciprocating wear against an as-received 52100 steel ball counterface. Pressures were estimated as outlined in Section 3.12. Wear performance can be best measured by considering the overall weight loss of the sliding pair, although noting the results in Figures 4.11 and 4.12, weight losses from the aluminum materials dominated the overall wear.

(I) HP AL

High Purity (HP) Aluminum is tested to show the limitations of the soft metal, which can flow easily to allow relative movement at the interface, a favourable property for lower friction induced mechanical damage during sliding, yet it also suffers from this merit, as ductility causes the severe limitation of dimensional instability. Pure aluminum furthermore demonstrates the differences between the rate of damage and the rate of wear. The HP Al matrix smears causing severe surface damage with minimal weight loss. Smearing of HP Al resulted in severe surface damage due to extrusion instead of fracture of the ductile metal, therefore generating and removing less debris, Figure 4.13. As a result, the wear rate based on weight loss does not adequately represent the extremely poor tribological performance.

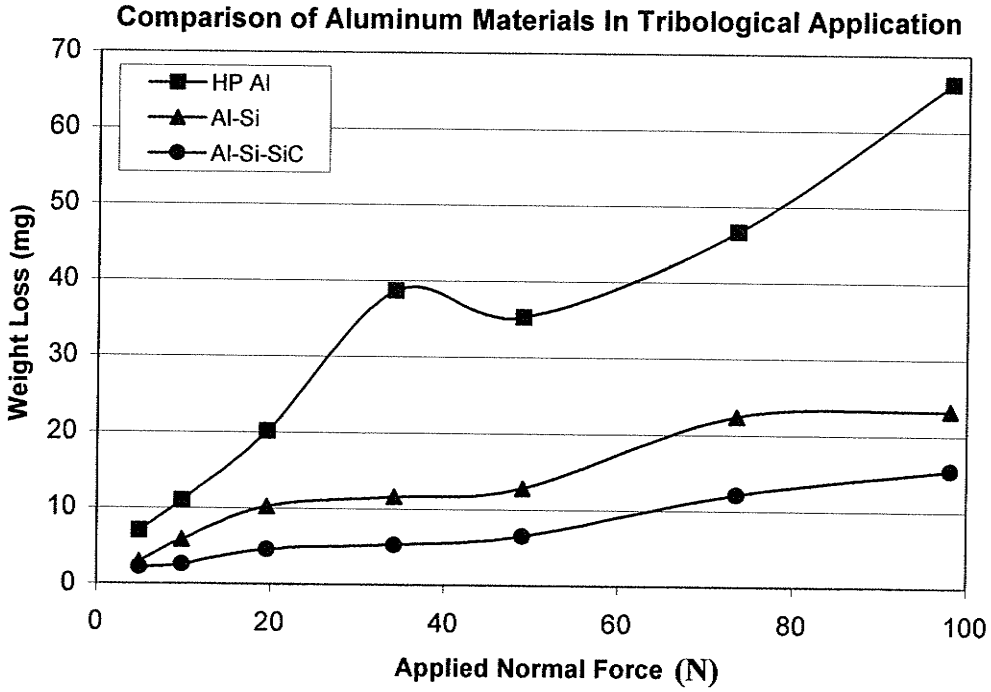

Figure 4.11 Wear indicated by weight loss of different aluminum materials. Tested using ¼" reciprocating track, 250m against an as-received 52100 steel counterface.

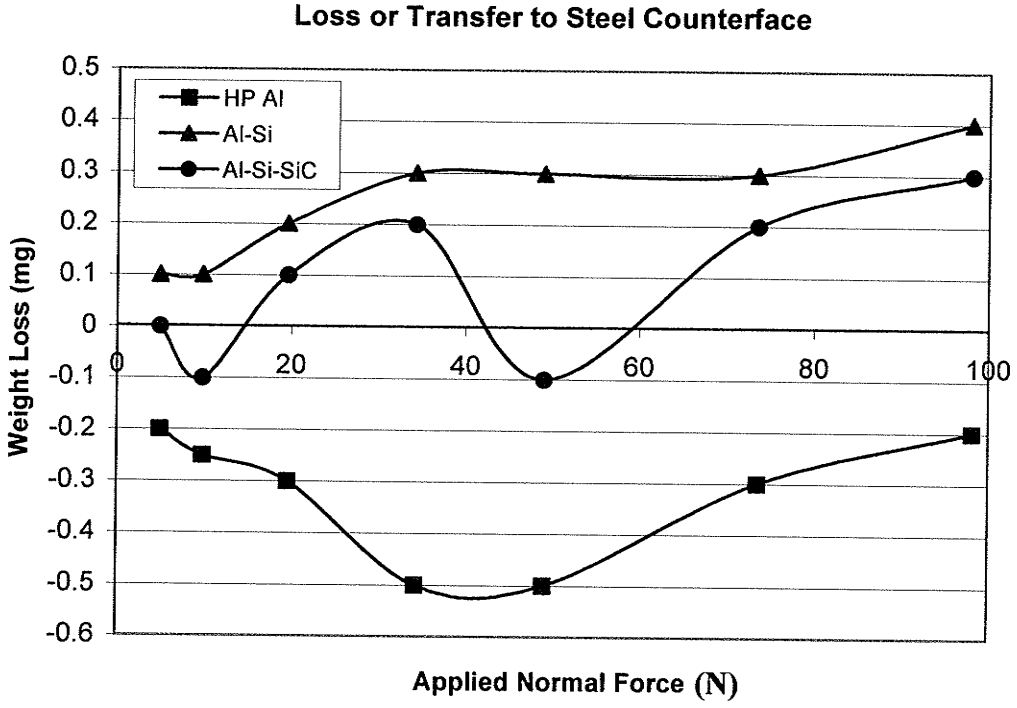

Figure 4.12 Weight change of the 52100 steel counterface for tests in Figure 4.11

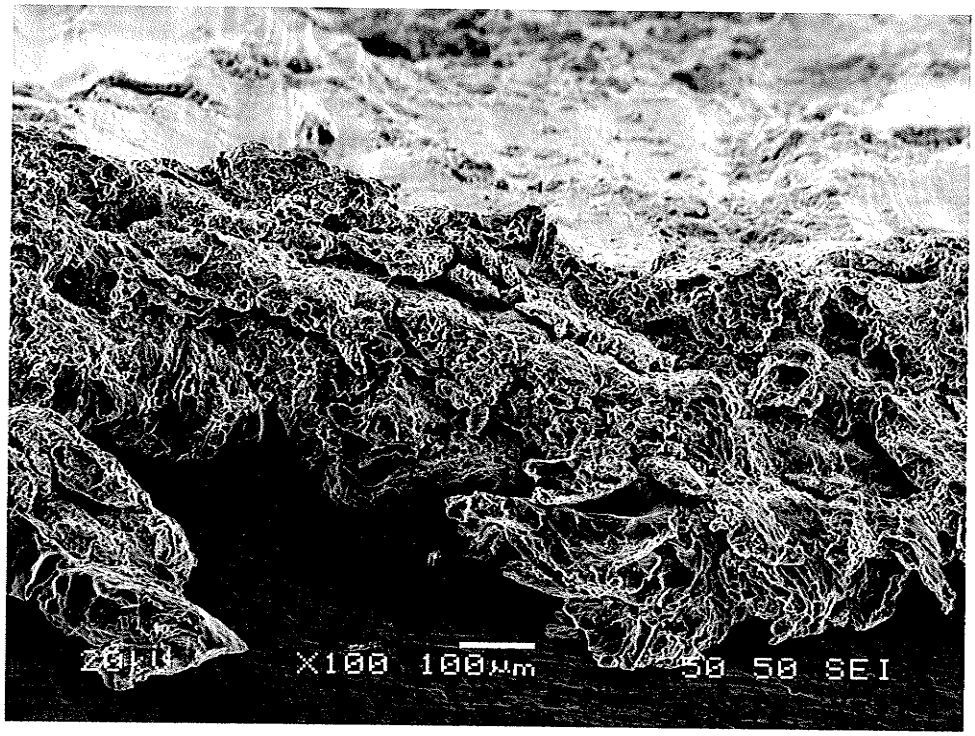

Figure 4.13 Extrusion of the HP Al surface by smearing with 50 N applied force after 250 m sliding contact. Approximately 3 MPa nominal pressure

A black mixed surface formed by the collection and smearing of particulate debris occurred for low load tests (below 1MPa) for HP Al. Black debris was pushed to the ends of the wear scar and accumulated readily on the Al surface up to approximately 2 MPa nominal contact pressure. At about 2 MPa the surface would begin to delaminate at too high of a rate for substantial mixing of particulate debris to remain on the surface. As the contact pressure approached 2 MPa, delaminations began to emerge at the center of the wear scar where the sliding velocity was highest. At higher contact pressures, in the range of 2-5 MPa, gross delaminations caused by seizure or excessive smearing negated all mixing effects and resulted in a bright metallic wear surface for HP Al, as demonstrated in the bottom picture of Figure 4.14. After 250m of sliding, contact pressures were most often reduced in the 2-5 MPa range, causing seizure or smearing to appear as most dominant wear mechanisms at the end of the test. At higher pressures of 5-25 MPa during initial

sliding, rapid disintegration of the surface through smearing and extrusion occurred. Delaminations due to seizure ceased to cause wear at high pressures, in the order of 10 MPa and greater, due to adequate hydrostatic pressure to "heal" the surface under high strain.

HP Al experienced the most transfer to the steel counterface of all three aluminum materials, Figure 4.12. This caused the surface to surface interactions to be predominated by deformed Al on Al contacts. As such, smearing of the Al surfaces was the principal mechanism of relative motion between contacting asperities. Both black particulate debris and delaminations were observed to adhere to the steel counterface, with both visible in the top picture Figure 4.14.

(II) AL-SI

In comparison to the HP Al which most often had a bright shiny wear scar appearance due to seizure delaminations at pressures above 2 MPa, the Al-Si alloy caused blackened (mixed) wear surfaces to develop over a larger range of nominal pressure, up to approximately 5 MPa. Nonetheless, past this approximate pressure level, the black mixed surface was observed to delaminate revealing an unmixed shiny metal subsurface during sliding [15,92]. At pressures where a black mixed surface existed, the surface was never uniformly formed, with long thin delaminations removing the protective mixed intermediate layer. Delaminations most often occurred at a depth below the mixed surface, not from the mixed surface as would be preferred. Of interest, delaminations were observed to originate from surface or near surface iron intermetallics, identified in Figure 3.18. Intermetallics were found to fracture in the subsurface causing the superjacent matrix and mixed surfaces to become unstable.

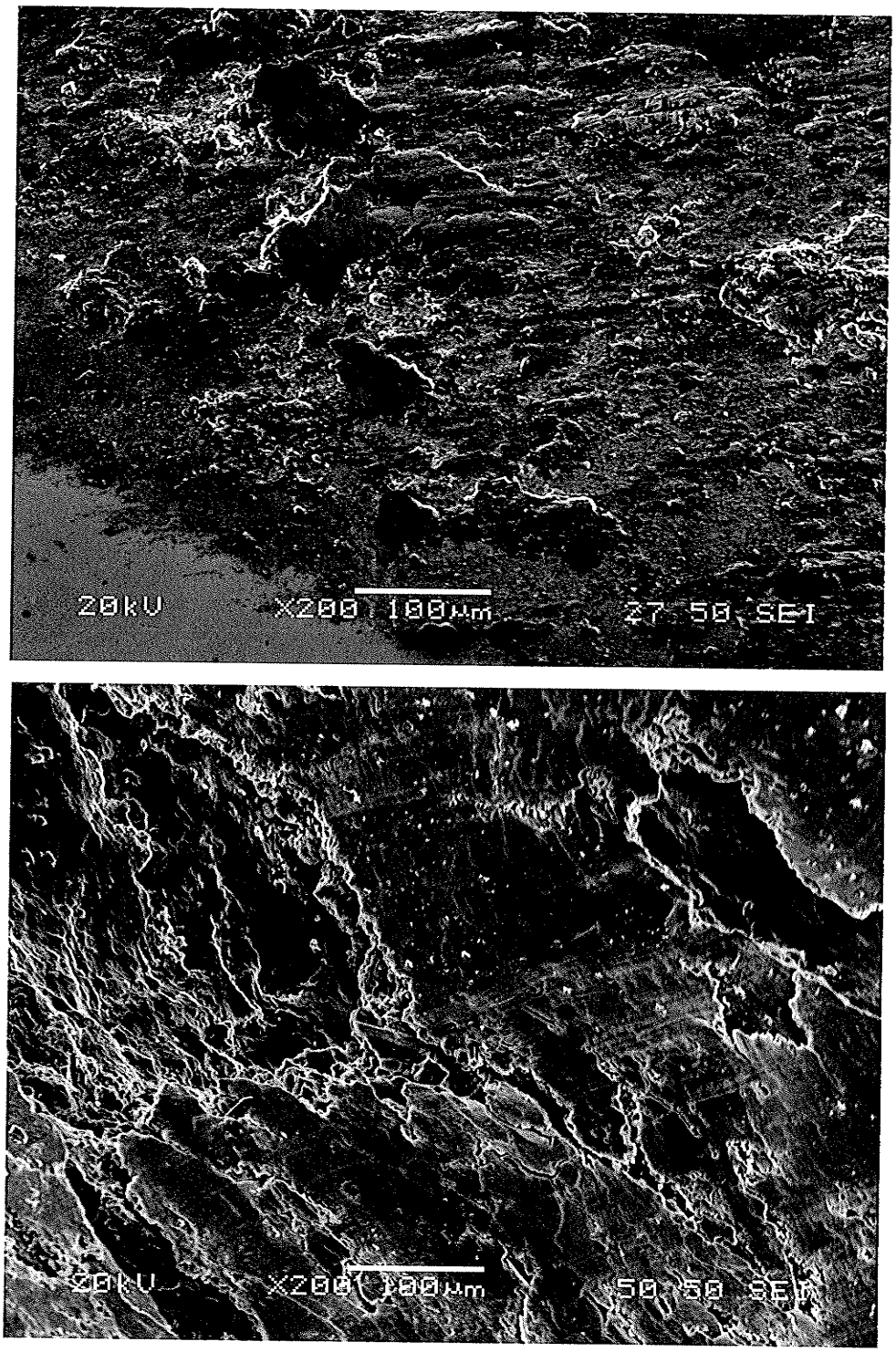

Figure 4.14 TOP: a thin layer can be seen to deposit on the steel counterface at any point of contact with the HP Al. Delaminations and mixed particulate debris can be seen to adhere to the surface (roughly 2 MPa). BOTTOM: Large delaminations of the HP Al surface caused by seizure or excessive smearing (roughly 5 MPa). At this higher pressure delaminations dominate transfer to the counterface.

The blackened surface was observed to form by the exchange of small particulate debris. Its formation depended upon the manner in which the debris was distributed on the wear surface, which was not uniform, with collections of debris at the ends of the wear scar where the direction of relative motion was reversed. Therefore, the blackened mixed surface phenomenon did not provide uniform surface wear resistance for the Al-Si material for two reasons: Firstly its formation depended on the distribution of debris once generated, and secondly, delaminations of the mixed surface were at a depth that exposed the unmixed surface.

For the initial range of high pressures where the pressure remained above 5 MPa (usually less than 100m sliding), only shiny delaminations occurred with bulk delaminations limiting mixing and resulting in a shiny wear surface, as similarly observed for HP Al. Black particulate debris and a mixed black surface morphology eventually formed at greater sliding distances where the surface pressure has dropped to levels that seizure and gross material transfer [75] could be resisted, Figure 3.14. Seizure pressures for a eutectic (11.7%Si) Al-Si alloy have been found to be between 2-5 MPa over a range of sliding speeds [89]. The seizure pressure for a hypoeutectic 7%Si alloy (used in this study) has been found to be slightly lower than for a eutectic composition, yet otherwise similar wear characteristics have been observed [75,87]. Once the conforming contact achieved low enough surface pressures to resist spalling due to seizure (or gross plastic delaminations) black debris particles began to emerge as the dominant participant in mixing and wear. A vertical region placed on a wear mechanism map represents the normalized contact pressure range experienced by the Al-Si during sliding and the dominant wear mechanism regions passed through as wear continued, Figure 4.15.

The onset of seizure of Al-Si alloys has been attributed to the removal of the "black" compacted protective layer [75], which forms congruent with the immergence of particulate debris. Observing the present reciprocal sliding, the wear scars could be seen to be metallic, blackened, or a combination of both (patchy). This wear surface formed cyclically, with a mixed surface forming, delaminating and regenerating. Delamination was apparent by harsh sliding noise between surfaces followed by a significant amount of black debris ejected from the wear scar, then smooth sliding until the process repeated. The reasonable conclusion was that for any applied load between 2-50N, or applied pressure in the range of 1-10MPa, the black mixed surface layer was not stable and could not form continuously under the reciprocal testing. Cyclic removal of the black mixed surface continued and did not stabilize sliding distance up to 1000m, which corresponds to a minimum nominal surface pressure of 0.5 MPa at 2N.

It was clear that once gross delaminations ceased to be the governing wear mechanism when operating in the proper range of contact pressures (past the first 100m), milder wear was achieved through mixing and formation of the black surface layer. The absence of this protective mixed layer has been qualified most commonly by the rate of fracture exceeding the rate of formation [32] and is proposed to explain the disappearance of the patchy mixed regions above 5 MPa.

In conclusion the wear performance was significantly improved through the use of the Al-Si alloy in comparison to the HP Al for like sliding conditions. The improvement in wear resistance could be best related to 1) a higher resistance to smearing, extrusion and large depths of plastic deformation into the subsurface and 2) a greater range of applied pressures where mixing occurred over delamination wear.

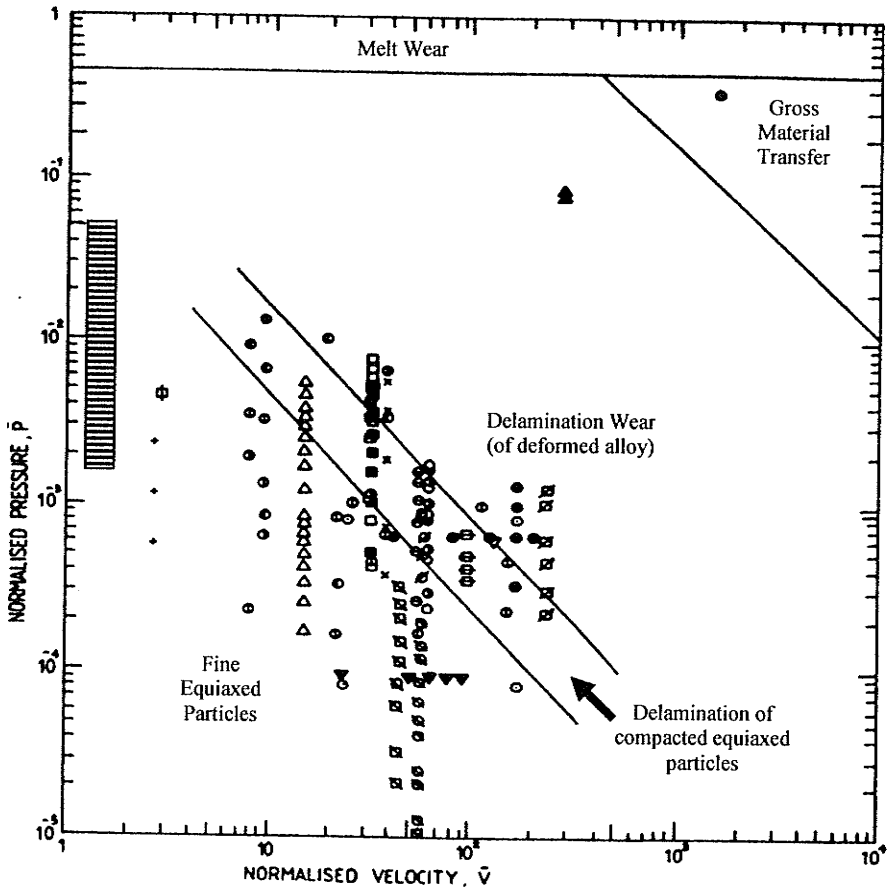

Figure 4.15 Wear mechanism map proposed for Al-Si alloys. Hatched region indicates range of sliding variables during testing. A transition from delamination wear to fine particulate debris was observed in agreement with this earlier work. Antoniou and Subramanian [34], 1988.

(III) AL-SI-SIC

A typical wear scar for the reciprocal testing is shown in Fig. 4.16. With secondary electron images (SEI) white patches indicate areas where recent delaminations have occurred. During steady-state wear the appearance of delaminations on the Al-MMC surface closely mimicked the transfer patterns on the steel surface, Figure 4.17. Small particles of fractured SiC remained on both surfaces, however protrusions were not common as most of the reinforcement was smeared into the aluminum matrix.

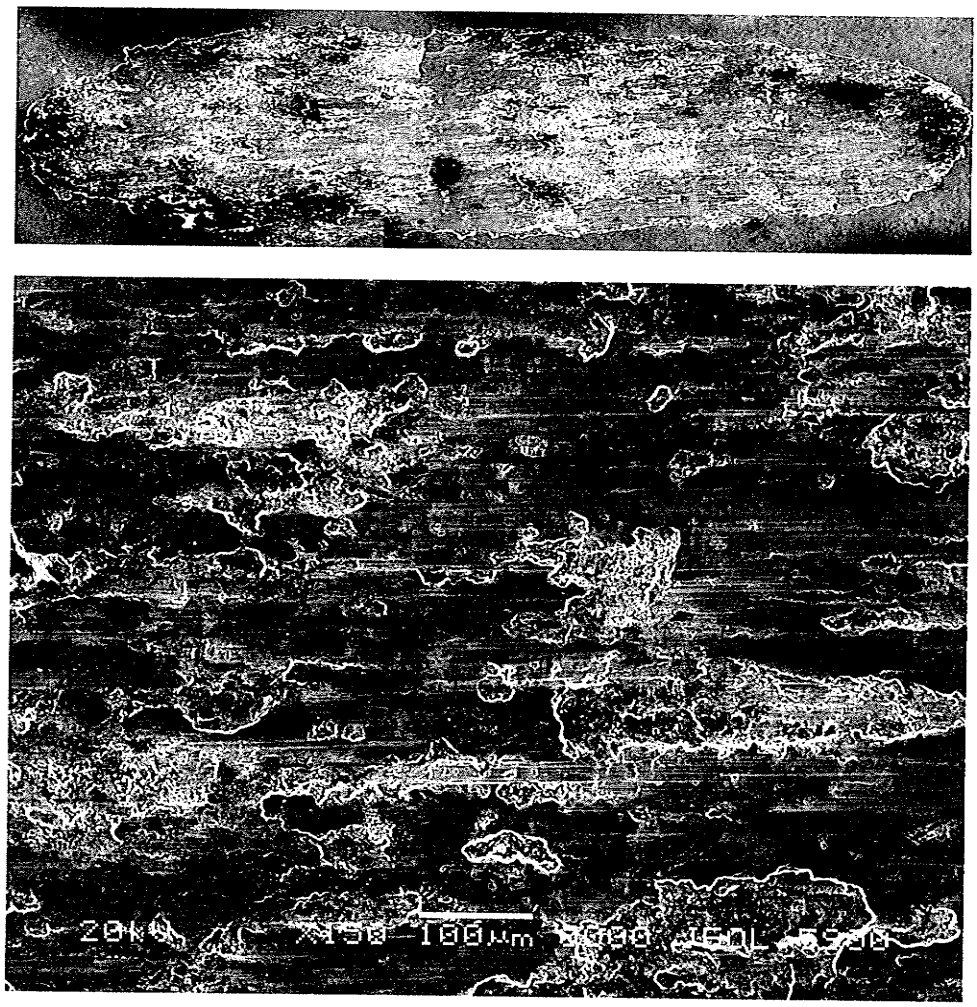

Figure 4.16 TOP: SEI image of ¼" Al-MMC wear scar for against 52100 steel, 250m, 20N, 20X magnification. BOTTOM: Surface at 1000m, 2N, approx. 0.5MPa. Abrasion, compact delaminations, superficial smearing and particle pull-out are observed

The composite experienced the same stages of wear as the HP Al and Al-Si: large shiny delaminations due to smearing and seizure at high pressures and small black particulate debris as the pressure decreased. Several important differences could be observed between wear of the monolithic alloy Al-Si alloy and the Al-Si-20%SiC composite. Firstly, delaminations due to subsurface fracture (indicated by a granular surface fracture appearance) were the more common cause of delaminations from the composite surface when compared to the unreinforced Al-Si alloy, which experienced a

greater degree of surface delaminations resulting from excessive smearing over the same range (2-5 MPa) of applied pressures. In other words, the composite resisted smearing delaminations at a higher range of applied pressures, up to approximately 10 MPa. This was indicated by a transition in the cause of delamination morphology, outlined in Section 4.22. Secondly, delaminations due to subsurface fracture were smaller for the composite in comparison the the unreinforced alloy. Finally, abrasion became a more dominant wear mechanism near 2 MPa when in contrast the unreinforced alloy continued to experience wear by large delaminations due to subsurface fracture. Abrasion was considered to be the most favourable dominant surface wear mechanism as it caused the least amount of weight loss from the sliding system. Overall, greater resistance to seizure and gross plastic delaminations due to smearing over the range of pressures experienced over the duration of a wear test could explain the consistently lower weight loss of the composite in relation to the unreinforced alloy, Figure 4.12. Abrasion as a more dominant wear mechanism over the range of applied pressures also could contribute to the lower weight loss of the composite.

Examination of the composite surface at the lowest contact pressures revealed superficial smearing, compact delaminations due to mixed surface fracture, abrasion, particle pullout and particle fracture to be simultaneously contributing to wear. These mechanisms can be identified in Figure 4.16. Delaminations can be seen to cause the most significant surface wear. Delaminations of the composite surface resulted even at the lightest contact pressure of approximately 0.5 MPa. Delaminations of the composite at the lowest pressures were smaller and therefore less damaging to the surface, in comparison to the unreinforced Al-Si tested at the same pressure. At any pressure between 0.5-5 MPa

surface wear could be characterized by a competition between smearing and mixing of the composite surface and subsequent fracture/ delamination of the smeared/mixed surface once formed.

(IV) COUNTERFACE WEAR

The change in weight to the steel counterface indicates differences in transfer that occur between the three aluminum materials. Clearly wear against HP Al caused significant Al transfer to the steel counterface, indicated by a weight gain, Figure 4.12. In contrast, wear against Al-Si caused a significant weight loss of the steel counterface. The weight loss of the steel counterface has been previously observed to increase with increased Si content for Al-Si alloys, although not proportionately [78]. In the current study, the presence of the Si phase caused a clear reduction in adhesive transfer in comparison to the HP Al. However in either case adhesion to the steel counterface remained as the dominant wear mechanism and the crux with regard to wear resistance of the aluminum material.

With SiC present, the wear of the steel counterface was erratic although consistently less than what was caused by the Al-Si alloy, Figure 4.12. This was unexpected in consideration of extra hard particles capable of abrading the steel when mated against the composite aluminum. Instead, introduction of the SiC particles from the composite aluminum was observed as promoting adhesive transfer to the steel surface, as well as act as a source of bonding instability for thick transfer layers to the steel surface, in agreement with previous published literature outlined in Section 2.43. This difference was observed by comparing wear scars of the Al-Si and Al-Si-SiC under the same sliding conditions, Figure 4.17.

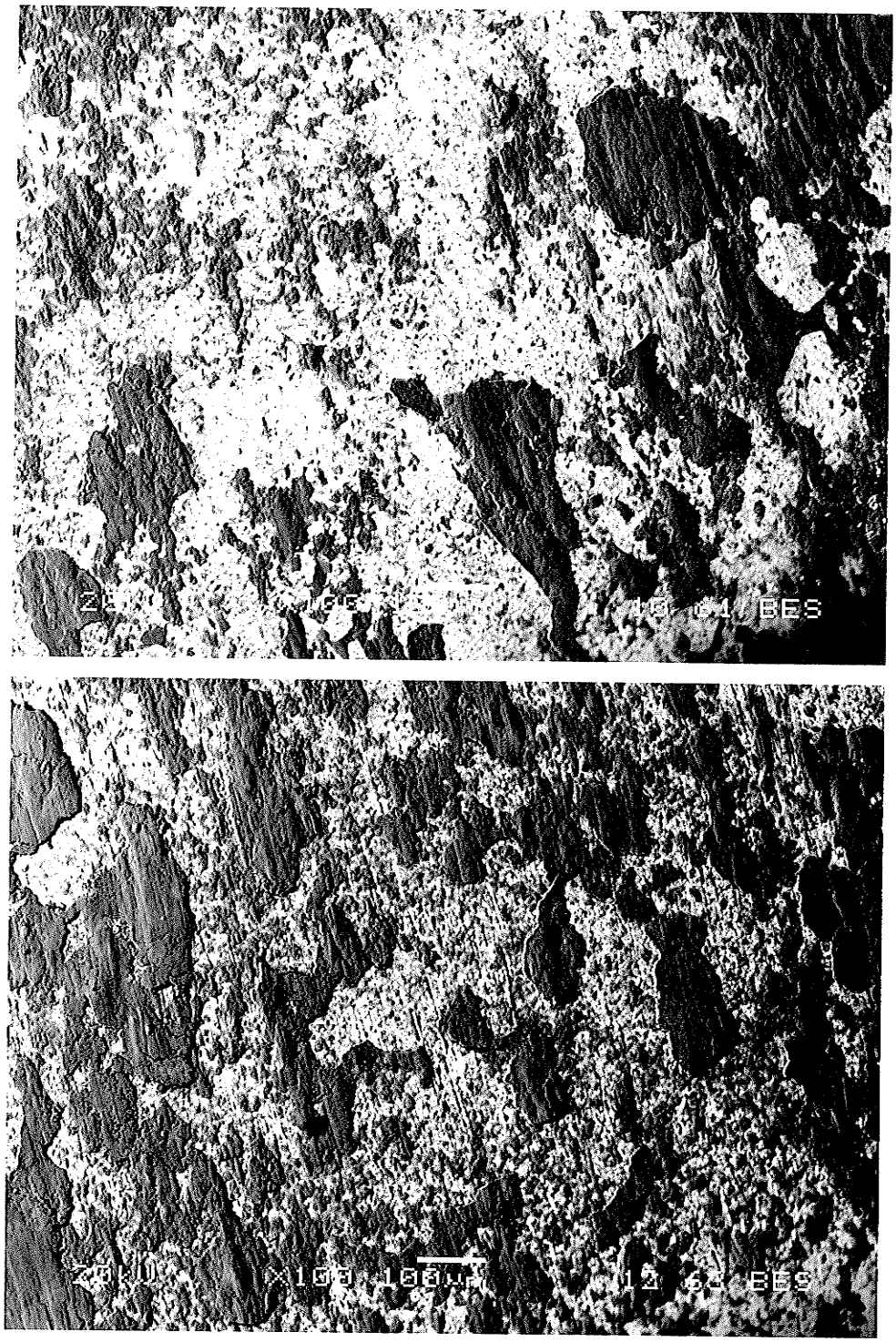

Figure 4.17 BSE images of transfer to steel counterface TOP: Al-Si, BOTTOM: Al-Si-SiC under equal test conditions. Aluminum appears dark in contrast to the steel. The composite Al caused greater transfer to the steel counterface while simultaneously causing greater abrasion of the surface, 20N, ¼", as-received 52100 counterface.

The instability of adhered Al-composite and the cyclic delaminations off the steel surface can explain in the irregular change in weight. The mechanisms of transfer to the steel counterface are further examined in Section 4.31.

4.12 WEAR PERFORMANCE FOR DIFFERENT RECIPROCATING LENGTHS

Different track lengths were examined for Al-SiC composite against the as-received 52100 steel counterface. The different combinations of reciprocating distance, reciprocating cycles and sliding velocity are given in Figure 3.16. These experiments were performed to examine the effect of reciprocating distance and sliding velocity on mixing and wear behaviour.

(I) ¼" VS ¾"

It was observed that for the same sliding distance, a greater number of cycles with a shorter reciprocating track (¼" vs. ¾") resulted in a lower weight loss, particularly as the normal contact force was increased, Figure 4.18. As the reciprocating track length was increased from ¼" to ¾" so was the surface area over which wear must occur to achieve a lower conforming contact pressure. Therefore the longer wear track area was expected to experience a greater weight loss logically due to the greater number of random points at which delaminations at high pressures must occur to expand the wear scar.

Despite this, significant differences were observed in how debris generated and lost from the sliding system when testing with a longer track length and higher average sliding velocity. The ¾" track caused delamination wear at the same nominal pressure that the

shorter ¼" track length would smear the surface without delaminating. In other words, for the same surface contact pressure a greater reciprocating length caused the surface to delaminate instead of smear. This had a profound effect on the initial wear rate. For example, ¾" reciprocating caused large delaminations to be immediately produced from the surface for 10 N applied force; no large delaminations (shiny debris) were produced for the same load with a ¼" track, only smaller mixed black particulate debris delaminations. The conclusion was that the slower average sliding speed allowed for the less damaging wear mechanism to dominate (adhesive particle transfer wear vs. delamination wear).

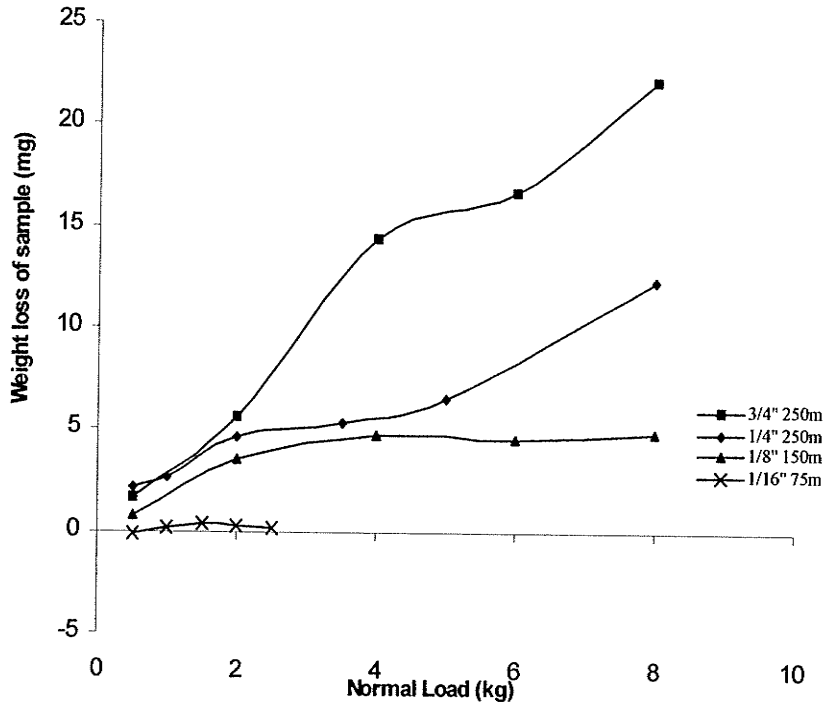

Figure 4.18 For the same sliding distance, a shorter reciprocating distance experienced a lower weight loss. At the shortest sliding distance debris was not ejected and little to no weight loss occurred.

A straight forward explanation for this difference was that at the shorter reciprocating distance contacting asperities did not strain to fracture before the contact stress was

reversed causing the smeared material to "fold back". The result was greater smearing and compaction of the surface over tensile fracture. A second explanation was that at the higher sliding speed a higher strain rate promoted surface fracture over surface deformation.

However, observing the weight losses in Figure 4.18, wear for the longer ¾" track length was nearly equivalent to the ¼" track length at 10N, despite the higher speed or longer track length causing large delamination wear at initial high pressures. This was accounted for by changes in the dominant wear mechanisms for long sliding distances between the ¼" and ¾" conditions. At the higher sliding speed setting of the ¾" track length abrasion became a more dominant wear mechanism as the pressure was reduced. This was in comparison to the shorter ¼" track length which continued to be dominated by adhesion/delamination wear and mixing. That is, abrasion never became a dominant wear mechanism for ¼" reciprocating conditions.

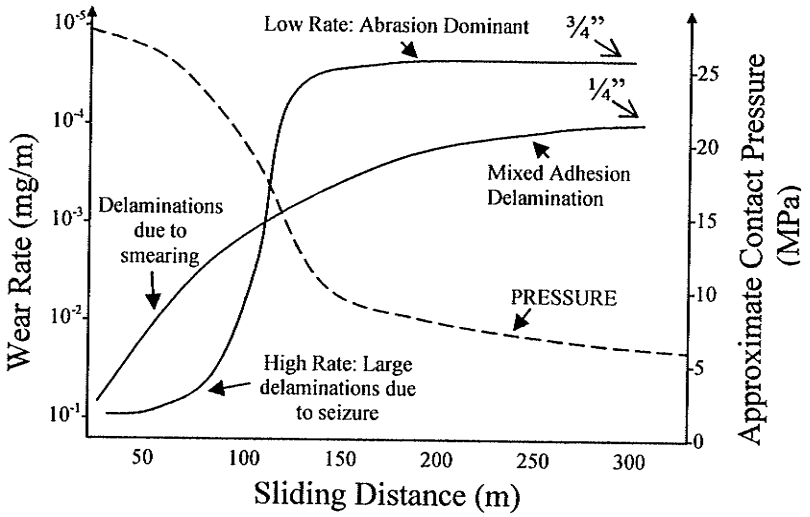

Figure 4.19 Representation of wear rates as affected by the dominant wear mechanisms as pressure decreased for the ball on block contact. Note that abrasion when dominant for ¾" reciprocating has the lower wear rate compared to mixed adhesion delaminations for long sliding distances. 10N applied contact force

In conclusion the longer track length and higher sliding velocity indicated that wear rates can be significantly decreased by these conditions promoting abrasive wear over adhesive-delamination wear when sliding at low enough pressure, Figure 4.19. However, when the pressures are high enough to cause seizure, smearing and subsurface fracture the higher velocity reciprocating condition caused a higher wear rate due to large delaminations occurring instead of surface mixing.

(II) ⅛" VS. $^1/_{16}$"

At ⅛" reciprocation only very small delaminations were observed in the center of the wear scar, Figure 4.110; at $^1/_{16}$" reciprocation there was little indication of delamination wear, only adhesive transfer between surfaces. It was believed that the majority of wear occurred by a process of adhesion-delamination, although the size of the delaminations were very small in comparison the visible surface spalling observed for longer track lengths. Despite increased small adhesive transfer particles found on both surfaces, cross sections did not reveal the formation of a mechanically mixed layer, only regions were a thick debris deposit could be observed on the surface, as can be observed in the top picture of Figure 4.111 or Figure 4.213.

(III) COUNTERFACE IRON AND IRON OXIDE TRANSFER

The most significant finding for the shorter wear scars was a rapid increase in iron and iron oxide transfer from the steel counterface to the aluminum composites surface. Using regional EDS scans, a maximum of 5wt% Fe content from the 52100 counterface was recorded due to points of abrasive transfer under ¼" and ¾" reciprocating sliding

conditions. In contrast, reciprocating at ⅛" caused high amounts of steel transfer, in the range of 15-40wt% Fe at the ends of the wear scar, increasing with increased load. For $^1/_{16}$" reciprocation a near uniform iron oxide layer was present on the surface at 5N, causing a red rust appearance to the wear scar, shown in the bottom picture of Figure 4.111. The iron oxide on the $^1/_{16}$" track caused a weight gain at low pressures, Figure 4.18. At higher loads the surface appeared mixed through adhesive transfer, with a black appearance and equally high Fe content.

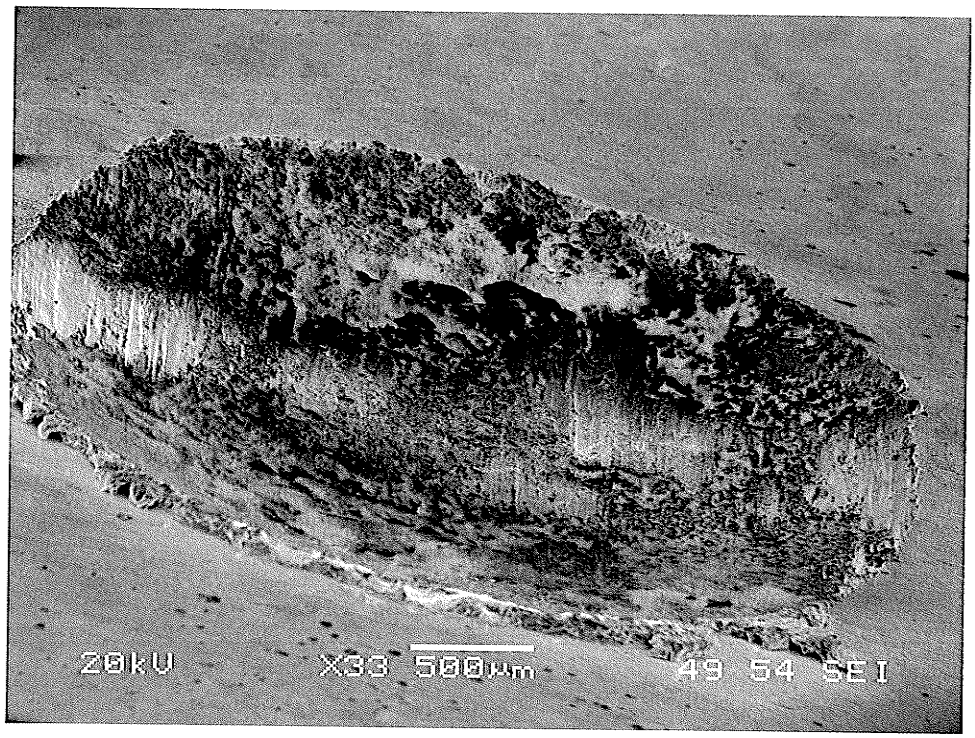

Figure 4.110 Whole wear scar, ⅛" reciprocating track with 50 N applied force for 125 m sliding contact.

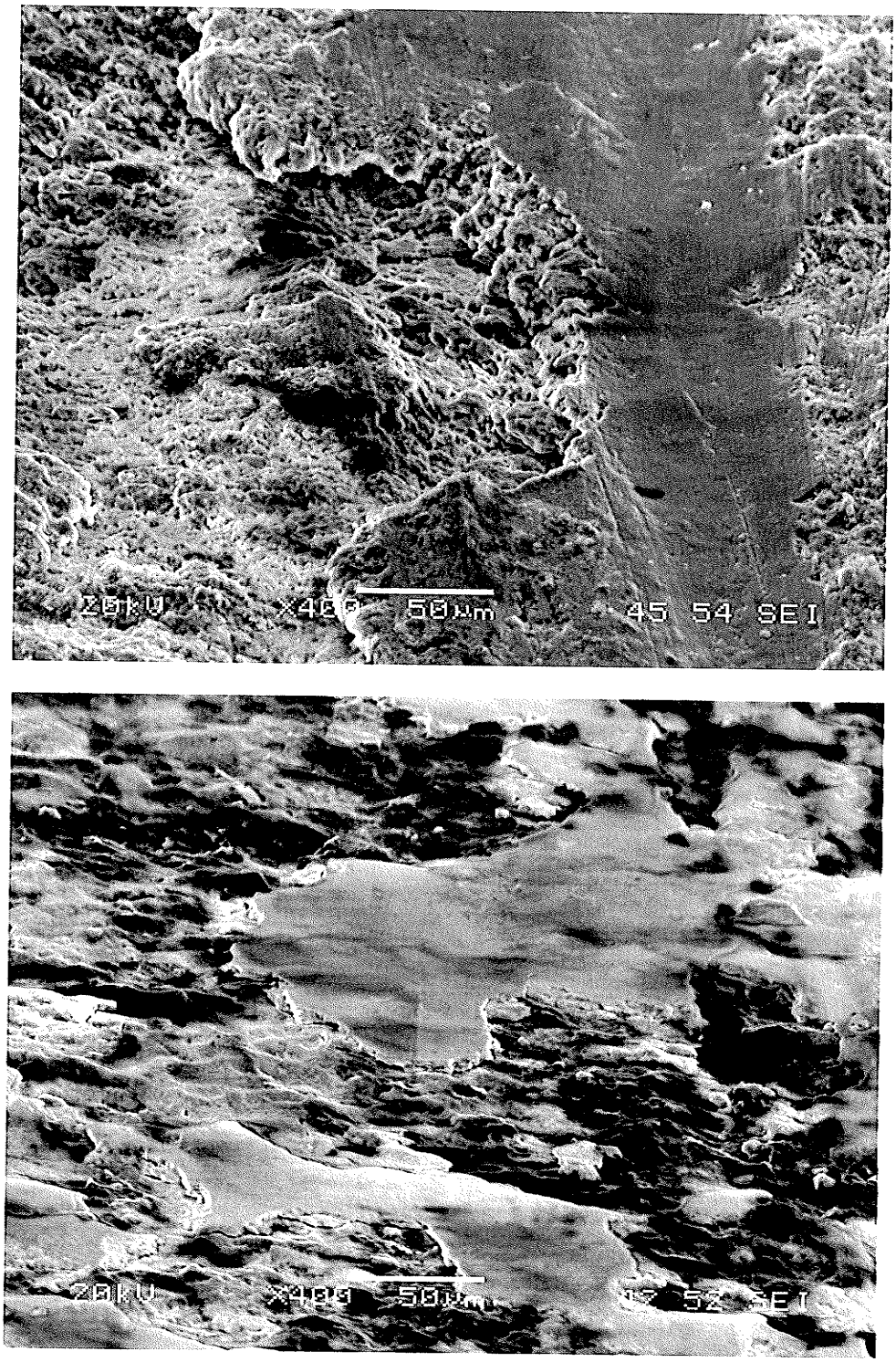

Figure 4.111 Differences in mixing at different sliding speeds. TOP: Center of wear scar with a mixed surface formed by adhesive transfer and exchange of debris. 15 % average Fe content was detected over the mixed region. BOTTOM: Edge of wear scar with deposited layers of iron oxide. Both images are from the wear scar shown in Figure 4.110.

(IV) DEBRIS

It was observed that debris particles were ejected with a greater momentum at the end of the wear scar as the track length was increased over the entire range of $^1/_{16}$" to ¾". A typical distribution of debris immediately after testing is shown in Fig. 4.112.

In general, as the reciprocating sliding distance and sliding velocity both decreased delamination wear was replaced by adhesive transfer wear. Also, as both of these extrinsic variables were decreased the iron and iron oxide particles in the debris were found to increase. It was surmised that the increase in iron transfer was due to greater abrasion of the debris trapped in the interface once generated.

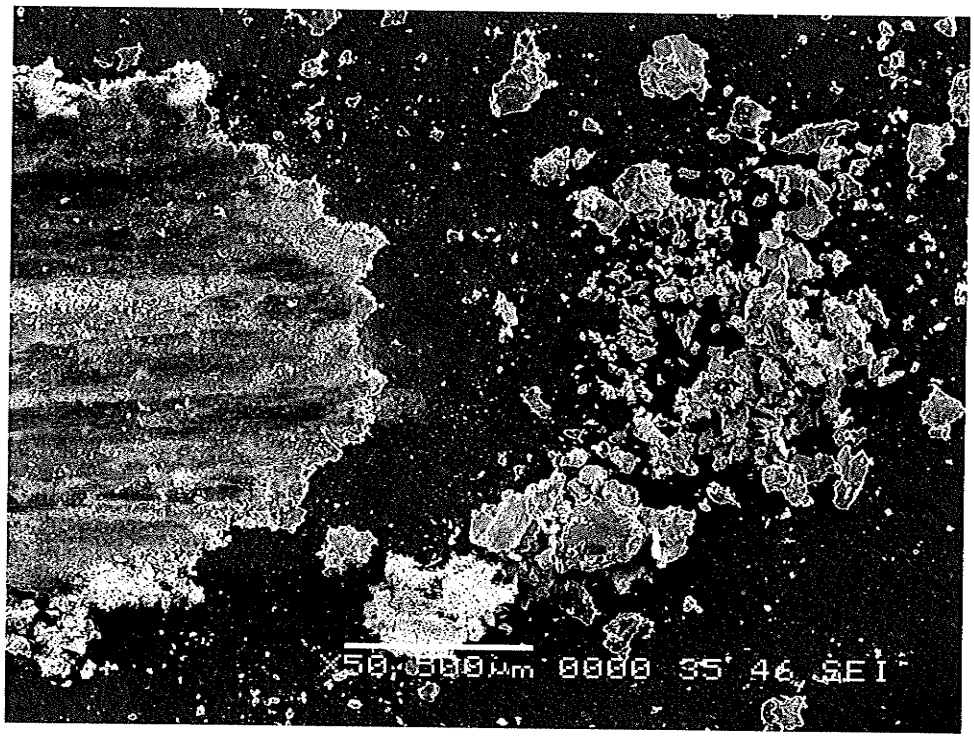

Figure 4.112 Ejection of debris particles at the end of the wear scar, 5N, 250m, ¼" reciprocating track. Larger debris was initially ejected with greater momentum for the ¾" reciprocating track and the higher sliding speed.

Shiny delaminations through smearing or fracture were produced for ¾" and ¼" track lengths, while black compact delaminations of mixed particle debris were the largest

source of surface wear for the ⅛" and $^{1}/_{16}$" sliding conditions. All reciprocating track lengths and sliding velocities produced black particulate debris.

Observing the overall results of changing the reciprocating distance it could be concluded that shortening the reciprocating distance promoted smearing, compression and adhesive transfer of the sliding surface at high contact pressures. As the reciprocating speed and distance was increased, abrasion as the dominant wear mechanism resulted in lower wear rates due to the least amount of debris produced, while as the reciprocating speed and distance were decreased lower wear rates resulted from the least amount of debris ejected.

4.13 EFFECT OF COMPOSITION OF THE STEEL COUNTERFACE

This section examines the effect of different counterface steels, 316, 440C and as-received 52100 tested against the Al-composite. The compositions and hardness values are given in Tables 3.2 and 3.3 respectively. Regarding the previous section, it was expected that greater difference in wear of the steel would occur at higher sliding speeds where abrasion became more dominant, however the focus of this section was on the effect of composition on adhesive transfer and mixing. Therefore the shorter ¼" reciprocating track length and average speed of 7.5 cm/s was chosen. The results are summarized in Figure 4.113.

Referring to Figure 4.113, differences can be seen in the resulting wear of the Al-SiC against three different counterface steel compositions. For a normal contact force less than 10 N the softest counterface, 316 stainless steel, caused the most Al-MMC wear. In

comparison, the 440C steel counterface caused a significantly lower weight loss of the Al-SiC MMC below this test load. The as-received 52100 steel caused the same trend of weight loss vs. normal contact force as the 440C steel; this was reasonable considering the change in hardness between the two counterface materials was relatively small. At the highest loads tested, where the wear of the composite can be considered to be severe, all three steels caused a very similar weight loss of the Al-MMC. Overall, it can be inferred that an increase in weight loss of the Al-MMC was not in proportion to an increase in hardness of the steel counterface. The wear rate caused by the counterface and applied load combination could be visibly defined as relatively high or low based upon the character of the debris, with fine black particulates being produced when the wear rate was relatively low and production of much larger shiny delaminations indicating a more severe rate of wear [11].

Greater insight into the fluctuations in weight loss with applied load can be found when comparing the change in mass transfer to the steel counterface. Weight loss of the steel counterface due to abrasion was observed to occur simultaneous with Al-MMC mass transfer, Figure 4.17. As a result mixing of the steel into the composite could have occurred despite an observed marginal weight loss of the steel counterface. Both as-received 52100 and 440C steel counterfaces had no weight loss or weight gain below 10 N, Figure 4.113. This indicated that the Al-MMC mass transfer to the steel counterface was greater than mass lost by the steel due to abrasion. The 316 stainless steel, the softest counterface, had the greatest likelihood of elemental mixing due to the greatest weight loss of the three counterfaces under 20N.

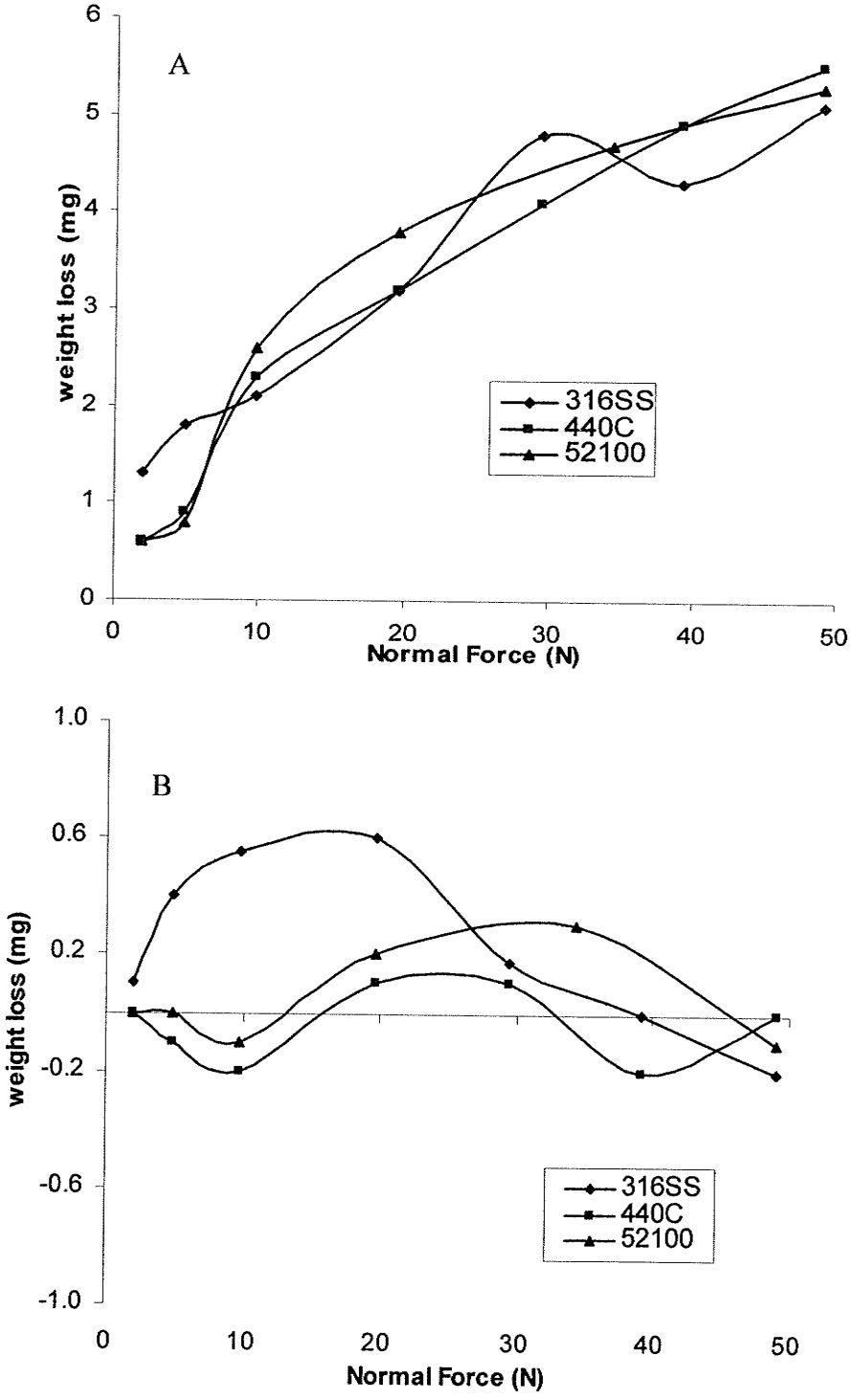

Figure 4.113 (A) Weight loss of Al-20%SiC against different steels. Similar wear rates were observed despite different counterface hardness and compositions. (B) Change in mass of the 3 different steel counterfaces. A negative weight loss indicates a weight gain by means of mass transfer. 250 m of ¼" reciprocal sliding, avg. 7.5 cm/s.

Fluctuations in the wear of Al-SiC correlate well to the change mass transfer occuring on the counterface. No detectable weight loss or gain of the as-received 52100 and 440C counterfaces below 5 N corresponded to the lowest wear rates of the Al-SiC. From 5 to 10 N a rapid rise in wear rate of the Al-MMC occurs in concurrence with a mass increase of the 440C and 52100 steel counterfaces, indicating that the stick-slip adhesive transfer of Al-MMC to the steel could be acting as a mechanism in increasing overall wear. A noticeable fluctuation to high wear for the Al-MMC at 30 N against the 316 counterface was observed. The fluctuation was correlated to the immergence of shiny flake delaminations from the Al-MMC surface at the beginning of the test that were subsequently produced at all higher loads. The high sudden increase in wear of Al-SiC at 30 N against 316 counterface can be observed in conjunction with the weight loss of the counterface being much reduced at this load, indicating more Al-MMC mass transfer to the 316 counterface must be occuring on average over time. In this case, a greater adhered volume of Al-MMC on the counterface during sliding contact would again indicate a greater rate of wear.

Variations in Al-MMC wear for different applied loads appeared to correlate well with the amount of mass transfer to the steel counterface or more specifically, the change in the delamination rate of the mixed Al-MMC transfer layer off of the steel counterface. Without a mixed Al-MMC transfer layer present on the steel, the ability of the steel counterface to cause direct delamination, abrasion, and plastic deformation controlled wear of the Al-MMC. However, this was rarely the case as a transfer layer was always present to some degree on the steel counterface over the range of applied pressures. The elemental transfer that could result depended on the thickness and uniformity of the mixed Al-MMC transfer layer since it controlled the ability of the Al-SiC MMC to directly abrade the steel.

4.14 EFFECT OF HARDNESS OF THE STEEL COUNTERFACE

52100 steel ball bearings were heat treated to achieve a range of hardness data. As received microstructure revealed a lathe martensite structure near center of ball bearing, with grain microstructure becoming more refined as distance from center increased. Retained austenite was visible on the as-received surface to a depth of 5-10 μm. Balls were annealed in vacuum to prevent decarburization and furnace cooled.

Figure 4.114 Center of as received 52100 ball bearing, 400x

Annealing Temperature (°C)	Time (hrs)	Hardness (HRC/ HV)
As received	-	64.8/ 827
300	1	59.8/ 693
300	3	55.2/ 598
300	9	46.7/ 469
300	20	45.0/ 448
350	1	53.7/ 575
400	1	49.7/ 509
450	1	40.8/ 401
500	1	37.4/ 367
550	1	34.0/ 335

Table 4.1 Heat treatments to achieve different hardness 52100 ball bearings

A vacuum of 10^{-5} Torr ($1.33x10^{-3}$ Pa) was, on average, obtained by evacuating silica glass tubes. Superficial oxidation was noted as a problem for obtaining consistent result as a black oxide layer would affect both hardness and wear rate when mated against the composite. When annealing at a relatively low temperature of 300°C in vacuum oxidation was insignificant. Consistent hardness values of the ball bearings could be obtained annealing at this temperature for progressively longer furnace times. Tempered Martensite Embrittlement (TME) represented a problem at the low annealing temperature, however the presence of grain boundary carbides was not observed by cross sections of the steel ball, Figure 4.114.

The annealed bearings allowed some separation between the role of the counterface material and the role of hardness alone. A high contact force of 50N was chosen to promoted stick-slip adhesive fracture. Observing 52100 bearing wear, Figure 4.115, a slight trend could be seen for increased mass transfer to the counterface as the hardness was increased. A similar result of increased weight loss for the softer 316 stainless steel counterface can be found in Figure 4.113 at 50N. Both sets of testing indicated that the hardness of the counterface may control the mass transfer more significantly than counterface composition. At any counterface hardness adhesion dominated wear, either by small transfer particles or adhesion-delaminations. Abrasion was never a dominant wear mechanism, even for the softest steels. In general, tests stopped at higher pressures had greater adhesion to the steel counterface and therefore greater composite wear. Variations in Al-MMC wear for different applied loads appear to be better described by: 1) the change in the delamination process of the transferred Al-MMC off of the steel counterface, i.e. the

degree of mass transfer, or 2) the ability of the steel counterface to cause direct delamination of the Al-MMC surface based upon the counterface's hardness.

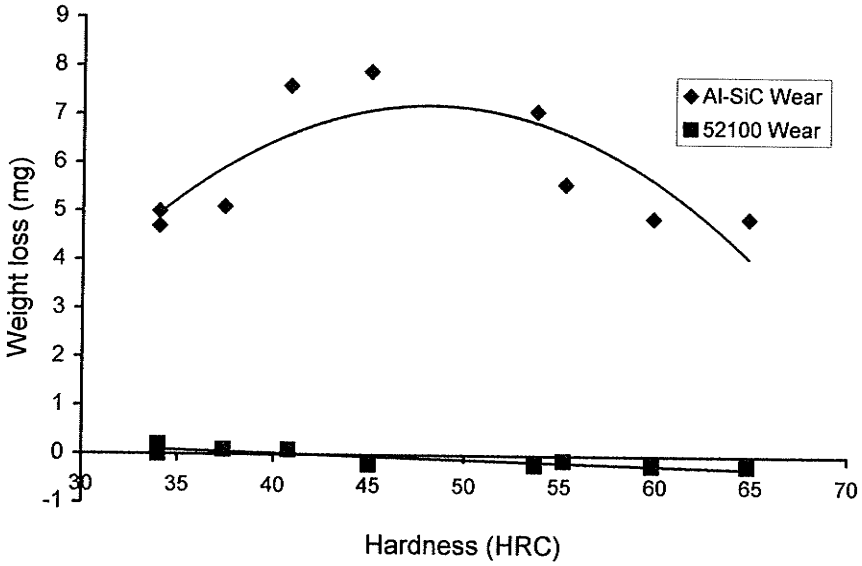

Figure 4.115 Effect of 52100 steel counterface hardness the on the wear of Al-MMC. Tested at 50 N for 250m using ¼" reciprocating track.

Moving from left to right in Figure 4.115, an increase in the hardness of the 52100 bearing from 30-40 HRC (300-400HV) can be seen to initially cause an increase in the wear of the aluminum composite. The peak in composite wear was observed between 40-50 HRC (400-500HV). Further increase in hardness up to the as received 65 HRC (833 HV) had the effect of decreased composite and counterface wear. The higher hardness steel counterface in general had an increase in mass. Since wear is occurring through simultaneous processes of adhesion and abrasion on both surfaces, increased mass must indicate that the aluminum composite has transferred to the steel counterface without significant loss of the counterface through abrasion. The weight loss observed for steel of

low hardness does not necessarily indicate less adhesion to the steel, as similar adhesive patterns were observed regardless of the hardness, but rather that abrasion of the softer steel may have become more significant. The soft steel (300 HV) caused similar wear of the composite as the hard steel (850 HV), nonetheless, when examining the tribological pair, the harder steel counterface would be preferred due to the lower overall weight loss.

4.15 CONCLUSIONS ON WEAR PERFORMANCE

The intrinsic wear resistant of the A356-20vol%SiC composite was established by comparison to the unreinforced alloy under equal test conditions. The increase was small but significant. Further increases in intrinsic wear resistance of these composites have been related to the formation of a MML, which was a phenomenon that did not occur under the sliding conditions used in this study.

Previous work has observed that reciprocal testing consistently produced a smaller size of debris than unidirectional sliding [47]. The change in reciprocal sliding distance was observed to have an effect on the size and composition of the debris produced and the dynamics of debris particle ejection. A change in the dominant wear mechanism from predominantly adhesion to mixed adhesion-delaminations and abrasion was observed to occur with increased sliding velocity and increased reciprocal sliding lengths.

In general, the hardness and composition of the steel mated against the composite did not greatly affect wear properties. A softer steel counterface, such as 316ss or annealed 52100, slightly increased the wear of the composite while simultaneously experiencing increased wear. Decreasing the hardness of the steel counterface could be concluded as

adversely affecting the wear performance of the sliding system. However, the effect of the counterface was not as significant as the extrinsic sliding conditions such as sliding velocity and reprocessing of debris.

Specific wear rates were found to be higher by order of magnitude when compared to those studies using a similar material pair [12,90]. It is proposed that wear rates observed in this study were high due to three major effects:

1) The cohesively weaker material (Al-composite) experienced intermittent contact. This may have reduced accumulation of debris and formation of stable surface mixed layers.

2) The reciprocal sliding condition better facilitated ejection of debris, again not allowing for debris mechanical mixing to contribute significantly to wear resistance.

3) The slow sliding speed promoted adhesion-delamination or stick-slip relative motion in contrast to higher speeds where abrasion can become more dominant.

All three of these proposed variables resulting in high wear are related to extrinsic sliding conditions. Therefore comparisons to previously published work are inaccurate since in most studies either 1) the aluminum composite was used as the continuous contact counterface for a block-on-ring apparatus [12,34] or 2) a pin-on-disk apparatus was used that maintained a constant contact pressure [31,90]. In comparison, the composite surface in this study experienced very high pressure over the course of the 250 m ball-on-block wear test. Either case of different contact geometries could significantly affect the specific wear rates and hence cannot be accurately compared.

4.21 STAGES OF AL-SI-SIC WEAR

For the ball on block contact steady-state wear is never fully achieved due to reduction of the contact pressure as the wear scar conforms to the counterface with increased sliding distance. The dominant surface wear mechanisms were related to the surface contact pressure by stopping the test for different sliding distances. With increased sliding distance (decreased pressure) the simultaneous dominant wear mechanisms can be organised into three broad categories:

1) Seizure spalling of the surface
2) Delaminations due to smearing

} **Category 1**: High Pressure

3) Delaminations due to subsurface fracture
4) Delaminations of the mixed surface

} **Category 2**: Intermediate Pressure

5) Abrasive wear

} **Category 3**: Low Pressure

This arrangement of wear mechanisms is in order of how they would appear with decreasing surface pressure. When delamination wear was the dominant mechanism [2), 3) and 4)] the plastic flow and compaction would cause the surface to appear smeared. When abrasion became a dominant wear mechanism very little or no smearing was observed on the surface. The transition of the dominant wear mechanism from 4) to 5) also corresponded to the limit of surface mechanical mixing. Abrasion as a dominant wear mechanism could however only be achieved at the contact pressures of approximately 1 MPa and lower, which were rarely achieved in the present study. Therefore abrasion and mixed delaminations most often had joint roles in wear at the lowest contact pressures.

All wear mechanisms except abrasion caused significant plastic deformation to extend into the subsurface. In category 1, seizure would cause overload fracture in the subsurface with very little subsurface damage accumulation. For all three mechanisms in category 2 the depth of subsurface damage accumulation determined the morphology of the delamination wear. Exceeding the maximum stable plastic tensile strain while under compression and shear at the surface caused smearing delaminations to occur for mechanism 2). Fracture due to deeper subsurface damage accumulation caused delaminations to occur for mechanisms 3) and 4).

(I) SEIZURE DURING INITIAL CONTACT

During initial contact surface pressures were extremely high causing extrusion of the Al surface at the point of contact of the steel ball. At the extreme pressures (>20MPa) the steel surface locks and pull apart the composite surface under the driving force of the wear-mechanism. The composite wear can be described as occurring due to seizure at points of contact and subsurface fracture. The result was surface spalling, with large shiny plate debris removed from the interface. No mixing occurs and wear rates are particularly high. For the Al composite, large shiny debris was observed to initially occur for normal contact forces greater than 20 N at ¼" reciprocating distance. At lower normal contact forces only black particulate debris was produced. This placed the seizure pressure in the range of 15-20 MPa at the average sliding velocity of 7.5 cm/s. As a result, seizure debris was only produced at the beginning of the test, characterized by long thin plates, up to 1mm in length, removed from the surface

When the average sliding velocity was *increased* (22.5 cm/s at ¾" reciprocating distance) shiny delaminations occurred at a lower normal force of 5N. This corresponded to a seizure pressure in the range of 10-15 MPa. As the sliding velocity was *decreased* (3.3 cm/s at ⅛" reciprocating distance) only black particulate debris was produced at any contact force. The conclusions are as follows. First, at high pressures seizure causes spalling of large shiny debris. Secondly, the resistance to surface spalling at high pressures decreases as velocity increases. Finally, longer reciprocating distances favour seizure delamination of the surface.

(II) SMEARING OF THE SURFACE

Surface spalling due to seizure should not be confused with gross plastic delaminations as different mechanisms are occurring. Seizure results in rapid disintegration of the surface as large regions of the surface are fractured and removed as debris without experiencing significant deformation. Gross plastic delaminations have experienced significant deformation prior to fracture and therefore resist wear to a much greater extent. Seizure of the surfaces would always cease to occur during the first few metres of sliding and be subsequently replaced by gross plastic delaminations as the dominant wear mechanism. This was true for HP Al and Al-Si, as well as the Al-SiC composite. Gross plastic deformations were dull grey or blackened through deformation in comparison to the shiny debris produced by seizure wear.

Smearing of the surface was observed to occur at any load for the Al-SiC composite. Initially smearing did not produce large delaminations debris under the high contact pressures and low speeds. The reciprocal stroke would "fold back" the surface; a

process which repeated until a smooth coherent Al-surface formed, Figure 4.21. The compression and elongation of the Al surface to large equivalent strains caused the coherent surface mixed layer to form. SiC are inundated and/or pulverized and inundated by matrix flow under the high hydrostatic pressure. Excessive strain in the smeared surface ultimately causes the surface to delaminate, Figure 4.24. These delaminations were observed to have a smooth underside fracture surface as the fracture would occur due to tensile strain of the layered material. Examples of large mixed delaminations of the smeared surface are shown in Figure 4.34

During the initial sliding contact the pressure was very high causing transfer of the Al-SiC to the steel counterface to occur. Layers of smeared Al-Si and pulverized SiC can be seen to deposit sequentially for each reciprocated pass. Under high pressures, from 10-20 MPa, smearing of the composite matrix dominates at the interface and the wear surfaces are rendered smooth, Figure 4.21. When smearing was dominant, matrix flow caused fracture and compaction of SiC particles which resulted in the formation of mechanical mixing regions in the subsurface. Subsurface morphologies formed by smearing as the dominant wear mechanism are shown in Figures 4.211 and 4.212.

Craze cracking of the surface provided evidence that the contact pressure is no longer adequate to retain the smeared surface. In Figure 4.23, an abrasive debris particle has caused significant surface traction causing severe damage to the smeared matrix surface. This occurred on the mixed composite surface.

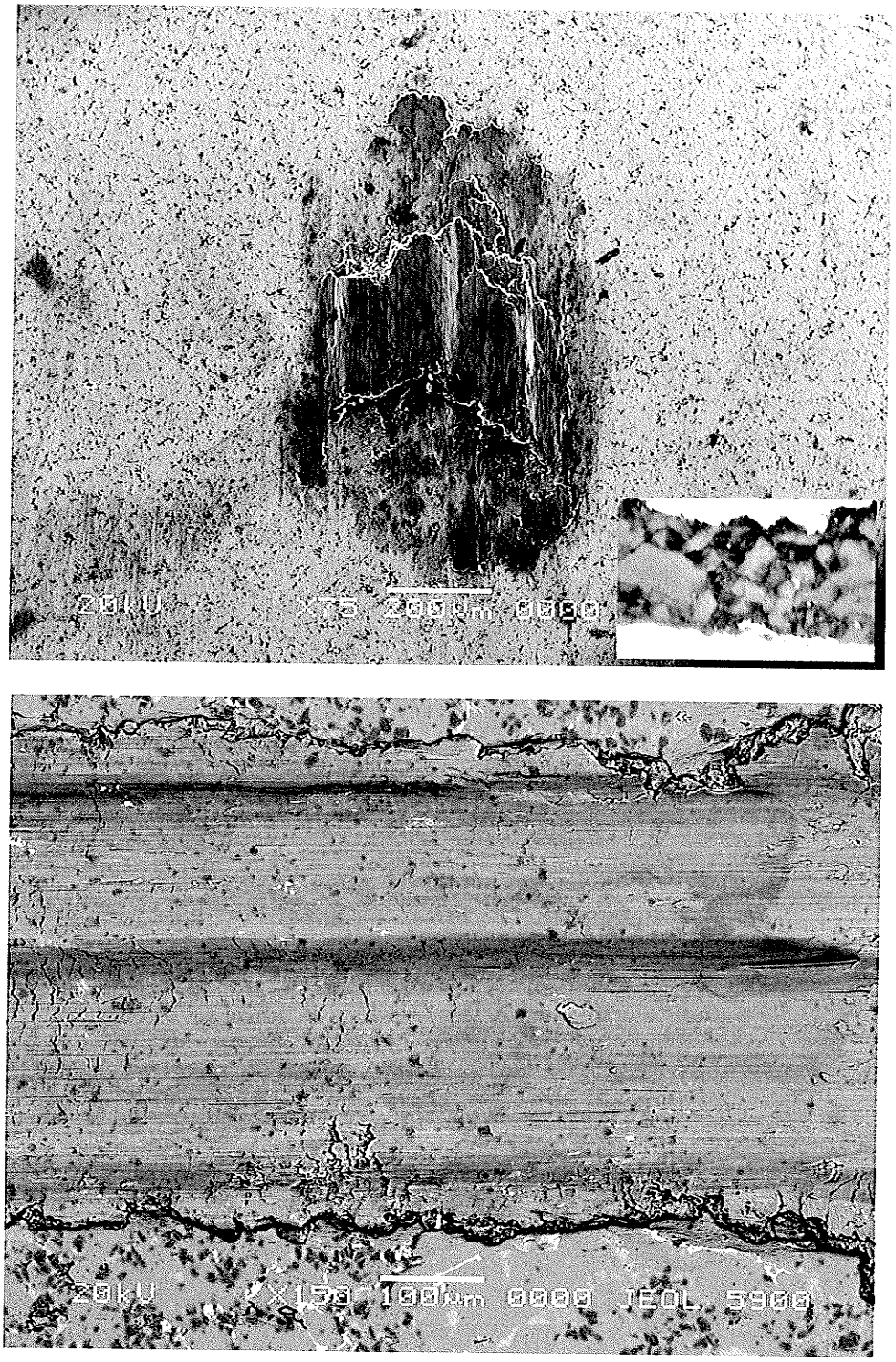

Figure 4.21 TOP: Layered material build-up from transfer of the Al-Si-SiC composite to the steel counterface. Inset shows the cross-section of the deposit. BOTTOM: BSE image of smeared composite surface. 5N, 10m, ¼", 316ss counterface, approximately 20 MPa

In comparison, craze cracking due to tensile fracture of smeared layers can be observed for HP Al however in this case there was no mechanical mixing due to the surface fracture being too severe, Figure 4.23.

(III) UNDULATIONS AND TRANSITION TO SUBSURFACE FRACTURE

As the state of contact pressure was reduced, undulations were observed to form. High loads were not required for undulations to form. Undulations developed as the sliding distance increased from 250 m to 2000m of sliding contact at a low normal load of 5 N. The surface undulations developed at shorter sliding distances for higher normal loads. For the high normal loads (greater than 50 N) that did not allow surface pressures to fall below 10 MPa, undulations would not form for any sliding distance and mechanical mixing through smearing and compaction continued to dominate, Figure 4.22. It can be observed that delaminations due to subsurface fracture are occurring most significantly from the valley regions of the wavy surface, and delaminations due to smearing are occurring at the crests. Undulations did not form for HP Al. Undulations that formed for the tested Al-Si alloy required much lower pressures.

Cross sections of the undulations revealed that they were not formed through debris deposition and mixing, with plastic deformation only visible of the ascending side of each undulation. The pattern of delaminations indicated that the peaks were formed due to preferential large delaminations occurring from the valley regions of the wear scar. Greater compression occurs on the ascending sides of the undulations in comparison to the lower points on the wear scar profile, causing a smoother smeared surface.

When undulations began to form a transition in the dominant wear mechanism was occurring from delamination wear by smearing to delamination wear by subsurface fracture. This observation was substantiated by rough fracture surfaces of the delaminations, Figure 4.25, in comparison the prior smooth folded fracture surfaces that resulted from smearing, Figure 4.24. Both smearing and subsurface fracture delaminations were observed to simultaneously occur on the wear surface as can be seen by examining Figure 4.27. That is, there was no particular contact stress at which a complete transition in the dominant wear mechanism occurred. This is as would be expected in consideration of the surface and subsurface variations in reinforcement, therefore causing variations in the flow stress and subsurface damage accumulation at points of counterface contact.

Sources of subsurface damage accumulation such as particle fracture and void formation had indications that they were exhibiting control over delamination wear. The fracture surfaces and debris revealed dimples and a tearing surface topography, Figures 4.25 and 4.33. Clarke and Sarkar [78] referred to wear particles with a rough fracture surface as "granular delaminations" for the Al-Si alloys, which appears equally valid for the delamination debris observed to be generated from the composite. During the transition between delamination mechanisms, debris produced often had a smeared surface although not substantial enough to form the layered structure before delamination from the subsurface occurred.

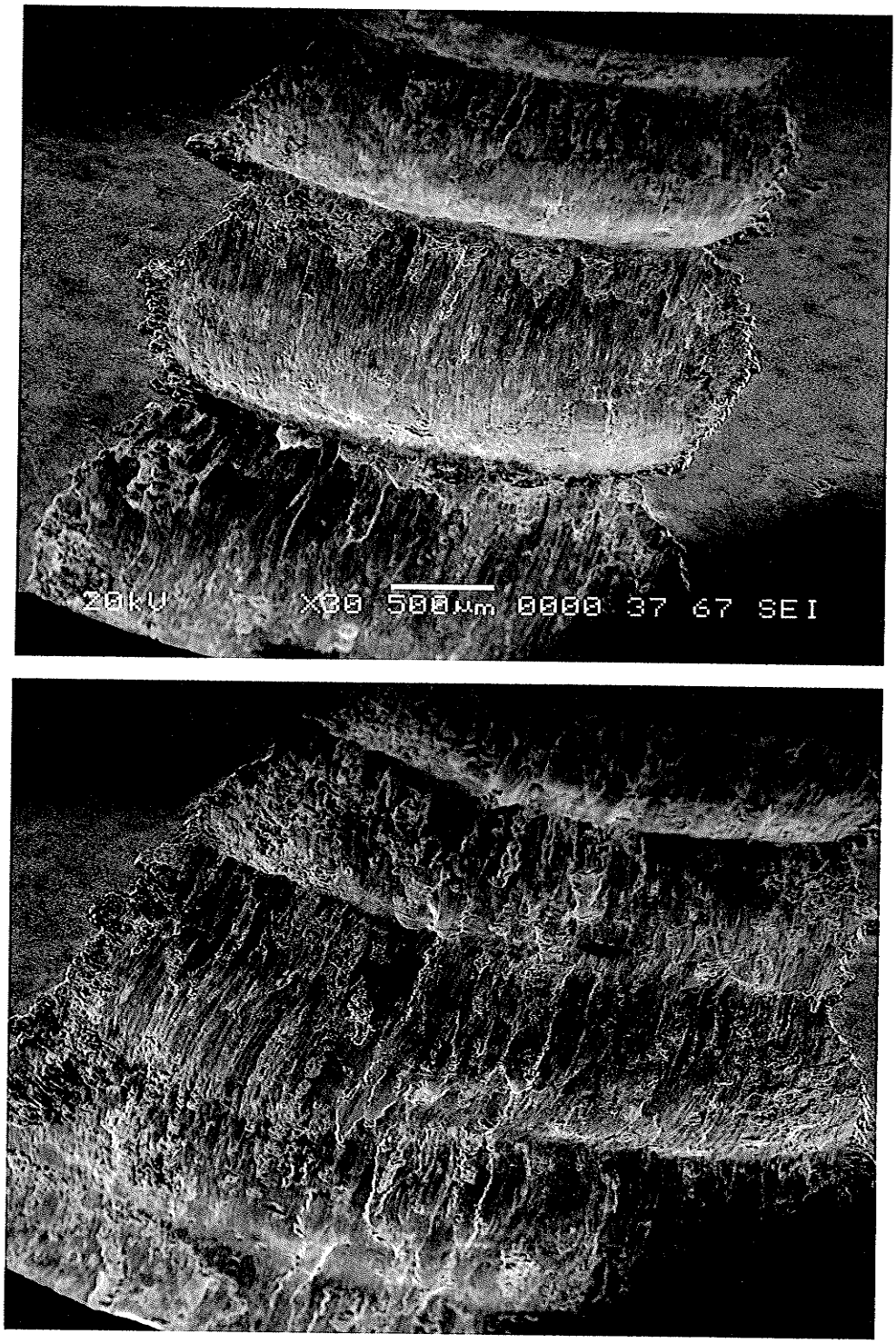

Figure 4.22 TOP: Undulations formed on the worn composite surface at 20N. BOTTOM: Undulations begin to be replaced by smearing of the surface at a higher load of 40N. Both tested for 250m. Delaminations due to smearing and subsurface fracture are observed as the dominant mechanisms of surface wear. Undulations were not present at higher pressures.

(IV) REDUCTION IN DELAMINATION SIZE

Delamination wear occurred at all test pressures, however the size and depth of delaminations were both reduced at lower pressures. The depth of delaminations caused by subsurface fracture was, in general, greater than delaminations originating from smeared layers. However as the pressure was decreased, compact delaminations and mixed delaminations were produced from the surface, causing significantly less surface damage, Figure 4.26. Surface damage can be considered proportional to the size of the debris produced, with the size of delaminations becoming reduced as the wear mechanism changes from 1) through 4).

Both compact and mixed delaminations were caused by some subsurface fracture. Incomplete compaction of particulate debris of the near surface was observed as a potential source of instability leading to mixed delamination wear. Compact delaminations were often found at particle clusters. Mixed delamination debris had two distinct surfaces: granular fine particulate debris at the fracture depth while smearing and compaction at the surface, Figure 4.34. This indicated that delaminations composed of fine equiaxed particles, proposed by Antoniou and Subramanian [15] could be a valid description of the wear observed at lower pressures. This was not chosen as the most accurate description as mechanical mixing of fine particulate debris did not always occur. Secondly, the depth at which delaminations were generated was often greater than the depth of surface mixing. Therefore for the current testing both compact (bulk) delamination and mixed delamination wear mechanisms must be used to described the composite wear best at lower pressures.

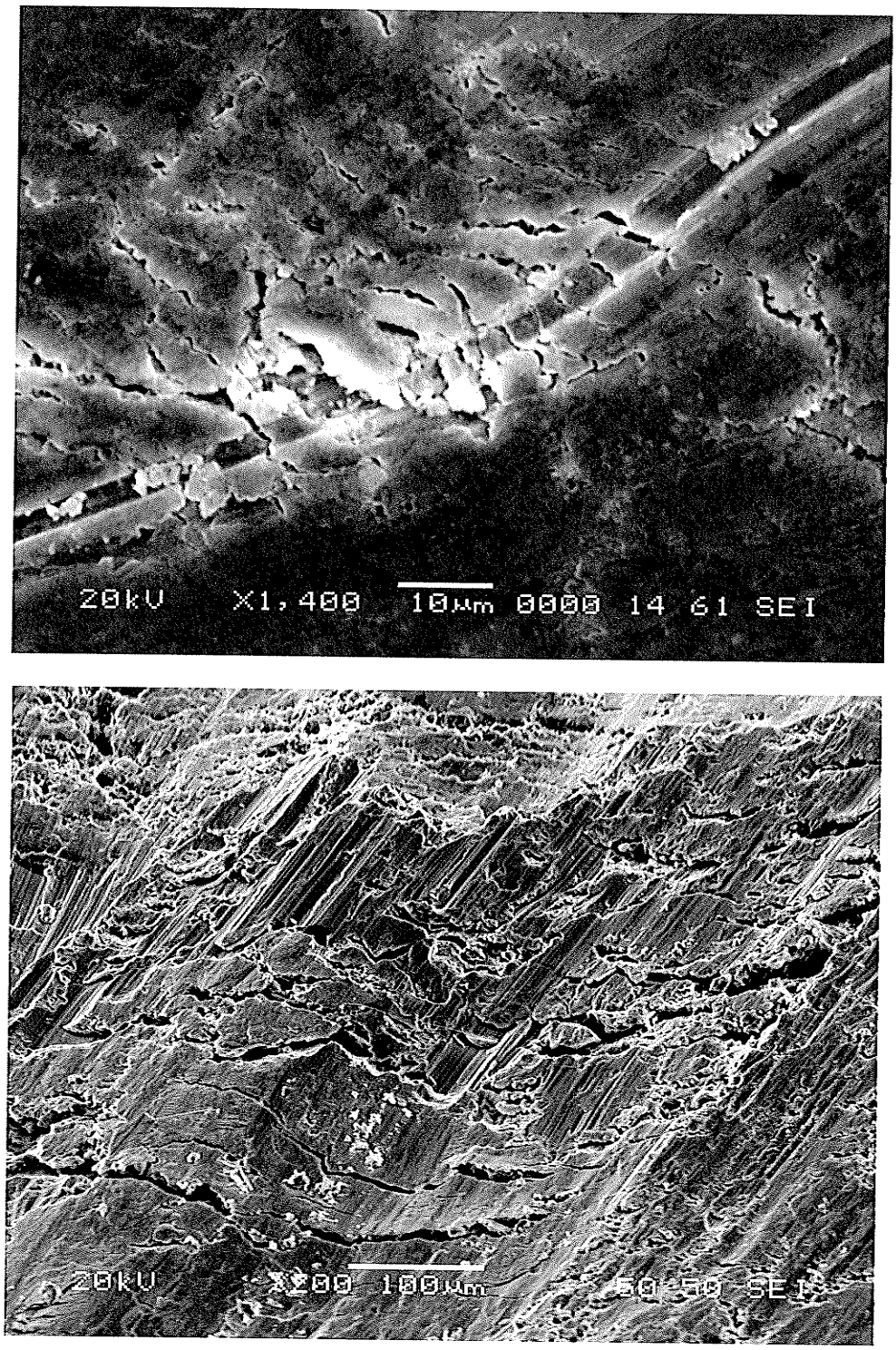

Figure 4.23 Breakdown of smearing as the dominant wear mechanism. TOP: Smooth SML exhibiting craze cracking due to abrasion of either a debris particle or transferred SiC from the composite. Traction of abrasive particles can be seen to provide impetus for small adhesion-delaminations to form. BOTTOM: Craze cracking due excessive plastic strain for HP Al. Due to the depth of plastic deformation the HP Al results in much larger delaminations

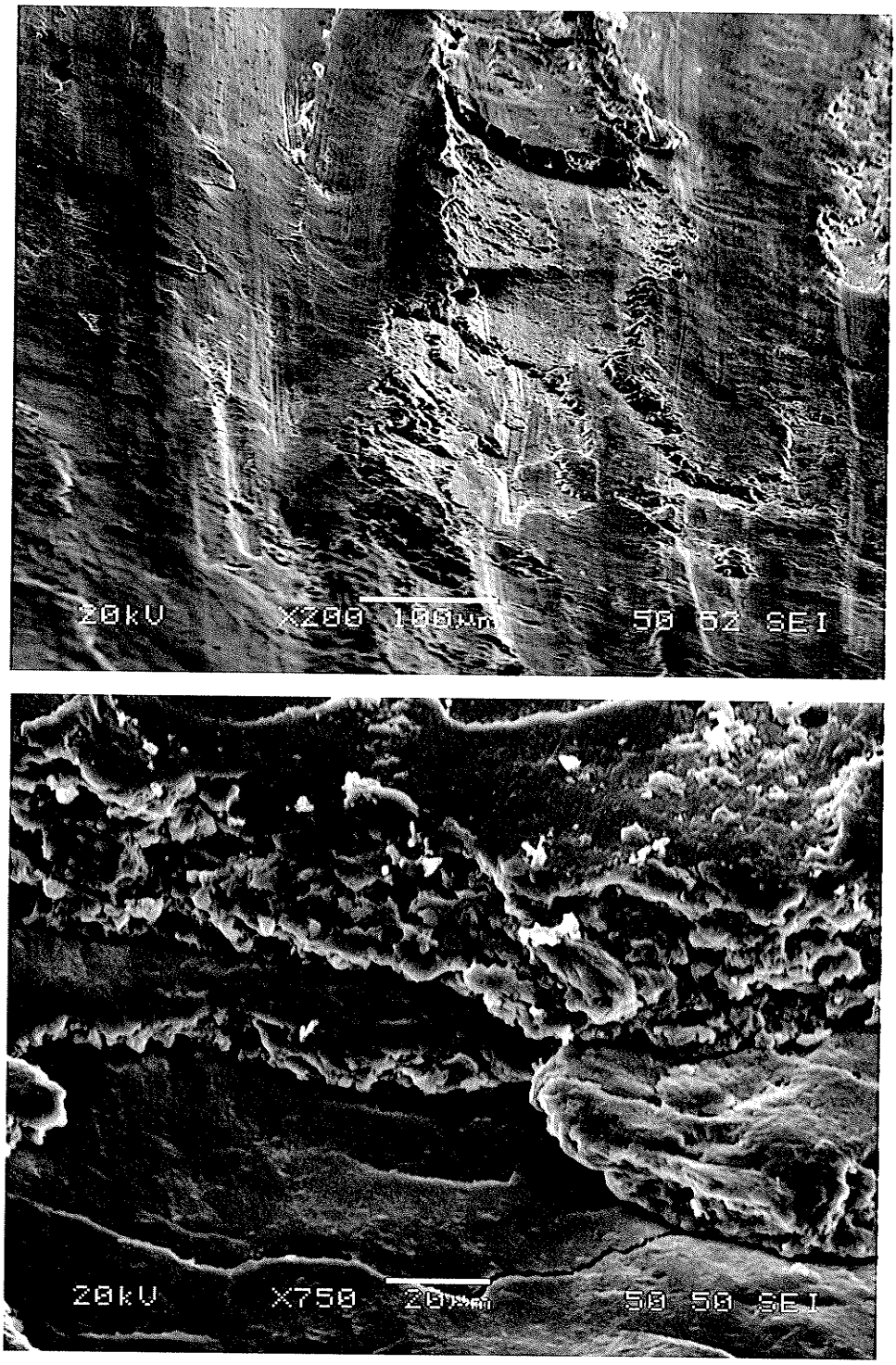

Figure 4.24 Gross plastic delaminations as the dominant wear mechanism. TOP: Compact layer delamination of the smeared surface. BOTTOM: Smooth underside of delaminations due to folding layers which form the smeared surface. Fracture surface is observed to be a combination of mixed debris and deformed Al-Si alloy. 50 N, 250 m

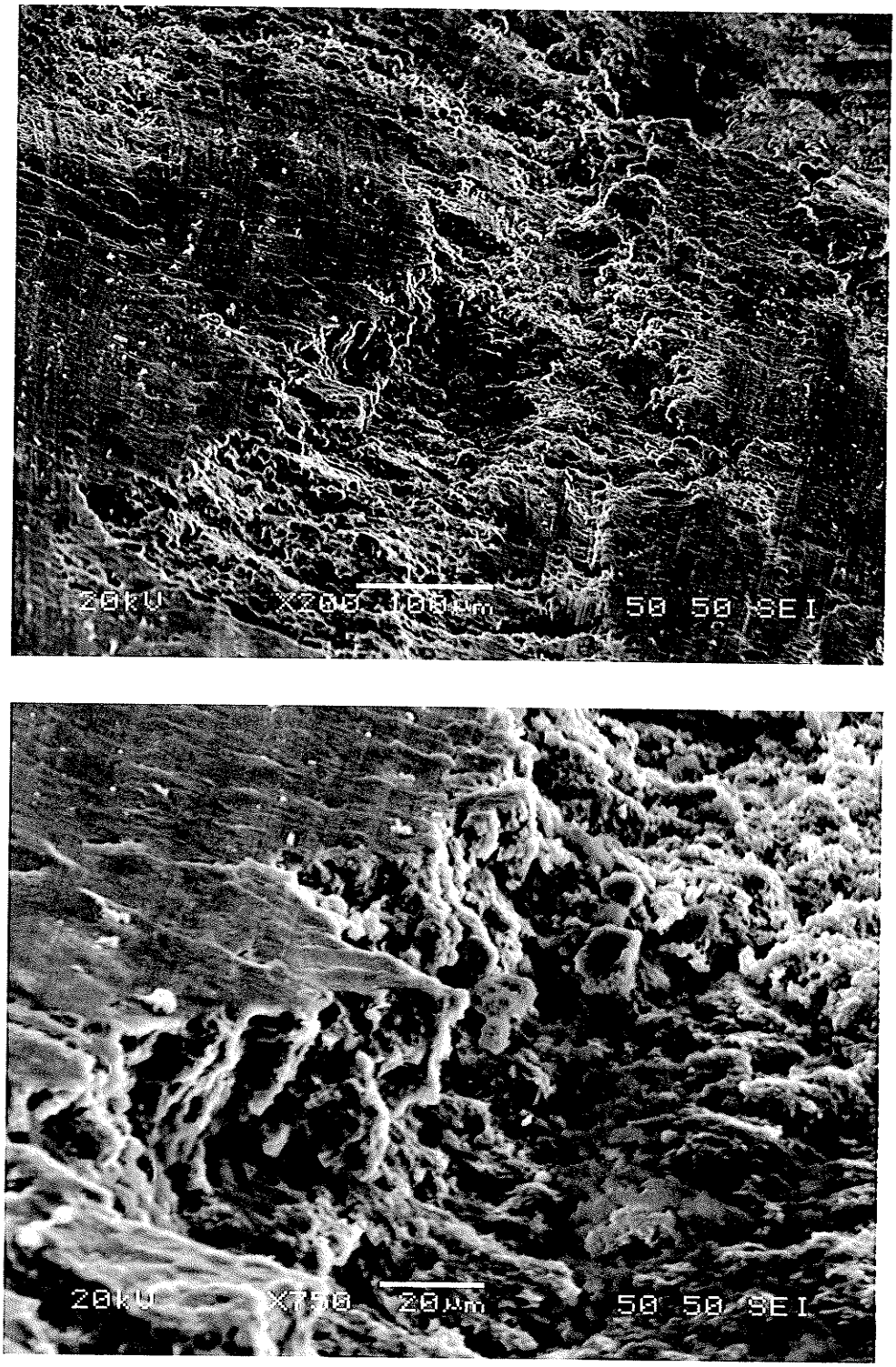

Figure 4.25 Delaminations due to subsurface fracture. Note the top surface of the composite has been smeared. Mixing of debris can be observed. Al-Si-SiC, ¼" reciprocating, 20N, 250 m.

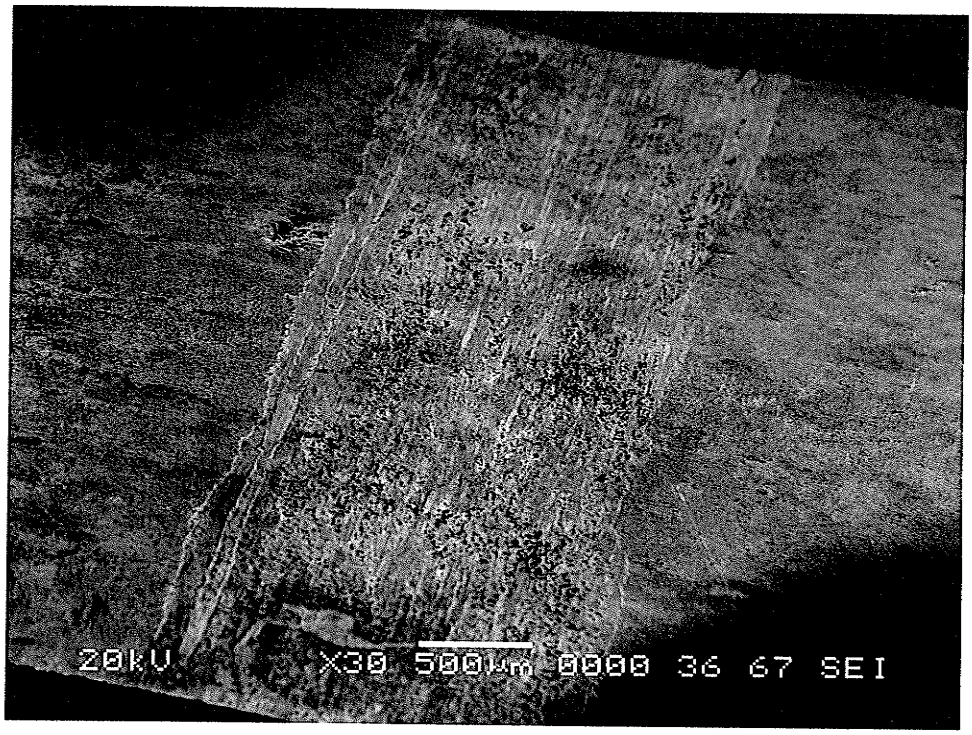

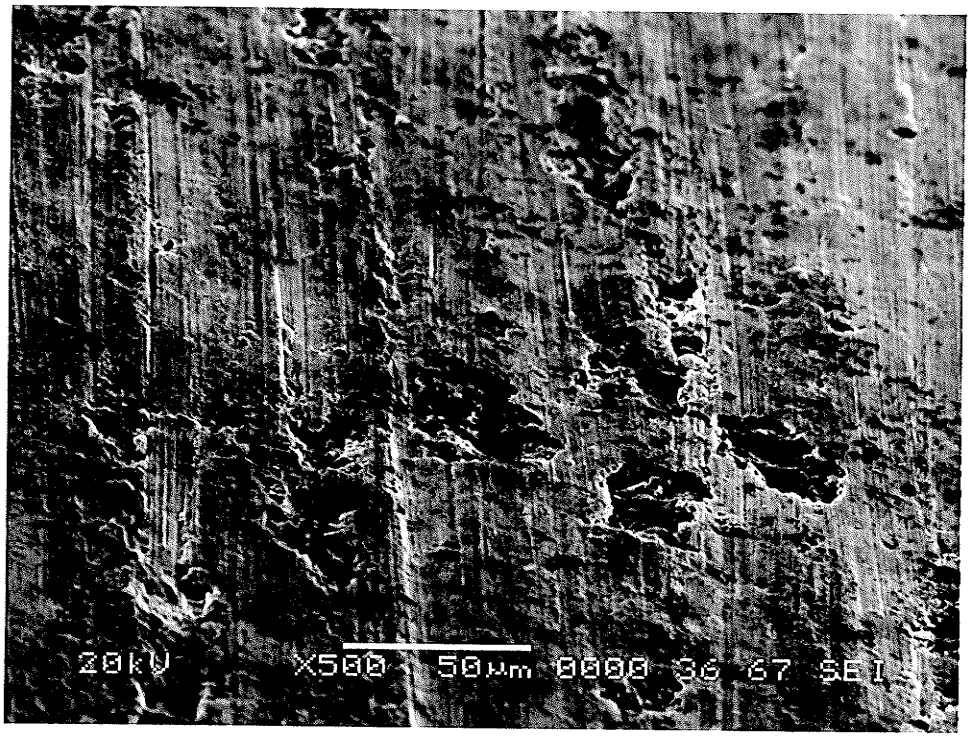

Figure 4.26 TOP: Low mag surface showing surface wear due to abrasion and compact delaminations. No possibility of a SML exists with these operating wear mechanisms. BOTTOM: High mag view of surface showing the small irregular bulk adhesion delaminations. 52100 counterface, ¾" reciprocating distance, 250 m, 5N, 1 MPa estimated contact pressure. With abrasion as a more dominant wear mechanism increased Fe transfer from the counterface occurred.

4.22 TRANSIENT SURFACE MIXED LAYER (SML)

(I) FORMATION OF A SML

The initial stage of formation of what would become a smooth surface mixed layer (SML) is shown in Figure 4.27. In this figure "tongues" or "wedges" of the aluminum composite are formed by smearing the aluminum matrix to large equivalent strains in the sliding direction. The wedges are observed to overlap and become smooth folded layers under the high initial pressure. With continued deformation the smooth folded layers would extend with each reciprocal pass and would eventually form a coherent SML, Figure 4.28. At greater sliding distances the SML would fracture in part due to excess strain, as can be seen in the top picture of Figure 4.23. Due to the reduction in contact pressure with continued sliding, once fracture of the SML began by smearing delamination wear, the sliding pressure was becoming insufficient to strain the surface into the layered structure. Consequently as pressure continued to decrease the fracture rate would exceed the formation rate until the SML was removed. Therefore due to the large change in pressure, the SML was a transient surface phenomenon under ball-on-block wear testing.

The role of reduced contact pressure in promoting delamination wear due to subsurface fracture over smearing can be observed in the wear scar morphology of Figure 4.29. In this figure the edges of the wear scar have a lower pressure due to the non-uniform pressure distribution of the ball-on block configuration. The center of a wear scar could be seen to have a smooth SML in the highest pressure contact region, Figure 4.29. Likewise little adhesive transfer existed on the ball in this region of contact due to dominant smearing of the composite surface.

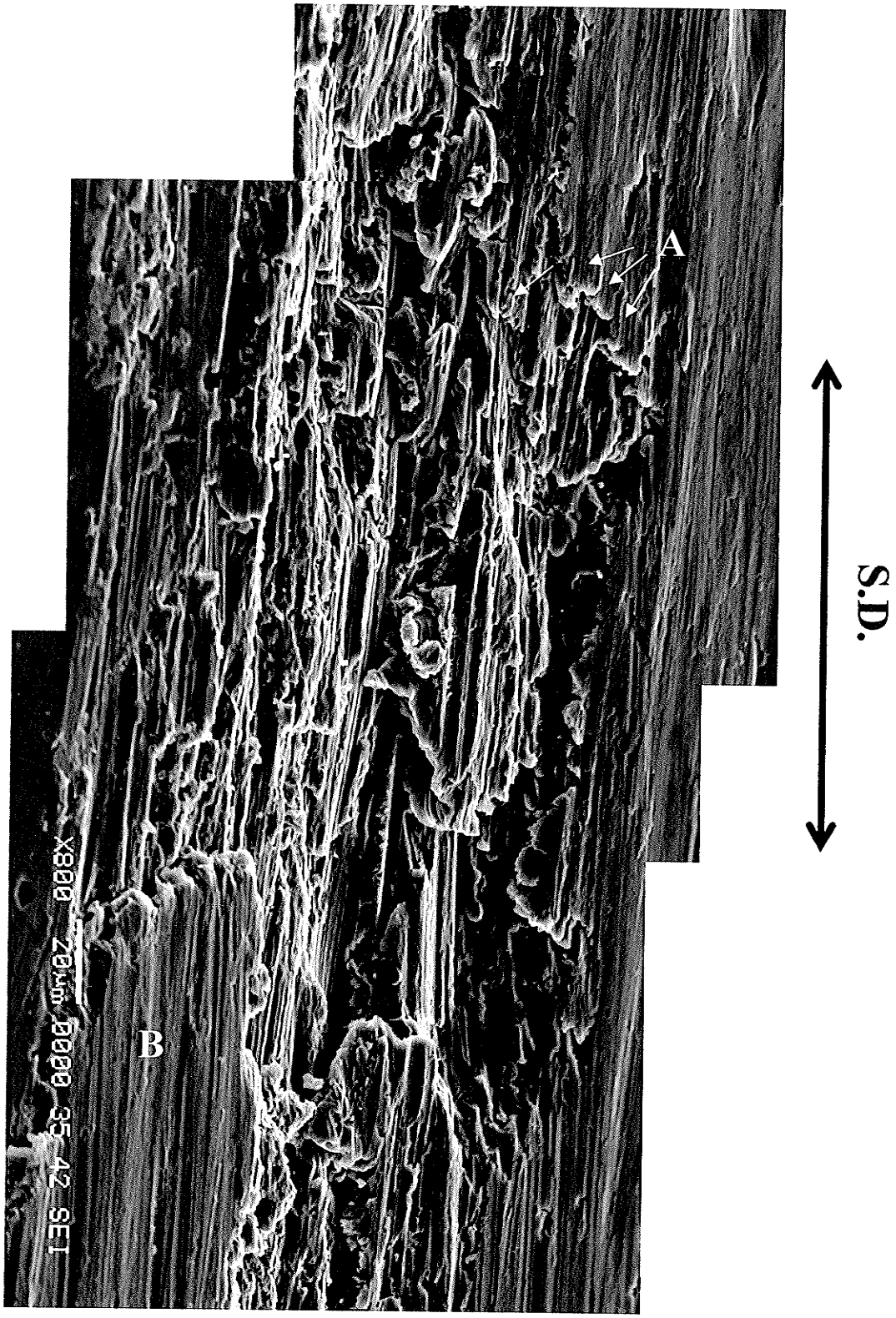

Figure 4.27 The initial stage of formation of a SML on the Al-SiC composite. (A) "Tongues" caused by contact points elongated to large strains are indicated by arrows. (B) The resultant layer formed by compaction of elongated contact points. 5 N, ¼", 52100 counterface, 1m sliding contact. Approximately 25 MPa.

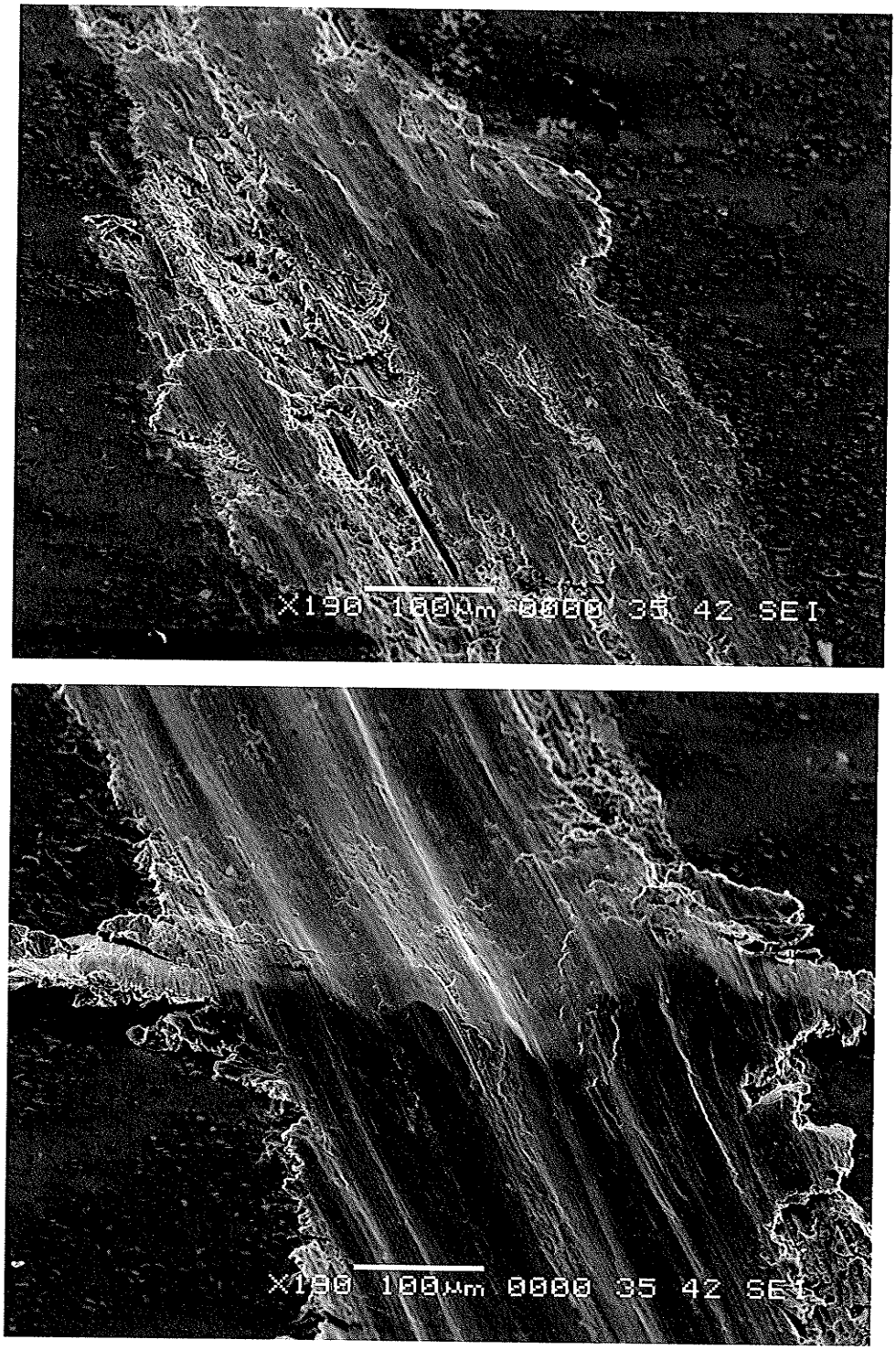

Figure 4.28 Formation of a SML TOP: 1m, BOTTOM: 10m, both tests at 5 N, against 52100 counterface. Delamination fracture due to smearing has not begun to remove the SML at this sliding distance.

The edges of the wear scar have evidence of both subsurface fracture and smearing delaminations. Both sources of delamination wear can be observed as causing the breakdown of the SML.

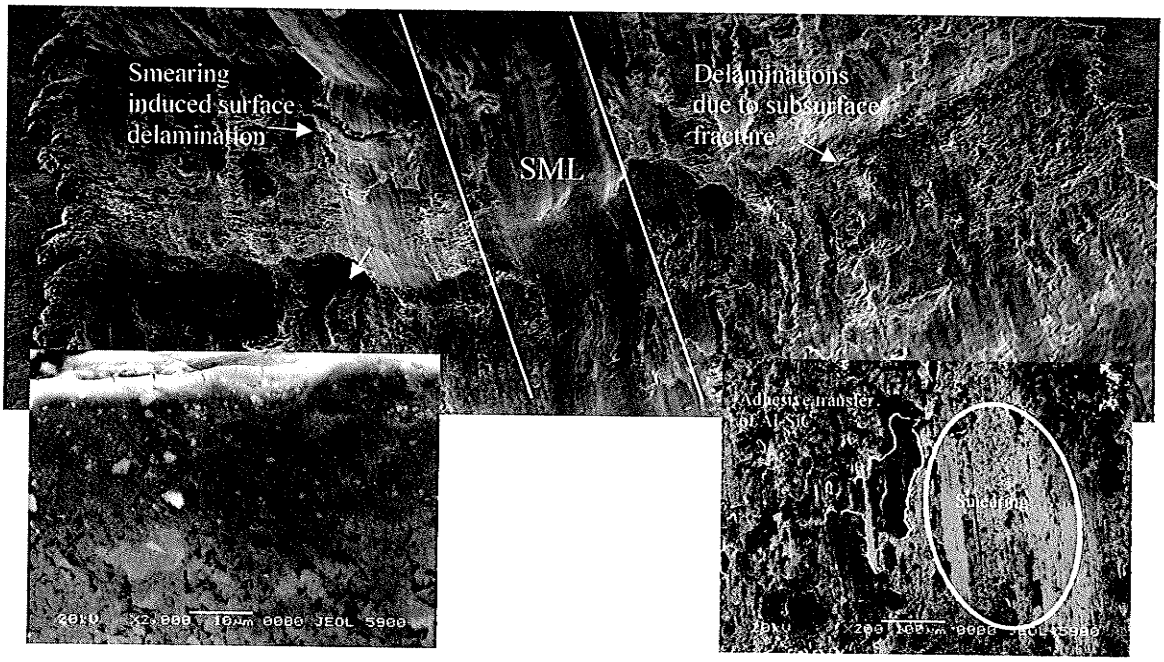

Figure 4.29 Wear scar showing SML at high contact pressure and adhesion/ delamination at lower contact pressure, 50 N, 250m, 52100 steel counterface (inset right). Est. p_{max} = 6 MPa. Highly deformed center cross section (inset left). SML removed at longer sliding distances (lower pressures)

(II) WEAR RATES AND FRICTION WITH A SML

Reduction in smeared delaminations by a larger particle size had been linked to lower wear rates in an earlier study of Al-SiC composites under low speed sliding conditions [109]. In this study, examination of debris revealed that delaminations due to smearing were large in size and caused significant damage to the surface. Mass loss of

sliding system appeared to remain high with a SML present due to whole SiC particles removed in delaminations of the smeared surface layers. Therefore it could be concluded that the SML in the present study was not particularly beneficial in terms of a lower wear rate due to large smearing delaminations removed from the surface. Based on the current testing, a larger surface particle size would be recommended to resist smearing and delamination wear under the high pressures (>20MPa) low sliding speed conditions to decrease wear rates.

Breakdown of the SML occurred for all wear tests. However, since there existed a period of time where a SML existed without smearing delaminations, further study of the cause of breakdown of the SML may reveal better potential for wear resistance by this phenomenon. The wear rate with a stable SML, Figure 4.29, could not be determined due to the short sliding distance over which this was the case.

When a SML exists, the force of sliding could be related to the force required to smear highly deformed aluminum contacts. Tabor [97] proposed the concept of a shear film during dry sliding, stating that relative motion will only occur at shear stresses (or applied tangential forces) equal to or greater than the surface "film" shear strength. The presence of a SML can be considered analogous to a surface shear film. Tabor further predicted the friction, μ, (and therefore surface traction) for junctions with an "interfacial film" to be:

$$\mu = \frac{1}{\delta^{1/2}\left[\left(\frac{\tau}{k}\right)^{-2} - 1\right]^{1/2}}$$

Where τ is the surface shear strength, δ the film thickness, and k is the surface shear stress which can be predicted by various slip-line asperity models[54,81,82]. A SML, once

formed, was determined to have a much higher hardness and therefore higher surface shear strength [32]. DPH indentions using 25 gram load were taken of the unworn surface and compared to the hardness of the SML shown in Figure 4.29.

Al-Si-SiC	HV (kgF/mm^2)
UNWORN	97
SML	138

Table 4.21 Increase in hardness due to SML using DPH indenter

Using Tabor's equation, the higher hardness SML would result in higher interfacial friction and shear stresses during sliding.

4.23 SMEARING AND MIXING OF SIC

For a ceramic material, a transition between the dominant cause of wear being plastic flow to it being dominated by fracture (spalling, delamination) has been observed to occur with the reduction in pressure [96]. For the current AL-MMC a transition has been identified as wear by smearing delaminations becoming wear by delaminations due to subsurface fracture with the reduction in pressure. This transition can relate to the size and volume fraction of ceramic in the composite. Pramilla Bai *et al.* provided evidence that smearing is significantly effected by the volume fraction of reinforcement [71]. In his study, an Al-Si-SiC composite with 15% SiC had a smoothened (mixed) surface and small fractured pits at 2.2 MPa. When the reinforcement volume fraction was increased to 25% the surface had an exclusively rough and fractured surface at the same pressure [71]. It can be therefore seen that at 2.2 MPa smearing was dominant for the composite with the lower 15% volume fraction, however the pressure was insufficient to smear the surface with 25

% reinforcement, and delamination due to surface fracture became was the dominant cause of wear.

How smearing relates to the size of reinforcement is illustrated in Figure 4.210. Under high stress the surface would either smear or fracture. Smearing instead of fracture could be related to the size (and volume fraction) of reinforcement [69,71]. As noted in Figure 4.210, for the tested Al-SiC composite the relatively small choice of reinforcement particles (avg. 10μm) was easily smeared. The surface mixed layer (SML) formed in Figure 4.28 has no SiC protrusions as they were inundated or pulverized under the plastic deformation.

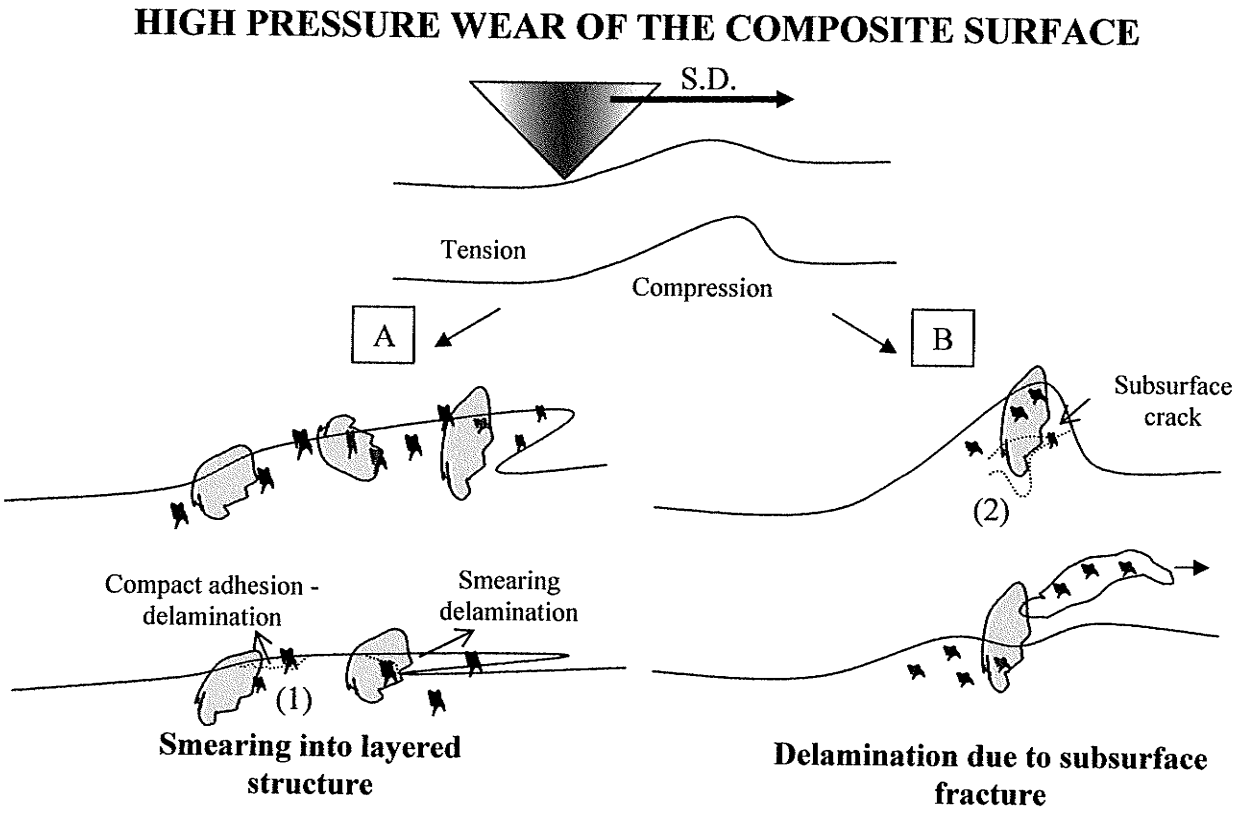

Figure 4.210 Observed wear mechanism occurring at initial high contact pressures causing smearing of the matrix. The average SiC particle size in the matrix is drawn to scale (black), as well as a 3x larger SiC particles (grey) for comparison. Larger particle may provide 1) better ability to retain surface and 2) better resistance to subsurface fracture though crack deflection

Whole particles are pressed into the surface, indicating that particle fracture was not debilitating wear resistance at these high applied pressures, but rather the particles are too small (or the volume fraction of particles to low) to provide the required matrix deformation resistance.

Based on the two examples given Figure 4.210, it can be hypothesized that a larger particle size could increase the resistance to smearing and possibly low-cycle fatigue fracture in the subsurface. This would be accomplished by 1) less likelihood of the SiC being inundated by matrix compliance and 2) a more substantial path of subsurface crack propagation [109]. The larger particles could also reduce the propensity of the material to flow at the surface and allow for increased transfer of iron through counterface abrasion [71]. Furthermore, larger SiC would be better able to reduce matrix adhesion, resulting in possibly lower Al transfer to the counterface.

4.24 DIFFERENCES BETWEEN A SML AND MML

A SML was identified in a previous study [64] on the wear of the same 356-20%vol SiC composite used in this study against a 52100 steel ball. At a load of 10 N and approximately 1" (25 mm) reciprocating distance, a surface mixed layer formed after 500 cycles but was removed by 5000 cycles (25-250 m). The pressure was estimated to drop from 30 to 10 MPa over this range of sliding cycles [64]. For sliding distances greater than 250m a greater nominal contact area existed due to widening of the wear scar, with contact stresses insufficient to form a coherent layer [99]. It was estimated that a minimum contact pressure of 5 MPa was required to maintain a SML [99].

Both Venkataraman and Sundararajan [33] and Li and Tandon [25] identified the formation a MML. The pin-on-disk apparatus used by Venkataraman and Sundararajan [33] provided a conforming contact that allowed for the nominal contact pressure to remain nearly constant as a function of sliding distance or test time. This study observed that when the fracture rate of the mechanically mixed layer exceeded the rate at which this layer was regenerated no MML would exist. This was related to a maximum applied pressure for stability. Breakdown of a stable MML was related to the occurrence of shear instability and delamination wear as the surface forces were increased past the maximum surface pressure [33]. Maximum applied pressures above which the MML was destroyed are summarized for two different composites in Table 4.22. It was noted that the hardness of the surface layer determined this maximum transition pressure; the higher the hardness of the MML the greater the resistance to adhesion delamination, and therefore a greater stable applied surface pressure could be accommodated.

Material	Maximum surface pressure for stable MML (MPa)	MML hardness (HV)	MML thickness (μm)
Al-40vol%SiC	2.9	575	10
Al-10vol%SiC	1.5	300	120

Table 4.22 Summary of results for stability of MML layers [33]. Pin-on disk, V =1 m/s, Steel counterface, 532±5HV

It can be clearly observed that the SML observed by Feng and Tandon [64] was formed at much greater pressures (in the order of 5-30 MPa) than the stable surface pressures for an MML determined by Venkataraman and Sundararajan [33]. In fact, the

minimum pressure for SML stability in the former study can be seen to be two times greater than the maximum pressure for MML stability in the latter study.

It is the opinion of the author that the two surface mixing cases observed were produced by different mechanisms. The MML observed by Venkataraman and Sundararajan [33] and Li and Tandon [25] was correctly stated as forming by compaction of debris from the prow of the sliding contact and turbulent plastic flow. In contrast the SML observed by Feng and Tandon [64], and similarly observed in this study, was formed by extensive subsurface deformation that did not delaminate as a result of very high hydrostatic pressure.

One of the major differences between SML and MML surface mixing phenomenons can be identified as the role of debris. This is validated by the fact that the former two unidirectional studies [25,33] observed very high levels of the iron transfer from the counterface in the MML. In the reciprocal study [99] little to no iron was found in the SML. The role of increased debris mixing could be further observed by comparing higher hardness values for MMLs in Table 4.22 to the SML hardness in Table 4.21. A significantly higher MML indicates that hard debris particles mixed into the surface in addition to strain hardening of the matrix. In conclusion, a SML as identified is a mixing phenomenon that occurs at higher pressure range and involves relatively low mixing of debris in comparison to a MML.

For the current reciprocal sliding, a stable MML did not form over the same pressure range that it was found to form under unidirectional sliding. It is proposed that unfavourable debris particle dynamics for the ball-on-block contact geometry prevented the formation of a stable MML under the reciprocal test conditions. Venkataraman and

Sundararajan [31] observed no MML for intermittent testing where the debris was removed. Therefore, collection of debris at the front of the sliding contact can be seen to have had high importance in the formation of the MML. When comparing wear geometries, the reciprocal testing did not accumulate debris in a prow as did the unidirectional pin-on-disk or block-on-ring.. As a result less reprocessing of debris occurred once generated due to easier removal from the wear scar. This unfavourable debris particle distribution in the current reciprocal testing is considered to explain the lack of MML formation.

A major conclusion from Section 4.1 was that abrasion wear quickly became the dominant wear mechanism as the sliding velocity was increased over this relatively low sliding velocity range. Since abrasion as the dominant wear mechanism excludes the possibility of a SML formed through smearing, surface mechanical mixing would be limited by both increased the velocity and at low pressures, both which promote abrasive wear. This leads to a conclusion that both upper and lower limits of the applied nominal pressure that allows for a SML to form, with both limits being set by surface fracture; the lower limit set by insufficient plastic deformation, the upper set by instability of the deformed surface causing a higher fracture rate of the mechanically mixed surface than the rate in which the mixed surface can re-form.

4.25 DOMINANT SURFACE WEAR MECHANISMS

In this section a brief overview of the observed wear mechanisms is given. A summary which wear mechanisms were dominant in relation to applied pressure is given in Table 4.23 under the current ball-on-block reciprocal testing.

1) SMEARING CAUSING EXTRUSION

At high compressive stresses the matrix can flow into flaws formed from wear induced large plastic strains at the surface or in the subsurface. The propensity of the wear surface to smear is principally related to the flow stress of the composite. The propensity of the wear surface to smear is equally related to damage accumulation. That is, when a contact junction is made between the two metal surfaces, the flow stress determines the magnitude of shear developed before the aluminum matrix plastically deforms; if the shear stress is greater than what can be tolerated with an existing flaw or crack the surface will fracture or delaminate, otherwise it will smear. The transient SML is a product of smearing as the dominant surface wear mechanism. Smearing causing wear by extrusion of the surface was observed as the wear mechanism at high pressures (>20MPa) for both HP Al and Al-Si, however at these higher pressures the composite would more commonly fracture before material could be extruded from the wear surface. Instead of extrusion, seizure spalling was the dominant wear mechanism at the highest sliding pressures for the Al-composite.

2) LAYERED DELAMINATIONS DUE TO SMEARING

Delaminations due to smearing occur when the surface can be smeared to large strains before fracture. The fracture surface of these delaminations is along the periphery of a long thin layer as a result of excess tensile strain in this layer. This contrasts subsurface crack initiation and propagation that causes fracture to occur for all other morphologies of delamination wear that were observed for the Al materials.

Delaminations due to smearing were identified as causing breakdown of the SML with decreasing contact pressure. Without sufficient hydrostatic pressure, any depth affected by the contact stress at the surface does not experience adequate healing due to matrix flow to compensate for the damage accumulation that occurs due to particle fracture and void formation [34]. As a result, delaminations occur. When the surface compression subsides to a magnitude that allows damage accumulation to occur large thin delaminations would fracture off the surface resulting in delaminations of the smeared surface.

3) Delaminations Due to Subsurface Fracture

Subsurface fracture became more dominant as the resistance to matrix flow increased. Increased flow stress can be related to the increased hardness for the three Al materials, Table 3.3. Therefore HP Al, Al-Si and Al-Si-SiC in order showed increase subsurface fracture and delamination wear as the steel counterface would attempt to smear the aluminum surfaces. Delamination wear due to subsurface fracture has been observed to increasingly dominate the surface wear with increased reinforcement volume fraction (increased surface shear strength) by two major studies [31,71]. Simply, higher shear forces due to higher surface shear strengths result in greater tendency for fracture in the subsurface where damage can accumulate. The result is delamination wear due to subsurface fracture replacing delamination wear due to smearing.

4) Adhesion, Compact Delaminations and Abrasion

The magnitude (depth) of delaminations due to subsurface fracture decreased as the pressure decreased, related to the depth at which damage nucleated. Delamination wear

due to subsurface fracture could occur in the plastically strained subsurface or from the mixed surface at intermediate pressures. From this point on, delaminations at a depth below the mixed surface are referred to as bulk or **compact delaminations**; delaminations where instability occurs within the mixed surface material will be referred to as **mixed delaminations**. This was illustrated in Figure 2.11. It is important to note that bulk delaminations can be smaller than mixed delaminations, as is the case when abrasion was the dominant mechanism, Figure 4.26. Compact delaminations occurred due to a shallower depth of subsurface fracture at the same contact pressure that abrasion and small adhesive transfer particles became the dominant surface wear mechanisms. Compact and mixed delaminations refer to debris produced of a much smaller size than delaminations due to subsurface fracture. Adhesion is presumed to be the genesis of compact and mixed delaminations much more than low cycle fatigue and subsurface fracture.

When the contact point between the two surfaces does not result in smearing of the composite aluminum, the junction must fracture is some manner. Smearing would not result when the shear strength at the surface was greater than the imposed shear stress at the junction. In this case very small delaminations (transfer particles) have been observed to result from adhesive transfer at asperity tips [91]. This process was presumed to be partially responsible for the formation of particulate debris.

Abrasion resulted in coarse cutting marks in the surface. Particulate debris can be observed to come from chip formation in front of the abrading particle, Figure 4.35. Since no mixed surface resulted when abrasion became a more dominant wear mechanism, delaminations at these corresponding low sliding pressures were from the plastically strained matrix, not from a mixed surface layer.

MATERIAL PAIR	HP Al against 52100	A356.2 Al-Si against 52100	A356-20vol%SiC against 52100
Contact Geometry	Reciprocating Steel ball on aluminum block	Reciprocating Steel ball on aluminum block	Reciprocating Steel ball on composite block (
Sliding Velocity	Avg. 7.5 cm/s (¼" Reciprocating)	Avg. 7.5 cm/s (¼" Reciprocating)	Avg. 7.5 cm/s (¼" Reciprocating)
Nominal Pressure	Dominant Wear Mechanism(s) Causing Weight Loss		
> 20 MPa	1) Extrusion	1) Extrusion 2) Delaminations due to seizure	1) Delaminations due to seizure 2) Delamination due to smearing
15-20 MPa	1) Extrusion	1) Delaminations due to seizure 2) Delamination due to smearing	1) Delamination due to smearing
10-15 MPa	1) Extrusion	1) Delaminations due to seizure 2) Delamination due to smearing	1) Delaminations due to smearing 2) Delamination due to subsurface fracture
5-10 MPa	1) Extrusion 2) Delamination due to smearing	1) Delaminations due to smearing 2) Delamination due to subsurface fracture	1) Delamination due to subsurface fracture 2) Delaminations due to smearing 3) Abrasion
2-5 MPa	1) Delaminations due to seizure 2) Delamination due to smearing	1) Delamination due to subsurface fracture 2) Delaminations due to smearing	1) Delamination due to subsurface fracture 2) Compact Delaminations and Particle Pull-out 3) Abrasion
1-2 MPa	1) Delamination due to smearing	1) Delamination due to subsurface fracture 2) Abrasion	1) Compact Delaminations and Particle Pull-out 2) Abrasion
< 1 MPa*	1) Delamination due to smearing 2) Delamination due to subsurface fracture 3) Abrasion	1) Delamination due to subsurface fracture 2) Abrasion	1) Abrasion 2) Compact Delaminations and Particle Pull-out
< 0.1 MPa*	1) Delamination due to subsurface fracture 2) Abrasion	1) Abrasion 2) Compact Delaminations	1) Abrasion 2) Compact Delaminations and Particle Fracture

Table 4.23 Summary of the dominant surface wear mechanisms, in order of which caused the most significant damage. The pressure range over which mixing could occur is also indicated. (*Pressures below 1 MPa were generally not achieved during sliding wear at the lightest loads; therefore the stated mechanisms are presumed from trends and literature)

4.26 SUBSURFACE DEFORMATION

When smearing was the dominant surface wear mechanism, some mixing of debris could considerably change the subsurface morphology. When debris was retained and mixed it formed a distinct surface layer, the bottom picture of Figure 4.213. A mixed debris layer due to smearing was found to be unstable due to the folded layers having an interface with the subsurface. Deformation can be observed to have been isolated in the transferred debris layer; therefore the debris had provided limited protection of the subsurface from strain and damage accumulation. Cracking can be seen to extend from the interface of the deposited transfer/debris layer, indicating that it is close to delamination.

Without a layer of debris, smearing would cause plastic deformation to considerably extend into the subsurface, producing a refined SiC surface and subsurface microstructure, Figure 4.211. This result of subsurface deformation was identified as a SML in previous work [64]. Only iron originally present in the composite alloy was found in the surface of the SML in previous work [99] or in Figure 4.211. In conclusion, with no counterface elements and little debris mixing the mixed surface/subsurface in Figure 4.211 could not be defined as a MML.

Figure 4.212 shows a SML surface region with a soft shear layer forming underneath that would likely cause it to delaminate. Delamination at the soft shear layers, formed by work softening of the locally unreinforced matrix, could be acting to prevent accumulation of SiC at the surface under the reciprocating stresses, consequently limiting stable mechanical mixing.

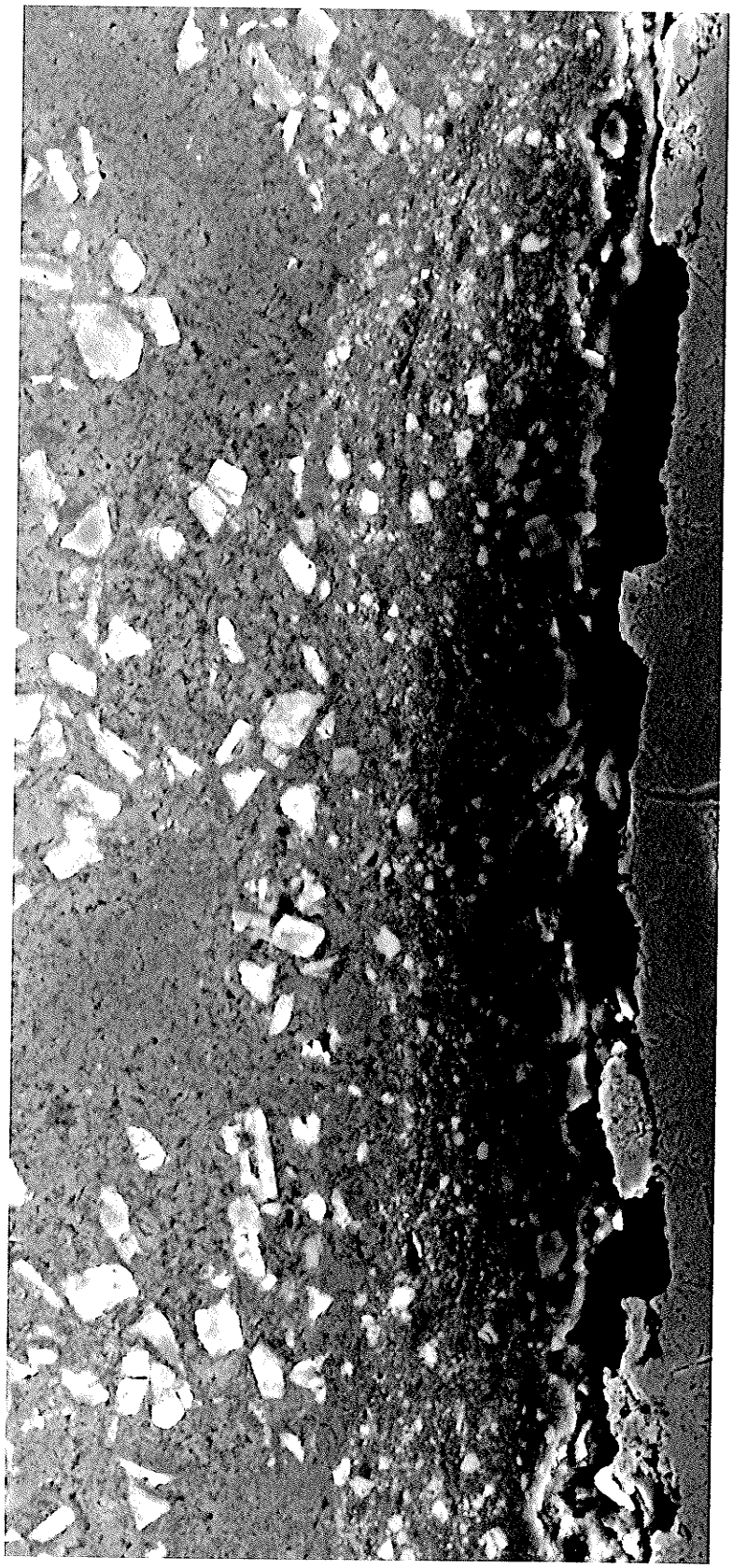

Figure 4.211 Subsurface damage accumulation caused during smearing of the surface. Counterface debris is not present. This surface mixed layer (SML) is becomes unstable at low speeds and low pressures. 10N, ¾" reciprocating, 100 m.

It was

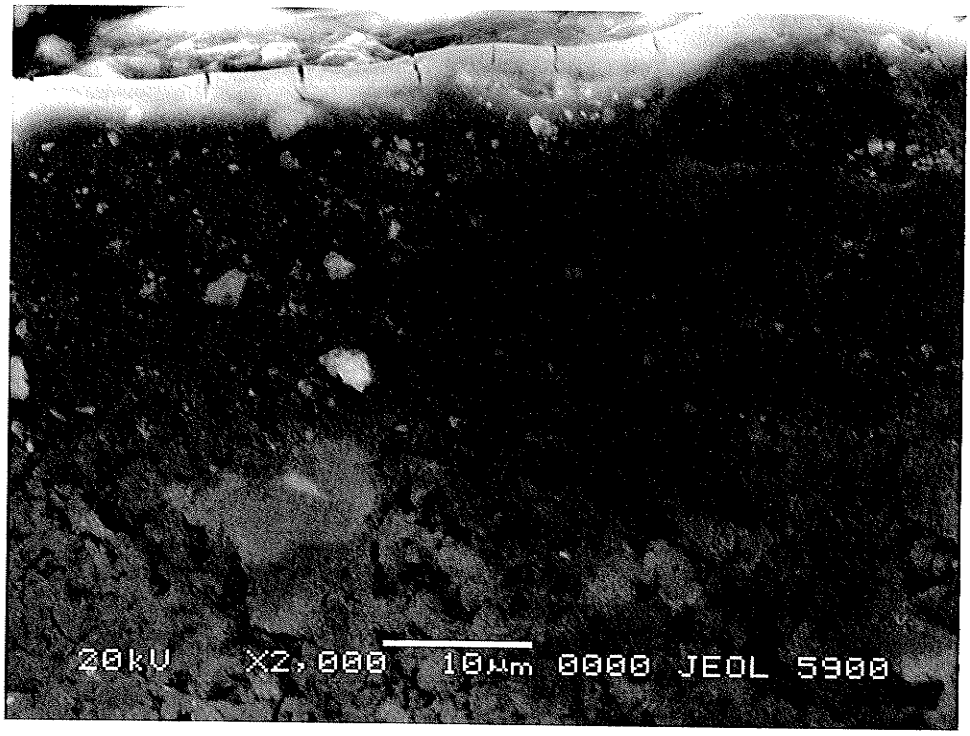

Figure 4.212 Deformation of the subsurface through surface smearing. Craze cracking can be seen on the surface and highly void density in the subsurface. This is an example of a cross section produced by smearing without any significant build-up from debris.

At high pressures, the subsurface plastic strains are observed to not only refine the reinforcement size but allow for flow of the matrix around the fractured particles under the compressive stress of the sliding contact, Figure 4.212 and 4.215. Brechet *et al.* observed particle refinement under strain to occur simultaneously with extrusion of the matrix between the cracked surfaces while under high compressive stresses for a like 356-20vol% SiC composite [120]. Although the compressive stress during sliding contact can "heal" the fractured SiC through matrix flow, Figure 4.212, a logical conclusion from the resulting substructure would be that a smaller, rounded and more evenly distributed reinforcement phase could ultimately provide similar plastic deformation resistance.

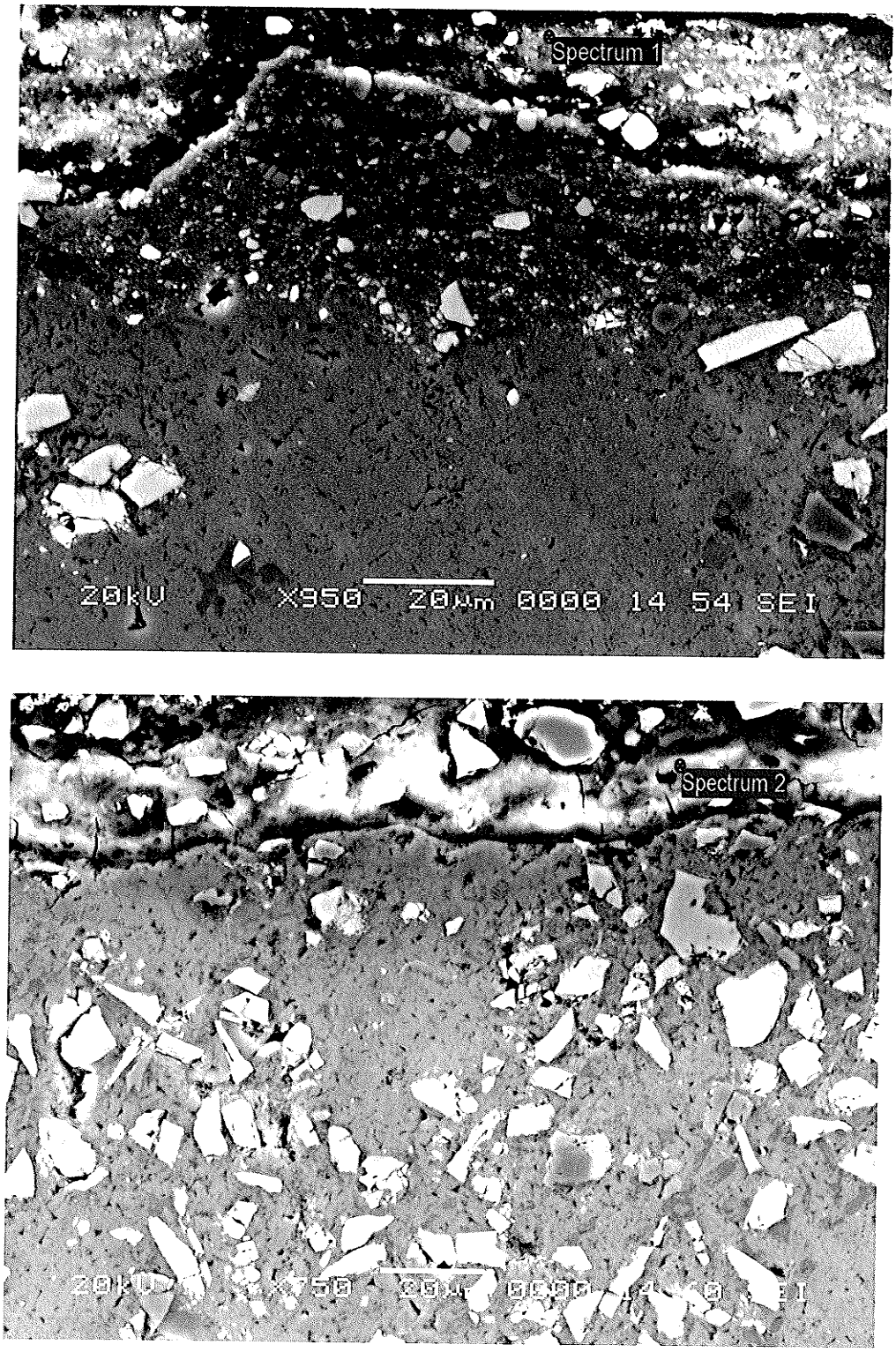

Figure 4.213 Two different subsurface deformation layers. TOP: Pulverization and compaction of reinforcement in the subsurface before fracture. BOTTOM: Transferred or smeared layer deposited on the surface but incoherent with the subsurface. Cracks can be observed to propagate from the bulk interface.

The coherent highly deformed composite in the top picture of Figure 4.213 has remained so due to the protection of the surrounding compacted and accumulated debris. At reduced pressures (<10 MPa, past about 100m sliding) a fragmented subsurface of this nature would delaminate before a substantial mixed depth could be achieved. As the reciprocating distance was increased to ¾" and at high pressures that did not cause seizure spalling, the tendency of the deformed surface to delaminate was less and a significant mixed depth could be maintained, Figure 4 .211.

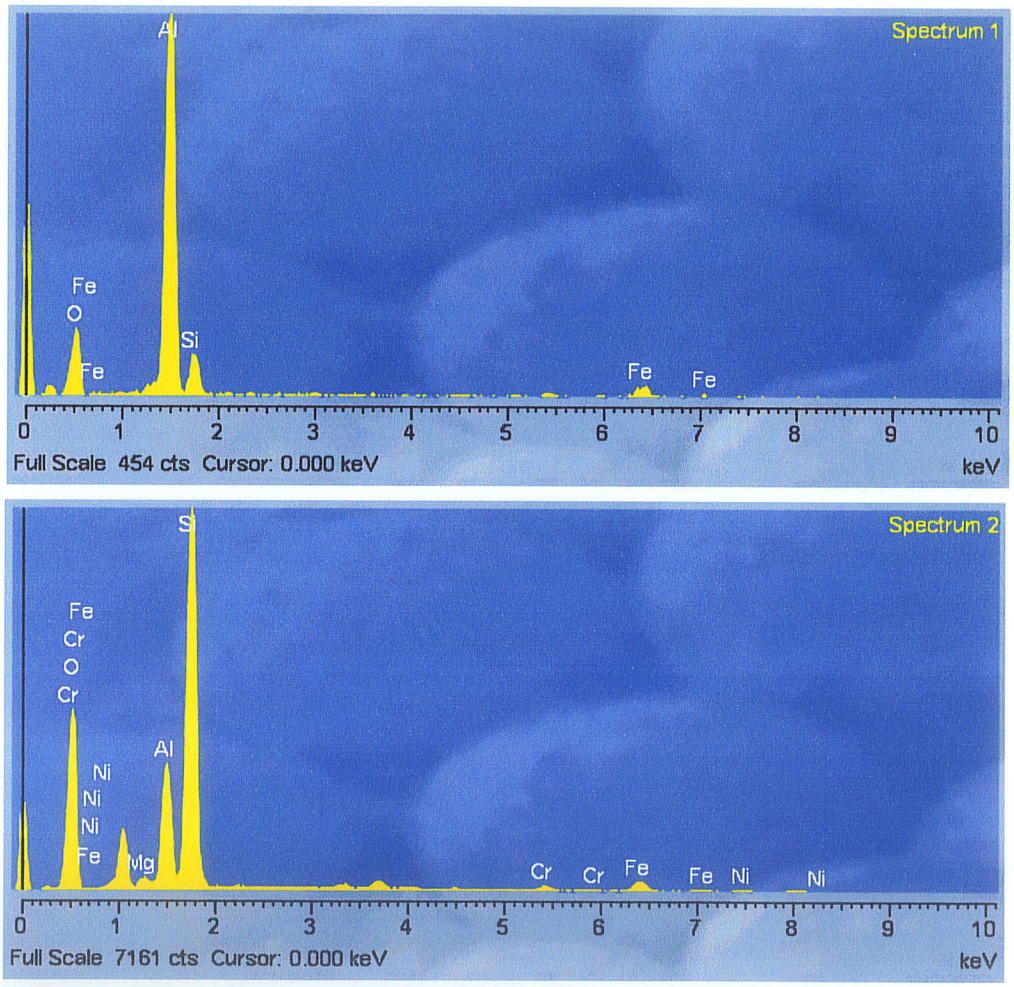

Figure 4.214 Semi-quantitative EDS point spectrums for mixed surfaces shown in Figure 4.213

In the top picture of Figure 4.213, the mixed debris surrounding the mixed composite peak had traces of the steel counterface through the transfer and back transfer events that allowed for its accumulation. In the bottom picture of Figure 4.213 smearing, compaction, and transfer as allowed a debris layer to form a coherent layer on top of the composite surface. As a result of the mixing process that formed this debris layer high oxygen content was present as well as traces of the steel counterface. Spectrums for the mixed surfaces are shown in Figure 4.214.

Mixing of iron from the counterface and the level of oxide was checked using EDS for the mixed and transfer layers shown in Figures 4.211 through 4.213. Quantification of oxygen content was considered to have an inaccuracy of up to 15%. It was concluded nonetheless, that high levels of oxygen were present in the debris transfer layers. The top cracked surface of Figure 4.212 had very high wt% of Si and O and low Al content, indicating that SiO_2 may have been formed at the surface. The detection accuracy however was insufficient to confirm this observation. No oxygen was found mixed into the SML subsurface of Figure 4.211, indicating that the mixed layer had formed without exposure to surface contacts. Fe, Cr, and Ni element detection from the counterface was much more accurate, in the order of a few percent. Both mixed surfaces of Figure 4.213 had very little iron, with mixing predominantly consisting of the original Al matrix and the SiC reinforcement.

The mixing cases shown in Figures 4.211 to 4.213 are exceptions in that surface mixing was in general unstable for the sliding conditions and only formed in patches on the wear surfaces. The most common subsurface morphology was a fractured interface with no

mechanical mixing and no debris deposit, clearly formed by subsurface fracture and bulk delamination wear.

Figure 4.215 shows a mechanism of SML breakdown for the tested sliding conditions. Soft shear layers as identified by Venkataraman *et al.* [32] can be observed to have formed between layers of pulverized SiC under the reciprocal sliding. Considering a non-uniform distribution of particulate as previously noted in Figure 3.19, each reciprocated cycle would deform a near-surface layer that may or may not contain SiC particulates that are pulverized under the high strain [120]. It was possible that a significant portion of the shear strain that must occur for the observed smearing of the Al-MMC surface occurred in local regions where the reinforcement effect was low.

Observing the size of the SiC exposed at the surface it is clear that an average particle size of 10 μm has a large effect in causing a non-uniform distribution of reinforcement to be smeared under the localized surface strain. The microstructure of the tested Al-MMC composite presents a wear surface/subsurface which may have relatively high or low reinforcement volume fraction as compared to the bulk 20vol%, especially considering the small size of asperity contacts. As the surface contacts induce surface plastic flow, subsurface regions containing low volume fractions of particles may yield first while particle-rich regions remain elastic to higher strains [121]. Alternatively, regions containing high volume fractions of particles could adopt disproportionately higher stresses causing them to fracture [122].

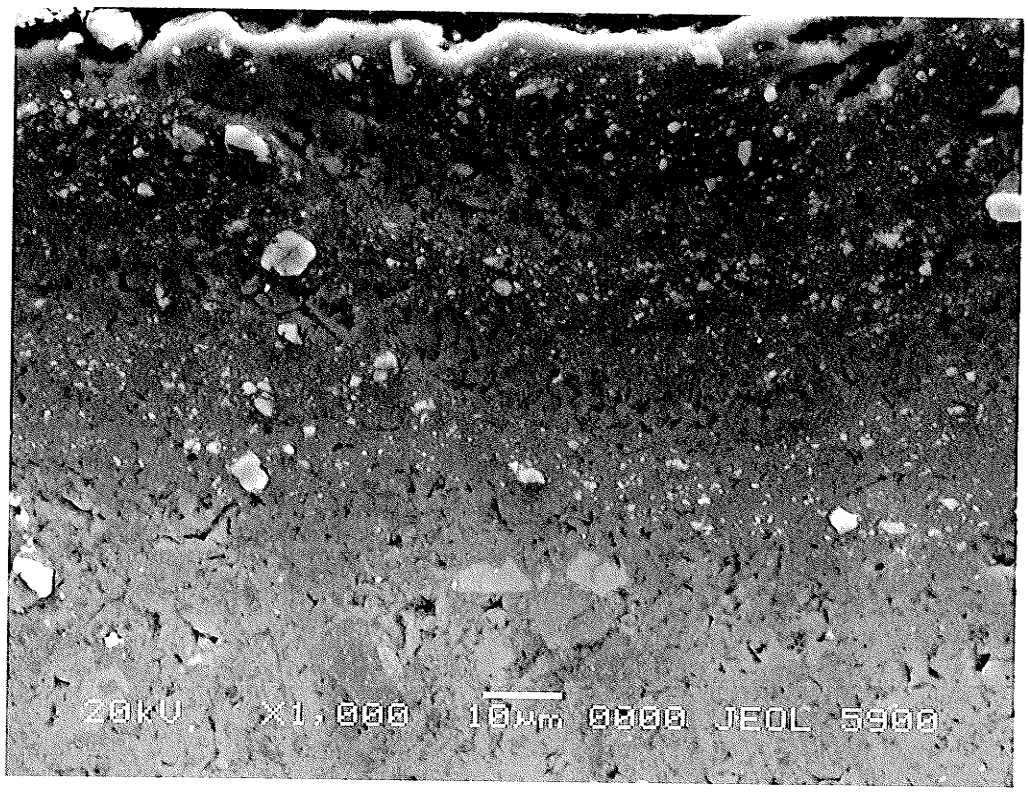

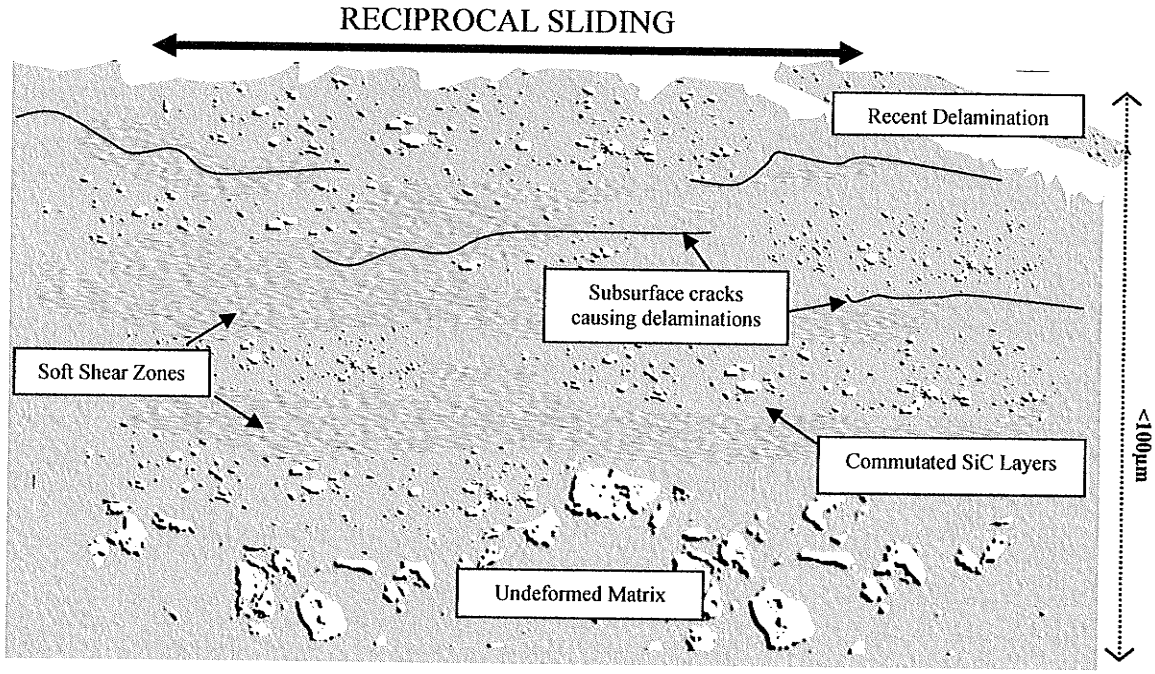

Figure 4.215 Effect of subsurface deformation during reciprocal sliding. Particle comminution occurred in the subsurface due to plastic strain. Areas without reinforcement particles have a high void density due to the disproportionate plastic strain

In either case the internal stresses in the subsurface would be relaxed, the resistance to fracture of the newly forming SML would be reduced, and local instability leading to delamination of the surface would be promoted. In conclusion, examination of the subsurface revealed that a smaller particle size, decreased particle spacing, and more uniform distribution of particles would be required to achieve more consistent SML formation due to a lower chance of intermediate soft shear layers forming.

A clear difference can be observed between the behaviour of SiC particles on the surface and SiC particles in the subsurface. At high pressures smearing of the surface occurred without particle fracture indicating that matrix yielding at the particle/matrix interface dominated the plastic relaxation behaviour [7]. In the subsurface, extensive particle cracking was observed, indicating that the particles fractured before the particle/matrix interface yielded. This indicated that prevention of elastic unloading and decreased subsurface damage could be achieved through smaller subsurface particles than the average size used in the present composite. By doing so, there would be less chance of release of elastic strain by particle fracture. Observing the surface particle behaviour confirmed the recommendation of Section 4.23; that a larger surface particle size was required to resist plastic deformation and smearing as a wear mechanism.

4.31 TRANSFER OF AL-SI-SIC TO THE COUNTERFACE

(I) STAGES OF TRANSFER AND MIXING

The transfer of Al-MMC to the steel counterface could be divided into three stages as sliding continued through the range of applied pressures:

1) Immediate abrasion by or transfer of SiC when exposed on the polished surface, Figure 4.31. SiC on the surface are quickly comprimised by smearing or transfer under the high pressure. Fracture, transfer and pull-out occurred at any tested normal contact force, indicating that the SiC on composite surface could not act as load bearing elements under the pressure of the ball on block contact.

2) Next, a coherent transfer layer formed after a short sliding distance through smearing and adhesive transfer, Figure 4.21. At high initial contact pressures a large mixed Al-MMC transfer patch on the counterface would form. Simultaneously, a SML would form and become the composite wear surface. It was proposed that adhesive transfer of the highly deformed aluminum asperity contacts dominated transfer to the counterface.

3) After a sufficient sliding distance to reach "steady-state", redeposition and removal of the adhered Al-MMC on the counterface occurred by random delamination, Figure 4.16, 4.17 and Figure 4.32. It was proposed that debris as a third body took on a more dominant role in transfer to the counterface in substitution of direct asperity contact.

(A) TRANSFER OF THE COMPOSITE TO THE COUNTERFACE

As proposed by Sarkar [61], tranferred deposits are built up to a critical thickness on the surface and then are fractured off. Current testing observed this behaviour with the formation of a coherent Al-MMC transfer patch on the steel counterfaces. The fomation of a coherent Al-MMC transfer layer was found to occur only at high pressures or short sliding distances. Under low pressures or long sliding distances, the transfer mass was observed to vary in a cyclic manner with time, as within a few cycles large Al-MMC deposits were seen to delaminate from the surface which would then take time to be replenished by subsequent transfer. Therefore, neither the coherent transfer layer on the counterface nor the SML simultaneously formed on the composite surface were stable surface phenomenons in terms of forming a uniform wear layer. The cause of the breakdown of the counterface Al-MMC transfer layer could have been related to build-up of a transfer mass past a critical thickness, surpassing stable levels of plastic deformation, or instability caused by reduction in contact pressure. A conclusion for all steels was that a thick transferred Al-MMC deposit on the counterface was unstable at low pressures.

As noted in Section 4.11, adhesive transfer of the composite fluctuated significantly at the low sliding speed as a function of applied pressure for each steel counterface. Section 4.12 provided evidence that adhesive transfer as the dominant wear mechanism caused much more severe rates of wear of the Al-composite as compared to when abrasive mechanisms dominate. Also noted in Section 4.13 and 4.14, transfer vs. abrasion could be related to the counterface hardness.

At low pressures the thickness of adhered Al-MMC transfer patches decreased. From observations of the steel surfaces at low pressures, the softest 316 counterface had

unstable Al-MMC transfer "patches" which would not build up to significant before delamination. In comparison, the harder 52100 steel counterface was more uniformly covered by mixed Al-MMC deposits. Although the cause was not clear, a higher hardness steel had promoted more stable adhesive transfer, decreasing delamination of the mixed Al-MMC deposits off the counterface and causing lower overall weight loss of the sliding couple. The 316ss had more of the steel contact surface directly exposed to mixed composite surface at low pressures and long sliding distances due to less adhesion. However at high pressures and short sliding distances, exposure of the steel surface caused pullout of whole SiC particles that readily anchored into the steel surface, increasing composite wear. The end result was the composite experiencing both increased adhesion-delamination rates off the counterface and greater particle pull-out, causing higher wear.

(B) TRANSFER OF THE COUNTERFACE TO THE COMPOSITE

The amount of surface covered by Al-MMC transfer deposits in relation to the amount of the steel counterface directly exposed during steady state wear could be expected to govern how much counterface steel mixing into the aluminum surface could occur. For all three Al materials tested under ¼" reciprocating conditions, little Fe abrasive particle transfer occurred from the steel counterface. Despite consistent weight loss of the steel counterface against the Al-Si alloy, no iron mixing was found on the Al-Si surface, indicating that any abraded or transferred steel must have been readily removed in the debris. Greater Fe transfer did not occur during wear against the composite despite the addition of hard particles to the sliding system.

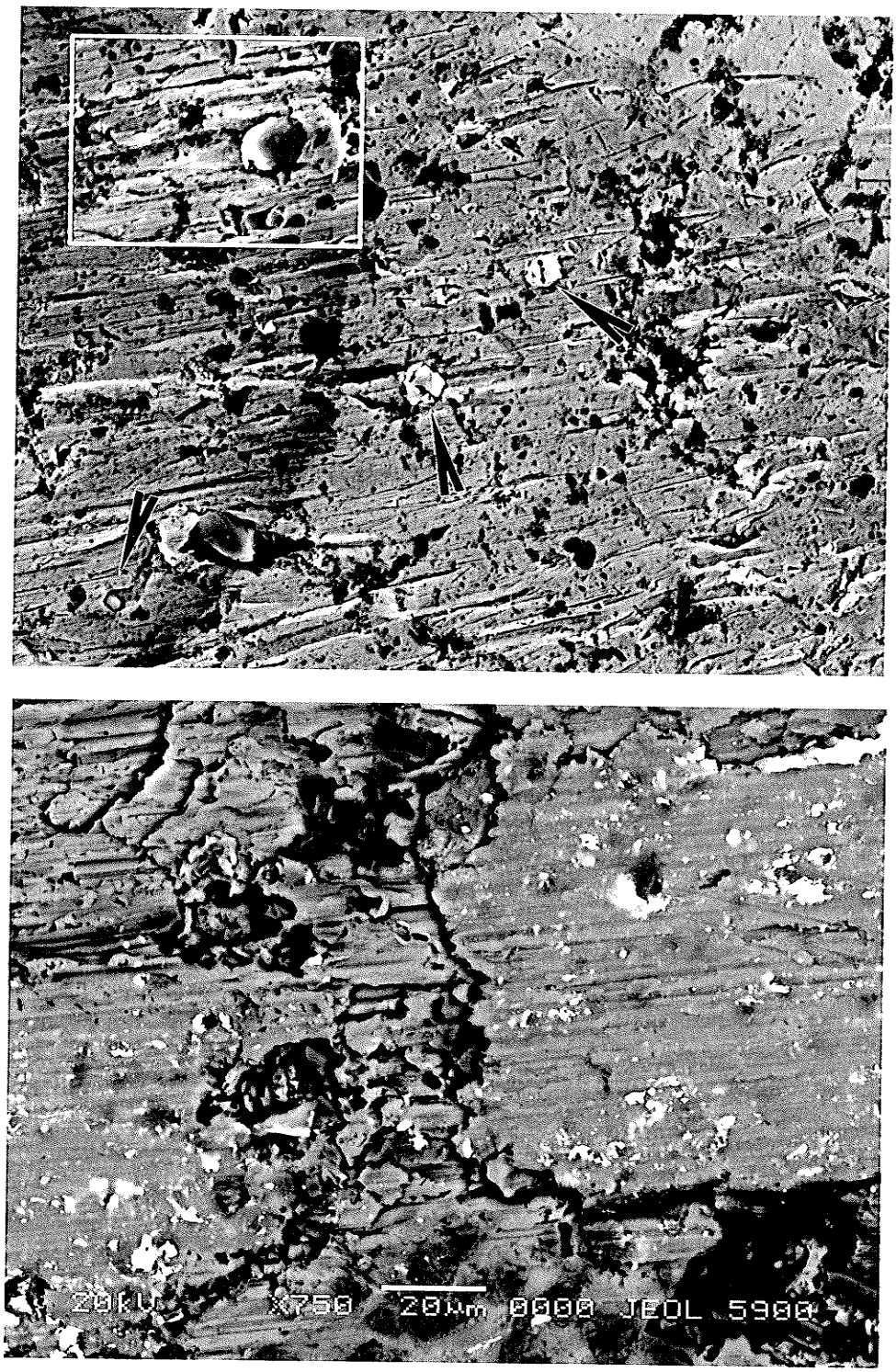

Figure 4.31 TOP: Transfer of whole SiC particles to the 316 counterface before Al significant adhesive transfer occurs. BOTTOM: BSE image of the composite surface showing abraded steel particles from the above counterface smeared into the surface. Surfaces are the result of 1 m ¼" reciprocal sliding at 5N.

The overall conclusion was that adhesion to the counterface controlled and prevented substantial transfer of the steel to the composite surface during sliding contact.

(II) ROLE OF ABRASION IN TRANSFER AND MIXING

Abrasive removal of the elemental Fe and iron oxide occurred when the steel counterface was in direct contact with the composite surface. This depended on the amount of Al-SiC transfer, which provided a protective layer that prevented direct steel counterface wear. The transfer layer to the steel was "patchy", Figure 4.32. Weight loss of the steel counterface due to abrasion was observed to occur simultaneous with adhesive Al-MMC transfer, making the wear process a combination of both abrasion and adhesion wear mechanisms.

Ploughing appeared to be a common abrasive wear interaction between surfaces. The top picture of Figure 4.23 and the debris shown in Figure 4.38 are examples of ploughing, which caused deep grooves to form in the surface, in comparison to abrasion which caused "chips" to be generated. In the top picture of Figure 4.33, it can be observed that ploughing has removed some of the transferred Al-MMC agglomerations from the steel counterface. Ploughing or abrasion can simultaneously be observed to generate particle debris from the Al-MMC counterface deposit. Small equiaxed deposits were often found at the ends of discontinuous abrasion lines, Figure 4.35. Therefore, for the steel counterfaces that resulted in high Al-MMC adhesion, particulate debris was observed to be generated from both the composite surface and from the transferred Al-MMC deposit.

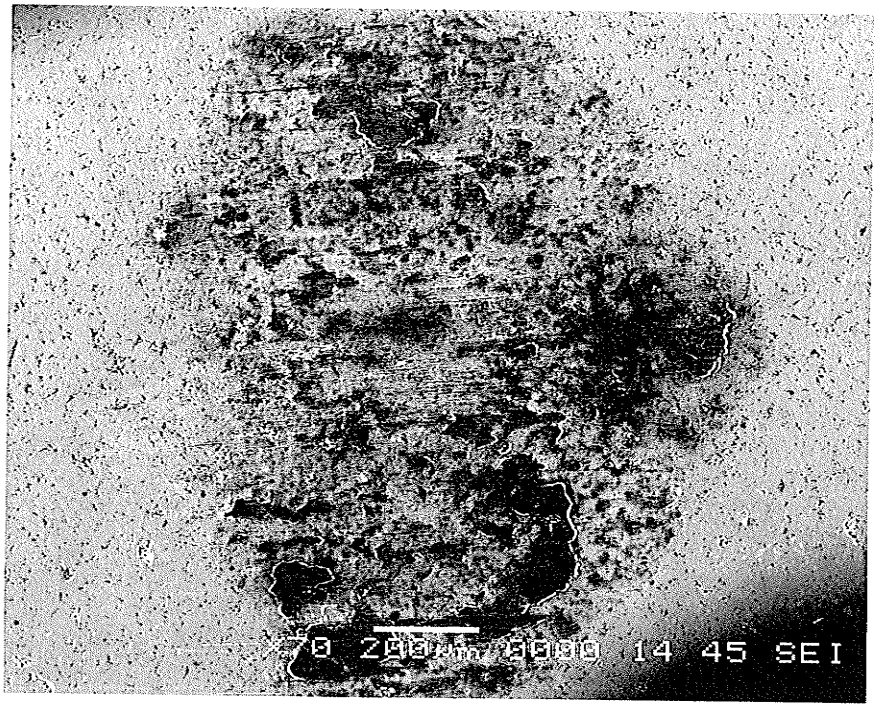

Figure 4.32 Low magnification of common patchy Al-MMC transfer to the 316 steel counterfaces. Similar, but less patchy transfer occurred for 52100 and 440C counterfaces at "steady state" pressures reduced below approximately 10 MPa or long sliding distances greater than 100m. 5N, ¼".

In summary the counterface transfer layer, originally formed by direct or debris particle transfer can subsequently be regenerated into particulate debris by abrasion and ploughing wear mechanisms. The surface with the highest hardness or greatest quantity of hard particles was expected to be dominant in abrasion and ploughing. In the current study the transfer deposit on the steel counterface had similar characteristics (hardness, composition) as the mixed composite surface from which it was formed. This could be observed in Figure 4.21 showing alike smeared surfaces. Therefore dominant abrasion or ploughing of one surface was not observed. Instead each surface had equal likelihood of abrading the other causing continual transfer and back transfer of particulate debris.

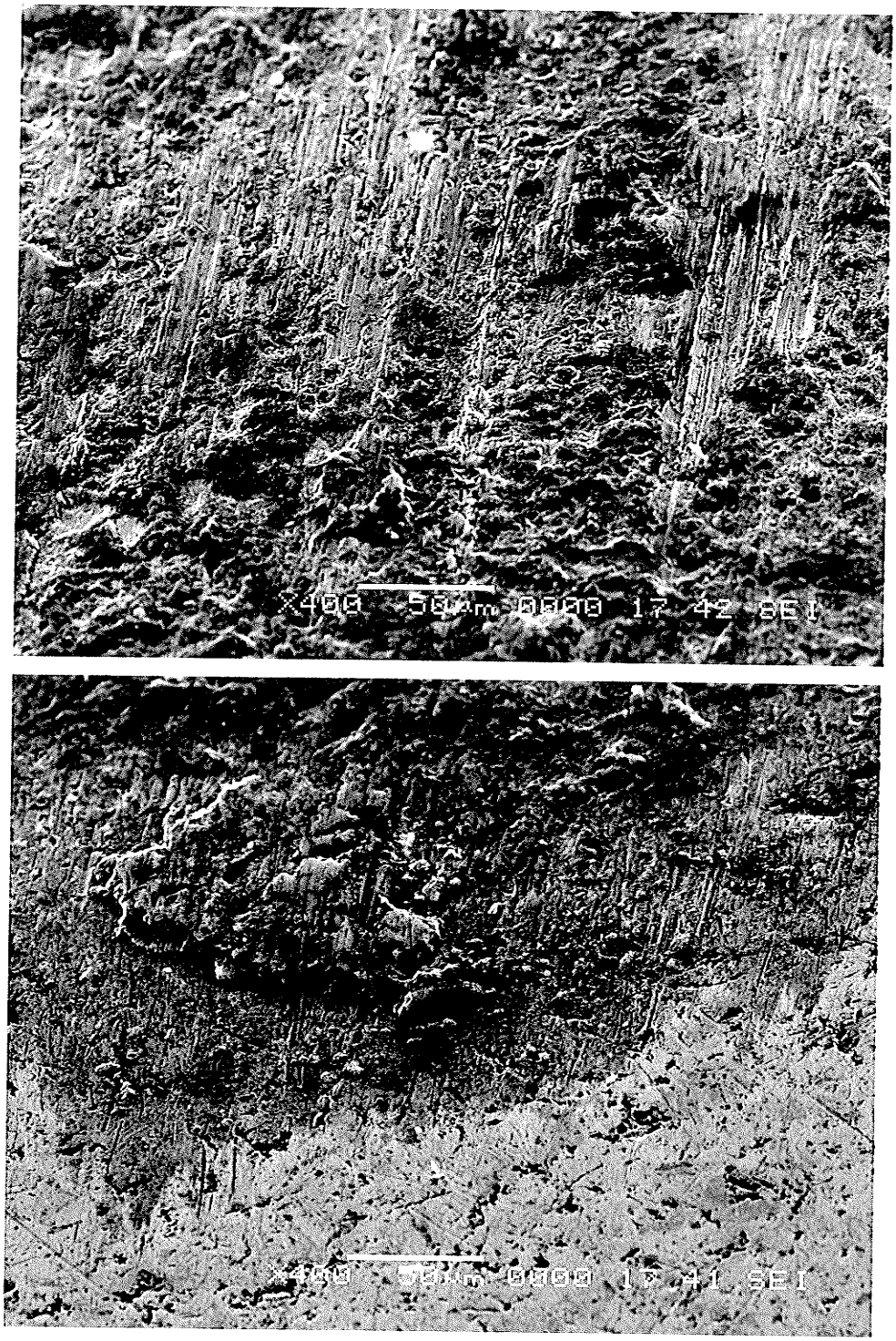

Figure 4.33 High magnification views of Figure 4.32 showing transfer of the mixed Al-MMC to the 316ss counterface. TOP: A combination of abrasion and smearing has removed the rough aggregations of small particles. BOTTOM: Edge of wear scar showing a thin layer remains on the steel surface of deposited aluminum/aluminum oxide, confirmed with EDS. In both cases particulate debris dominates transfer.

When accumulation of hard SiC particles was observed in the formation of a MML, dominant abrasion of the steel counterface by the composite could have occurred. This explained the significant increase in Fe transfer over the observed SML composition [33]. With abrasion of the MML dominant, Al-MMC transfer would be less and any exposed steel surface could be directly abraded into particulate debris. Li [34] found fine particles of iron to be exclusively mixed into aggregates of Al particles under unidirectional sliding with MML formation. In this study little mixing of the steel into the composite would occur, despite the observed marginal weight loss of the steel counterface, Figure 4.33. Fine Fe particles were found to be similarly intermixed; however the magnitude of abraded iron particles was much less due to the difference in high adhesion of the composite. Consequently, although adhesive transfer remained the dominant wear mechanism under the current sliding conditions, abrasion could be considered an important ancillary mechanism in mixing and transfer of the counterface.

(III) ROLE OF OXIDATION IN TRANSFER AND MIXING

At the low sliding speeds in this study, transfer of iron oxide (or chromium oxide) to the composite surface was not a dominant wear mechanism in reducing wear through *in situ* lubrication [11,101], even at the lowest applied loads. The exception was the $^{1}/_{16}$" reciprocating condition at low load (<10 N) which did cause a transfer layer of iron oxide to form and which was explained by increased abrasion of the debris trapped in the interface. The increased iron oxide was considered have occurred due to approaching fretting wear conditions for $^{1}/_{16}$" reciprocating conditions compared to sliding wear at higher reciprocating distances. Generally based on previous studies and present testing, the

formation of an iron oxide transfer on the composite surface would have been more influential at higher sliding speeds or lower applied pressures [11,24,39] than used in the current low speed reciprocal sliding.

Black aluminum oxide films were observed sporadically to form on the mixed counterface surface, Figure 4.34. The films were analyzed to consist entirely of Al and O and had a visible but very fine substructure of Al particles. The black appearance was observed using SEI mode while no elemental contrast was observed between the oxide film and surrounding Al-MMC deposit using BSE images. Similar black "films" were observed by Bai *et al.* [24], who also observed that the oxide films became continuous as the reciprocal sliding velocity was increased from 7.5 cm/s to 30 cm/s. Unfortunately, the effect of velocity on the formation of this oxide was not examined in this study.

No black oxide was observed on the mixed composite surface, only on the mixed Al-MMC counterface deposits. The presence of the black oxide on the counterface from sliding against the unreinforced Al-Si alloy was not found. The oxide appeared to form on the counterface transfer deposit in regions that had remained affixed for some time without delamination. Fine particulate debris consisted of the Al-MMC deposit on which the oxide was formed. It was found that the greatest likelihood of black oxide surface formation was at low sliding loads, in this study less than 10N, which would produce predominantly particulate debris that was readily transferred. The black oxide was therefore considered a product of the Al-MMC particulate debris, and found to form on the transferred Al-MMC deposit regardless of 316, 440C or 52100 counterfaces acting as the substrate.

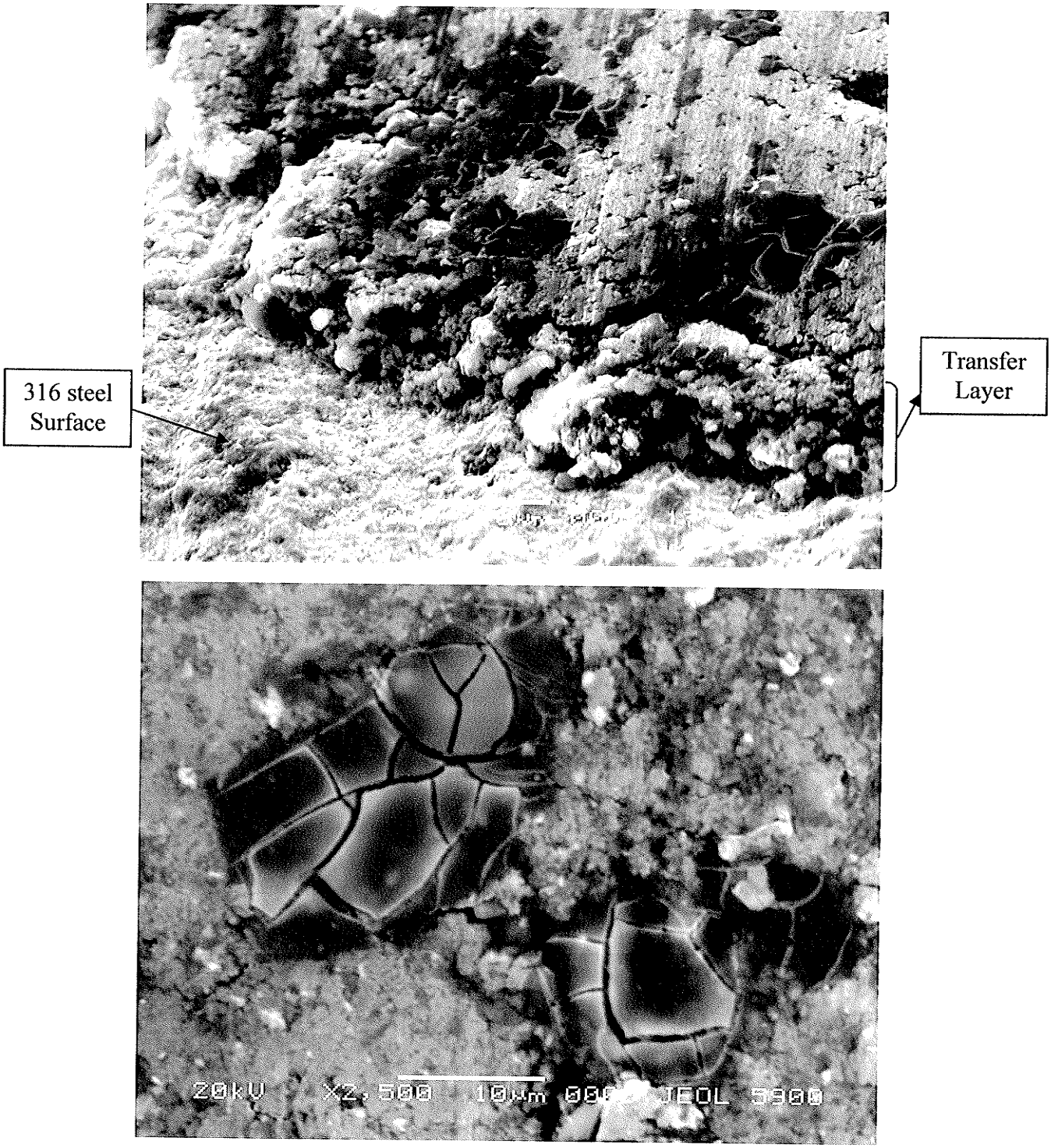

Figure 4.34 TOP: Black aluminum oxide developed on the mechanically mixed Al-MMC transferred to the steel ball. 316ss, 5N, 100m. BOTTOM: Mud-cracked aluminum oxide deposits on a 440C stainless steel ball, 250m, 2N. The occurrence of this oxidation was patchy and non-uniform.

It was proposed that the black cracked oxide surface was the product of high strain, oxidation and deformation of fine particulate debris. The transition to a continuous oxide layer at higher sliding velocities in the previous study [24] may have been related to higher oxidation kinetics in relation to the delamination rate of the transferred composite material off the steel counterface. Overall since this black mixed surface phenomenon was superficial on the mixed surface and did not form readily enough to dominate surface interactions, it was considered to not significantly affect wear properties during sliding.

4.32 DEBRIS MORPHOLOGIES

The character of the debris provides insight into the interactions and amount of re-processing that occurs during the wear test. Agglomerated particles and mixed delaminations are formed through an increased amount of debris interaction as compared to bulk delaminations. The prerequisites for third- body transfer and mixing are ultimately controlled by the size of the debris.

The debris produced in this study is compared to the debris observed by Li [34], who using the same A356-20%vol SiC composite against a M2 hard steel in a block-on-ring setup found the formation of a MML. This study found no MML formation, only patches of mechanical mixing, and a SML at high pressures. The changes in debris morphology provided evidence of the effect of the different ball-on-block contact geometry used in this study and provided some explanation as to why a MML was not observed to form.

(I) SIZE OF DELAMINATIONS

A delamination due to smearing is shown in top picture of Figure 4.35. The average sized delamination shown is approximately 100 x 100 x 6 μm^3. Figure 4.35 was an intermediate size of delamination produced during wear, with larger delaminations due to smearing occurring at high pressure, as shown in Figure 4.310. The maximum size of smearing delamination found was in the order of 300 x 200 x 10 μm^3. The length of smearing delaminations decreased with decreased pressure causing more symmetric delaminations to be produced.

Thin delaminations of the size and morphology shown in Figure 4.35 were likewise observed by Zhang *et al.* [22,80] who stated that the "flakes" were produced by adhesive wear. In this study by Zhang no MML was stated as forming, and the average wear flake dimension was determined to be 600 x 200 x 8 μm^3 [80]. Venkataraman and Sundararajan [32] observed similar delaminations that were described as "irregular shaped platelets". In this case platelet delaminations were found to be produced from a MML at the surface [33]. The size of the "platelets" was determined to be in the order of millimetres at high load and a few hundred micrometers at low load. Both studies [22,32] observed pressures less than 10 MPa and sliding speed of near 1 m/s. The Al-SiC composites had smaller average reinforcement sizes of 1.8 μm [22] and 2.5 μm [32] than the average 10μm particles of the composite used in the present study. Comparing debris produced by smearing delamination from current reciprocal testing with the platelets or flakes observed in these previous unidirectional sliding studies [22,32] it was apparent that the smearing delaminations were in general much smaller in size.

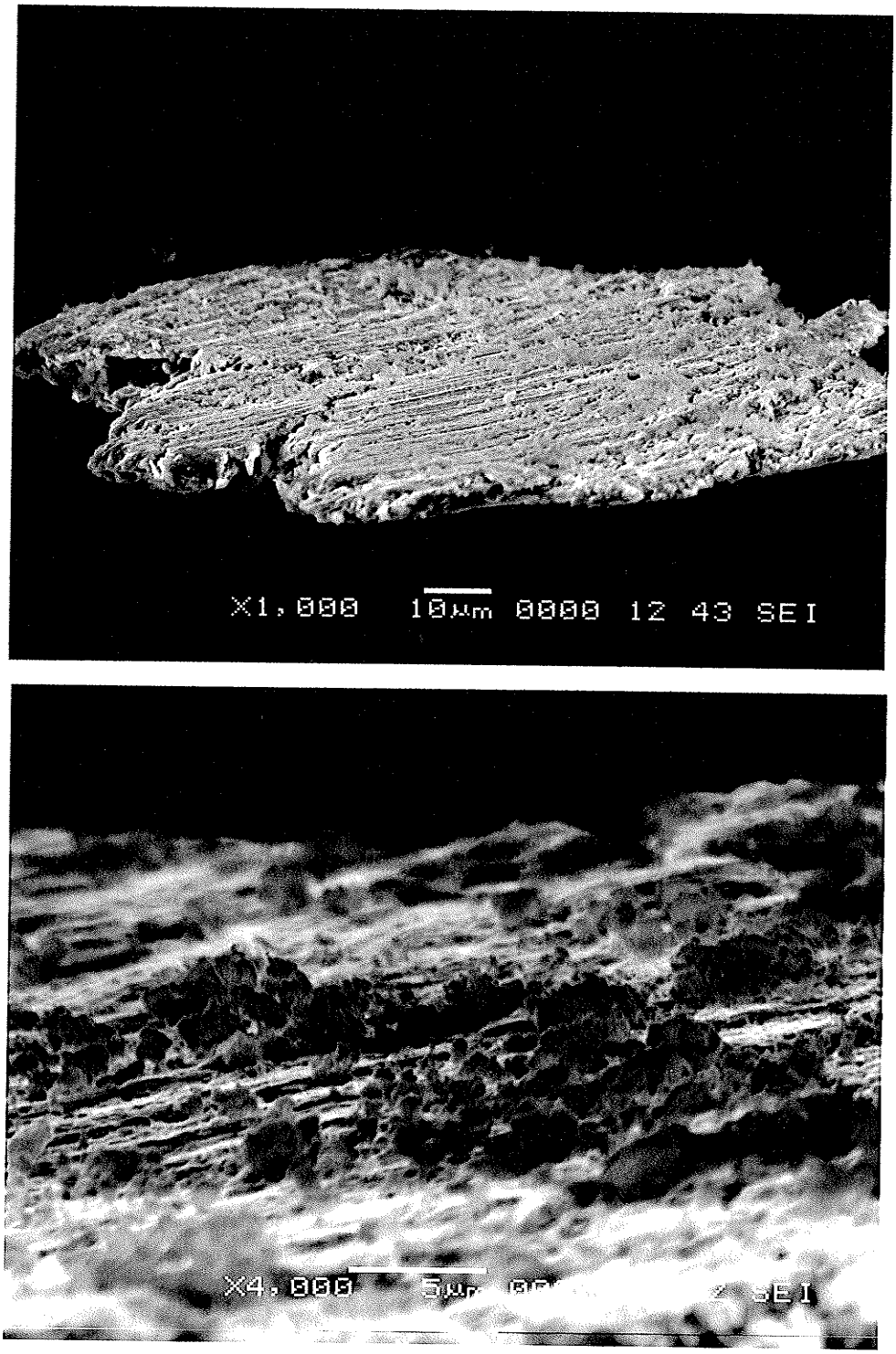

Figure 4.35 TOP: Average smearing delamination from the composite surface. The thin layer can be seen to have experienced tensile fracture at the edges. BOTTOM: High magnification of the delamination showing fine abrasion lines and the resulting thin chips formed. This provided evidence that abrasion can be partially responsible for the production of fine particulate debris.

At a lower unidirectional sliding speed of 0.2 m/s and using the same composite, Li [34] observed plate like debris of similar size as the smearing delaminations found in the current reciprocal sliding study, except that the plate debris he found was formed from the MML layer with significant mixing of iron. Considering the above mentioned studies it was concluded that the plate, flake, or thin delamination size did not drastically change with or without a MML present. It could also be inferred that larger thin delaminations were produced due to either a smaller reinforcement size or a higher sliding velocity. Finally, since flake or plate debris of this size and morphology has been similarly observed for unreinforced aluminum alloys [13,27], delamination wear of this nature can be established as the principal cause of weight loss during dry sliding wear of aluminum and aluminum composites regardless of the surface mixing behaviour that is occurring.

(II) SMEARING AND SUBSURFACE FRACTURE

Distinguishing between a delamination produced by smearing and a delamination produced by subsurface fracture was often difficult due to the interplay of plastic deformation and the cracks it would form. Most delamination debris could be seen to be produced by both excess smearing and a crack propagating to fracture. Delamination debris often had of a cracks extending from the surface to the subsurface, formed by excess tensile strain due to smearing. The initiation of surface cracks that propagate to the subsurface could be identified by development of craze cracking, shown in Figure 4.23 and Figure 4.313. Propagation of a surface crack often corresponded to visible shear bands along the periphery of the fractured particle. Both delaminations shown in Figure 4.39 were produced by propagation of a crack down through several shear band layers.

Long subsurface cracks parallel to the sliding direction formed between smeared layers facilitating fracture of the thin flake or smeared delaminations. The result was a free surface beneath the smeared layer before tensile fracture at the edges occurred. Figure 4.36 shows a recently formed thin surface delamination with evidence of tensile fracture at the edges due to smearing (A). A surface crack can be seen to have crack propagated along the bottom of the debris, in the subsurface under the smeared layer (B). A smeared surface can be seen at the bottom of the debris plate indicating that this delamination was smeared overtop the bulk matrix as a separate layer before fracturing (C). When the crack propagated to an unstable depth underneath the smeared layer, the wear particle fractured, causing dimples and striations to form in the center (D). Consequently both smearing and subsurface fracture are simultaneously controlling the delamination wear.

Long subsurface cracks caused smearing debris to be elongated in the sliding direction, Figure 4.310. When pressure decreased smearing of the surface into a layered structure was reduced and surface cracks no longer propagated between smeared layers. Rather surface cracks would propagate along shear bands into the subsurface. This caused delamination debris to be produced by instability and fracture at a greater depth into the subsurface, instead of tensile fracture of a surface smeared layer. When subsurface fracture began to have greater dominance on the production of debris wear particles would become more symmetrical and thicker in response to how the crack propagated, Figure 4.37.

In other words, without large displacements at the surface occurring due to smearing, a subsurface crack would produce a delamination of the bulk composite matrix, instead of from a smeared layer. In the bottom picture of Figure 4.37, shear bands along which the crack propagated are magnified. In this figure, superficial smearing of the

surface can be observed, and a more symmetrical debris size. In addition, since fracture does not occur from smeared layers but rather from crack propagation into the subsurface, the depth of the delamination can be seen to considerably increase. While the maximum thickness of a smeared layer delamination was about 10 μm, delaminations due to subsurface fracture were found be the up to 70 μm thick.

Both smearing delaminations and delaminations due to subsurface fracture had similar smeared surface appearances. In fact, smearing and ploughing could be observed on the contact surface for all delamination debris morphologies. Delaminations due to subsurface fracture often had a fracture surface apparent at the bottom of the particle indicating tearing topography surface (TTS), dimple rupture (DR) or crack propagation. Unfortunately debris once produced, must leave the wear scar for observable weight loss to occur. Therefore a clear distinction between surfaces was often obscured through interactions before ejection from between wear surfaces.

Delaminations produced by fracture of thin smeared layers, as shown in Figure 4.310, had a dull metallic silver appearance. As the delamination size decreased the debris darkened from shiny metallic silver to dark grey to black. The delamination in Figure 4.37 would visibly appear as dark grey. Larger delaminations were found to be ejected a considerable distance from the contact surfaces. As expected, smaller compact delaminations would better remain in the interface once produced, causing greater surface mixing and darkening the debris appearance. The longer a delamination remained in the interface meant greater mechanical mixing was capable of occurring. Mixing that occurred on a delamination that remained in the interface can be seen in the bottom picture of Figure 4.39.

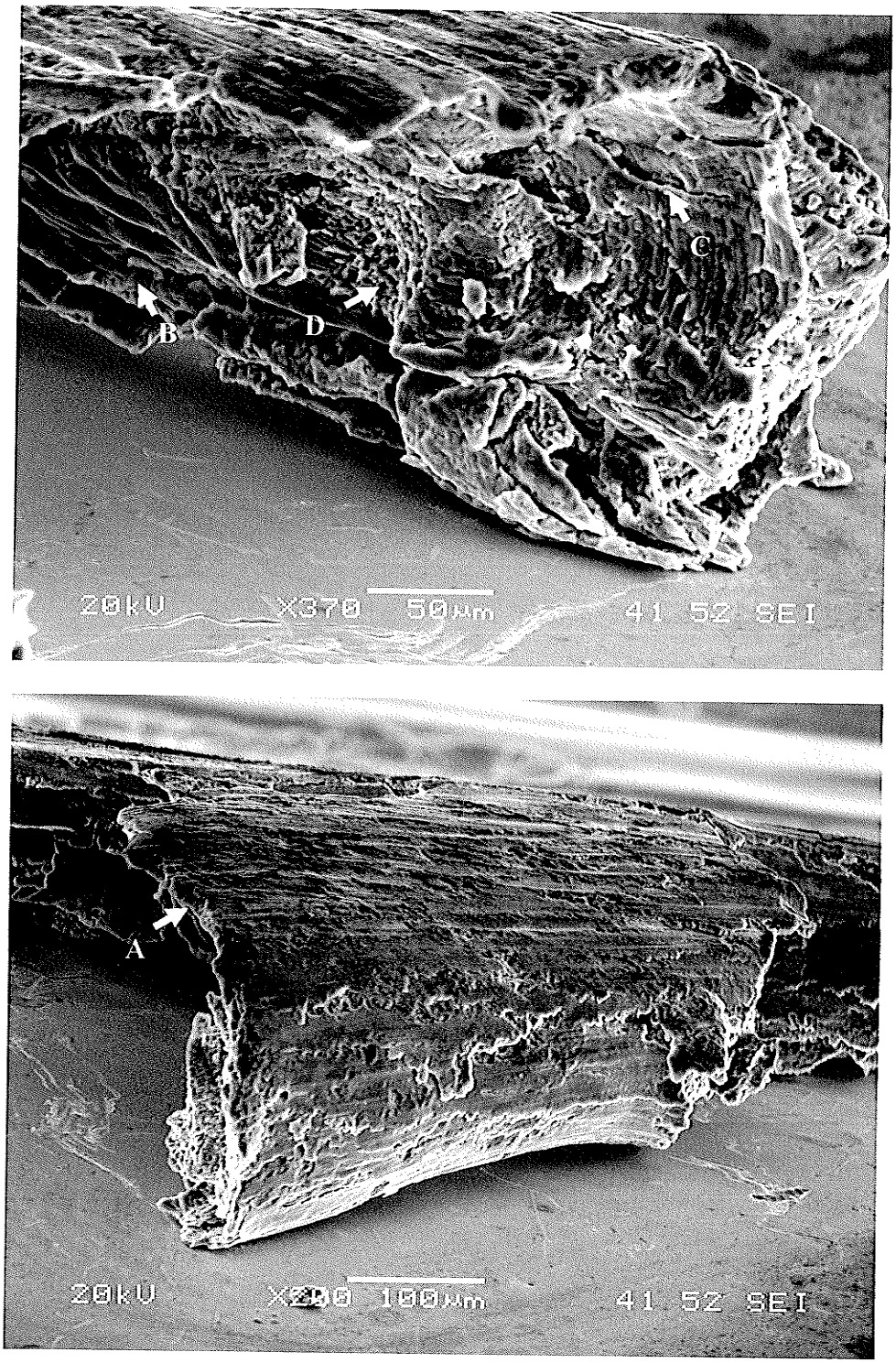

Figure 4.36 Recent delamination removed from contact surface, Al-Si 50 N. Tensile fracture at the periphery indicates that this delamination morphology was formed predominantly due to fracture of a smeared layer, (A). Shear bands of subsurface crack propagation, (B). Smearing of a free surface at the bottom of the delamination, (C). Dimples show evidence of ductile subsurface fracture as the final cause of the delamination, (D).

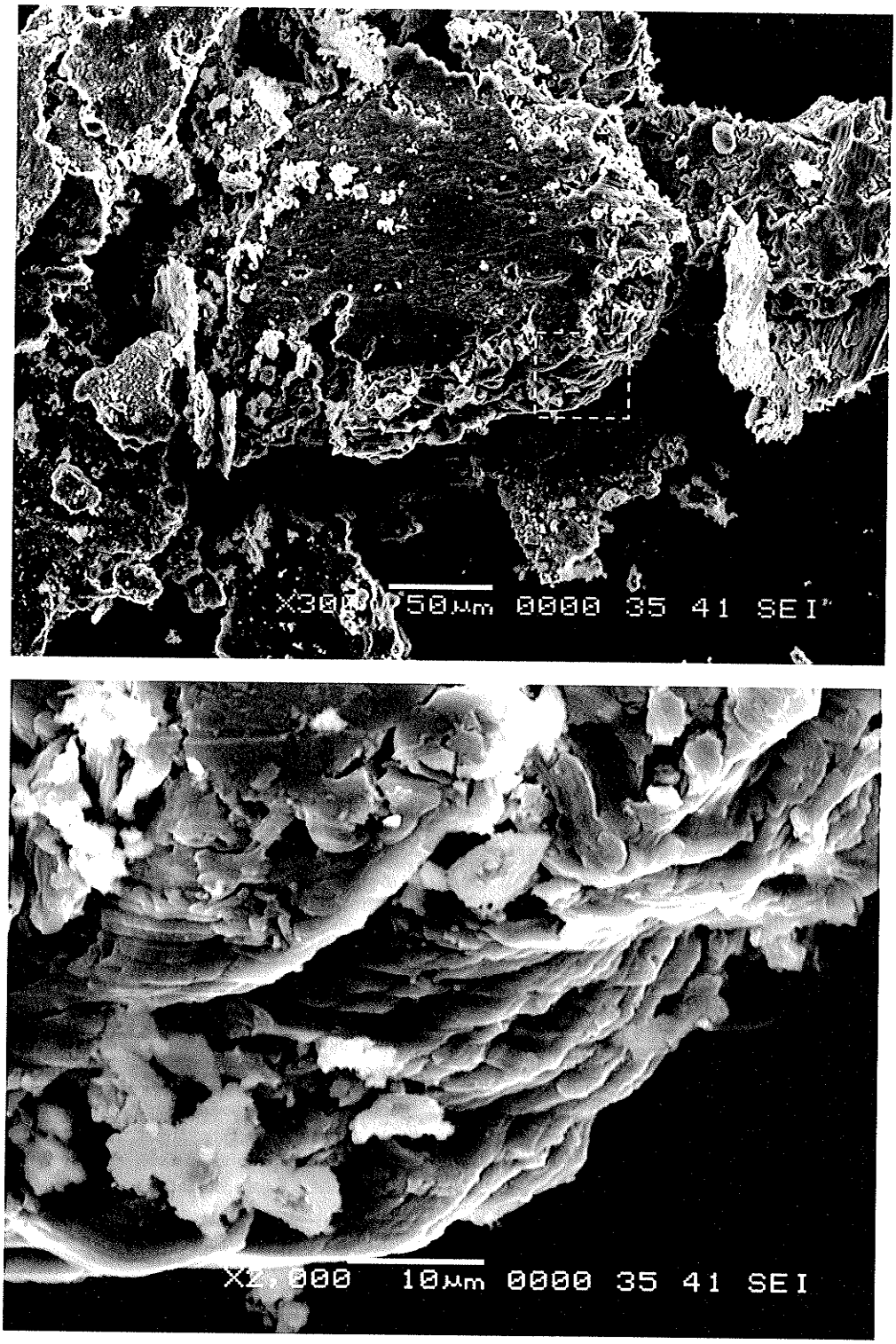

Figure 4.37 TOP: A thick, symmetrical delamination due to subsurface fracture from the Al-composite. The edge of the debris has been magnified to show the fracture surface along which a crack propagated. The striations appear to be formed due to shear bands in the subsurface, indicating extensive subsurface deformation occurred. Debris was magnified from Figure 4.112.

Large delaminations of smeared layers were formed by high deformation of the composite surface, a process that did not result in much intermixing of abraded particulate debris. Consequently the large delaminations due to smearing were found to have the same composition as the surface of the base alloy with a marginal increase in oxidation, Figure 4.310. Abrasion was observed on the smeared surfaces of the delamination debris, Figure 4.35, as well as ploughing, Figure 4.38, both of which expectedly caused production of Al and SiC particle debris. Therefore fine debris particles were both produced from and collected on delamination surfaces. The fine particle debris on the surface of the delaminations was analyzed to be predominantly Al. Accumulation of the particles, compaction, and smearing may have resulted in build-up of the delamination surfaces. However as previously noted for the smeared Al-MMC surface, significant Fe particle mixing was not present in the delamination debris, as was revealed by X-Ray mapping.

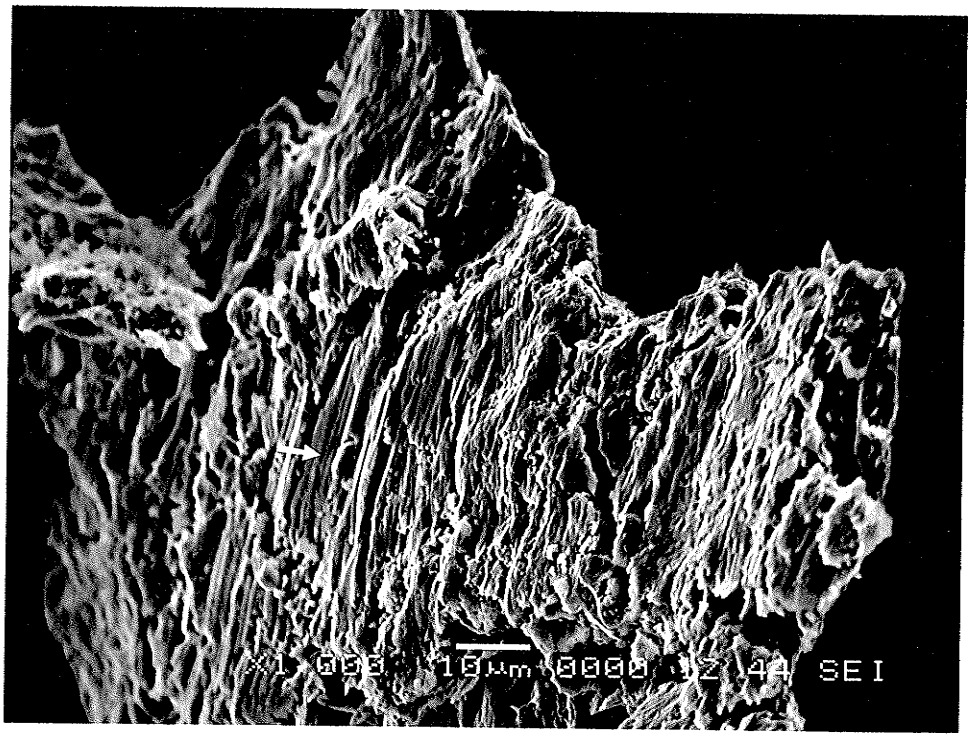

Figure 4.38 Extensive ploughing of a smeared delamination before removal from the interface. Tensile fracture observed at edges. SiC identified with arrow.

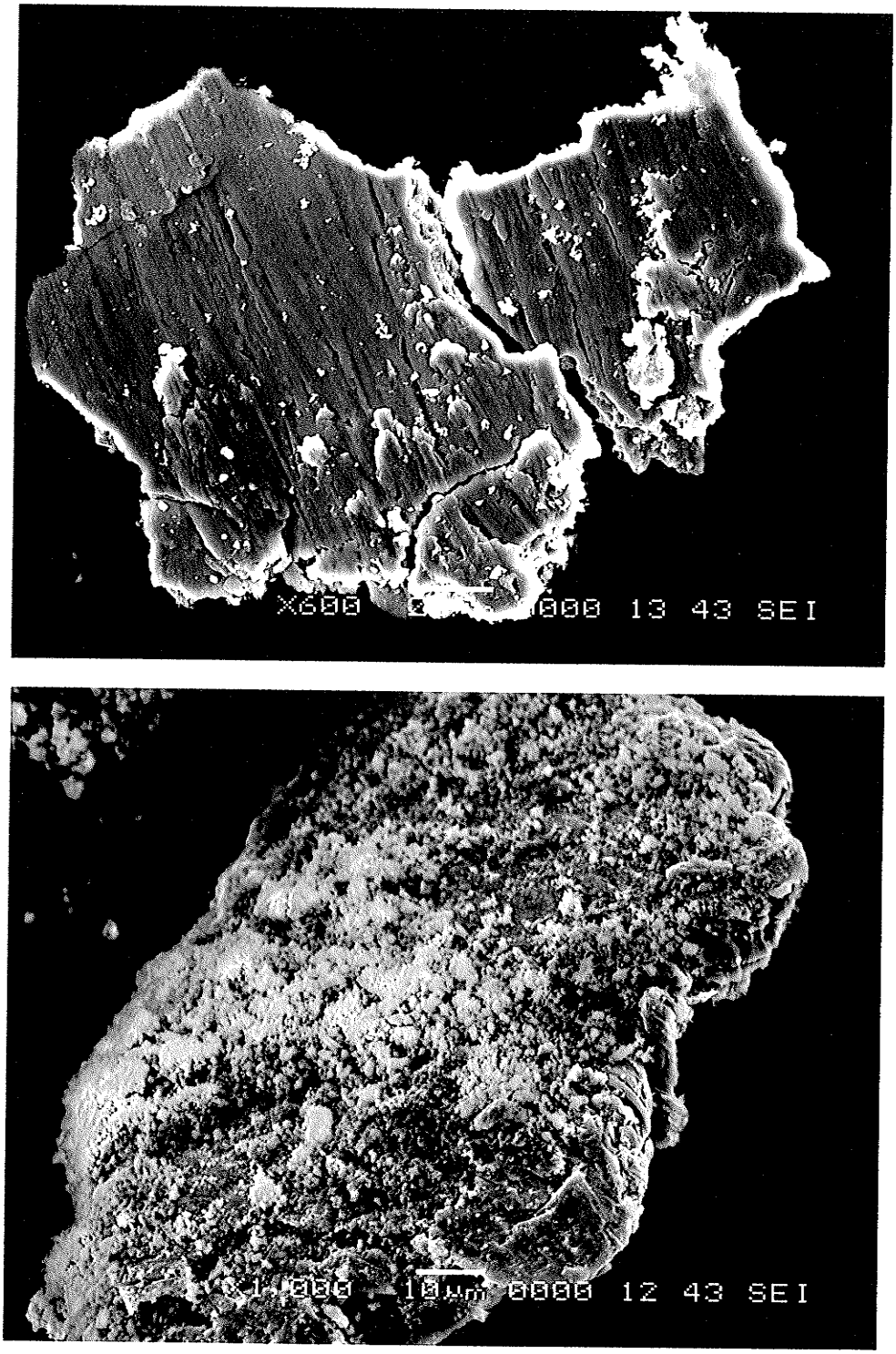

Figure 4.39 TOP: Debris consisting of several partially smeared layers, and therefore produced by combined mechanisms of smearing and subsurface crack propagation causing fracture. BOTTOM: Thick delamination due to subsurface fracture with fine particulate debris mixed on the surface. White particles are oxidized aluminum.

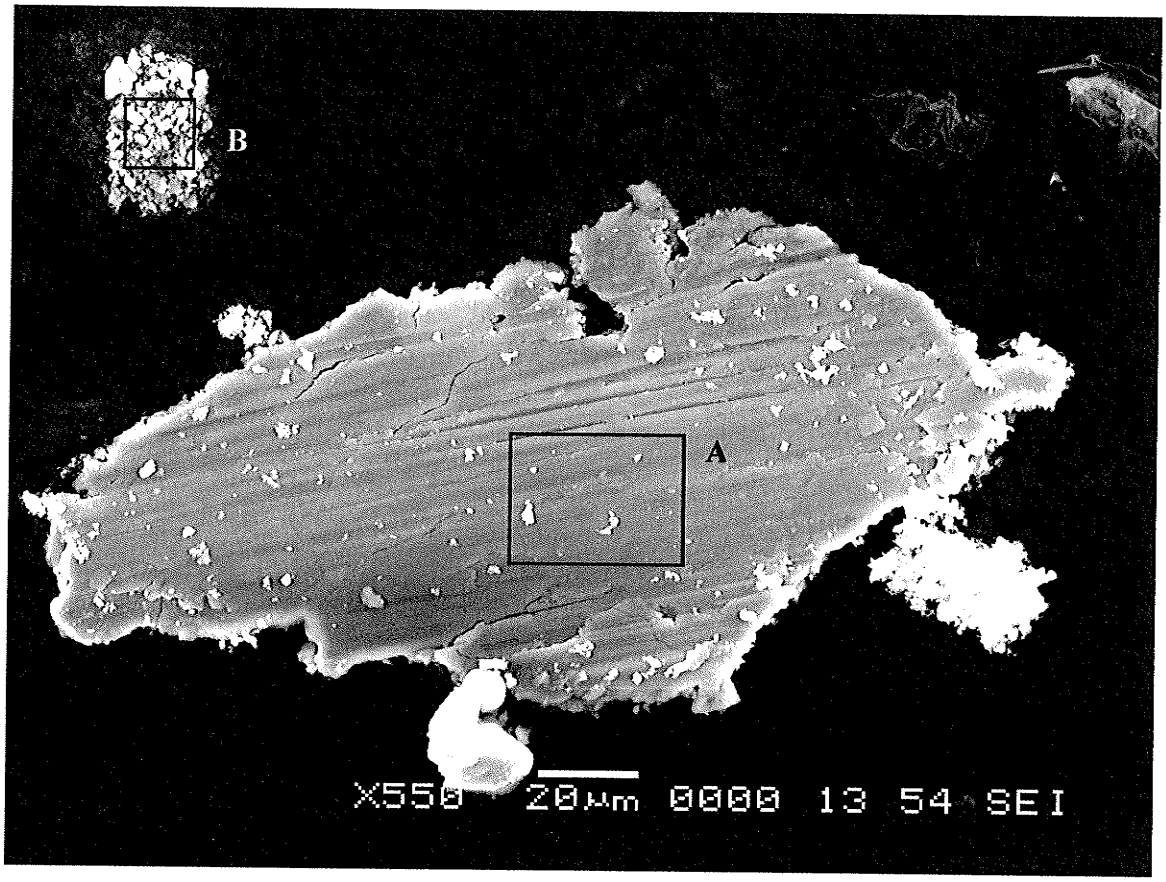

[A] Shiny thin delamination

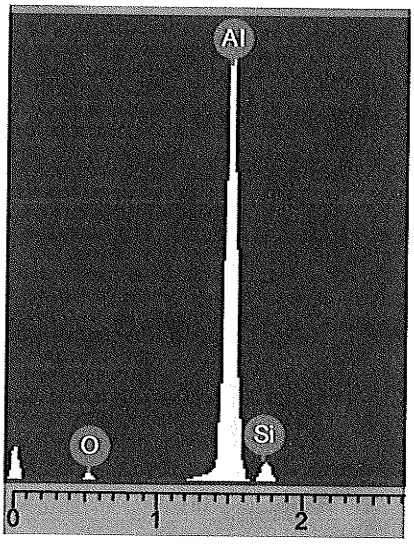

[B] Black particle debris

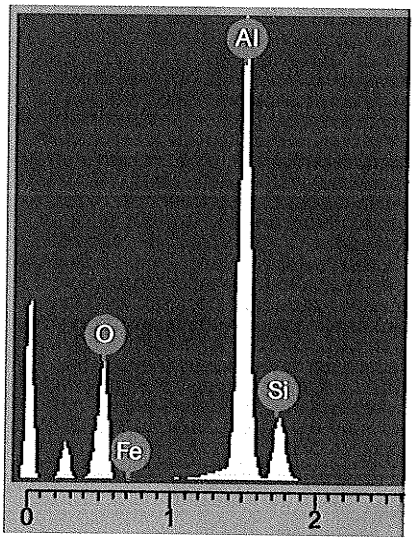

Figure 4.310 Shiny thin delamination due to smearing [A] and black particulate agglomeration debris [B] that were ejected from Al-MMC surface at different pressures. The long thin delamination was produced due to smearing at high pressure, while the agglomeration of compact delaminations was produced at much lower pressure with continued sliding. Debris produced against 52100, 10N, ¼".

(III) MIXED DELAMINATION DEBRIS

If a MML forms a coherent layer from which fracture causes weight loss and wear, fractured MML delaminations should be observable in the debris. Venkataraman and Sundararajan [32,33] observed irregular shaped plates/delamination debris from the MML, with Fe content increasing with %SiC. Through cross-section examination and the observed high mixing of the counterface it was concluded that this debris originated from the MML. Similarly, Li [34] observed MML debris to consist of compacted plates of particulate debris, which contained up about 50 wt% Fe as the sliding load was increased. The iron was determined to be distributed throughout the composite as ultra fine particles. In both studies [33,34] the MML can be seen to be distinctly different than the SML shown in Figure 4.211-4.213 by the drastic increase of hard particles in this layer.

Some mixed delaminations of irregular shaped morphology were collected in the current study, Figure 4.311. These delaminations were separated from bulk compact delaminations due to the fine aggregate fracture surface, indicating the debris delaminated from a mixed depth. X-ray mapping of the particulate fracture surface indicated small Fe particles were dispersed in the region however the percentage of mixed Fe was in the range of 1-5 wt%, Figure 4.312, much less than the previously observed MML content.

Mixed debris that would have become a MML was considered to have formed from debris particle accumulation. Debris from a SML had a refined SiC microstructure due to surface smearing and deformation and since it was formed without debris particle mixing it would be better described as a compact delamination.

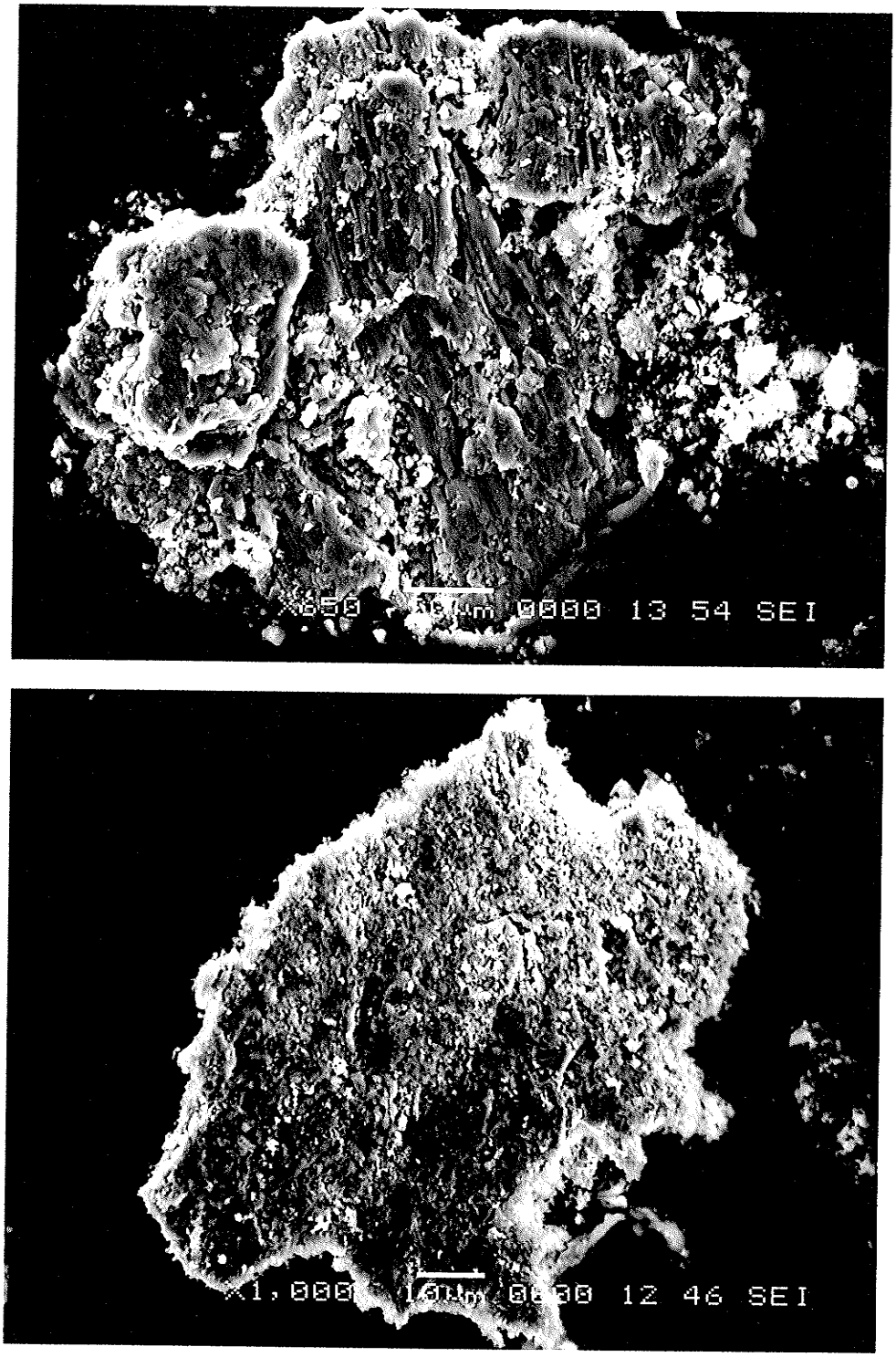

Figure 4.311 TOP: Agglomeration of mixed delaminations caused by subsurface fracture. Note that smearing has occurred on the surface. BOTTOM: Fracture surface belonging to the above debris morphology, showing incomplete agglomeration of particulate debris, crushed reinforcement and dimple fractures. Traces of iron indicate that the subsurface particles were once in contact with the counterface.

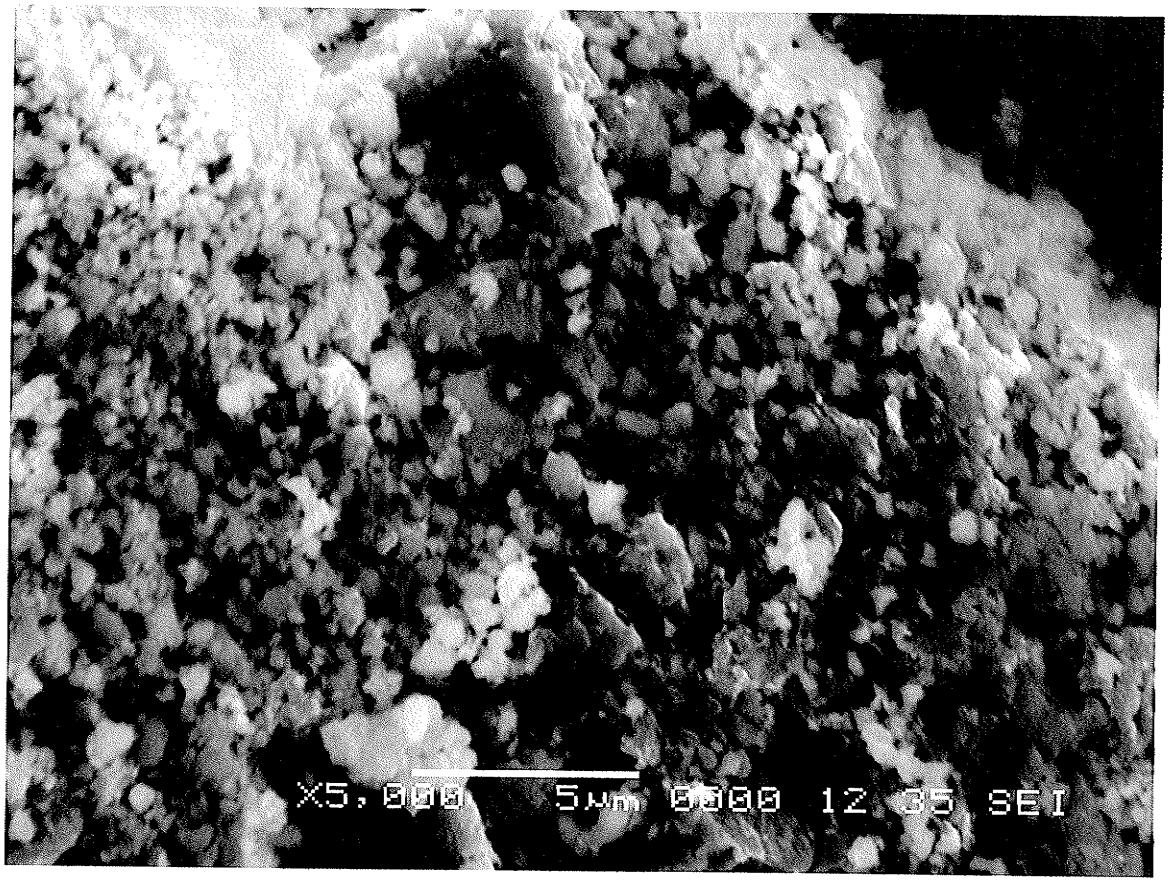

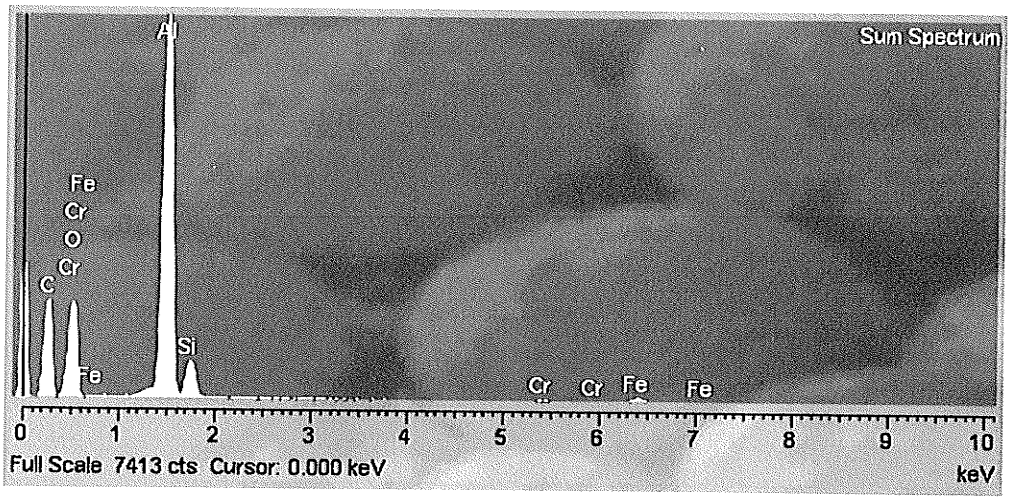

Figure 4.312 High magnification view of fracture surface from the lower picture of Figure 4.311. The presence of elements from the 316 counterface was detected; however the original composite matrix dominated the particle mixing which occurred. The sum spectrum was taken from entire region.

The production of highly deformed compact delaminations and mixed delaminations can be observed to be simultaneously occurring in Figure 4.313. In this figure craze cracking has produced very small delaminations from the smeared layer. Accumulation of mixed particles can be observed to occur at the discontinuity left by the delaminations, which would be smeared into surface with continued sliding. In the captured state of surface wear delaminations that are produced may be composed from either mixed debris or the bulk composite.

Since compact delaminations were considered to have mostly formed through deformation not debris accumulation, no Fe content from the counterface was again observed in individual debris flakes. Many compact delaminations were too large to mechanically remix into the surface once produced, however were also too small to easily be ejected from the interface. As a result, compact delaminations often formed aggregations before becoming ejected from the wear scar, Figure 4.314. Compact delaminations and SiC reinforcement were rarely ejected from the interacting surfaces as separate particles, but rather were accumulated into these aggregates before removal. The aggregates produced at low pressure were most often less than 50 x 50 μm^2 and usually contained whole SiC particles. Some iron was found in the aggregate debris most likely due to abrasion of the counterface before ejection from the wear scar, as noted in Figure 4.310. The agglomerations of compact delaminations/particle debris were visibly black when ejected.

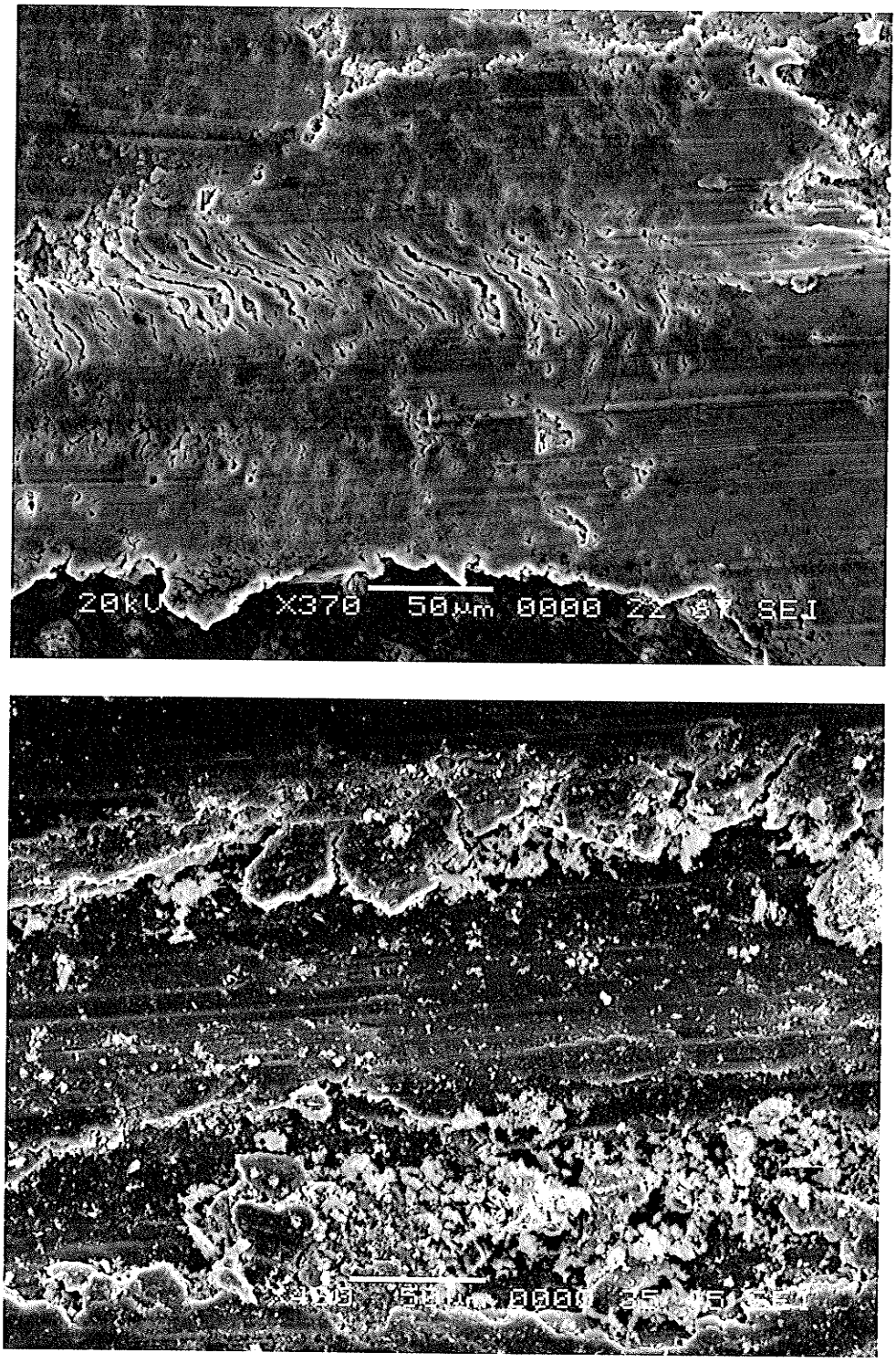

Figure 4.313 Delamination of the smeared surface due to craze cracking. Fine particle debris has accumulated in recesses left by the delamination. The ejected debris from this delamination is shown in Figure 4.214. The formation of compact and mixed delaminations can be seen.

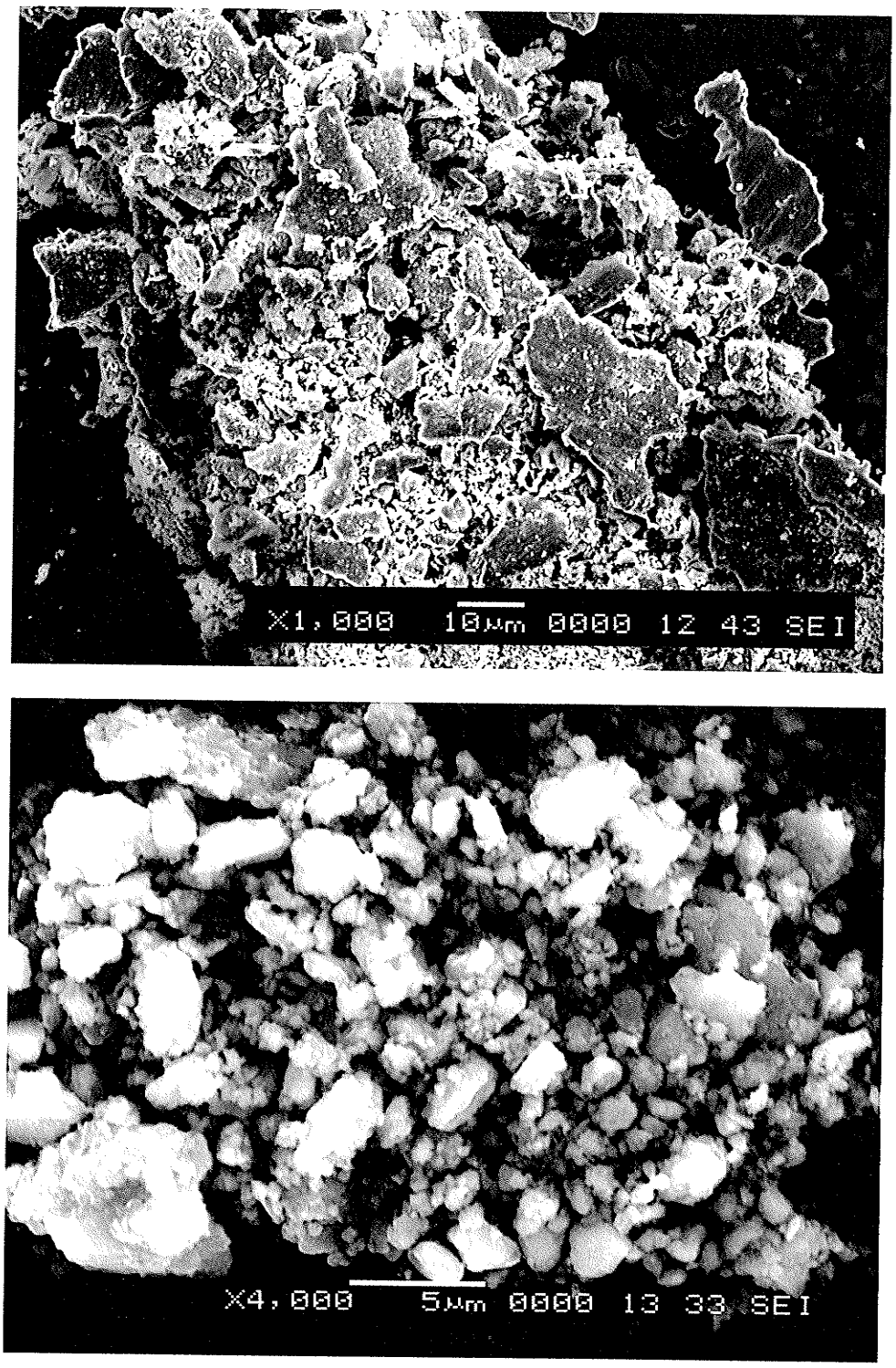

Figure 4.314 Debris agglomerations formed at contact pressures that produce compact delamination wear particles more readily than abraded fine particulate debris. TOP: Collection of compact delaminations on the edge of the wear scar. BOTTOM: Magnified view of aggregate. EDS of aggregate revealed points of abraded iron and whole SiC particles agglomerated before the debris particle was ejected

As pressure decreased so did the size of the delaminations. Nothing separated a delamination due to subsurface fracture from a compact delamination except for both size and thicknesses were much reduced in the latter case. Sizes for compact delaminations were considered to range from 5-50 μm and less than 5 μm. thick Compact and mixed delaminations were produced at pressures less than approximately 15 MPa and were substantially replaced with production of fine particulate debris as the pressure fell below 5 MPa. Debris flakes less than 10 μm were common and could either be mixed of compact delaminations. This small flake debris was fractured of the surface after any combination of mixing, compaction and smearing by a delamination process, and was therefore distinct from particulate debris, produced by abrasion or small adhesive transfer, by the operating wear mechanisms.

(IV) PARTICULATE DEBRIS

A fine aggregate debris was observed, characterized by an agglomeration of small, 0.2-2 μm average diameter, equiaxed particles, with a visible black soot appearance, as has been identified in previous studies [25,34], Figure 4.316. The fine aggregate debris was found to contain small amounts of Fe, with Cr and Ni also present for a 316 counterface, Figure 4.317. SiC particles and increase oxide level were revealed by x-ray mapping.

Particulate debris was produced for all three Al materials. The particulate debris was similar in size and morphology in all three cases, with the exception of the odd SiC particle intermixed amongst the fine particles from the composite. The rationalization was that the particles were produced by a same process related the Al matrix, regardless of the presence of Si or SiC phases, since fine particulate debris was readily produced during wear

of HP Al. The Al particles were most often highly oxidized, causing charging of the image in SEI pictures.

Abrasion or ploughing, as observed on this debris flake in Figure 4.35, caused wedges to form of amassed metal chips was identified as a potential source of the particulate debris. Adhered wedges due to abrasion are seen on the surface, 0.2 – 1.5 μm in size. EDS of abraded particles is limited by depth of beam penetration being greater than the particle size, however only Al was detected. The nascent abraded chips or equiaxed particles are expected to rapidly oxidize.

Adhesion between surfaces was also assumed to produce particulate debris, with Al contact asperities fracturing and transferring between surfaces. This process was related to the almost snowflake like debris observed at high magnification. The proposed process of small adhesive transfer is Figure 4.315.

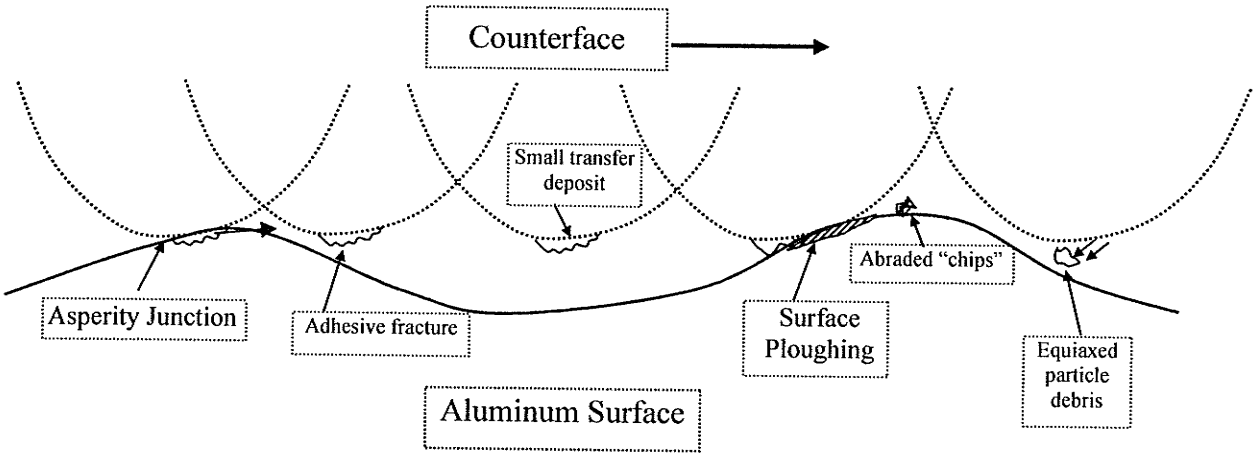

Figure 4.315 Proposed mechanisms adhesion producing small transfer elements and debris from the aluminum matrix. Note that abrasion or ploughing of the surface producing fine particulate debris from abraded chips could occur by contact with the steel counterface, hard debris particles or contact by the deformed aluminum transfer deposit as shown.

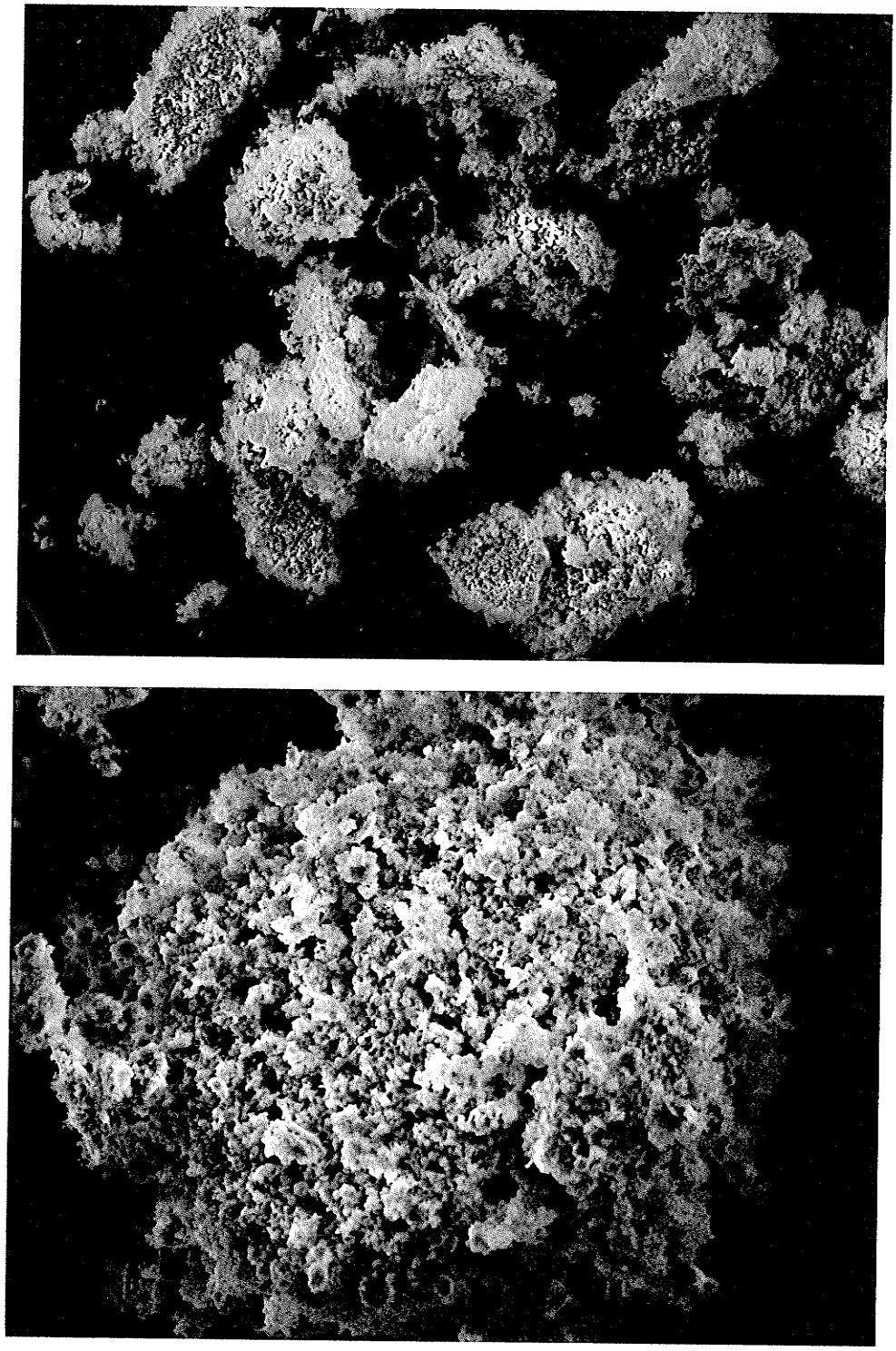

Figure 4.316 Aggregates of fine particulate debris produced at low pressure where abrasion and compact delaminations dominate surface wear. TOP: Small delaminations act as a substrate from the particles to accumulate on, 400X. BOTTOM: Magnified view of an agglomeration, 2000X.

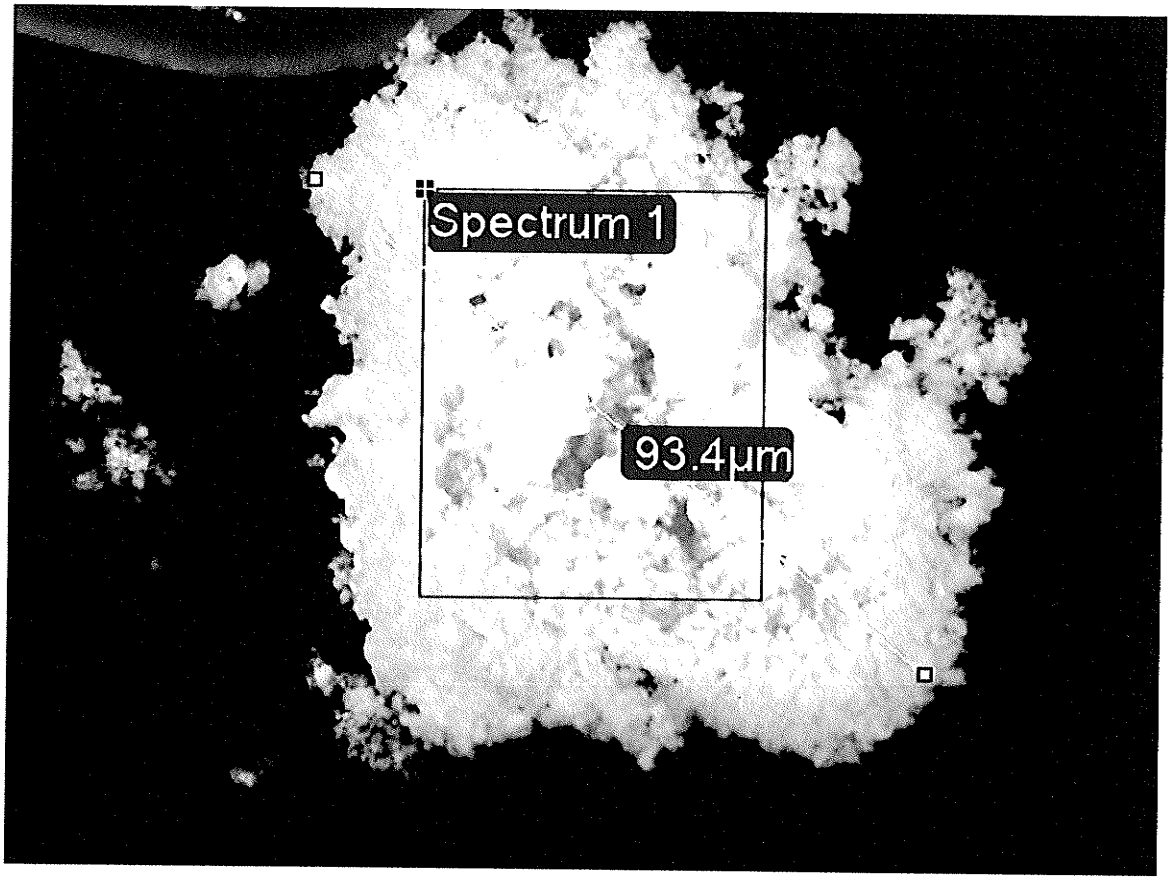

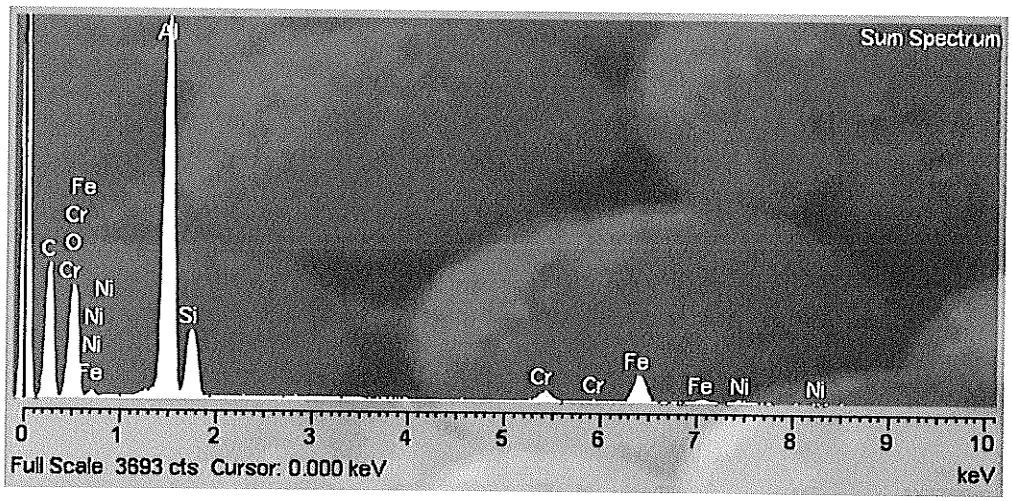

Figure 4.317 Very fine particle debris agglomerated most likely on the composite surface before ejection from the interface. EDS scan indicated the fine particles to be predominantly composed Al. 316ss counterface, 5N

A transition from metallic wear to oxidative wear has been proposed to occur with the immergence of fine particle debris [6,16], as shown in Figure 4.317. Although the X-Ray mapping of this debris particle indicated that the level of O was high, it was not high enough to conclude that the very fine particles came from an Al_2O_3 oxide layer. The fine particles must have consisted of highly oxidized particles of the aluminum alloy, in agreement with previous studies [25,92].

For block-on-ring testing, wear particles tend to pile up on the leading edge of the ring. When the leading edge debris accumulation would become an unstable size the mass would break apart and scatter in-between contact surfaces and compacted. However, the current ball-on-block reciprocating tests did not exhibit the same debris prow formation behaviour due to the change in direction. In the current testing particulate debris accumulated on the surface to form very fine, almost snowball-like aggregates. However, these aggregates were ejected as shown in Figure 4.316 and 4.317 without compaction into plates as observed by Li [34]. Debris accumulated at the edges of the wear scar due to the change in direction. The greatest chance of a mechanically mixed surface and iron from the counterface was found at the ends of the reciprocating wear scar. Therefore noting the round agglomerations of debris not observed in the unidirectional study, the formation of a MML out of the debris particles was not occurring possibly due to the lack of compaction of fine particulate debris into the surface before ejection from the interface.

4.41 INFLUENCE OF THE COUNTERFACE

In this final section effort is taken to establish if the wear mechanisms and mixing behaviour determined so far were specifically related to the use of a steel counterface, or if the wear properties of the composite were similar regardless of the counterface material. Low mixing of the steel counterface elements has been observed for the ball-on-block geometry. This has been related to dominant smearing of the surface, high adhesive transfer to the counterface and insufficient re-compaction of the debris into the wear surface once produced. The adhesive compatibility, which surface dominates asperity interactions, and how counterface debris is produced and transferred, are all extremely dependant on the counterface hardness and composition.

(I) METHODOLOGY OF DETERMINING RELATIVE INFLUENCE

To examine the effect of different counterface materials on SiC interactions, a low load of 2N was applied and exposed to 100 cycles of ¼" sliding (approximately 1m). SiC could clearly be observed to either inundate, fracture or act as load bearing elements at the short sliding distance, before cumulative wear damage made identifying SiC behaviour difficult. Wear and transfer at the very short sliding distance also provided indication of how the counterface and composite would respond when in brief dry sliding contact due to breakdown of a protective oil film under lubricated conditions.

To examine if a transient surface mixed layer would form, tests were interrupted after 10m cumulative sliding at 2N. This was the same sliding condition that caused the formation of an SML against a 52100 counterface, Figure 4.28.

Finally to examine how the wear resistance of the composite was directly affected by counterface material, tests were run for 250m causing the surface to experience a range of applied pressures. The counterfaces were tested at a high and low range of pressures, expected to respectively cause mild and severe wear conditions. A low load of 2N allowed better chance of the SiC acting as load bearing elements to resist smearing, while at 20N SiC were expected to be mixed and smeared under the high pressures.

(II) WEAR PERFORMANCE RESULTS

A summary of the composite and counterface wear is given in Figure 4.41. The weight of the collected debris had a much higher weight than the sum of the composite and counterface weight losses due to oxidation occurring to a greater degree on all surfaces at lower loads. In general the weight loss results can be considered as low pressure (2N) and high pressure (20N) sliding conditions.

(A) Low Load

Considering the wear resistance of the composite, 316 stainless steel caused the greatest weight loss, while K-Monel caused the composite to gain weight, Figure 4.21. Therefore the nickel alloy made the best choice based on composite wear. Considering the wear resistance of the counterface, both ceramics gained mass and therefore experienced nil wear in comparison to the metal materials. The Al_2O_3 caused the least transfer and therefore was clearly the best choice for minimum counterface wear at low pressure.

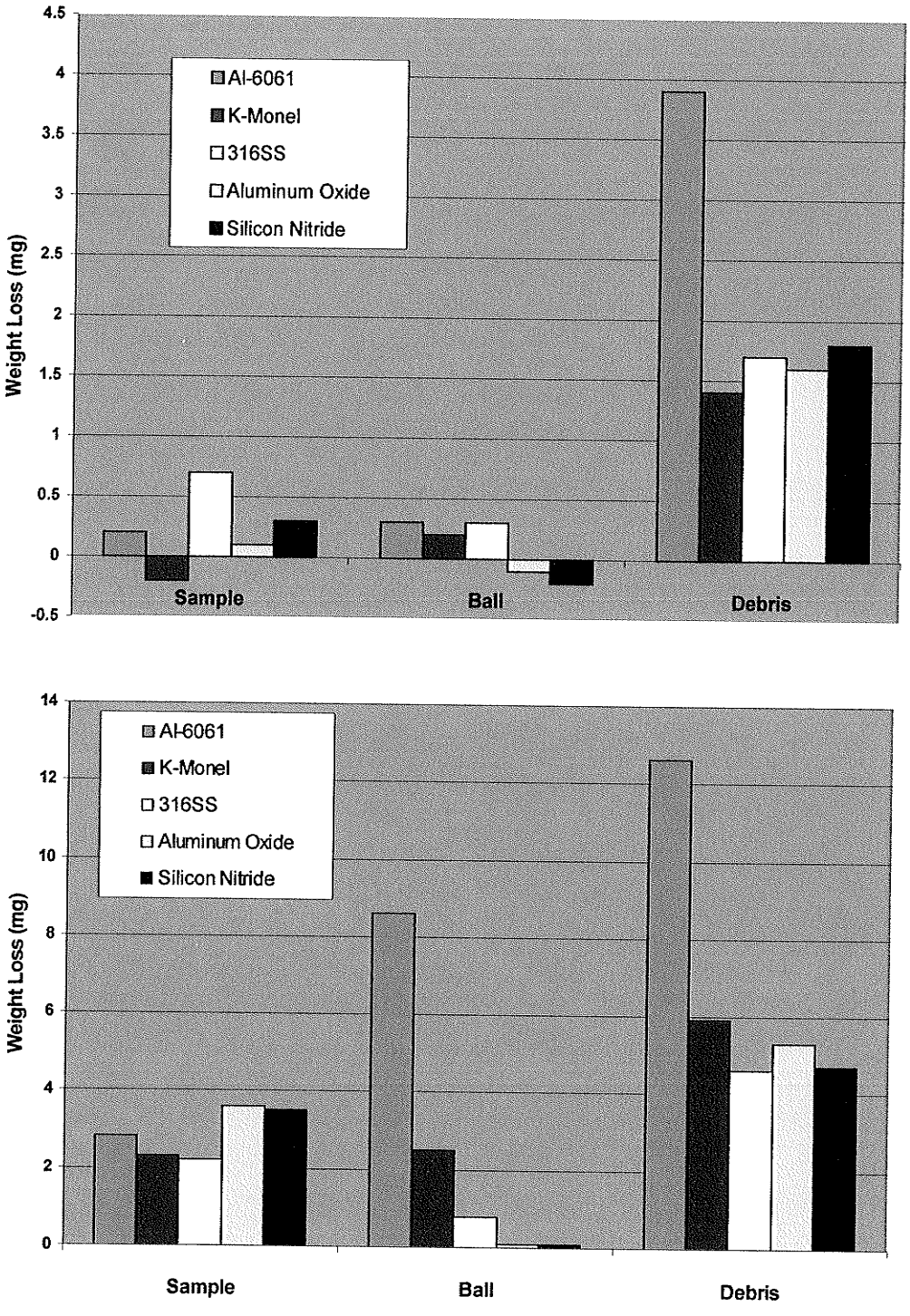

Figure 4.41 Wear performance results for different counterfaces against the Al-SiC composite. TOP: 2N, BOTTOM: 20N. 250m of ¼" reciprocating sliding contact.

Considering the wear resistance of the tribological pair, which was determined by the total weight loss from the sliding system, a clear choice of best counterface material between, K-Monel, Al_2O_3, and Si_3N_4 was unclear due to mutual transfer between surfaces causing essentially no weight loss. Al-6061 was clearly the worst counterface choice based on weight loss. 316ss was a worse choice than K-Monel at the lower applied load.

(B) HIGH LOAD

At the higher 20N contact force weight loss of the composite did not vary significantly based on the counterface. Examination of the surfaces revealed that smearing dominated most of the composites wear. However, transfer of the composite to the counterface varied significantly. Al_2O_3, and Si_3N_4 did not loose or gain weight, corresponding to consistent transfer deposits on the counterface contact surface. K-Monel experienced significant transfer to the composite, while Al-6061 had a very high weight loss due to abrasion. 316 was the best choice at the higher applied load when considering both weight loss and surface damage indicators of wear.

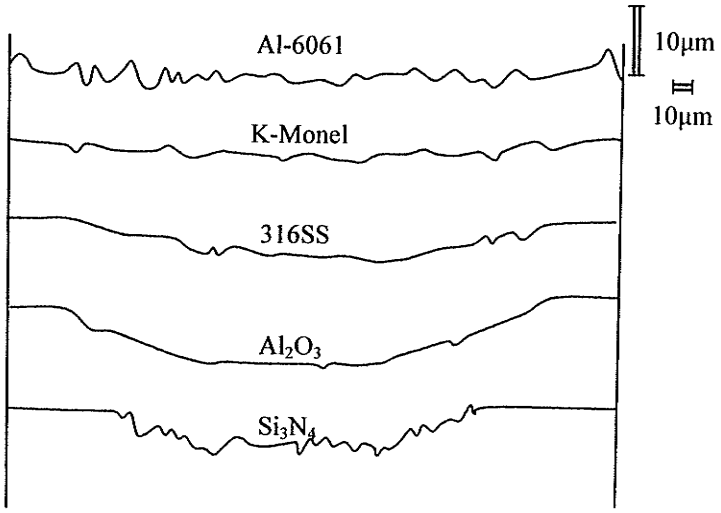

Figure 4.42 Counterface profiles at 20 N. The Al-6061 had the greatest roughness due to large thin delaminations in the sliding direction and random mutual transfer.

4.42 DIFFERENT COUNTERFACES

In both low and high conditions examination of the surface wear mechanisms and mixing behaviour better elucidates how to rank of the counterface materials at low load which had no net weight loss.

(I) AL-6061

(A) TRANSFER AND MIXING

The unreinforced aluminum counterface was expected to have high adhesive compatibility [47] with the Al-composite. Also, having a lower cohesive strength the Al-6061 was expected to experience greater transfer of the two [49]. High adhesive transfer did occur between the surfaces. However, it was observed that a preferred direction of adhesive transfer did not exist, as the Al-Si composite base alloy was found deposited on the Al-6061 ball and vice-versa, Figure 4.43. The compositions of A356 and 6061 were not very different considering that the room temperature solubility of Si in the Al composite matrix is less than 0.2 at% [9]. Therefore adhesive surface energies between the 6061 counterface Al and composite Al matrix Al were expected to be similar and not cause the development of a preferred transfer direction [50]. Transfer of the mixed Al-MMC to the Al-6061 counterface was confirmed in the bottom picture of Figure 4.44.

(B) SML BEHAVIOUR

A stable SML was never observed to form against the Al-6061 counterface. Mutual transfer between surfaces occurred, with no stable transfer layer forming on either surface. In contrast, all other counterface-composite combinations had stable Al-MMC transfer deposits form on the counterface surface at high pressure, from which smearing between like mixed composite surfaces resulted in the formation on a SML, as previously shown in Figure 4.21.

In Figure 4.43 two regions of surface mechanical mixing can be identified. On the left of the wear scar a composite SML has formed as a result of an adhered Al-MMC delamination on the counterface. The thick delamination caused increased interfacial separation and higher contract pressure this region. The result was smearing of the composite matrix and fracture of SiC in this region that formed an SML. On the right of the wear scar a SML has formed without mixed reinforcement present. Smearing and transferred of the Al-6061 counterface material to the composite surface has deposited a layer of mixed Al over the SiC reinforcement. As a result surface mixing occurs between smeared Al matrix contacts only. In conclusion, transfer only in direction (Al-MMC to the counterface) can be observed as a prerequisite for stable SML formation, and which was lost with a soft counterface was used.

(C) WEAR MECHANISMS AND PERFORMANCE

Both surfaces had similar wear morphologies at the low 2N load. Each surface was smeared and had significant ploughing during initial sliding. Large delaminations immediately occurred from both surfaces. The wear scar caused by 250m sliding contact is

shown in Figure 4.45. SiC were fractured through smearing despite the soft Al counterface (black regions in BSE image). As in the initial formation of a SML, mixed delaminations adhered to the counterface and created long smearing grooves through high contact pressures in these regions. A dominant wear mechanism was elongated smearing delaminations as shown in Figure 4.45. Mixing and smearing of particle Al debris into the surface was noticeable. The result was high oxygen content detected throughout the worn composite surface. The dominant wear mechanisms changed from "oxidative" small particle to "metallic" large smearing delaminations as the load was increased to 20N. Lower oxidation explained the proportional weight of debris at the lower load. Oxidation caused satisfactory performance at low load, on par with the 316ss. At high load large metallic delaminations caused the Al-6061 high wear and the worst wear performance.

(D) DEBRIS

At low load a very large weight difference existed between the collected debris and combined losses of the ball and block, Figure 4.45. This was found to be caused by small highly oxidized particulate debris produced by the wear couple. The agglomerated particulate debris not mixed into the surface and had a "fluffy cloud" appearance (Figure 4.45) and was not rounded into "snowballs" like with the steel counterfaces (Figure 4.317), but rather was loosely dispersed and mixed between surfaces.

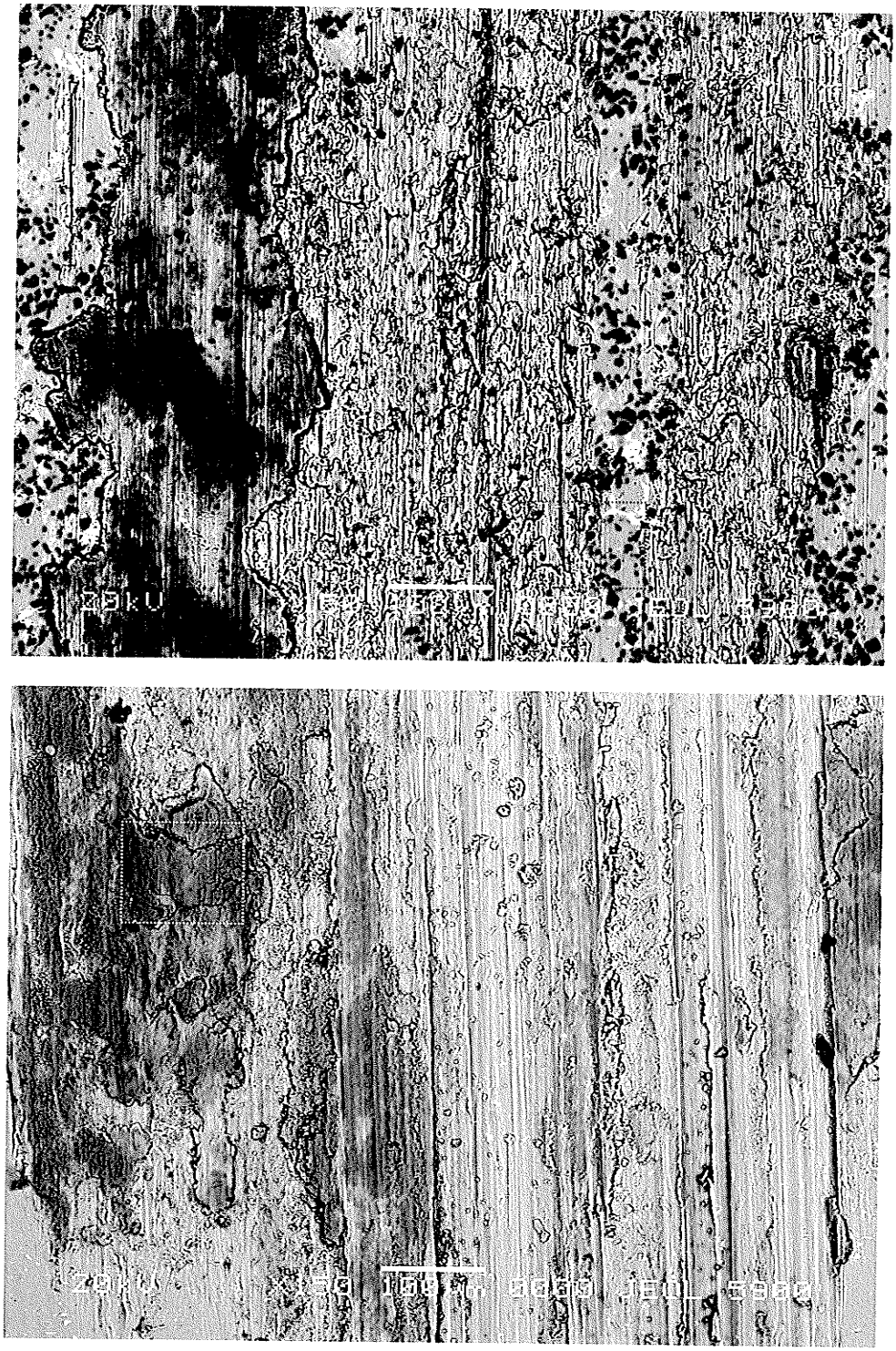

Figure 4.43 Al-6061 (BOTTOM) against the composite (TOP) 10m, 2N. Two distinct regions of SML formation are observed. On the left transfer of the Al-Si composite matrix caused a highly oxidized and smeared surface including crushed SiC. On the right transfer and back transfer of the Al-6061 matrix has caused a SML of the deformed matrix alloys overtop the reinforced composite surface.

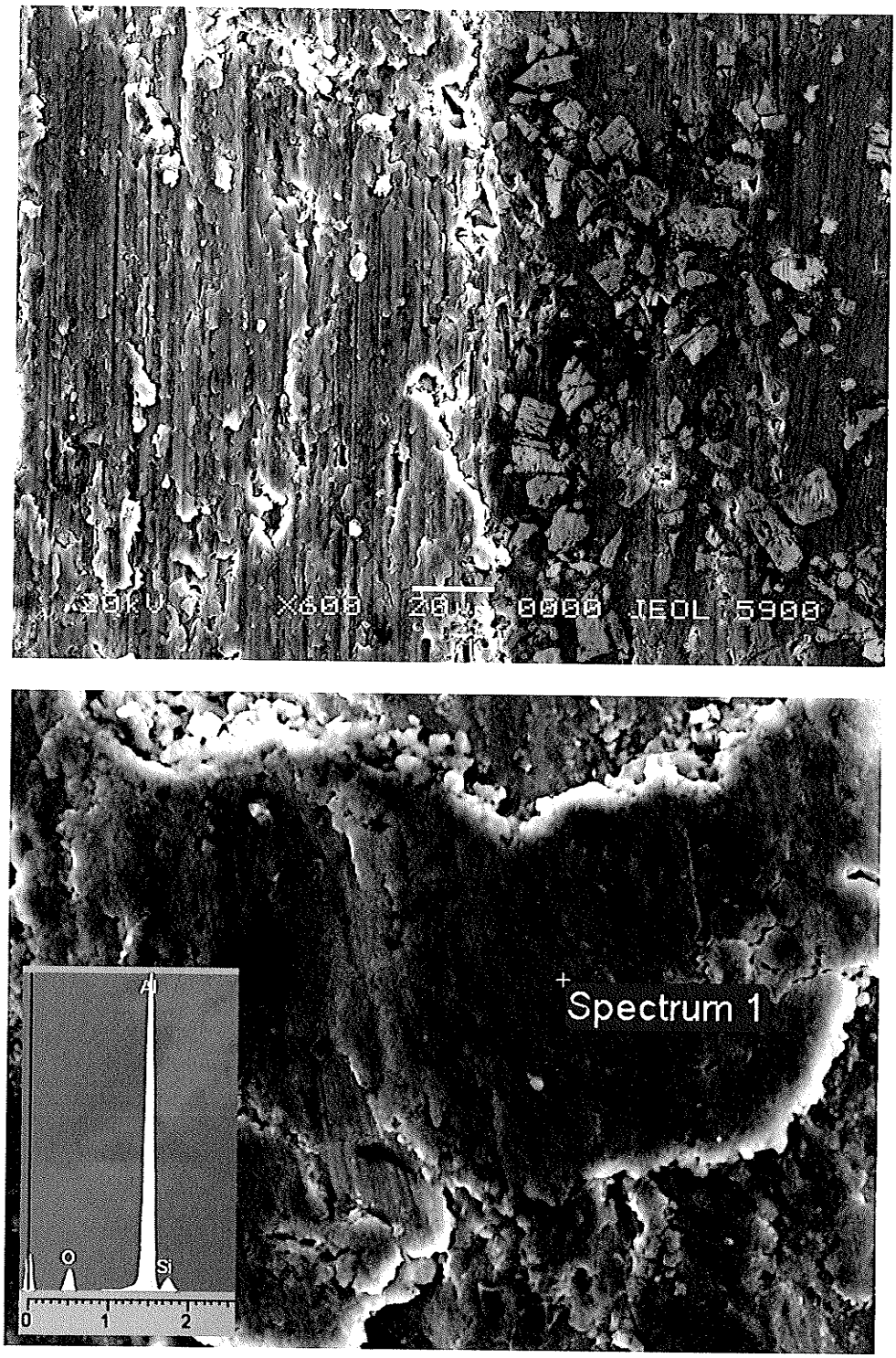

Figure 4.44 SEI images of the indicated regions in Figure 4.43. TOP: Smeared surface comprised of the Al matrix alloys deposited overtop the reinforced composite. BOTTOM: Transferred Al-MMC to the Al-6061 counterface containing fractured SiC particles.

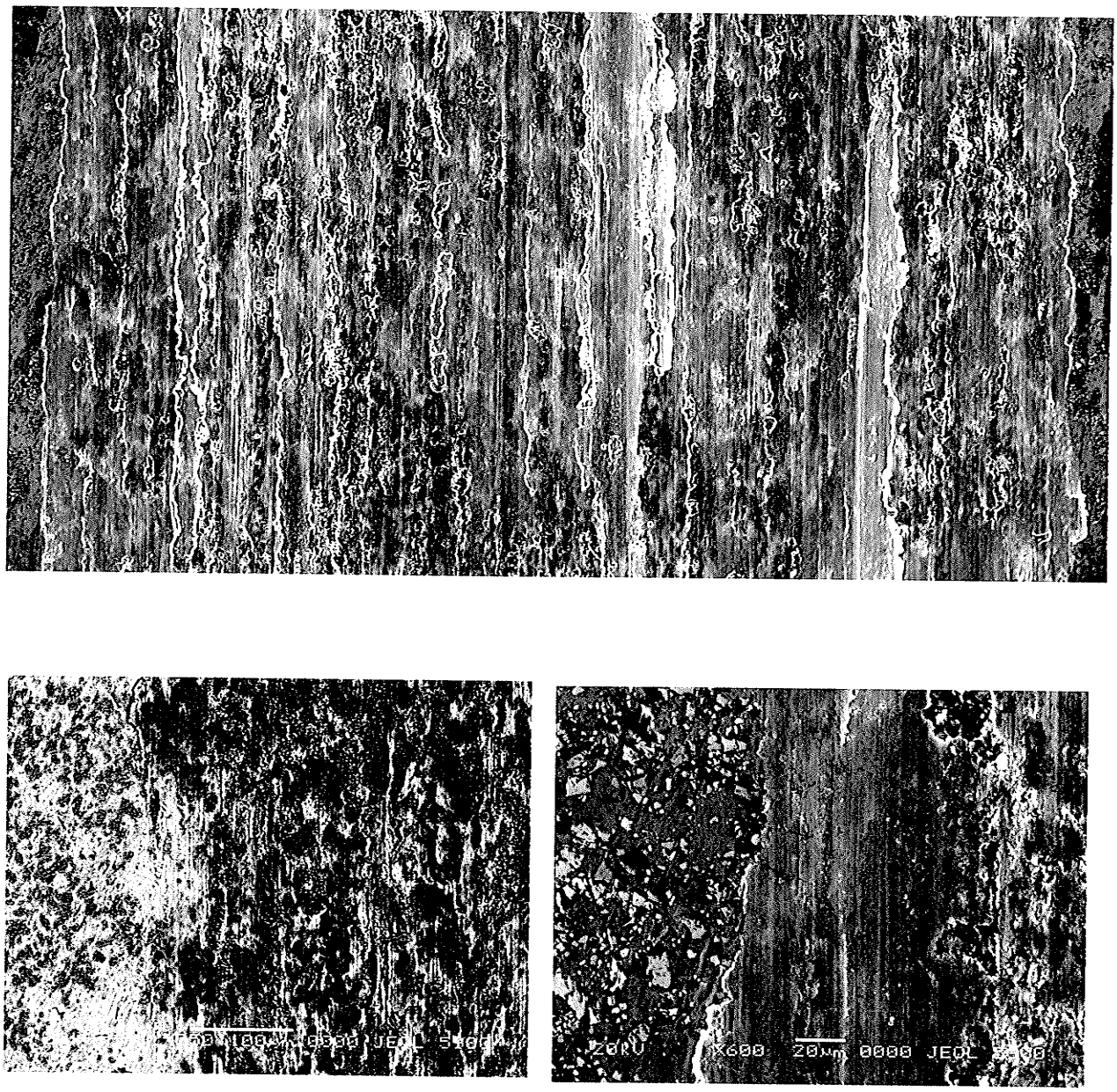

Figure 4.45 Wear of the composite surface against Al-6061, 250m, 2N. TOP: whole composite wear scar, 75X. Long smeared layer spalling is observed. BOTTOM LEFT: BSE image of the side of the wear scar showing high pulverization of the SiC reinforcement due to smearing. BOTTOM RIGHT: SE image that indicates that no SiC remains exposed at the surface.

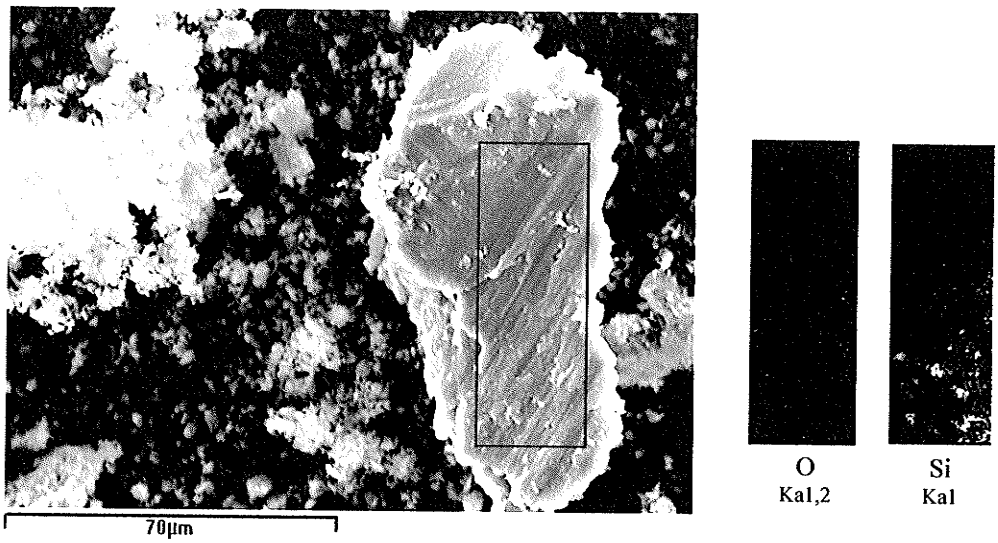

Figure 4.46 Debris from Al-6061 counterface against the 20%volSiC Al-Si composite, 2N, 250m. Elongated delaminations of the composite revealed by SiC present in x-ray mapping. The highly oxidized particle debris caused significant increase in weight of collected debris.

(II) K-MONEL VS. 316 STAINLESS STEEL

(A) SML BEHAVIOUR

Clear differences were observed in the high pressure mixing behaviour of the hard nickel alloy counterface compared to 316ss. At high pressures K-monel smeared the composite forming an uneven transferred Al-MMC deposit. In Figure 4.47, transfer of Al-MMC to the counterface at high pressure was patchy, thick, and not uniform. Large mixed Al-MMC "peaks" accumulated on the nickel alloy counterface, Figure 4.47, causing SiC in the SML to be crushed under the high local pressures. In contrast, 316ss amassed a large but uniform Al-MMC deposit on its surface, Figure 4.21, and inundating instead of crushing SiC particles, Figure 4.410. Comparing the SML wear scars of Figures 4.47 and 4.411 it is apparent that the stainless steel counterface caused more severe damage by a greater wear depth.

While adhesive transfer was unstable at initial pressures, little to no adhesive transfer occurred at low pressures. At low pressures only small mixed delaminations transferred to the K-monel counterface. Instead, at low pressures abrasion of the K-monel counterface dominated its wear. This again contrasted the 316ss where high adhesive transfer continued at low pressures, causing the sliding between mixed Al-contacts. As a result, high elemental transfer occurred for the K-monel at low pressures due to abrasion, while the 316ss experienced minimal transfer. This could be directly related to the higher work hardening rate of the stainless steel, which would cause a more rapid increase the steels resistance to abrasion, in comparison to K-monel. The work hardening effect on interface modification would have been exacerbated when considering that the ball counterface was the continuous contact surface, which causes it to experience a higher rate of work hardening based on the sliding geometry alone. The overall conclusion was that at any applied pressure adhesive transfer of mixed Al-MMC to the K-monel counterface was less stable.

(B) TRANSFER AND MIXING

K-monel was chosen to examine how a different a counterface metal can affect transfer and wear. It was observed that despite having similar hardness to the 316ss, Table 3.4, greater abrasion caused transfer of very high transfer Ni and Cu transfer to the Al-MMC surface, BSE image of Figure 4.48. While 316ss caused rarely above 5 wt% mixing randomly in the surface, a uniform mixed surface was formed against the K-monel counterface with up to 30 wt% of the nickel alloy elements present. It was therefore determined that K-monel counterface can form a MML against the composite under the

current sliding conditions. However, accumulation of hard particles in the mixed surface layer still did not occur as found for unidirectional studies [33,34]. This allowed the importance of debris mixing to be established in relation to MML formation. For the steel counterfaces, it was concluded that accumulation and compaction of hard debris on the mechanically mixed surface was sufficient to cause dominant abrasion of the steel counterface under unidirectional sliding, resulting in Fe micro-particle transfer and MML formation. However, beneficial accumulation and compaction of hard debris did not occur under reciprocal sliding, causing the *in situ* hardness increase of the composite surface to be primarily due to strain hardening effects. Consequently the dominant wear mechanism did not transcend from Al adhesion to harder Al-MML surface micro-abrasion of the steel. However, the hardness of the surface mixed layer without debris mixing was sufficient to cause dominant abrasion of the K-monel, resulting in Ni-Cu micro-particle transfer and MML formation. Since micro-abrasion of the K-monel occurred without significant debris mixing the overall wear rate was worse at the higher load, causing the MML phenomenon to not be particularly beneficial.

(C) Wear Mechanisms and Performance

The MML formed increased the mass of the Al-composite at the 2N load due the nickel alloy transfer, Figure 4.41. After 250m of sliding small MML adhesion-delaminations were observed as the dominant wear mechanism of the composite.

At the high 20N load larger mixed adhesion delaminations were fractured from the MML surface. This caused greater weight loss from of the composite by adhesion-delamination and increased abrasion of the counterface, reducing overall wear performance.

In comparison, the 316ss counterface had significant adhesion of Al-MMC on the contact surface at the 20N high load, preventing its abrasion. The 316ss counterface therefore experienced less wear, causing a lower overall weight loss from the sliding system. Observing wear scar depth, Figure 4.42, the K-monel counterface caused less surface damage compared to the 316ss. Abrasive wear of the K-monel and MML formation caused a uniform wear scar, while a very rough wear scar was produced by patchy adhesive delaminations against the 316ss counterface.

(D) DEBRIS

There was much less particle debris produced against K-Monel due to less transfer and back transfer events when abrasion of the counterface was dominant. K-monel formed large particle agglomerations in comparison to stainless steel, Figure 4.410. Ni and Cu from the K-monel counterface are intimately mixed into the debris indicating that micro-abrasion of the mixed surface was an active mechanism in transfer and mixing of the composite surface. Delaminations of mixed material produced and were larger than the small round agglomerations found against the 316ss counterface. This is in agreement with section 4.32(i) which found larger debris sizes for MML conditions.

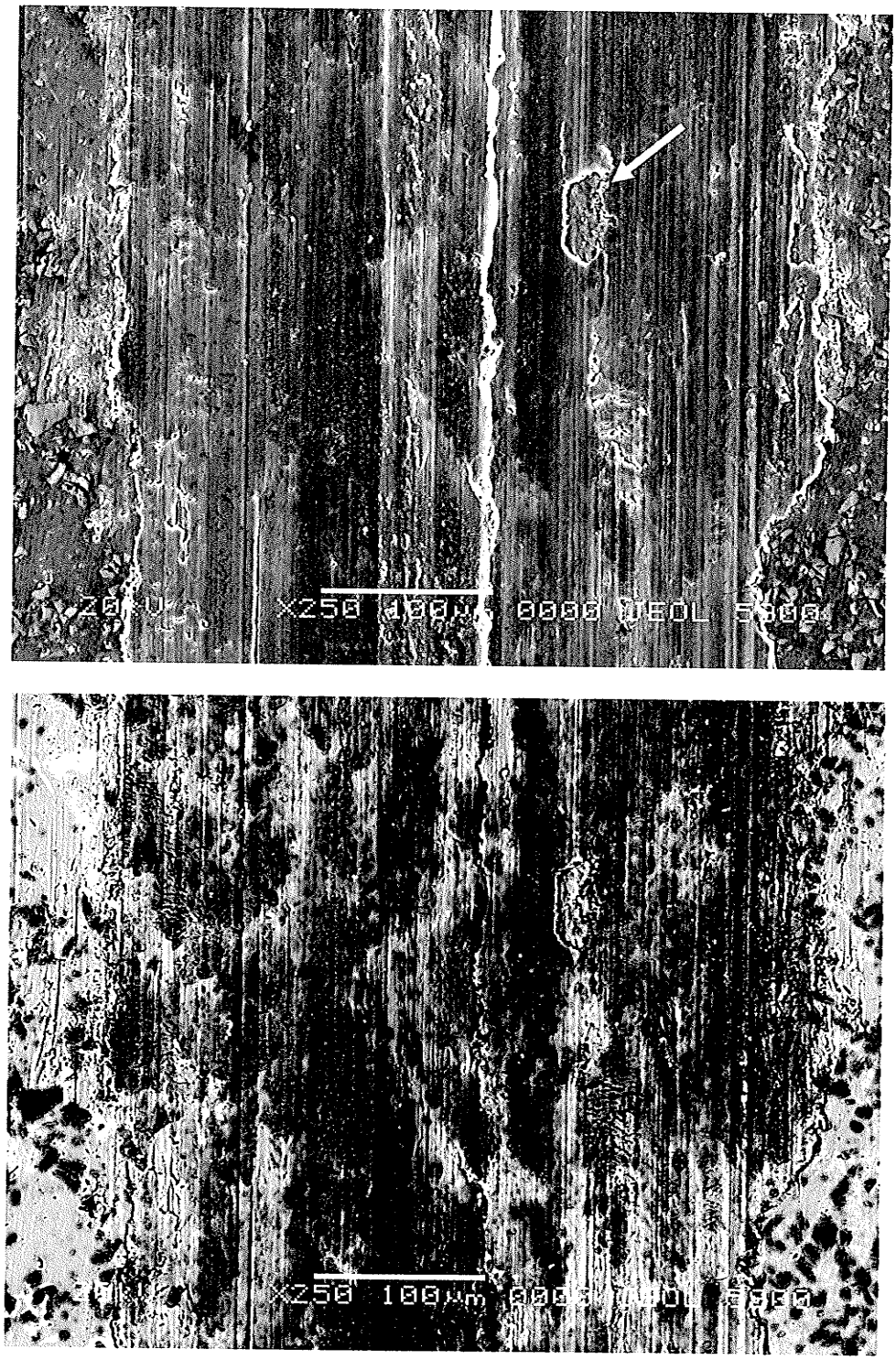

Figure 4.47 SML behaviour of the composite against K-monel, 10m, 2N. TOP: SE image showing the SML groove formed by a thick mixed Al-MMC transfer deposit on the nickel alloy counterface (figure 4.48). The SML was thin (note delamination indicated by arrow). BOTTOM: BSE image showing that mixing, fracture of SiC, and oxidation occurred in on the mixed surface

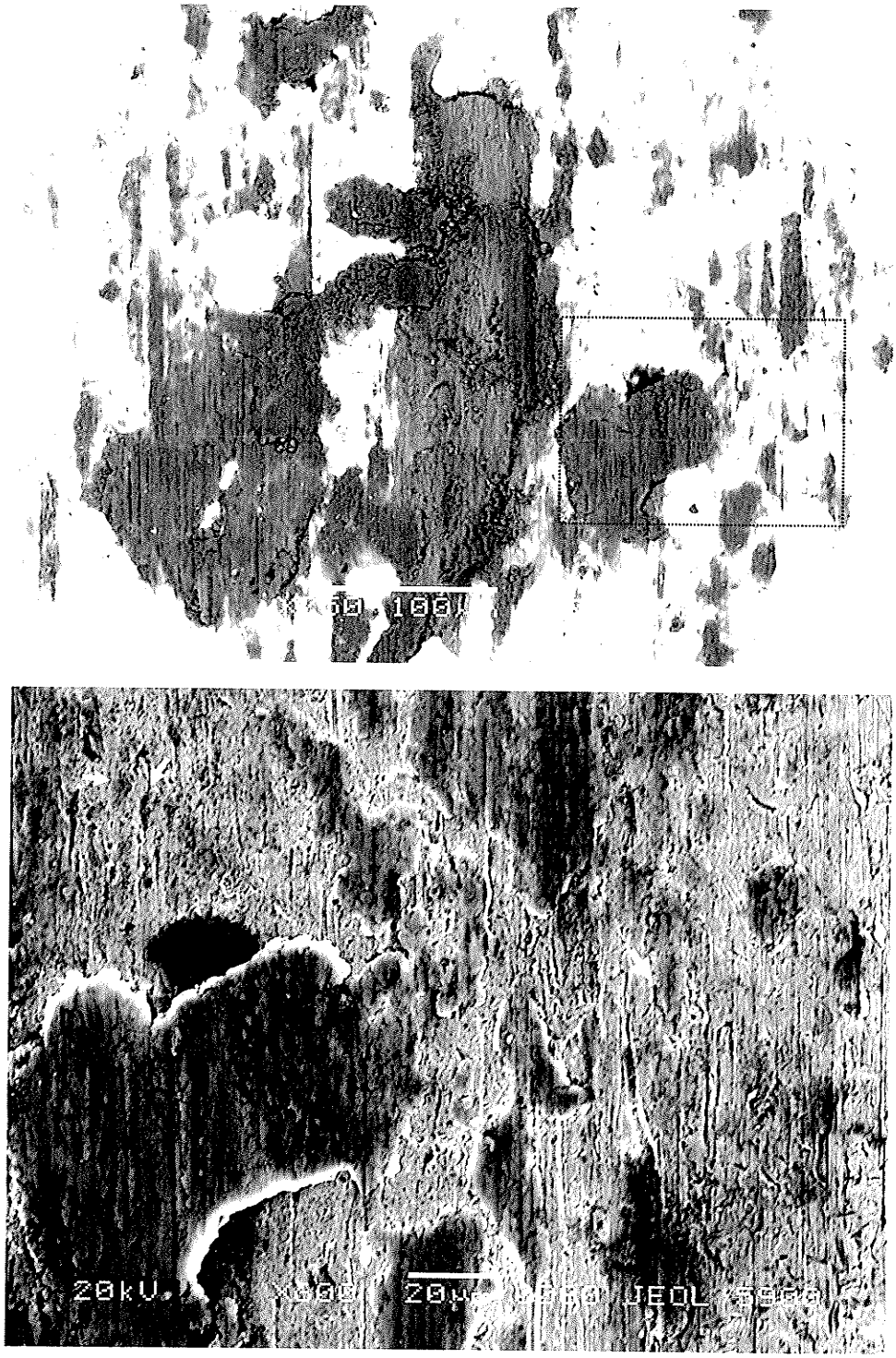

Figure 4.48 High pressure adhesive transfer to K-monel, 10m, 2N. TOP: BSE image of the uneven wear deposit on the counterface. The transferred Al-MMC appears grey on the Ni-Cu ball. BOTTOM: SE image has small delaminations (arrows) and abrasion visible on the K-Monel surface. Initial Transfer to the K-Monel takes the large mixed patches, which were nearly completely removed at lower pressure or longer sliding distances. Compare top image to Figure 4.21

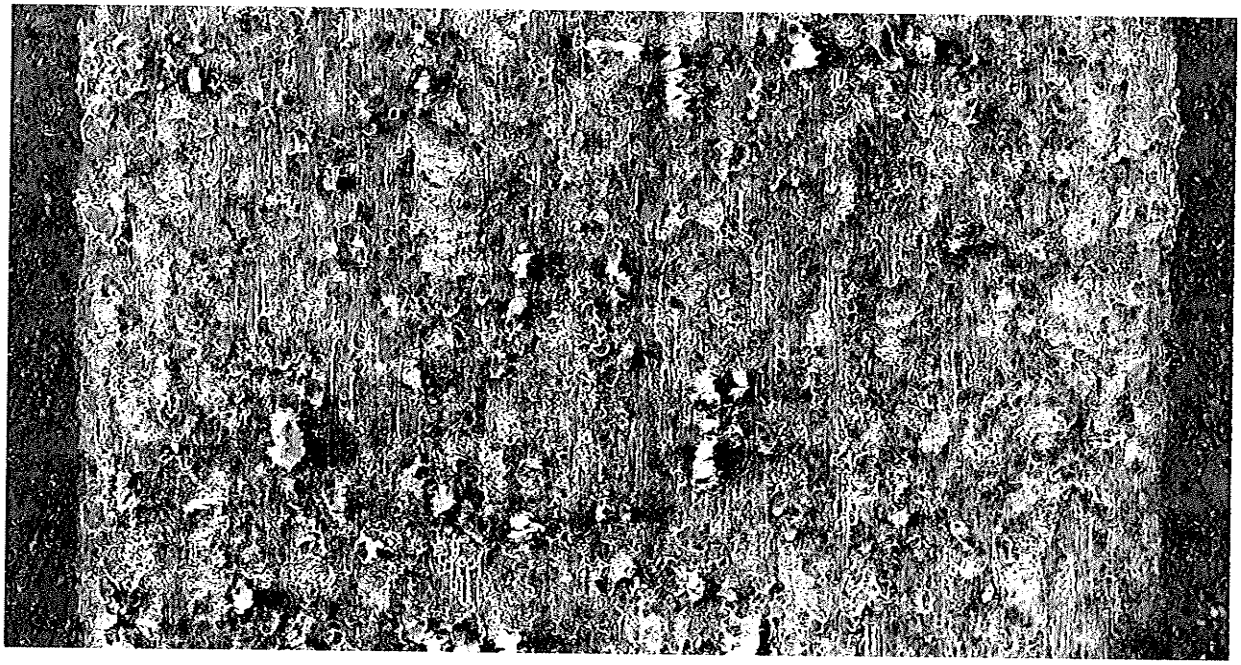

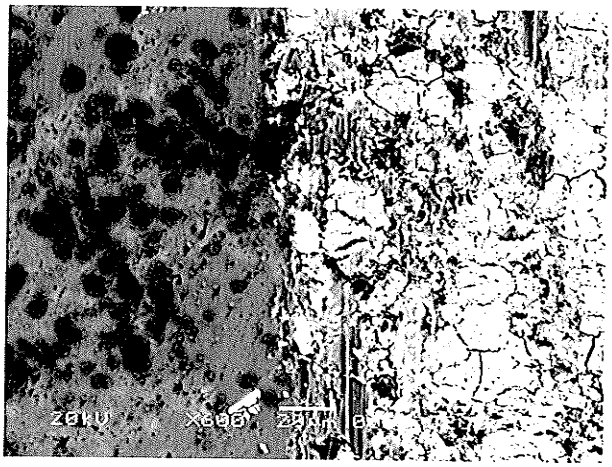

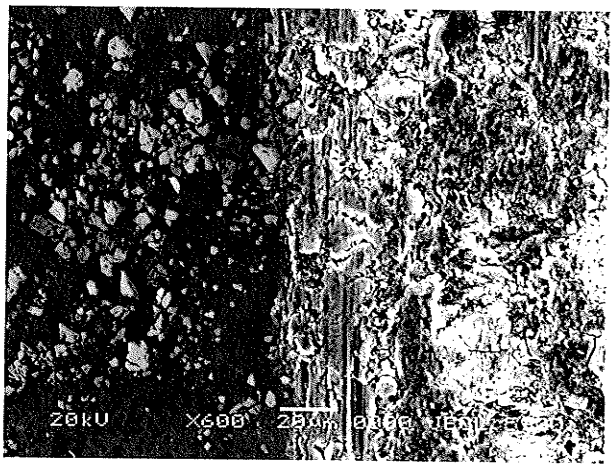

Figure 4.49 Wear of the composite surface against K-Monel, 250m, 2N. TOP: SEI image of whole composite wear scar, 75X. Very small mixed delamination pits and abrasion are the most common sources of wear. BOTTOM LEFT: BSE image of the side of the wear scar showing high amount of transferred Ni and Cu from the counterface. BOTTOM RIGHT: SE image indicated deformed Al-matrix debris has agglomerated and partially compacted to form the wear surface.

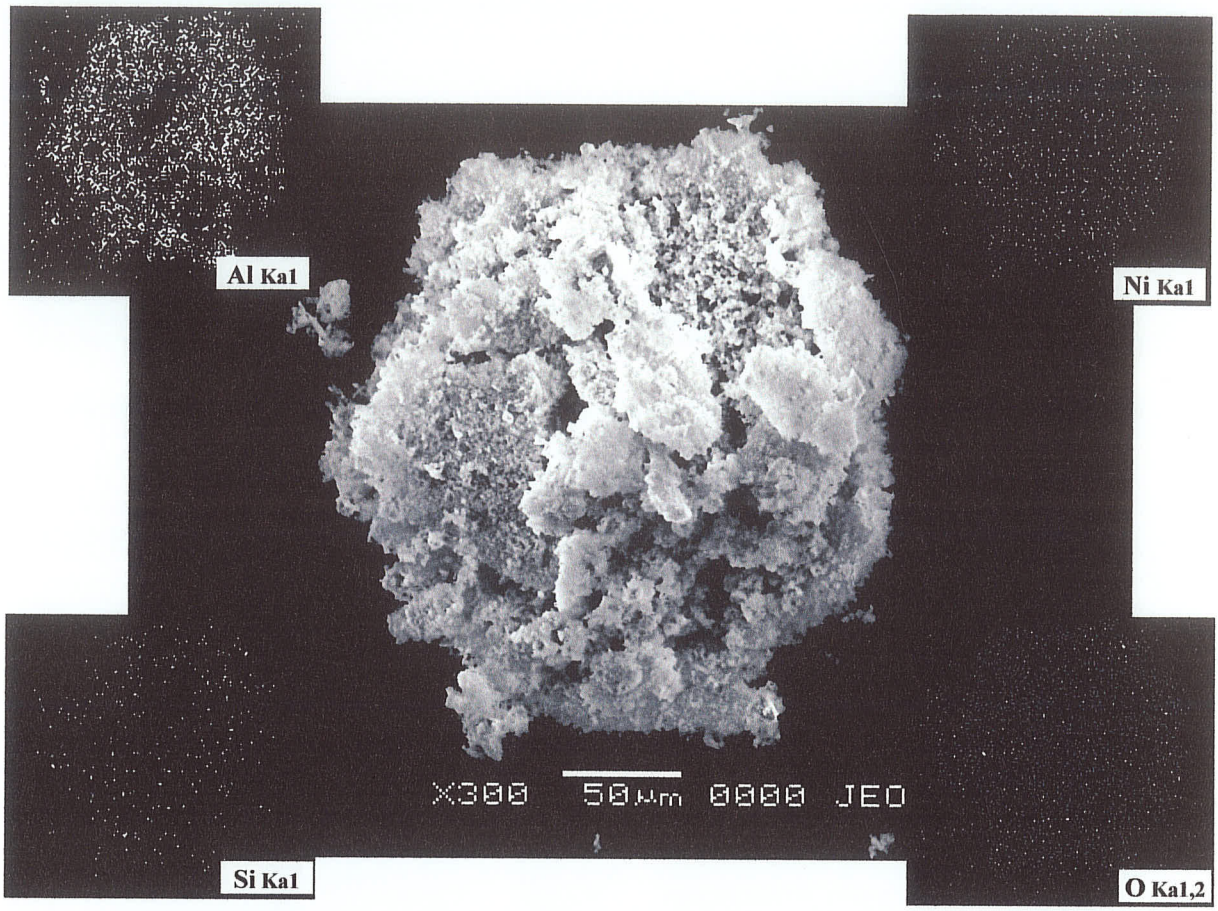

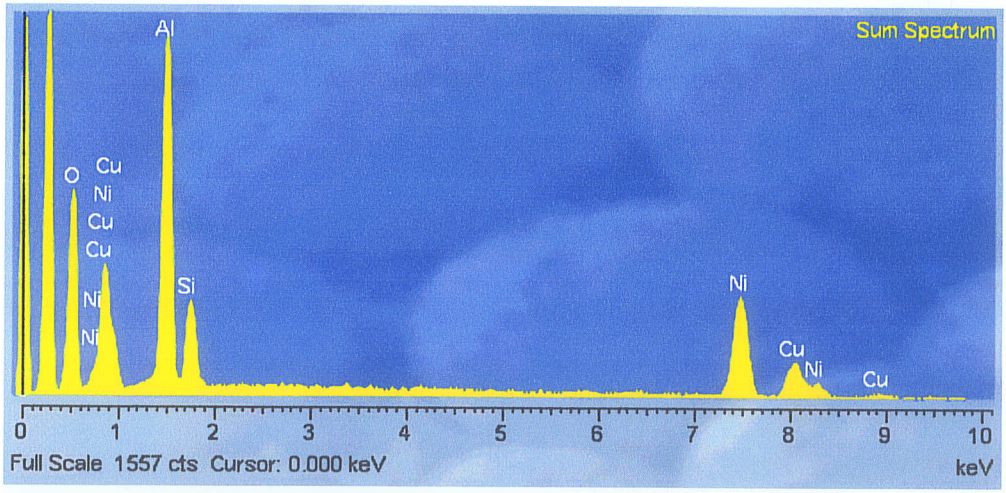

Figure 4.410 X-ray Mapping of debris agglomeration formed by Al-20vol% SiC against K-Monel, 250m, 2N. The size of the agglomerations were much larger than formed by wear against 316 stainless steel (Figure 4.217)

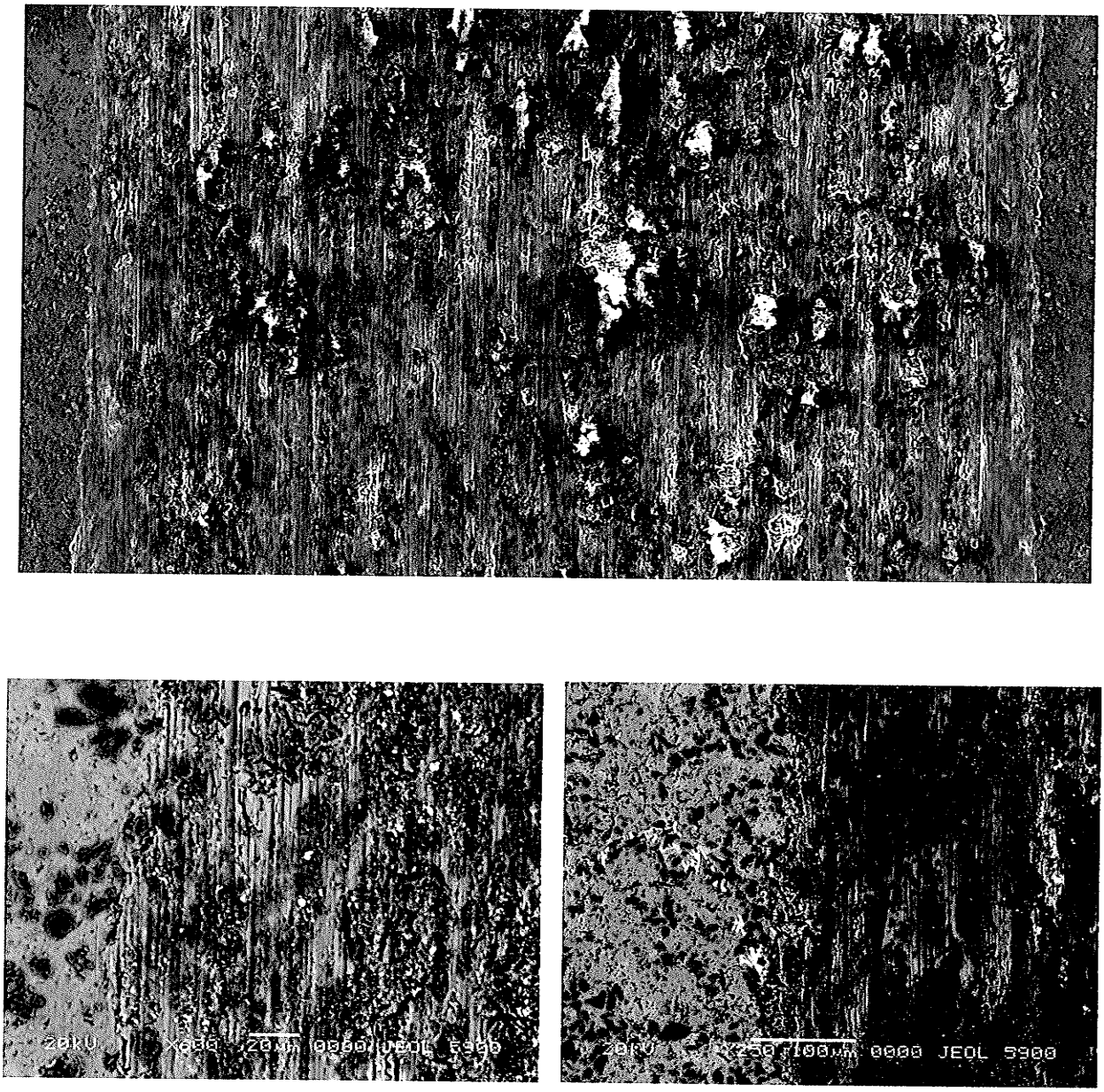

Figure 4.411 Wear of the composite surface against 316ss, 250m, 2N. TOP: whole composite wear scar, 75X. Ploughing and delamination dominated wear. Surface interaction remain between mixed composite contacts at low load. BOTTOM LEFT: BSE image of the for low 2N applied load, showing mixing of a few Fe particles. Whole SiC particles remain under the smeared surface. BOTTOM RIGHT: BSE image for the high 20N applied load, showing a black area due to smearing and pulverization of SiC. The images indicate that a minimum pressure between 5-10 MPa was required for fracture of SiC in the composite surface.

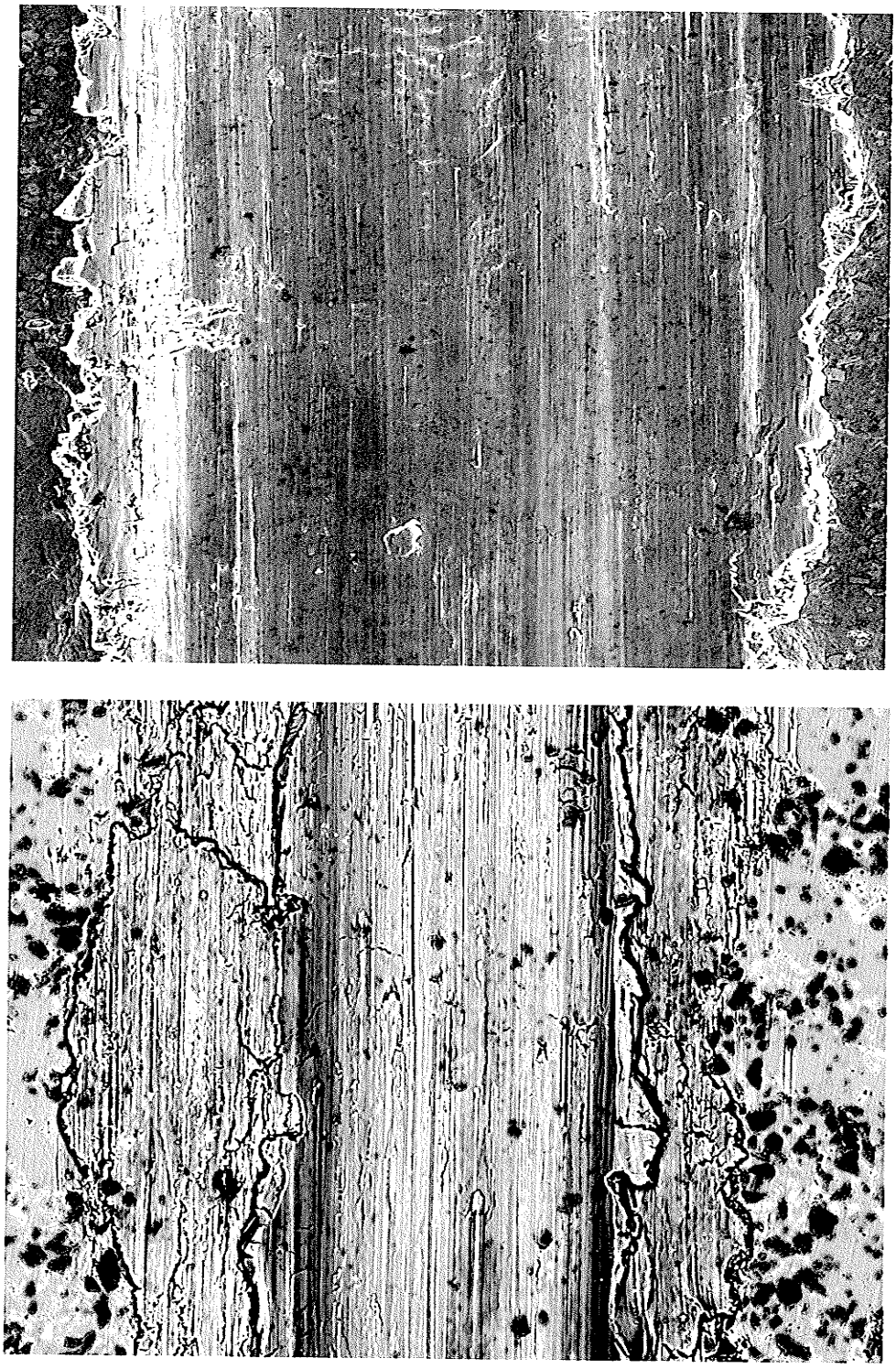

Figure 4.412 SML behaviour of the composite against 316ss, 10m, 2N. Wear scar is deep caused by a thick uniform Al-MMC transfer patch. Smearing of the matrix occurred inundating SiC particles without instead of fracturing. Counterface image was similar to the top picture of Figure 4.21.

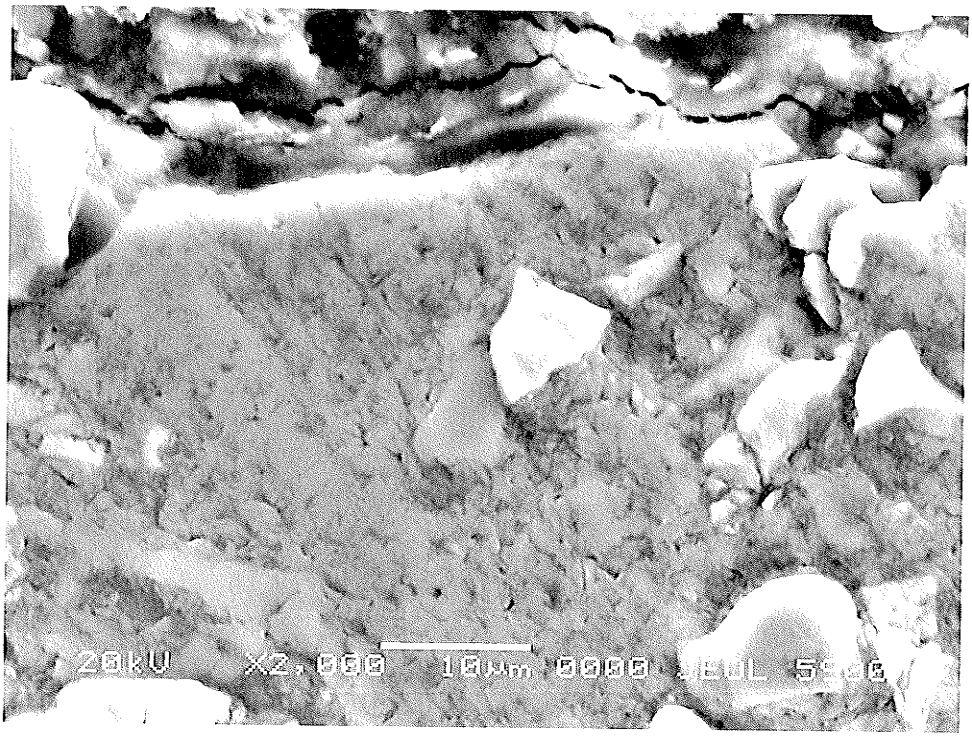

Figure 4.412 MML which contains uniformly mixed Ni and Cu from K-monel counterface. Surface is about to delaminate.

(III) CERAMICS VS. 316SS

(A) SML BEHAVIOUR

The surface mixed layer formed by wear of the composite against Al_2O_3 ceramic was very similar to that formed by 316 stainless steel, Figures 4.412 and 4.414. Both materials developed thick uniform Al-MMC transfer patches the width of the wear scar, causing even SML formation. This confirmed that metallic compatibility was not a factor in adhesive transfer to the counterface. The same transfer behaviour was observed against Si_3N_4, except that the harder ceramic allowed a thicker transfer layer to become stable. As a result the local high pressure of the mixed Al-MMC contact extruded a deep groove down the centre of the wear scar.

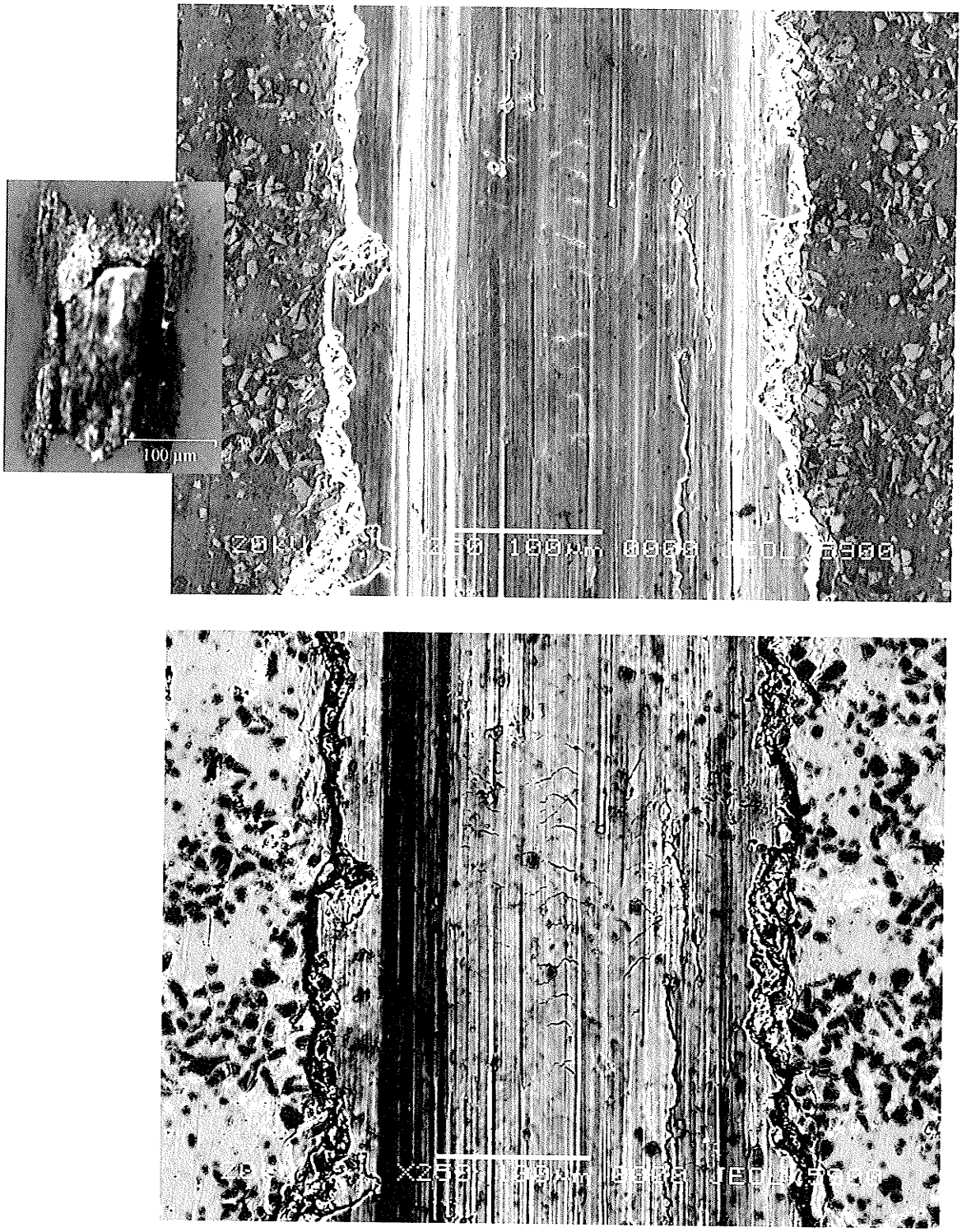

Figure 4.414 SML behaviour of the composite against Al_2O_3, 10m, 2N. The wear scar is very similar to that produced by 316ss, Figure 4.411. Inset shows optical image of the counterface deposit, which has wide and uniform.

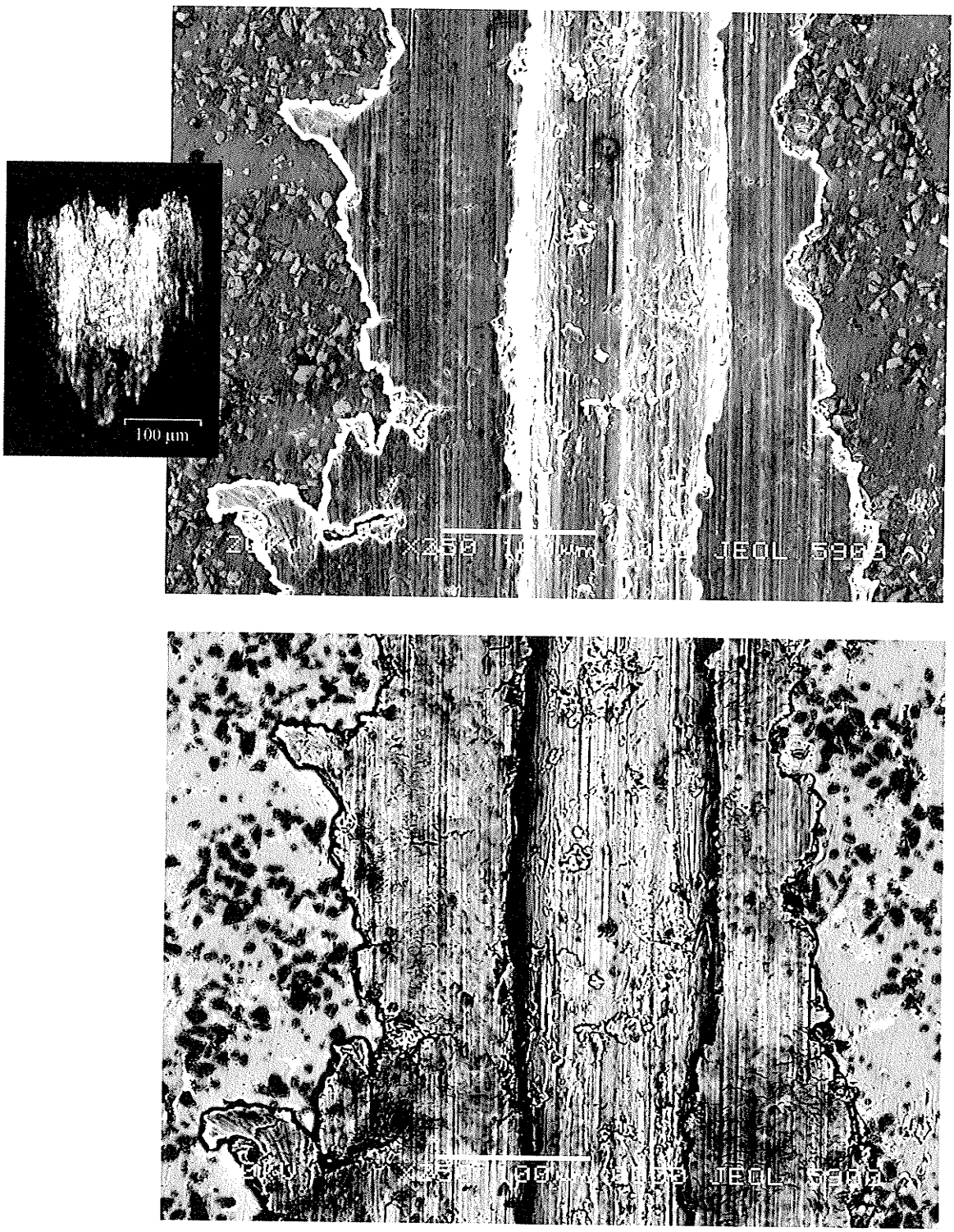

Figure 4.415 SML behaviour of the composite against Si_3N_4, 10m, 2N. The harder ceramic had caused a smaller and thicker transfer patch to form compared to Al_2O_3 (inset). This caused severe damage with deep grooves in the center, extrusion from the wear scar and smearing delamination wear due to high pressures and strain.

(B) TRANSFER AND MIXING

Transfer and mixing of either ceramic did not occur due to the thick mixed adhesion layer that remained stable on the surface. At low pressures transfer of the composite to the adhered Al-MMC surface on the counterface continued and the transfer amassed did not decrease in thickness, causing an increase in the mass. At high pressures minimum thickness of the deposit uniformly covered the surface, preventing direct contact of the ceramic. A previous study using a block of Si_3N_4 against a 20vol%SiC Al-Composite observed that a transfer layer of smeared composite on the ceramic wear surface formed. As a result, wear occurred between the composite and a transferred composite film, not directly with the ceramic counterface [79]. Transfer stability may have been promoted by elastic restraint of transferred mixed Al-MMC due to the higher modulus elasticity of the ceramic counterface acting as a substrate.

(C) WEAR MECHANISMS AND PERFORMANCE

A comparison of wear scars between the steel and ceramic counterfaces after 250m of sliding is shown in Figure 4.416. The Si_3N_4 counterface caused large delamination debris to adhere to its surface and causing a very rough wear surface to develop, Figure 4.42. Increased adhesion to the Si_3N counterface allowed the debris to remain in the interface which caused a lower track depth due to greater surface separation. However the high contact stress of the adhered delamination debris caused greater surface damage overall, Figure 4.42. Al_2O_3 did not accumulate delamination debris but rather maintained a uniform transfer layer.

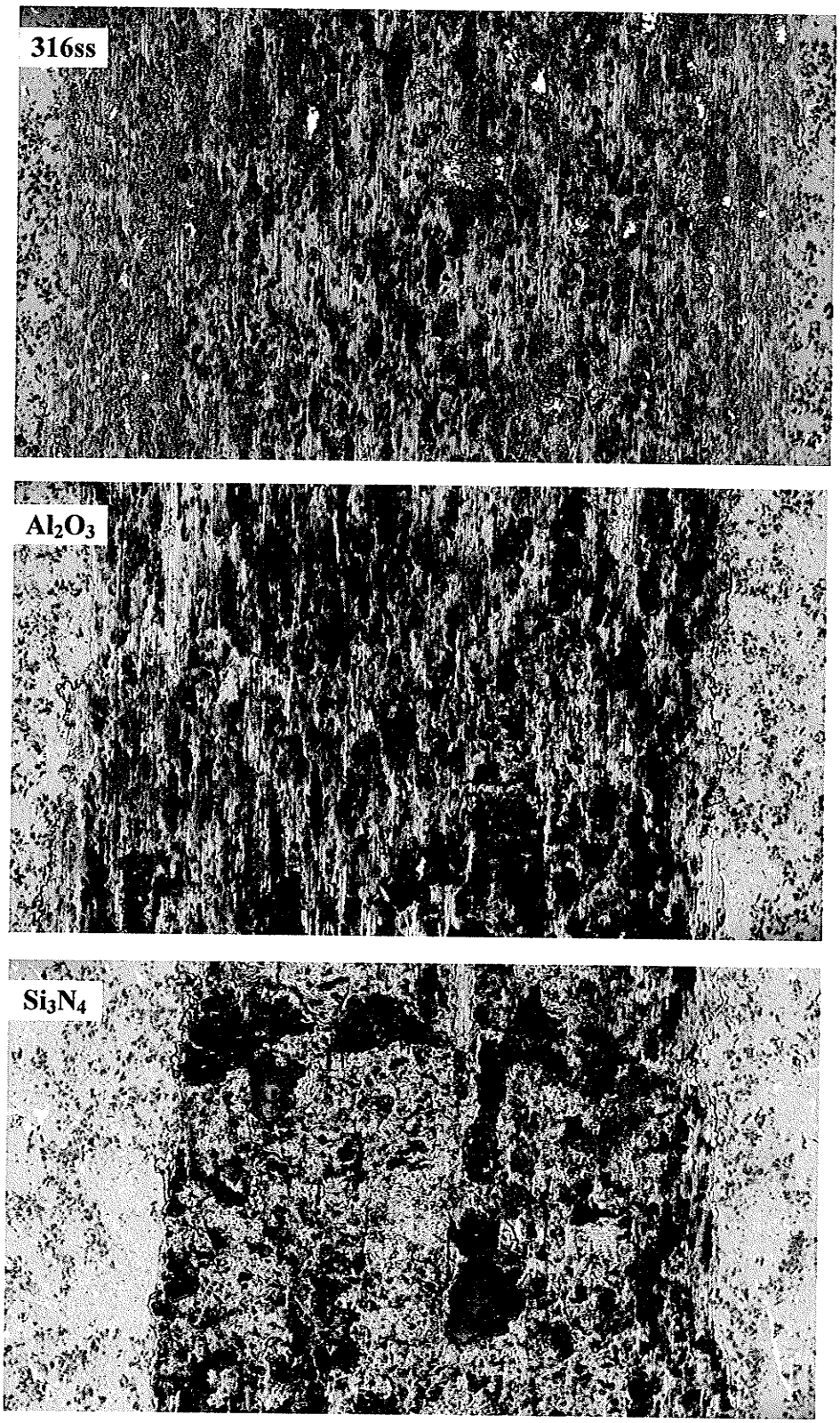

Figure 4.416 BSE images showing how oxidation and crushed SiC distributed for the different counterfaces. 2N, 250m. The large patches of mixed and oxidized Al-MMC (black) agglomerated against the Si_3N_4 counterface causing increased wear as compared to the uniform mixed surface from Al_2O_3. Wear occurred between mixed Al-on-Al contacts resulting in smearing delamination wear and ploughing. Ploughing was highest against the patchy 316 transfer material and surface debris compaction was greatest against Si_3N_4.

The result was wear dominated by smearing delaminations and high transfer and back transfer of mixed Al material. The thick transfer layer on Al_2O_3 concentrated surface ploughing, causing worse surface damage when compared to the patchy adhesive transfer that occurred with steels. Overall Al_2O_3 was considered to be the best choice of the two ceramic counterfaces under the current sliding conditions

(D) DEBRIS

Debris consisted of smearing delaminations and aggregations of small particulate debris, as found against steel counterfaces. Oxygen content was found to increase in some aggregates. These two debris morphologies were considered a product of mixed Al-on-Al contacts during sliding.

4.45 SIC INTERACTIONS

The counterface has a direct influence on the surface interactions that will occur during wear. In the absence of a mechanically mixed layer the counterface asperities can contact 1) the metal matrix, 2) protruding SiC particles or 3) Si and intermetallics in microstructure. These interactions can be significantly different depending on the counterface. For example, contact of an Al-6061 asperity with a composite matrix asperity can result in small adhesive transfer between surfaces, while contact of the Al-6061 asperity against a reinforcement particle can lead to its abrasive removal. It was observed that the steel counterface can pull out SiC particles due to the particles mechanically anchoring into the steel surface [53]. Hard contact points for aluminum oxide and silicon

nitride counterfaces against SiC may promote particle fracture. In all cases of counterface contact, the size of the SiC reinforcement is important in the surface interactions that would result. SiC particles in the range of 0.25 to 10μm can be considered to be in the range of asperity contact sizes for most metal counterfaces. SiC particles greater than 10 μm would increasingly dominate the contact the composite would make with the counterface. Hard particles acting as asperities under most sliding forces would only experience small elastic deformation, and would fracture before plastically deforming, causing the Tabor model [97] of asperity junction growth to no longer apply. Potential SiC interactions are shown in Figure 4.417. SiC fracture readily occurs except for very light loads during sliding wear against ceramics (CASE D) and it becomes unclear how the fractured SiC will be reinitiated into local contacts. Current testing established that the hard ceramic or hard steel counterfaces would mix in debris and be removed from the interface as readily as it was pressed into the surface, causing no net gain of hard particles. Pressed in and fractured SiC occurs in the formation of a SML (CASE B); while exclusive surface re-deposition of fractured SiC debris occurs in the formation of a MML (CASE C). In the latter case greater small particle SiC-SiC interactions are occurring to lower overall wear rates. Therefore CASE C is considered to be the most desirable case of SiC interaction. Removal of SiC from the interface due to fracture (CASE D) can result in greater occurrence of aluminum matrix-counterface contact and, to be expected, higher rates of wear.

A goal for improved wear resistance of both the composite and counterface is to prevent the generation of abrasive wear debris. Therefore, the soft 316 steel counterfaces which had potential to cause increase particle pull-out and therefore made a worse choice for counterface compared to the hard steel, which experience less particle penetration and

more surface mixing. Increased roughness of the worn Al-SiC surface was observed against the Si_3N_4 counterface as compared to the Al_2O_3 counterface. This may be explained by the harder ceramic pulverizing SiC which abrade the original composite surface as third body debris. The highly mixed debris that contacted the hard ceramic counterface was then at a higher hardness than the composite surface and caused severe ploughing before leaving the interface. The aluminum oxide had a relatively smooth wear scar appearance, possibly due to more elastic and inundating interactions with the SiC particulate (CASE E).

(I) DUCTILITY OF COUNTERFACE

1) At low-speed particle pull-out occurs due to mechanical anchoring into the counterface surface (CASE B) for intermediate hardness counterface metals. This corresponds to discontinuous ploughing tracks with embedded SiC particles on the stainless steel counterface, Figure 4.31. For this to occur, the counterface must be soft enough to allow deep enough penetration of the particle however not so soft that the particle causes direct abrasion. The Al-6061 counterface experienced direct abrasion without SiC pullout because it was too soft. K-Monel also experienced the abrasive nature of SiC more than the potential benefit of the hard particle "switching sides". The 316 stainless steel however had sufficient hardness to mechanically anchor the SiC particles causing abrasion of the *composite*. Here we see a transition in wear behaviour may be occurring around 30 HRC. The steel counterfaces experienced SiC interactions cases A,B, and C most readily with penetration and pullout decreasing for the harder steels.

2) At higher speeds impacted SiC particles coherent in the Al-matrix offer a greater resistance to particle pull-out. Therefore, for the same applied contact stress and hardness of the counterface, higher sliding velocities can allow greater composite resistance to wear by CASES C and E. Therefore, wear resistance is increasing due to increased SiC ploughing and abrasion of the *counterface*. However, impact between a SiC and very hard ceramic counterfaces does not allow for a preferential increase in counterface abrasion leaving two options for the interaction, SiC pulverization or elastic resistance to the contact pressure. As observed under dry sliding wear, the contact stresses are too great to allow for elastic resistance of reinforcement particles, hence the end result is a deposited layer of smeared and mixed matrix by comminuted SiC continually fractured in the interface.

3) As can be seen by the above description, a lot depends upon the hardness of the counterface. The immediate question is: what occurs for an intermediate counterface hardness between the soft aluminum, nickel, and stainless steels and the hard ceramics? It has been established that the hard tool steels between 58-68 HRC make the best counterface paired for overall tribo-system wear performance. A explanation to this exists again in the penetration potential of the SiC particles. For the harder steels SiC particles cannot penetrate as deeply into the matrix material. Therefore during sliding the particles partially penetrate the surface and fracture causing fragments to remain on both surfaces during continued sliding. This causes the observed wear surface of thin abrasion lines [79], smaller than the original SiC particles. Since the particles are mixed more evenly between surfaces a more uniform transfer layer may be allowed to form. This causes a more stable

mechanically mixed layer, and offers a possibility as to why higher on average transfer of the Al/SiC mixed surface occurred for the harder steel counterface.

Overall, the observed changes in composite wear, counterface wear, and material transfer could be excellently correlated with the ability of SiC particles to penetrate (and mechanically interlock) into both surfaces. As a first approximation of particle penetration a Vickers indentation may be offer insight to the hardness ranges that have the greatest chance of 1) particle pull-out, 2) particle penetration and fracture and 3) particle comminution.

(A) ABRASIVE TRANSFER

The initial stages of elemental transfer could be observed for the short 100 cycle sliding distance and low load, where the SiC on the polished surface were directly exposed to the counterface, Figures 4.417 and 4.418. All three metal counterfaces, Al-6061, K-Monel, and 316ss, were transferred to the composite surface. Resistance to abrasion by SiC was increased with increased counterface hardness. Therefore as expected, more abrasive transfer occurred for Al- 6061 and the K-Monel counterfaces, as compared to the harder 316ss stainless steel. Decreased abrasive transfer was similarly observed for the harder 52100 counterface compared to the 316ss in Section 4.14. Very fine abrasion lines could be seen on the Al_2O_3 and Si_3N_4 counterfaces.

(B) ADHESIVE TRANSFER

Observing which surfaces were smeared in the SEI pictures at 100 cycles it was apparent that a mixed Al-Si surface layer on the composite by adhesive transfer resulted in smearing and ploughing wear.

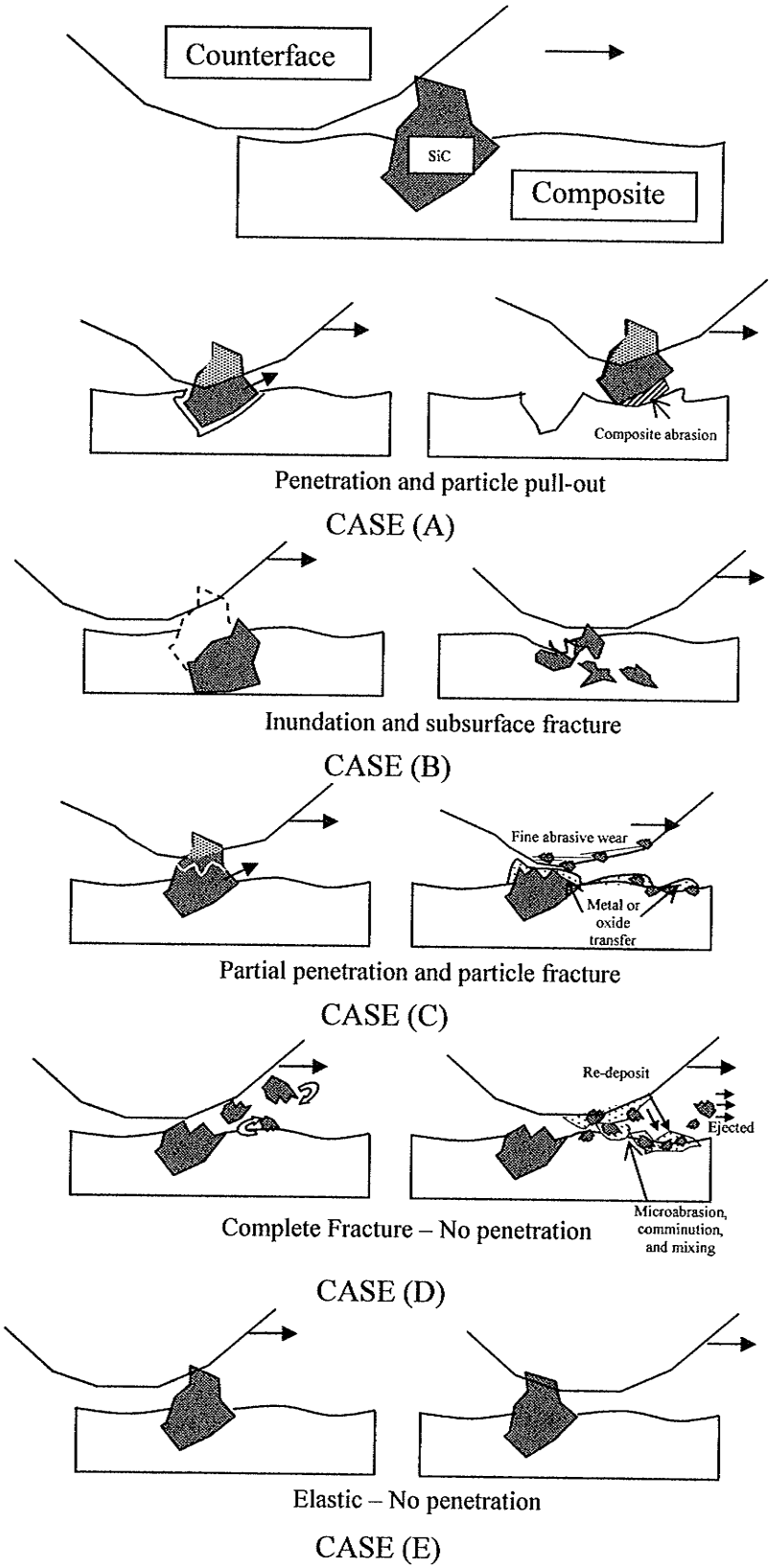

Figure 4.417 Possible outcomes from counterface interaction with SiC particles.

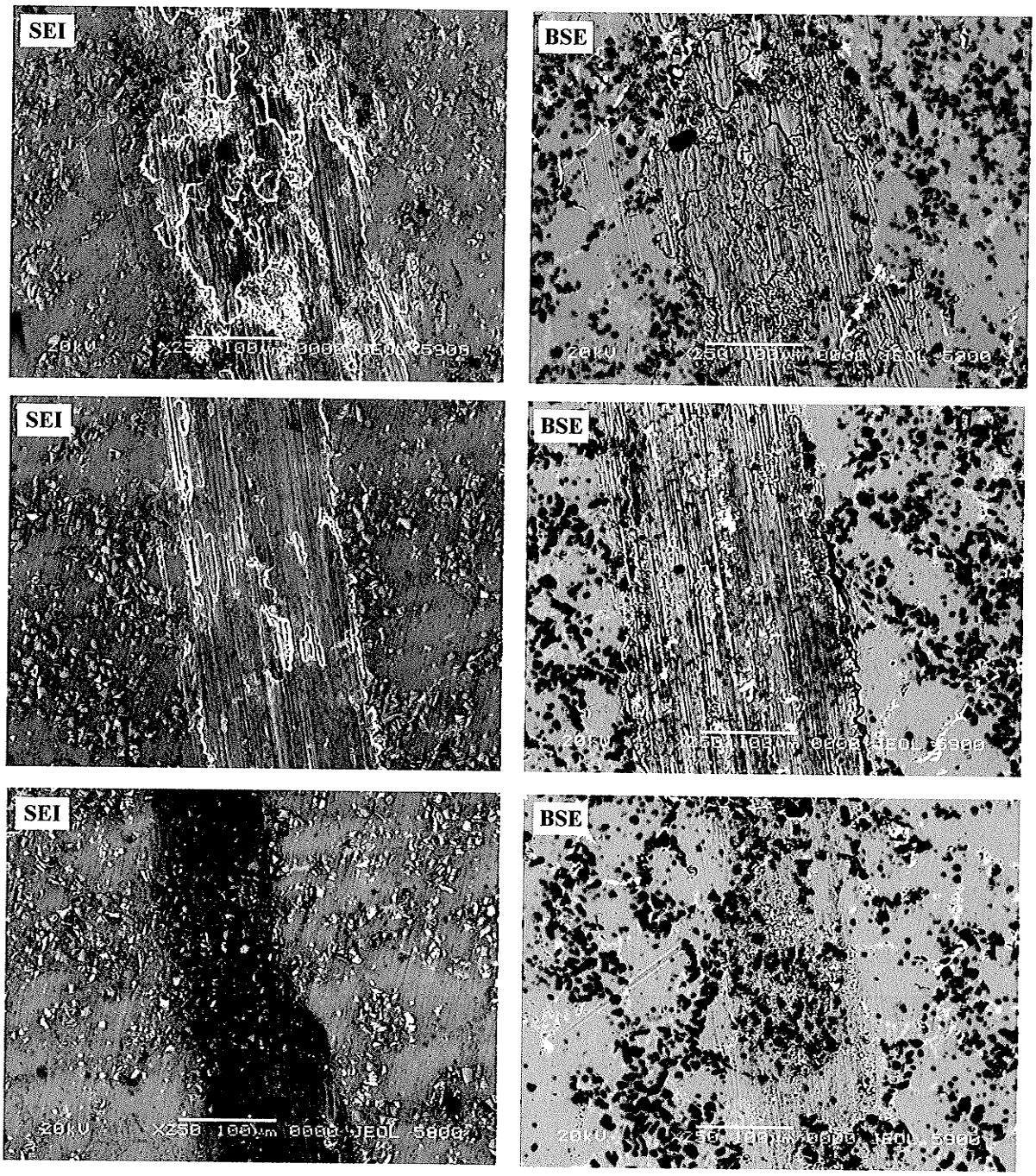

Figure 4.418 The composite surface wear scars under low pressure conditions (2N) after 100 cycles (≈ 1m) sliding. Tests were intended to indicate SiC particle interactions. The counterfaces are: TOP - Al-6061, MIDDLE - K-Monel, BOTTOM - 316 stainless steel.

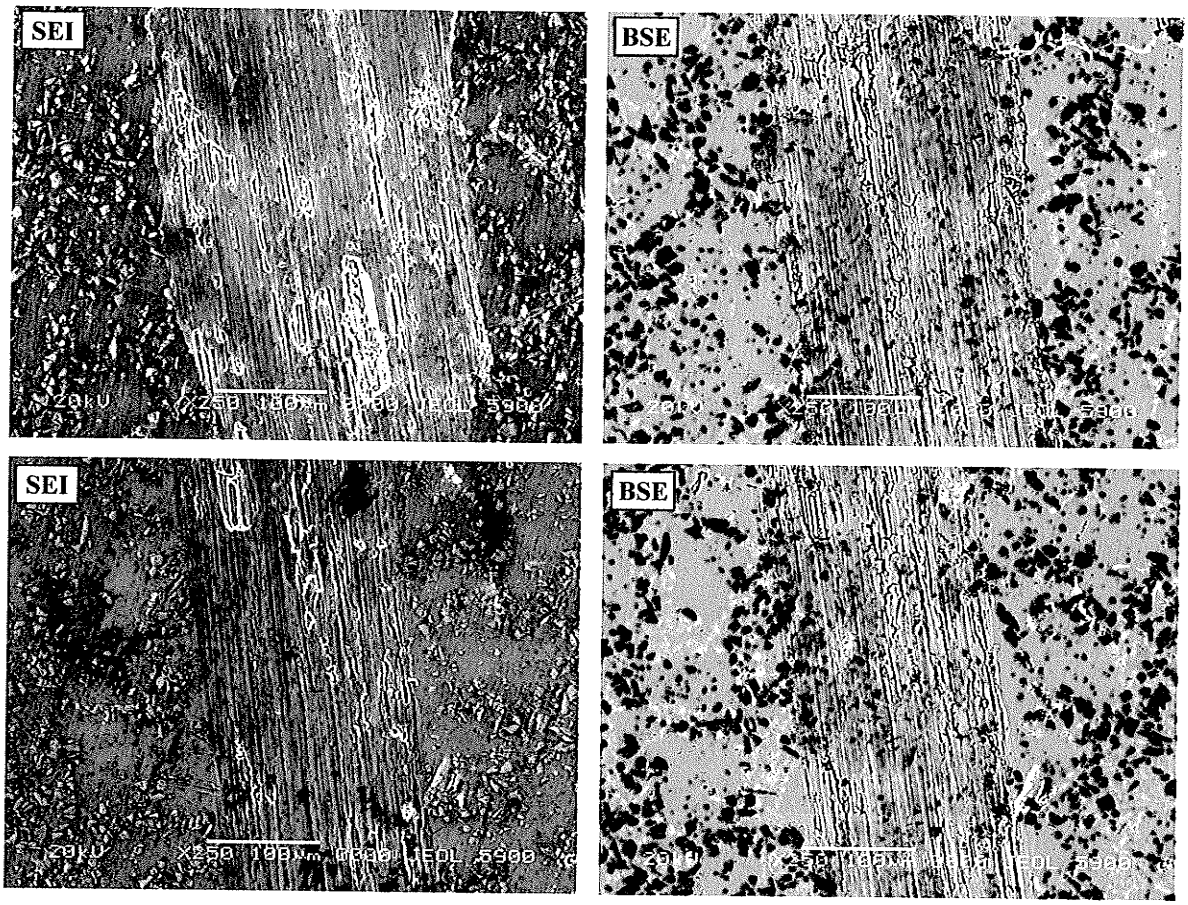

Figure 4.419 The composite surface wear scars under low pressure conditions (2N) after 100 cycles (≈ 1m) sliding. The counterfaces are TOP: Al_2O_3 BOTTOM: Si_3N_4

How the counterface mass accumulated determined the wear track morphology. Al_2O_3 had a thin flat transfer layer of mixed Al-MMC on the surface after 100 cycles sliding, resulting in a highly smeared composite surface. Mutual adhesive transfer between the Al-6061 alloy and the composite occurred.

When direct exposure of the K-Monel surface occurred before a transfer layer was developed (100 cycles) SiC particles could be seen to be crushed, Figure 4.417. When direct exposure of the 316ss occurred against the composite, SiC were not fractured, but instead were inundated in the surface.

CHAPTER 5 CONCLUSIONS

5.1 CONCLUSIONS FROM LITERATURE REVIEW

1) SLIDING CONDITIONS:

The literature review focused on low speed, high applied pressure sliding conditions. It has been determined that these sliding conditions favour mechanical mixing during sliding contact. Transfer, back transfer, and the interaction of debris in the interface are more prominent at low sliding velocities. Transfer and debris interactions have been related to high friction fluctuations, the process that forms a mechanically mixed layer, and relatively high or low transitions in the rate of wear. A low sliding velocity considered below 1 m/s where frictional temperature rise was low. A high pressure was considered over 1 MPa based on nominal contact area.

2) Al-Si MATRIX:

Overall, the increase in hardness through precipitation hardening has not been proven to significantly reduce wear of Al-MMC composites, and in fact may have a detrimental effect on wear resistance though increased SiC particle debonding or particle fracture. In most wear studies peak age hardening was not found to be effective in reducing wear of aluminum composites. Reduction in tensile stress in the matrix is beneficial regardless of the sliding condition.

Debris size is affected by the %Si content and morphology. Increasing Si content can decrease debris size by reducing delaminations due to smearing. However, at high

pressures hypereutectic Al-Si alloys (high %Si) can have increased delamination due to subsurface fracture as a result of cracking of large primary Si particles. Therefore, for unmodified cast Al-Si alloys a near eutectic composition was most likely to benefit from the formation of a mechanically mixed surface. This has been related to smaller debris sizes, reduced subsurface instability and favorable ratio of hard and soft phases to allow mixing to occur. For the aluminum matrix adhesion consistently limited wear performance and remained an obstacle for Al-MMCs. Increasing %Si in the Al-Si alloy has been consistently shown to reduce adhesion.

The mixing of the Si phase in the active layer was found highly dependent on the microstructure, specifically the Si morphology and size. A very small Si particle distribution was found not to increase wear resistance due to easier removal of the Si particle phase from the surface. In all the studies cited, mixing of the Si phase in addition to a mechanical mixed surface containing counterface elements was found unanimously to increase wear resistance whenever it was observed to occur.

3) SiC REINFORCEMENT:

Concerning the choice of reinforcement a specific range of particle sizes between 2-15μm showed the most promise under high pressure, low speed conditions. Smaller particles than 2μm were not commonly tested, however increased adhesion, smearing, and pull-out instead of mixing were all indicated to limited wear resistance of these smaller particles. Larger particles than 15μm suffered from particle cracking, severe surface damage with the removal of a particle, worse surface distributions to protect the aluminum matrix from counterface asperity contact, and increased potential for softening due to the

Bauschinger effect under reciprocal sliding. The conclusion was that under high pressure, low speed sliding conditions the use of smaller particle in this range would be superior to larger sized particles. The optimum particle size appeared to be determined by two opposing wear mechanisms: particle size should be decreased in response to particle cracking in the subsurface while particle size should be increased in response to smearing and pull-out at the contact surface.

In all studies an even surface distribution of SiC particles improved wear properties. Fibers normal to the sliding direction was the better reinforcement geometry due to better load bearing capacity of surface tensile forces. However, the use of fibers has not been shown to be particularly beneficial in comparison to the use of particles, in part due to cracking of the fibers. Uniform reinforcement shapes (spheres) were preferred in terms of less discontinuities, lower particle stresses and less likelihood of fracture. Cast Al-Si-SiC composites with particle volume fractions greater than 30% have demonstrated lower wear resistances due to increased fracture.

4) COUNTERFACE:

Hard ceramics at low sliding speeds appear to act as a worse choice for a counterface material for both Al-Si alloys and aluminum metal matrix composites compared to hardened steel. A soft steel was found to be a worse choice of counterface compared to a harder steel. Counterfaces that promoted low adhesion of the Al-matrix had the best wear performance when tribologically paired with aluminum alloys and composites. The iron oxide transfer layer effect was not effective at high pressures, with

transfer of elemental iron particles more likely to occur for the sliding conditions focused upon in this review.

5) DEBRIS:

Generation of fine particulate Al debris is preferred in terms of greatest potential for mechanical mixing and least surface damage. The role of SiC as debris particles during Al-composite wear has not been established. The possible role of hard ceramic phase is very different on the surface as compared to in the interface. A further conclusion may be that if abrasion does not significantly increase (as noted for small ceramic particles) *and* surface mixing occurs, presence of a hard ceramic phase on the surface may act to reduce wear by hard ceramic particles in the interface.

5.2 CONCLUSIONS FROM STUDY

1) AL MATERIAL WEAR PERFORMANCES

The wear performance was significantly improved through the use of the Al-Si alloy in comparison to the HP Al for like sliding conditions. The Al-SiC composite had lower weight losses than the unreinforced Al-Si alloy. This was explained by greater resistance to seizure and large plastic delaminations due to smearing over the range of pressures experienced over the duration of a wear test. The conclusion was that the addition of 20%SiC was beneficial to wear resistance of the base Al-7%Si alloy under low speed, high pressure sliding conditions.

2) RECIPROCATING DISTANCE AND SPEED

Tests were performed with average sliding speeds approximately in the range of 2-22 cm/s and reciprocating track lengths of 1/16"-3/4". At high initial pressures (>10MPa) a slower average sliding speed (7.5cm/s vs. 22.5cm/s) allowed for the less damaging wear mechanisms to dominate (debris mixing and transfer vs. seizure delaminations). In contrast, at long sliding distance where the pressure was low (<1MPa) the higher sliding velocity caused less surface damage by promoting abrasive wear (particle debris) over adhesive-delamination wear (large plate debris). Shortening the reciprocating distance promoted smearing, adhesive transfer of the sliding surface and debris mixing at all contact pressures. At 1/16" reciprocating debris remained where it was generated causing an iron oxide layer to form on the composite surface through increased abrasion of the steel counterface. This was an exception, as under all other test conditions debris adequately escaped the interface and an abraded iron oxide layer did not form.

3) EFFECT OF STEEL COUNTERFACE

Stainless and hardened steel counterfaces in the range of 25-65 HRC were tested against the Al-20vol%SiC composite. The change in steel hardness in this range did not drastically alter the composite wear rate. An increase in weight loss of the Al-MMC was not in proportion to an increase in steel hardness or vice versa. Hardness had the greatest effect on adhesive transfer of the composite surface.

Observing the weight loss of the material pairs, 316 steel experienced the greatest wear and caused the greatest weight loss of the Al-MMC at low pressures, making it the

worst tribological pair tested in terms of wear performance. A soft annealed 52100 counterface had worse tribological performance similar to the 316ss, indicating that hardness was more important than composition. At high pressures wear rates were similar for the composite, however the softer steels had increased weight loss due to abrasion compared to the harder steels. Overall a soft steel regardless of composition was the worst choice of counterface.

4) ADHESION AND TRANSFER OF Al-COMPOSITE

Transfer of Al-MMC to the steel counterface was found to preferentially occur. For all steels, a thick transferred Al-MMC deposit initially formed at pressures greater than 10MPa and became unstable at low pressures. The hardness of the counterface was found to affect the amount of the mechanically mixed transfer material deposited on the steel surface. Although the cause was not clear, a higher hardness steel promoted a more stable adhesive transfer layer. A more stable transfer layer decreased delamination of the mixed Al-MMC deposits off the counterface and caused lower overall weight loss of the sliding couple. The overall conclusion was that adhesion to the counterface controlled and prevented substantial transfer of the steel to the composite surface during sliding contact.

5) MECHANICAL MIXING

For any applied load between 2-50N, or applied pressure in the range of 1-10MPa, a black mixed surface layer was not stable and could not form continuously under the

reciprocal testing for either HP Al, 7%Al-Si, or the A356-20%vol SiC composite against a steel counterface. Current testing has established that surface mechanical mixing for Al-20% SiC can consist of (I) layered deposits of both Al-SiC and steel counterpart (MML), as found in the previous study [34], (II) A mechanically mixed layer of Al and SiC only (SML), (III) patchy deposits of Al, commutated SiC, mixed oxides, and small amounts of counterface material transfer, or (IV) no mixed surface deposits or layers present.

Since very limited counterface elements and little debris mixing occurred during the current reciprocal testing, the mixed surface/subsurface found could not be defined as a MML. A SML was identified as a mixing phenomenon that occured at a higher pressure range and involves relatively low mixing of debris in comparison to a MML. The SML was formed under sliding conditions of severe surface smearing and a thick mixed transfer layer on the composite. The MMLs previously identified were formed by a continuing process of debris agglomeration, mixing, compaction, and subsequent delamination. Therefore, a conclusion of this study was the an SML and MML are different phenomenons, with the latter being more beneficial in terms of wear resistance. It was concluded that both upper and lower limits of applied nominal pressure exist that allow for a SML to form, with both limits being set by surface fracture; the lower limit set by insufficient plastic deformation, the upper set by instability of the deformed surface causing a higher fracture rate of the smeared surface than the rate in which the mixed surface can re-form.

6) INSTABILITY IN THE SUBSURFACE

Examination of the subsurface revealed that severe reinforcement fracture occurred in the subsurface at high pressures (>10MPa) causing soft shear layers to form in-between SiC particles. The conclusion was that particle fracture remained a problem for the tested composite with an average 10μm particle size at the highest pressures. At intermediate pressures (2-10MPa) subsurface crack propagation and delamination caused debris to be generated before particle cracking significantly occurred. The transition between subsurface particle behaviour was related to a transition in debris from delaminations due to smearing to delaminations due to subsurface fracture. It was concluded that a smaller particle size, decreased particle spacing, and more uniform distribution of particles would be required to achieve less elastic unloading due to particle cracking and decrease the probability of soft shear layers forming.

7) WEAR MECHANISMS

Wear of the Al-materials was classified by three categories of wear mechanisms as pressure decreased. Seizure and smearing delaminations were identified as contributing the greatest weight loss at high pressures, while delaminations due to subsurface fracture began to dominate as the pressure was reduced. Increased seizure delamination occurred in response to increased sliding velocity at high pressures. Smearing of the surface occurred at any tested apparent pressure.

Undulations were observed to form by delamination due to subsurface fracture in the valley regions and delaminations due to smearing on the crests of what would become a wavy wear surface at intermediate pressures. Delaminations due to subsurface fracture were thicker than smearing delaminations. The dominant surface interaction between a SiC

asperity and the counterface changed from predominantly fracture and inundation at high pressures (>10MPa) to ploughing and abrasion at low pressures (<1MPa). Plastic deformation of Al-asperities always occurred due to the high asperity pressures during dry sliding. Stick-slip adhesive transfer of the Al matrix asperities to the counterface occurred at all pressures.

8) DEBRIS MIXING

Debris agglomerated unfavourably under the reciprocal sliding conditions for mechanical remixing into the surface. "Snowballs" formed by agglomerations of particulate debris were created in the interface and easily ejected from the wear scar. This was in contrast to unidirectional sliding which allowed "flakes" or plates of compacted debris to be mixed into the wear surface. Since compaction of fine particle debris occurred more readily under unidirectional sliding MML formation was hence promoted. A thick adherence of soft Al material on the counterface caused debris generation and mechanical mixing predominately from like Al-SiC material in contact.

9) ADHESION - DIFFERENT COUNTERFACES

Adhesion of the Al-composite limited wear performance regardless of the choice of soft or hard counterface materials. Both Al_2O_3 and Si_3N_4 ceramic counterfaces resulted in thick transfer patches of mixed Al-MMC material forming on the counterface's contact surface. The transfer patches were thicker and therefore more stable on the harder Si_3N_4 ceramic counterface. In contrast transfer patches on the K-Monel counterface were small and relatively unstable, which caused direct exposure of the nickel alloy surface to abrasion

by the composite. As a result a MML was formed with fine Ni and Cu particles mixed into the composite surface. The softest Al-6061 had no preferential direction of adhesive transfer. This caused large adhesively transferred delaminations between surfaces, resulting in large delaminations eventually ejected from the interface and severe wear rates. A clear trend of increased stability of adhesive transfer material was observed in conjunction with increased hardness of the counterface.

10) WEAR PERFORMANCE – DIFFERENT COUNTERFACES

Classifying wear performance of the different counterfaces varied depending upon what would be considered the worst indicator: overall weight loss of the pair, greatest adhesive transfer of the composite, or the severity of surface damage. At low load K-monel was the only material to form a MML and clearly had the best wear performance. At high loads the ceramics resulted in high adhesive transfer, low weight loss and deep wear scars. Although the overall weight loss was similar, the use of a steel counterface was clearly superior over the ceramic counterfaces due to less adhesive transfer and therefore less damage to the Al-composite surface. At high load K-monel experienced relatively high abrasive wear, limiting the overall performance of the tribological pair.

CHAPTER 6 FUTURE DESIGN/ RESEARCH CONSIDERATIONS

6.1 IMPROVED DESIGN OF AL-MMCS FOR WEAR RESISTANCE

Al-Si and Al-Si-SiC improve dimensional stability through the use of a hard phase that supports the load on the soft Al phase. As such the friction and wear properties can be potentially tailored, with the soft Al matrix acting as its own "lubricant" during contact due to the low shear strains required to deform this phase. The hard reinforcement phase, normally associated with higher friction coefficients than the matrix, allows for interface stability and lower subsurface strain. Using the benefits of both hard and soft phases is the basic premise behind the use of Al binary or composite materials in improving tribological performance. The goal is to produce a stable interface where adhesive transfer does not cause high wear, or smearing does not cause loss of dimension. To achieve this goal the best case scenario is development through sliding of a thin surface layer that can dissipate friction work and minimize the depth of sliding damage. This is possible through the incorporation of load bearing reinforcement to reduce subsurface deformation (SiC), a soft matrix phase with low friction (Al), as well as a counterface which allows for proper thin surface layer to form.

Since counterface contact with the aluminum matrix and reinforcement phase will inevitably occur during sliding wear, improving upon the wear resistance of metal matrix composites can be simplified by first looking at what would improve the wear resistance of the individual constituents.

6.11 IMPROVING WEAR RESISTANCE OF THE MATRIX

As is well known, improving wear resistance must be approached differently depending upon the application. If adhesion limits wear resistance, the matrix hardness can be increased somewhat to compensate. Age hardening may improve adhesion resistance through increased hardness, although studies to date have not found significant improvements by this method with reinforcement present [35,108]. Alloying is more effective in increasing matrix hardness than greater reinforcement content [8]. However, solid solution strengthening of Al is severely limited by solubility [9]. The most promising developments are the use of nanocrystalline aluminum alloys such as $Al_{92.5}Ti_{2.5}Fe_{2.5}Cr_{2.5}$ formed by rapidly solidified powder [137]. Al-Fe alloys (<10wt%Fe) formed by mechanically alloying can result in a matrix with excellent strength and ductility combination for wear resistance at low temperatures [138-140]. SiC dispersion strengthening provides stabilization of the microstructure [137,141]. Unfortunately, increased matrix hardness through alloy powders requires high energy input (ball milling) and complex P/M processing methods to achieve the high hardness matrix material [142].

In comparison, the use of Al-Si alloys can be cast at a fraction of the cost. Increased %Si can be used to obtain much higher levels of matrix hardness. A recommended limitation to the use of Al-Si alloys is that the processing method/ composition should not allow large primary Si phase to form, which is detrimental to surface stability under high pressure, low sliding speed conditions [88]. Iron intermetallics were observed to crack and cause surface delaminations for the Al-Si alloy and therefore must not be present near the wear surface. Residual tensile stress in the matrix has to be avoided in attempts to harden the matrix due to the negative effect of promoting micro-

pitting and increased stresses at the particle/matrix interface. Non-precipitating alloy elements can be recommended for solid solution strengthening of the matrix.

Despite increased hardness with the Si phase, small particle debris removed by adhesion of the Al-matrix is expected to occur and needs to be reduced. Incorporation of a soft phase in the cast alloy that could easily shear and reduce Al adhesion could allow significant improvement by limiting the Al metallic transfer ever-present during wear of the Al-Si and Al-composite materials tested. Alloying with a soft metals such as Sn or Bi, or a metal with a low melting point such as In, are options for introduction of a potential third phases that could promote "shear film" formation over the Al-matrix and SiC reinforcement during sliding. Reducing adhesion requires vital focus in further research to improve wear properties of cast Al-Si and Al-Si composite materials.

6.12 IMPROVEMENT IN WEAR RESISTANCE THROUGH REINFORCEMENT

In general using a relatively unaltered aluminum matrix a significant amount of SiC reinforcement must be utilized to achieve wear resistance. Addition of significant amount of alloying elements to the aluminum matrix in combination with techniques such as rapid solidification and powder metallurgy can significantly reduce matrix ductility, so that considerably less SiC reinforcement is required to achieve the desired deformation or wear resistance. Brittle inclusions and void formation in the subsurface has been identified as a major cause of delamination wear and therefore the use of brittle ceramic particles to make a wear resistant material raises red flags. The use of very small reinforcement particles (for example 1μm) and high volume fraction (for example 30-50%) appears as a good solution to elastic unloading of particles due to cracking that can lead to delamination wear. This

provides a good solution for subsurface stability and reduced plastic deformation. However subsurface cracks can be more easily linked at the higher volume fraction of reinforcement and with evenly distributed small particles. Therefore if the composite is designed with this reinforcement philosophy effort must be taken to decrease crack propagation and increase toughness in the matrix. This could be accomplished by the addition of a third phase to the composite.

If a very small particle size is used for the benefits of subsurface stability, surface adhesion becomes a problem. Very small reinforcement particles can be easily removed from the surface due to the lower particle/matrix surface bonding area. Consequently the rate of particles removed from the surface could increase, especially at high volume fractions, causing increased surface weight loss while simultaneously not protecting the Al-matrix from direct contact. Therefore a larger surface reinforcement particle (for example 5μm) may be required. Further research into particle surface/subsurface size distributions may reveal how further improvement can be made through the use of different sizes of SiC reinforcement. Improving the fracture resistance of the SiC reinforcement, matrix bonding, and homogeneity of the particle distribution in the cast composites all have significant potential to increase wear resistance.

REFERENCES

[1] J.F. Archard, Friction between metal surfaces, Wear 113, 1986, p. 3-16

[2] J.K. Lancaster, Material-specific wear mechanisms: relevance to wear modelling, Wear 141, 1990, p.162-166

[3] E. Rabinowicz, Penetration hardness and toughness indicators of wear resistance, Proceedings of the Institution of Mechanical Engineers, Part C, Vol. 198, 1987, p. 197-203

[4] M.J. Winter, University of Sheffield and WebElements Ltd., 2002 http://www.webelements.com/ , Physical data of elements

[5] J.D. Embury, Strengthening mechanisms in Al alloys – An overview of natural limits and engineering possibilities, Material Science Forum Vols. 217-222, 1990, p. 57-70

[6] F.A. Davis, T.S. Eyre, Effect of silicon content and morphology on the wear of aluminum-silicon alloys under dry and lubricated sliding conditions, Tribology International, Vol. 27, No. 3, 1994, p. 171-181

[7] Y. Brechet, J.D. Embury, S. Tao, L. Luo, Damage initiation in metal matrix composites, Acta metallurgical et Materialia, Vol 39, No. 8, 1991, p. 1781-1786.

[8] G. Straffelini, Experimental observations of subsurface damage and oxidative wear in Al-based metal-matrix composite, Wear 245, 2000, p. 216-222

[9] C. Subramanian, Some considerations towards the design of a wear resistant aluminum alloy, Wear 155, 1992, p. 193-205

[10] D.A. Rigney, Transfer, mixing and associated chemical and mechanical processes during the sliding of ductile materials, Wear 245, 2000, p. 1-9

[11] A.T. Alpas and J. Zhang, Effect of Microstructure (Particulate Size and Volume Fraction) and Counterface Material on the Sliding Wear Resistance of Particulate-Reinforced Aluminium Matrix Composites, 1993, p. 974-976

[12] S. Wilson, A.T. Alpas, Wear mechanism maps for metal matrix composites, Wear 212, 1997, p. 41-49

[13] J. Zhang, A.T. Alpas, Transition between mild and severe wear in aluminium alloys, *Acta Metall.*, v 45, 1997, p. 513-528

[14] R. Lawrence, K.N. Tandon, Transfer of elements and MML across the interface during reciprocal dry sliding wear of Al-SiCp MMC against steels, Proceedings of CIM Light Metals Conference, 2002, p. 589-602

[15] R. Antoniou, C. Subramanian, Wear mechanism map for aluminum alloys, *Scripta Metall.* , Vol. 22, 1988, p. 809-814

[16] Y. Liu, R. Asthana, P. Rohatgi, A map for wear-mechanisms in aluminum alloys, Journal of Material Science, Vol. 26, 1991, p. 99-102

[17] S.C. Lim, Recent developments in wear-mechanism maps, Tribology International, Vol. 31, No. 1-3, 1998, p. 87-97

[18] J.K.M. Kwok, Tribological properties of metal-matrix composites, Ph.D. thesis, National University of Singapore, 1996

[19] J. L. Young, D. Kuhlmann-Wilsdorf, R. Hull, Generation of mechanically mixed layers (MMLs) during sliding contact and the effects of lubricant thereon, Wear 246, 2000, p.74-90.

[20] A.P. Sannino, H.J. Rack, Dry sliding wear of discontinuously reinforced aluminum composites: review and discussion, Wear 189, 1995, p. 1-19

[21] J.K.M. Kwok, S.C. Lim, High-speed tribological properties of some Al/SiCp composites: II. Wear mechanisms, Composites Science and Technology, Vol. 59, No. 1, 1999, p. 65-75

[22] Z.F. Zhang, L.C. Zhang, Y.W. Mai, Wear of ceramic particle-reinforced metal-matrix composites: Part I. Wear Mechanisms, Journal of Material Science, Vol. 30, 1995, p. 1961-1966

[23] A. Wang, H.J. Rack, Dry sliding wear in 2124 Al-SiC_w/17-4 PH stainless steel systems, Wear 147, 1991, p. 355-374

[24] M. Bai, Q. Xue, H. Guo, Reciprocal sliding wear of SiC particle reinforced Al-Cu aluminum matrix composites against stainless steel, high speed tool steel and ceramics II. Wear mechanisms, Wear 194, 1996, p. 126-136

[25] X.Y. Li, K.N. Tandon, Microstructural characterization of mechanically mixed layer and wear debris in sliding wear of an Al alloy and an Al based composite, Wear 245, 2000, p. 148-161

[26] A.R. Rosenfield, A shear instability model of sliding wear, Wear 116, 1987, p. 319-328

[27] J. Zhang, A.T. Alpas, Delamination wear in ductile materials containing second phase particles, Materials Science and Engineering A, Vol. 160, 1993, p. 25-35

[28] A.T. Alpas, J.D. Embury, Wear mechanisms in particle reinforced and laminated metal matrix composites, Wear of Materials: International Conference on Wear of Materials, Vol. 1, 1991, p. 159-166

[29] A. Kapoor, F.J. Franklin, Tribological Layers and the wear of ductile materials, Wear 245, 2000, p. 204-215.

[30] Sture Hogmark, Staffan Jacobson and Olof Vingsbo, Surface Damage, ASM Handbook Vol.18: Friction, Lubrication, and Wear Technology, 1992, p. 177

[31] B.Venkataraman, G. Sundararajan, The sliding wear behaviour of Al-SiC particulate composites-I. Macrobehaviour, *Acta Mater.*, Vol. 44, No. 2, 1996, p. 451-460

[32] B. Venkataraman, G. Sundararajan, The sliding wear behaviour of Al-SiC particulate composites-II. The characterization of subsurface deformation and correlation with wear behaviour, *Acta Mater.*, Vol. 44, No. 2, 1996, p. 470-473

[33] B. Venkataraman, G. Sundararajan, Correlation between the characteristics of the mechanically mixed layer and wear behaviour of aluminum, Al-7075 alloy and Al-MMCs, Wear 245, 2000, p. 22-38

[34] X.Y. Li, Wear behaviour and Microstructural characterization of worn surfaces and wear debris of a high purity Al and Al-Si alloy and an Al-Si/SiCp composite sliding against an M2 steel, PhD Thesis, 1999

[35] X.Y. Li, K.N. Tandon, Subsurface microstructures generated by dry sliding wear on as-cast and heat treated Al metal matrix composites, Wear 203-204, 1997, p. 703-708

[36] K. Varadi, Z. Neder, K. Friedrich, Evaluation of the real contact areas, pressure distributions and contact temperatures during sliding contact between real metal surfaces, Wear 200, 1996, p. 55-62

[37] Pan, Y.M., Fine, M.E., Gheng, H.S., Sliding wear of an alloy SiC whisker composite, *Tribol. Trans.*, Vol. 35, 1992, p. 482-490

[38] G. Straffelini, F. Bonollo, A. Molinary, A. Tiziani, Influence of matrix hardness on the dry sliding behaviour of 20 vol% Al_2O_3 – particulate-reinforced 6061 Al metal matrix composites, Wear 211, 1997, p. 192-197

[39] A. Ravikiran, M.K. Surappa, Effect of sliding speed on wear behaviour of A356 Al-30wt% SiC_p MMC, Wear 206, 1997, p. 34-36

[40] D.W. Borland, S. Bian, Unlubricated sliding wear of steels: towards an alternative wear equation, Wear 209, 1997, p. 171-178.

[41] M. Narayan, M.K. Surappa, B.N. Primila Bai, Dry sliding wear of Al alloy 2024-Al_2O_3 particle metal matrix composites, Wear 181-183, 1995, p. 563-570

[42] A.T. Alpas and J. Zhang, Effect of SiC particulate reinforcement on the dry sliding wear of aluminum-silicon alloys (A356), Wear 155, 1992, p. 83-104

[43] A.T. Alpas and J. Zhang, Delamination wear in ductile materials containing second phase particles, Material Science & Engineering A, Vol. A160, No. 1, 1993, p. 25-35

[44] M.F. Ashby, S.C. Lim, Wear-Mechanism Maps, *Acta Metall.* , Vol. 35, No. 1, 1987, p. 1-24

[45] Wang, A., Rack, H.J.; Transition wear behavior of SiC-particulate- and SiC-whisker-reinforced 7091 Al metal matrix composites, Materials Science & Engineering A: Structural Materials: Properties, Microstructure and Processing, v A147, n 2, Nov 15, 1991, p 211-224

[46] Hwang, D.E. , D.E. Kim , S.J. Lee ; Influence of wear particle interaction in the sliding interface of metals, Wear 225-229, 1999, p. 600-614

[47] Dong-Hwan Hwang, In-Ha Sung, Dae-Eun Kim, Sang-Jo Lee, Effects of material pair properties on the frictional behavior of metals, Wear 225-229, 1999, p. 427-439

[48] D.E. Larsen, D.A. Rigney, Sliding behaviour of an Al/SiC composite against H-13 tool steel and PSZ, 6th Intl. Congress on Tribology, Vol. 3, 1993, p.83-88

[49] D.A. Rigney, The roles of hardness in the sliding behaviour of materials, Wear 175, 1994, p. 63-69

[50] L.H. Chen, D.A. Rigney, Adhesion theories of transfer and wear during sliding of metals, Wear 136, 1990, p. 223-235

[51] T. Akagaki, D.A. Rigney, Sliding friction and wear of metals in vacuum, Wear 149, 1991, p. 353-374

[52] I.R. McColl, S.J. Harris, G.J. Spurr, Fretting wear of a fine particulate reinforced aluminum alloy matrix composite against a medium carbon steel, Wear 197, 1996, p.184

[53] I.R. McColl, S.J. Harris, Q. Hu, G.J. Spurr, P.A. Wood, Influence of surface heat treatment on the fretting wear of an aluminium alloy reinforced with SiC particles, Wear 203-204, 1997, p. 507-515

[54] K. Komvopoulos, N. Saka, N.P. Suh, Plowing friction in dry and lubricated metal sliding, Journal of Tribology, Vol. 108, 1986, p. 301-311

[55] K. Komvopoulos, N. Saka, N.P. Suh, The significance of oxide layers in boundary lubrication, Journal of Tribology, Vol. 108, 1986, p. 502-513

[56] D.E. Kim, N.P. Suh, On microscopic mechanisms of friction and wear, Wear 149, 1991, p. 199-208

[57] R.L. Deuis, C. Subramanian, J.M. Yellup, Dry sliding wear of aluminum composites—A review, *Composites Science and Technology*, Vol. 57, 1997, p. 415-435

[58] C. Subramanian, Wear of Al-12.3 wt.% Si Alloy slid against various counterface materials, *Scripta Metall.* , Vol. 25, 1991, p. 1369-1374

[59] R. A. Antoniou, L.J. Brown, J.D. Cashion, The unlubricated sliding of Al-Si alloys against steel: Mössbauer spectroscopy and x-ray diffraction of wear debris, *Acta metal.* , Vol. 42, No. 10, 1994, p. 3545-3553

[60] Q. Hu, I.R. McColl, S.J. Harris, R.B. Waterhouse, Role of debris in the fretting wear of a SiC reinforced aluminum alloy matrix composite, Wear 245, 2000, p. 10-21

[61] N. Emori, T. Sasada, Effect of fine ceramic particles interposed between sliding surfaces on wear of metals, International Conference of Wear of Materials, 1987, p. 185-190

[62] A.T. Alpas, J. Zhang, Effect of SiC particulate reinforcement on the dry sliding wear of aluminum-silicon alloys (A356), Wear 155, 1992, p. 83-104

[63] X.Y. Li, K.N. Tandon, Subsurface microstructures generated by dry sliding wear on as-cast and heat treated Al metal matrix composites, Wear 203-204, 1997, p. 703-708

[64] Z.C. Feng and K.N. Tandon, Behavior of surface layers during the reciprocating wear of SiC-Al/Si metal matrix composites, *Scripta Metall.*, Vol. 32, No. 4, 1994, p. 523-528

[65] X.Y. Li, K.N. Tandon, Effect of ion implantation on the dry sliding wear behavior of SiC reinforce Al-Si composite, Surface & Coatings Technology, Vol. 90, 1996, p.136-142

[66] X.Y. Li, K.N. Tandon, Mechanical mixing induced by sliding wear of an Al-Si alloy against M2 steel, Wear 225-229, 1999, p. 640-648

[67] Quinn, Terence F. J., Nasa interdisciplinary collaboration in Tribology, a review of oxidational wear, 1983

[68] A. Sato, R. Mehrabian, Aluminum matrix composites: Fabrication and properties, *Metall. Trans.*, Vol. 7B, 1976, 443-450

[69] Hu, M.S., Some effects of particle size on the flow behavior of Al-SiC_p composites, *Scripta Metall.*, Vol. 25, 1991, p. 695-700

[70] Wang, A., Rack, H.J., Transition wear behavior on SiC-particulate and SiC-whisker reinforced 7091 Al metal matrix composites, Materials Science and Engineering A, Vol. 147, 1991, p. 211-224

[71] B.N. Pramila Bai, B.S. Ramasesh, M.K. Surappa, Dry sliding wear of A356-Al-SiC_p composites, Wear 157, 1992, p. 295-304

[72] M.A. Martinez, A. Martin, J.L. Wear of Al-Si alloys and Al-Si/SiC composites and ambient and elevated temperatures, *Scripta. Metall.*, Vol. 28, 1993, p.207-212

[73] Pramila Bai, B.N., Biswas, S.K., Characterization of dry sliding wear of Al-Si alloys, Wear 120, 1987, p. 61-74

[74] D. Kuhlmann-Wilsdorf, D.A. Rigney (editor), Fundementals of Friciton and Wear of Materials, ASM, 1981, p. 119-186

[75] S.A. Reddy, B.N. Pramila Bai, K.S.S. Murthy, S.K. Biswas., Wear and seizure of binary Al-Si alloys, Wear 171, 1994, p. 115-127

[76] F.M. Hoskings, F.F. Portillo, R. Wunderlin, R. Mehrabian, Composites of aluminum alloys: Fabrication and wear behaviour, Journal of Material Science, Vol. 17, 1982, p.307-314

[77] G.J. Howell, A. Ball, Dry sliding wear of particulate-reinforced aluminum alloys against automobile friction materials, Wear 181-183, 1995, p. 379-390

[78] J. Clarke, A.D. Sarkar, Role of transfer and back transfer of metals in the wear of binary Al-Si alloys, Wear 82, 1982, p. 179-195

[79] J.K.M. Kwok, S.C. Lim, High-speed tribological properties of some Al/SiCp composites: I. Frictional and wear-rate characteristics, Composites Science and Technology, Vol. 59, No. 1, 1999, p. 55-63

[80] Z.F. Zhang, L.C. Zhang, Y.W. Mai, Wear of ceramic particle-reinforced metal-matrix composites: Part II. A model of adhesive wear, Journal of Material Science, Vol. 30, 1995, p. 1967-1971

[81] A.J. Black, E.M. Kopalinsky, P.L.B. Oxley, Asperity deformation models for explaining the mechanisms involved in metallic sliding friction and wear – a review, Proceeding of the Institution of Mechanical Engineers, Part C: Journal of Mechanical Engineering Science, Vol. 207, No. 5, 1993, p. 335-353.

[82] I.J. Ford, Roughness effect of friction for multi-asperity contact between surfaces, Journal of Physics D: Applied Physics, Vol. 26, No. 12 , 1993, p. 2219-2225

[83] A.D. Sarkar, Wear of aluminum-silicon alloys, Wear 31, 1975, p. 331-343

[84] T.S. Eyre, F. Abdul-Mahdi, Wear resistance of aluminum and its alloys, Proceedings of the International Conference of Aluminum Technology, 1986, p. 485-492

[85] O.P. Modi, B.K. Prasad, A.H. Yegneswaran, M.L. Vaidya, Dry sliding wear behaviour of squeeze cast aluminium alloy-silicon carbide composites, Materials Science & Engineering A: Structural Materials: Properties, Microstructure and Processing, Vol. 151, No. 2, May , 1992, p. 235-245

[86] L. Cao, Y. Wang, C.K. Yao, Wear properties of an SiC-whisker-reinforced aluminium composite, Wear 140, 1990, p 273-277

[87] B.K. Prasad, K. Venkateswarlu, O.P. Modi, A.H. Yegneswaran, Influence of the size and morphology of silicon particles on the physical, mechanical and tribological properties of some aluminum-silicon alloys, Journal of Materials Science Letters, Vol. 15, No. 20, 1996, p. 1773-1776

[88] B.K. Prasad, K. Venkateswarlu, O.P. Modi, A.K. Jha, S. Das, R. Dasgupta, A.H. Yegneswaran, Effects of primary silicon particles on the sliding wear behavior of aluminum-silicon alloys, Journal of Materials Science Letters, Vol. 17, No. 16, 1998, p. 1381-1383

[89] B.K. Prasad, K. Venkateswarlu, O.P. Modi, A.K. Jha, S. Das, R. Dasgupta, A.H. Yegneswaran, Sliding wear behavior of some Al-Si alloys: role of shape and size of Si particles and test conditions, Metallurgical and Materials Transactions A: Physical Metallurgy and Materials Science, Vol. 29, No. 11, 1998, p. 2747-2752

[90] M. Bai, Q. Xue, H. Guo, Reciprocal sliding wear of SiC particle reinforced Al-Cu aluminum matrix composites against stainless steel, high speed tool steel and ceramics I. Tribological properties and construction of tribo-maps, Wear 195, 1996, p. 152-161

[91] D. Tabor, Friction and wear – developments over the last fifty years, Proceedings of the Institution of Mechanical Engineers, Part C, Vol. 245, 1987, p. 157-172

[92] R. Antoniou, D.W. Borland, Mild wear of Al-Si binary alloys during Unlubricated sliding, Materials Science and Engineering, Vol. 93, 1987, p. 57-72

[93] A. Ravikiran, S.C. Lim, A better approach to wear-rate representation in non-conformal contacts, Wear 225-229, 1999, p.1209-1314

[94] J.A. Greenwood, Analysis of elliptical Hertzian contacts, Tribology International, Vol. 30, No. 3, 1997, p.235-237

[95] Hardness Testing, 2nd Ed., Harry Chandler, ASM International, p.141-157

[96] S.J. Cho, H. Moon, B.J. Hockey, S.M. Hsu, The transition from mild to severe wear in alumina during sliding, *Acta Metall.* , Vol. 40, 1992, p.185-192

[97] D. Tabor, Junction growth in metallic friction, *Proc. Roy. Soc. London*, 1959, Vol. A251, p. 378-392

[98] Yeong-gi Cho, Su-young Kin, Ikmin Park, Kyung-mox Cho, Wear properties of particulate reinforced aluminum alloys, Light Weight Alloys for Aerospace Applications IV, 1997, p. 235-236.

[99] Z. Feng, The reciprocal sliding wear behavior of SiC particulate reinforced aluminum composite, M.Sc Thesis, 1995, p. 86

[100] P.K. Rohatgi, Y. Liu, S.C. Lim, Wear mapping for metal and ceramic matrix composites, in: Advances in composite Tribology, ed. K. Friedrich, Elsevier, Amsterdam, 1993, p. 291-309

[101] M. Bai, Q. Xue, Investigation of wear mechanism of SiC particulate-reinforced Al-20Si-3Cu-1Mg aluminum metal matrix composites under dry sliding and water lubrication, Tribology International, Vol. 30, No. 4, p. 261-269.

[102] S.J. Harris, I.R. McColl, Z.W. Huang, Influence of thermo-mechanical processing on the tensile and fatigue properties of a SiC particle reinforced aluminum alloy, Proceedings of International Symposium on the developments & applications of ceramics & new metal alloys, 1993, p.117-126

[103] M. Bai, Q. Xue, W. Liu, Sliding wear of Al-Fe-Ce-SiC composites lubricated with several typical additives, Tribology transactions, Vol. 40, No. 2, 1997, p. 267-272

[104] P.C. Nautiyal, J.A. Schey, Transfer of aluminum to steel in sliding contact: Effect of lubricant, Journal of Tribology, Vol. 112, p. 282-287

[105] Y. Wan, Q. Xue, Friction and wear characteristics of P^- containing antiwear and extreme pressure additives in the sliding of steel against and aluminum alloy, Wear 188, 1995, p. 27-32

[106] H. L. How, T.N. Baker, Dry sliding wear of Saffil-reinforced AA 6061 composites, Wear 210, 1997, p. 263-272

[107] F.A. Davis, T.S. Eyre, Wear of plain bearing materials with particular reference to role of soft phases, Material Science and Technology, Vol. 7, 1991, p. 746-756

[108] Y.M. Pan, M.E. Fine, H.S. Cheng, Aging effects on the wear behavior of P/M aluminum alloy SiC particle composites, *Scripta Metallurgica et Materialia*, Vol. 24, 1990, p. 1341-1345

[109] S. Chung, B.H. Hwang, A microstructural study of the wear behaviour of SiC_p / Al composites, Tribology International, Vol. 27, No. 5, 1994, p. 307-314

[110] S. Skolianos, T.Z. Kattamis, Tribological properties of SiC_p reinforced Al-4.5%Cu-1.5%Mg alloy composites, Material Science and Engineering A, Vol. 163, 1993, p. 107-113.

[111] A.P. Sannino, H.J. Rack, Tribological investigation of 2009Al-20vol% SiC_p/17-4 PH – Part I: composite performance, Wear 197, No. 1-2, 1996, p. 151-159

[112] A. Jokinen, P. Anderson, Tribological properties of PM aluminum alloy matrix composites, Proceedings of the Powder Metallurgy Conference and Exhibition, pt. 2 of 3, 1990, p. 517-530.

[113] K.J. Bhansali, R. Mehrabian, Abrasive wear of aluminum metal matrix composites, Journal of Metals, Vol. 34, No. 9, 1982, p. 30-34

[114] D.J. Lloyd, H. Lagace, A. McLeod, P.L. Morris, Microstructural aspects of aluminum-silicon carbide particulate composites produced by a casting method, Materials Science & Engineering A, Vol. 107, No. 1-2, 1989, p.73-80

[115] Samuel, A. M., Samuel, F. H., Influence of casting and heat treatment parameters in controlling the properties of Al-10wt% Si-0.6wt% Mg/SiC/20p composite, Journal of Material Science, Vol. 29, No.14, 1994, p. 3591-3600

[116] P. Heilmann, J. Don, T.C. Sun, D.A. Rigney, W.A. Glaeser, Sliding wear and transfer, Wear 91, 1983 p.171-190

[117] N. Okabe, I Murakami, H. Hirata, Y. Yoshioka, H. Ichikawa, Environmental deterioration and damage of ceramic matrix composites, Ceramic Engineering and Science Proceedings, Vol. 16, No. 5, 1995, p. 885-892

[118] D.Z. Wang, H.X. Peng, J. Liu, C.K. Yao, Wear behaviour and microstructural changes of SiCw-Al composite under Unlubricated sliding friction, Wear 184, 1995, p. 187-192

[119] D.Z. Wang, H.X. Peng, J. Liu, C.K. Yao, H. Han, Effects of ageing and whisker-orientation on wear behaviour of SiC_w/Al composites under unlubricated sliding friction, Composite Science and Technology, Vol. 53, No. 1, 1995, p. 21-25

[120] Y. Brechet, J. Newell, S. Tao, J.D. Embury, A note on particle comminution at large plastic strains in Al-SiC composites, *Scripta Metall.*, Vol.28, 1993, p. 47-51

[121] S.F. Corbin, D.S. Wilkinson, J.D. Embury, The Bauschinger effect in a particulate reinforced Al alloy, Materials Science and Engineering A, Vol. 207, 1996, p. 1-11.

[122] D.S. Wilkinson, E. Maire, J.D. Embury, The role of heterogeneity on the flow and fracture of two-phase materials, Materials Science and Engineering A, Vol. 233, 1997, p. 145-154

[123] E. Maire, D.S. Wilkinson, J.D. Embury, R. Fougeres, Role of damage on the flow and fracture of particulate reinforced alloys and metal matrix composites, *Acta Mater.* , Vol. 45, No. 12, 1997, p. 5261-5274

[124] R.B. Waterhouse, University of Nottingham, "Fretting wear", ASM Handbook – Friction, Lubrication, and Wear, Vol. 5, 1994, p.253

[125] H. Goto, S. Omori, Tribological Characteristics of Particle and Chopped Fiber-Reinforced Al-Si Alloy Matrix composites, Tribology Transactions, Vol. 43, No. 1, 2000, p. 57-65

[126] H. Nakanishi, K. Kakihara, A. Nakayama, T. Murayama, Development of aluminum metal matrix composite (Al-MMC) brake rotor and pad, JSAE Review, Vol. 23, 2002, p. 365-379

[127] Z.W. Huang, I.R. McColl, S.J. Harris, Notched behaviour of a silicon carbide particulate reinforced aluminium alloy matrix composite, Materials Science and Engineering A, Vol. 215, 1996, p. 67-72

[128] P.N. Bindumadhavan, T.K. Chia, M. Chandrasekaran, H.K. Wah, L.N. Lam, O. Prabhakar, Effect of particle-porosity clusters on tribological behavior of cast aluminum alloy A356-SiC_p metal matrix composites, Materials Science and Engineering A, Vol. 315, 2001, p. 217-226

[129]C. C. Perng, M. C. Jeng, J.L. Liang, Wear behavior of Al_2O_{3p}/6061-T6 aluminum alloy matrix composite, Journal Wuhan University of Technology, Materials Science Edition, Vol. 15, No. 2, 1994, p 118-127

[130] A. Ravikiran, M.K. Surappa, Oscillations in coefficient of friction during dry sliding of A356 Al-30wt% SiC_p MMC against steel, *Scripta Metall.* , Vol. 36, No. 1, 1997, p. 95-98

[131] F. Rana, D.M. Stefanescu, Friction properties of Al-1.5 Pct Mg/SiC particulate metal-matrix composites, Metallurgical Transactions A, Vol. 20, No. 8, 1989, 1564-1566

[132] C. Verdu, H. Cercueil, S. Communal, P. Sainfort, R. Fougeres, Microstructural aspects of damage mechanisms of cast Al-7Si-Mg alloys, Materials Science Forum, Vol 217-222, Pt. 3, 1996, p. 1449-1454

[133] S. Barnes, I.R. Pashby, D.K. Mok, Effect of workpiece temperature on the machinability of an aluminum SiC MMC, Journal of Manufacturing Science and Engineering, Transactions of the ASME, Vol. 188, No. 3, 1996, p. 422-427

[134] A. Martin, J. Rodriguez, J. Llorca, Temperature effects on the wear behavior of particulate reinforced Al-based composites, Wear, Vol. 225, 1999, p. 615-620

[135] R.S. Lee, G.A. Chen, B.H. Hwang, Thermal and grinding induced residual stresses in a silicon carbide particle-reinforced aluminum metal matrix composite, Composites, Vol. 26, No. 6, 1995, p. 425-429

[136] J.Lu, B. Miege, J-F. Flavenot, S. Thery, Study on the effect of the surface treatment on the residual stress gradient in silicon carbide (SiC) reinforced aluminum metal matrix composites, Journal of Composites, Vol. 12, No. 4, 1990, p. 232-238

[137] Makoto Takagi, Hidenobu Ohta, Toru Imura, Yoshihito Kawamura, Akihisa Inoue, Wear Properties of Nanocrystalline aluminum alloys and their composites, *Scripta Mater.*, Vol. 44, 2001, p. 2145-2148

[138] X.P. Niu, L. Froyen, L. Delaey, C. Peytour, Effect of Fe content on the mechanical alloying and mechanical properties of Al-Fe alloys, Journal Of Material Science, Vol. 29, 1994, p. 3724-3732

[139] X.P. Niu, L. Froyen, L. Delaey, C. Peytour, Fretting wear of mechanically alloyed Al-Fe and Al-Fe-Mn alloys, Wear 193, 1996, p. 78-90

[140] K.L. Sahoo, C.S.S. Krishnan, A.K. Chakrabarti, Studies on wear characteristics of Al-Fe-V-Si alloys, Wear 239, 2000, p. 211-218

[141] T. Koike, H. Yamagata, Development of SiC-composite-PM aluminum alloy piston, Journal of the Japan Society of Powder and Powder Metallurgy, Vol. 46, No. 5, 1999, p. 519-523

[142] F. Zhou, R. Lück, K. Lu, M. Rühle, Phase transformation of a dual phase Al-Fe alloy prepared by mechanical alloying, *Z. Metallkd*, Vol. 92, 2001, p.675-681

[143] F. Bin, G.S. Cole, Scuffing resistance of selected materials as protection for bores in aluminum engine blocks, SAE paper 920285, 1992, p. 1-9

[144] Y. Fujii, M. Hirata, K. Maeda, K. Fujii, S. Yamamoto, New retainer material for high speed and high temperature cylindrical roller bearing, Tribology Interactions, Vol. 42, No. 4, 1999, p.783-788